SOME ASPECTS OF THE DEVELOPMENT OF AN OPTICALLY SENSED GRAVITATIONAL-WAVE DETECTOR

BRIAN J. MEERS

Submitted for the degree of Ph.D. in the Faculty of Science of Glasgow University, December 1983.

CONTENTS

ACKNOWLEDGEMENTS

I would like to express my gratitude to all members of the Glasgow gravitational-waves group, without whom this work would not have been possible: Ron Drever, Jim Hough, Gavin Newton, Harry Ward, Andrew Munley, Norna Robertson, Stuart Hoggan and Graham Kerr; together with the excellent technical staff of Angus McKellar, Jim Pittillo and Allan Latta. Thanks are also due to Professors Sir J.C. Gunn and E. Laing for their help.

Financial support was gratefully received from SERC and the University of Glasgow.

PREFACE

Construction of a 10 m laser interferometer for the detection of gravitational radiation was started in Glasgow in 1978. This thesis describes various aspects of the development work covering the period October 1980 to October 1983.

Chapter 1 starts by discussing the nature of gravitational radiation and reviews the likely strengths, frequencies and rates of occurrence of various astrophysical sources. Different types of possible detector are also considered.

Chapter 2 discusses in detail laser interferometers which contain optical cavities in each of their arms in order to enhance the phase change produced by the gravitational wave. The effect of the gravitational wave, for arbitrary cavity storage time, fringe visibility and modulation depth, is calculated. The limitations imposed by various noise sources are then considered, though much of this material is not original. The effect of beam geometry changes is extensively discussed in Chapter 3, in an elaboration of previous work. The demonstration that beam geometry fluctuations must be reduced is followed, in Chapter 4, by the successful development of two techniques, an active beam position controlling system and a resonant cavity mode-suppressor (an idea developed in Munich), to do this. A spatial filtering system is also analysed and shown to have some potential for reducing complex beam shape changes.

In collaboration with the rest of the group, a recon-

structed interferometer was brought into operation. Experimental investigations into its performance, including the placing of limits to the sensitivity set by various noise sources are described in Chapter 5.

Some implications of this work and possible future developments are discussed in Chapter6.

The Appendices describe an experiment, carried out with the rest of the group, to place an upper limit on the gravitational radiation from the millisecond pulsar PSR 1937+214, together with various calculations which are relevant to the material discussed earlier but which would otherwise clutter-up the text.

SOME ASPECTS OF THE DEVELOPMENT OF AN OPTICALLY-SENSED GRAVITATIONAL-WAVE DETECTOR

SUMMARY

Gravitational radiation, a wave-like variation in the curvature of spacetime, is predicted by all relativistic theories of gravity, notably General Relativity. Produced by variations in mass distribution, its effect is to alter the distance between separated bodies.

The single sign of mass, together with energy—momentum conservation, means that monopole and dipole gravitational radiation are forbidden, a change in the quadrupole (or higher) moment of the souce being necessary for the generation of gravitational radiation. Together with the inherently weak nature of the gravitational interaction, this has the consequence that rapid, coherent motions of a large amount of matter are required if a significant amount of gravitational radiation is to be generated. These are the characteristics of violent astrophysical situations. Some possible sources are collapsing stellar cores in supernovae or collisions of compact objects (for bursts) , binary stars or rotating neutron stars (for periodic radiation) or the big bang (for a stochastic background). Observation of such radiation would provide valuable, qualitatively new, astrophysical information.

All detectors of gravitational radiation try to observe the apparent changes in tidal forces between separated masses. Resonant detectors, such as Weber bars, attach a

spring between the masses to magnify the effect of continuous radiation and prolong the effect of pulses; their properties are reviewed. If the test masses are free, then their separation may be increased to reduce the effect (relative to the gravitational-wave signal) of stochastic forces on the masses and noise in the detection process. They are also broad band. It is argued that this makes them potentially good detectors of gravitational radiation: the reason why it was decided to build such a detector, using laser interferometry to sense the motion, at Glasgow.

Laser interferometers are discussed; in particular, the variant, which is used at Glasgow, containing optical cavities in the arms of the interferometer is extensively analysed and possible noise sources in the operating region of ~100 Hz to ~20 kHz discussed. Considerable attention is devoted to one noise source: fluctuations in the size, shape or position of the laser beam. Its significance is demonstrated, with measurements being made both of the size of the positional fluctuations and of their effect on the interferometer. An active system was developed to suppress positional fluctuations of the beam, together with a resonant cavity mode-suppressor to reduce all types of change. The usefulness of a spatial filtering system is considered.

Experimental investigations into the performance of a prototype detector using optical cavities of length 10 m are presented. The significance of various noise sources, including laser frequency, intensity and positional fluctuations, is evaluated. Lessons for the future development

of the detector are drawn.

Finally, an experiment using a bar detector to place an upper limit to the gravitational radiation from the millisecond pulsar PSR 1937+214 is briefly reported; the observed limit was $h \sim \left(0{\cdot}8^{+1{\cdot}5}_{-0{\cdot}8}\right) \times 10^{-20}$ at 1284 Hz.

CHAPTER ONE

GRAVITATIONAL RADIATION: PROPERTIES, SOURCES AND DETECTORS

(1•1)The Nature of Gravitational Radiation.

The existence of some form of gravitational radiation is a prediction common to all theories of gravity which incorporate a version of local Lorentz invariance, with the consequent requirement for a finite propagation velocity. It is current belief that this velocity is not the "speed of thought" as suggested by Eddington(1922), but that gravitational radiation represents a genuine transfer of energy from one place to another. Now in any metric theory of gravity (e.g. Misner, Thorne and Wheeler 1973) all freely falling particles move on geodesics of the metric. A gravitational field is not "felt" by such particles, its action being to change the curvature of spacetime and so alter the path taken by the geodesics. Despite the lack of local action, the effect of the gravitational wave is thus to change the separation of free masses.

If a particle is a distance x^k from the centre of a local inertial frame at which the Riemann curvature tensor is $R_{\alpha\beta\gamma\delta}(t)$, then the apparent acceleration produced by the curvature is

$$d^2x^j/dt^2 = -R_{j0k0}(t)x^k \qquad (1•1)$$

In general, this allows six independent polarisations (e.g. Thorne 1983) which are various combinations of longitudinal and transverse deformations. General Relativity, however, only possesses two polarisations,

which correspond to the purely transverse deformation patterns indicated in figs 1•1 and 1•2. The "+" polarisation has $R_{x0x0}(t-z/c) = -R_{y0y0}(t-z/c)$ and all other R_{j0k0} equal to zero, while the "x" polarisation has $R_{x0y0} = R_{y0x0}$.

It is conventional to define the amplitude of a gravitational wave by

$$h_{jk} = -2R_{j0k0}(t-z/c) \qquad (1•2)$$

The change in separation of two test particles then becomes

$$\delta x^j = \tfrac{1}{2}h_{jk}(t-z/c)x^k \qquad (1•3)$$

The effect of the gravitational wave can thus be interpreted as the production of a change in the separation of two free particles which is proportional to that separation, a "strain in space".

Just as electromagnetic waves are produced by a change in the charge distribution, gravitational waves are produced by a change in the mass distribution. Just as monopole electromagnetic waves are forbidden by conservation of charge, monopole and dipole gravitational waves are forbidden by conservation of energy and momentum, at least in General Relativity. Those theories of gravity, however, in which the active gravitational mass depends on the gravitational binding energy (such as the Brans-Dicke-Jordan theory) predict unequal inertial and gravitational masses, thus allowing dipole radiation. The production of gravitational radiation in General Relativity requires a change in the reduced <u>quadrupole</u> moment Q_{jk} of the rad-

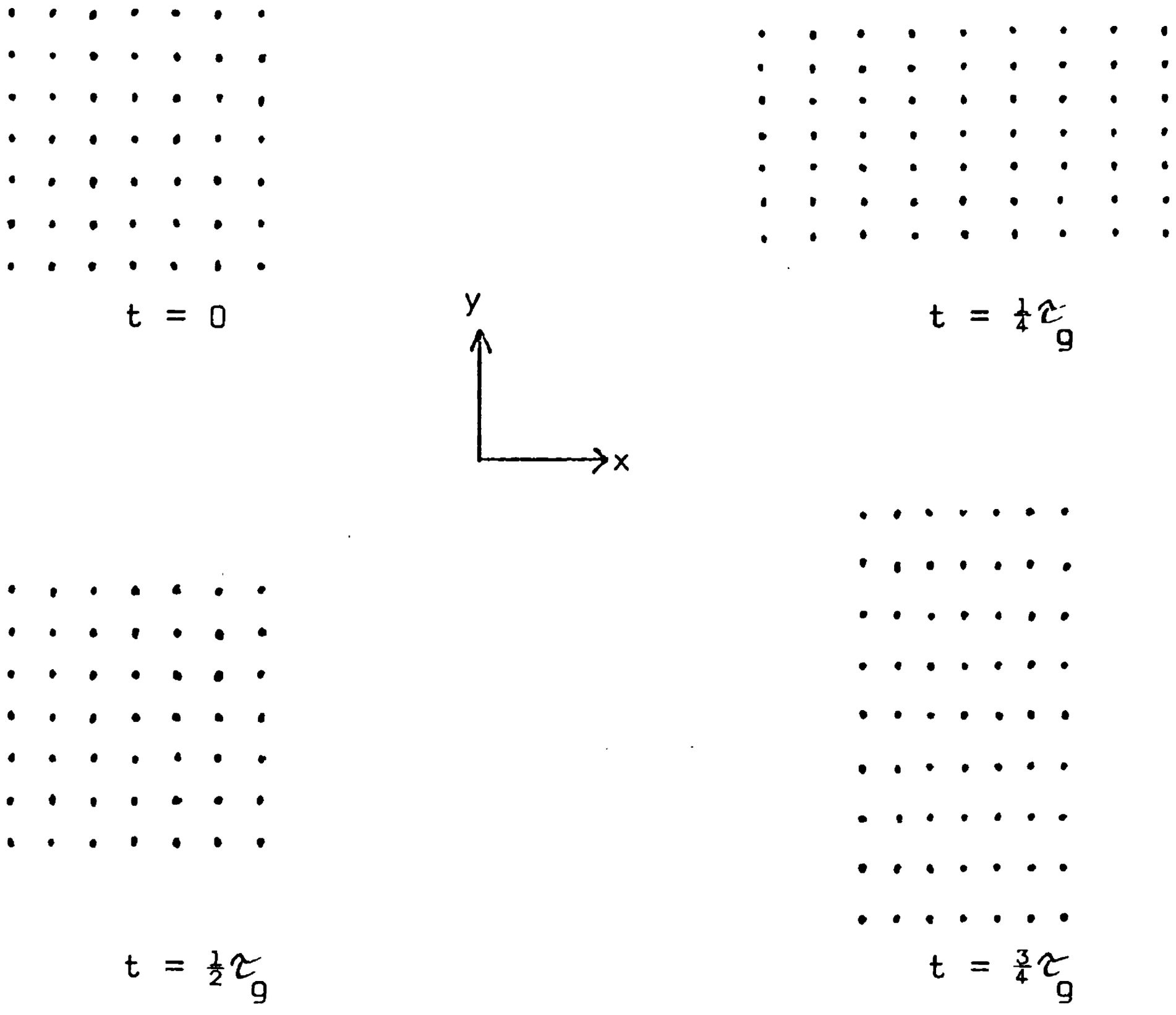

Fig.(1·1): The effect of the "+" polarisation of gravitational radiation on an array of test particles. The diagrams show the deformation patterns produced at intervals of a quarter of the gravitational-wave period τ_g. Note that orthogonal directions are affected oppositely by the gravitational wave. It is also apparent that the change in the separation of two particles increases with their initial separation. If the gravitational wave was of the "x" polarisation, the deformation pattern would be rotated by 45^o. The x and y directions would then be affected equally.

That the rotation angle is 45^o (not 90^o) reflects the spin two nature of the gravitational field. A 90^o rotation is just equivalent to a phase change.

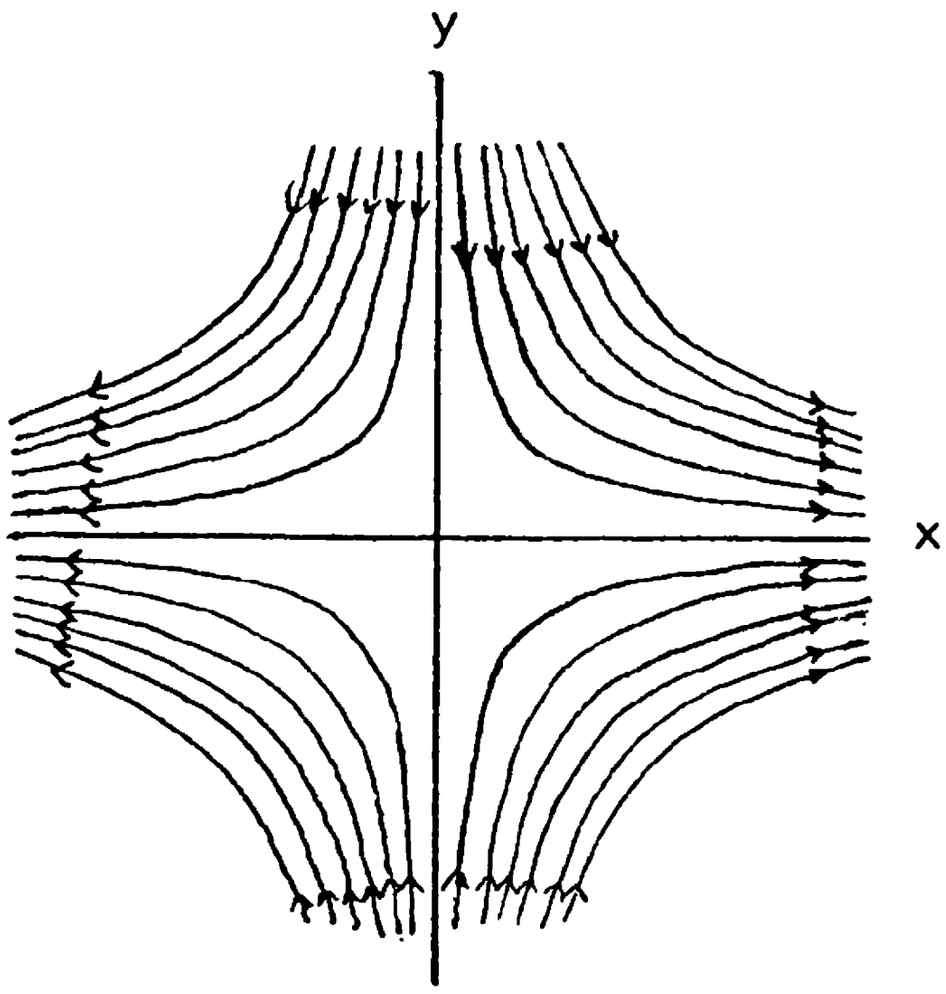

Fig.(1·2(a)): The effect of a gravitational wave may also be represented by a line-of-force diagram (Misner, Thorne and Wheeler 1973). As usual, the magnitude of the forces are indicated by the spacing of the lines. This diagram shows the effect of the "+" polarisation. Again, the diagram should be rotated by 45^{o} to see the effect of the "x" polarisation.

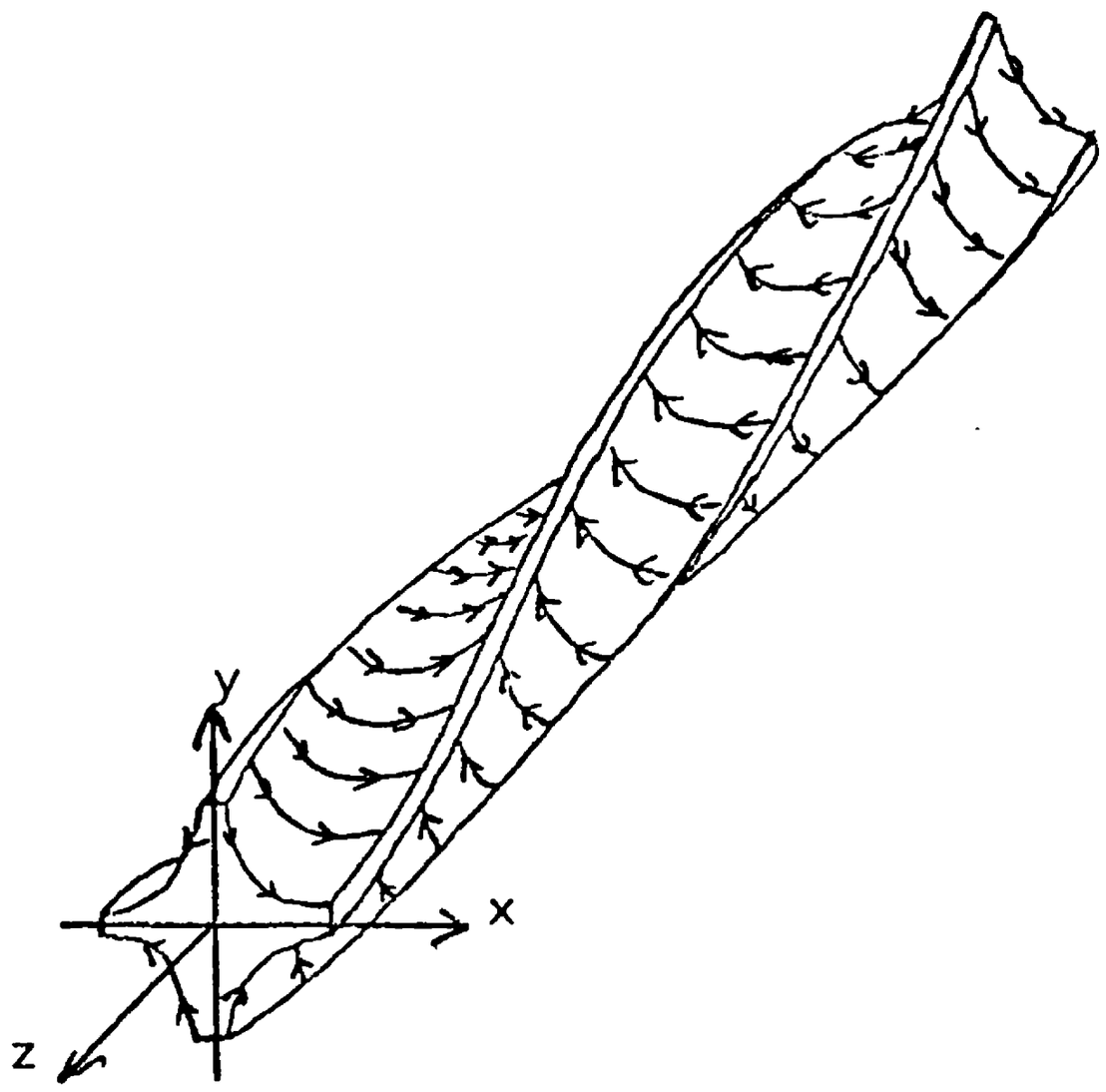

Fig.(1·2(b)): A three-dimensional force diagram, showing a circularly polarised gravitational wave. The line-of-force diagram rotates once every gravitational-wave period. The circularly-polarised wave is composed of the "+" and "x" polarisations with a 90^{0} phase lag.

iating system, where

$$Q_{jk} = \int \rho(x^j x^k - \tfrac{1}{3}\delta_{jk} r^2) d^3x \qquad (1\cdot4)$$

For slowly moving sources, the power radiated in gravitational waves L_{GW} is

$$L_{GW} = \frac{G}{5c^5} \langle \dddot{Q}^2_{jk} \rangle \qquad (1\cdot5)$$

It is convenient to express this in terms of a universal luminosity:

$$L_0 = c^5/G = 3\cdot6\times10^{52} W = 2\times10^5 M_\odot c^2/s$$

and the power flow L_{int} associated with non-spherical motions internal to the source:

$$L_{GW} \approx (L_{int}/L_0)L_0 \qquad (1\cdot6)$$

So large internal power flows are required if appreciable energy is to be radiated as gravitational waves. Equation (1·6) may be rewritten, for a source of dimension l and gravitational radius r_g, moving at typical velocity v, in the form

$$L_{GW} \approx (r_g/l)^2 (v/c)^6 L_0 \qquad (1\cdot7)$$

This clearly shows that matter moving at high velocity quite close to its gravitational radius is needed for the production of a large flux of gravitational radiation.

At a distance r from the source, the gravitational wave flux I_{GW} is

$$I_{GW} = L_{GW}/4\pi r^2 \qquad (1\cdot8)$$

For a monochromatic wave of frquency f, the resultant amplitude is (Weiss 1979)

$$h = (2G/\pi c^3)^{\frac{1}{2}} I_{GW}^{\frac{1}{2}}/f = (G/\pi^2 c^3)^{\frac{1}{2}} L_{GW}^{\frac{1}{2}}/rf \qquad (1\cdot9)$$

This may also be written as

$$h \sim 10^{-17}\left(\frac{\text{internal kinetic energy}}{\text{total mass-energy of sun}}\right)^{\frac{1}{2}}(r/10\text{kpc})^{-1} \quad ;(1\cdot9)$$

While strictly applicable only to slow motion sources, it seems likely that these relations will be at least approximately valid for realistic astrophysical sources (Thorne 1983).

The number of polarisation states is not the only property of gravitational radiation that varies between different theories of gravity. The propagation speed c_{GW} can also depend on the theory (e.g. Will 1979). If both the gravitational radiation and the light produced by a supernova in the Virgo cluster of galaxies could be observed (see next section) and the time discrepancy limited to about one day, then it would be possible to place the limit

$$\left|\frac{c_{GW}-c_{EM}}{c}\right| \lesssim \frac{1 \text{ day}}{4\times10^{7}\text{yr}} \sim 10^{-10}$$

(1·2) Sources of Gravitational Waves

We have seen that the generation of significant quantities of gravitational radiation requires compact systems of large mass, moving in such a way as to have a rapidly varying quadrupole moment. A method of realising this in the laboratory might be to rotate a massive rod as fast as possible. The maximum obtainable gravitational-wave luminosity, however, would only be of the order 10^{-14}W (Douglass and Braginsky 1979) and there seems little prospect of detecting such a small flux. The detection of gravitational radiation must therefore rely on the existence of astrophysical or cosmological sources. Such

a detection should provide valuable information about events which, by their very nature, are violent or catastrophic.

The possible strengths and rates of occurrence of some likely sources are discussed below. Others, of which we have not been sufficiently clever to think, may well exist.

(1·2(i))Bursts of Gravitational Radiation

One possible source of gravitational radiation is the collapse of massive stars as they finish nuclear burning, leaving either a neutron star or a black hole. Core collapse to a neutron star is probably the trigger for Type II supernovae, but may also occur with relatively little accompanying optical radiation (e.g. Blair 1983). Typical models (e.g. Arnett 1979, Saenz and Shapiro 1979, Wilson 1979 and Eardley 1983) envisage a gradual increase in the size of a degenerate core in stars of $\sim 5M_{\odot}$, followed by a sudden collapse when the mass of this core exceeds the Chandrasekhar limit of $\sim 1{\cdot}4M_{\odot}$. This collapse occurs in approximately one second, with possible bounces of the neutron star having periods of the order of a millisecond. The energy released in this collapse is perhaps $0{\cdot}1M_{\odot}c^2$; much of this is lost in the form of neutrinos and it is still highly uncertain what fraction is radiated as gravitational waves. One reason for this is that gravitational radiation is only emitted if the collapse or bounce is asymmetric, the deviation from symmetry

being particularly difficult to predict astrophysically. In addition, the relevant three-dimensional numerical simulations are exceedingly difficult, even if it is assumed that all of the physics is known.

It can be said, however, that there may well be collapses with efficiences ϵ of conversion of energy into gravitational waves of the order of 1%, or

$$h \sim 10^{-21}(\epsilon/1\%)^{\frac{1}{2}}(10\text{Mpc}/r) \qquad (1\cdot10)$$

where r is the distance to the source (the Virgo cluster is 10Mpc away). The gravitational radiation from these collapses will be emitted in a short burst, possibly with a waveform similar to that shown in fig 1·3. This consists of two components: an initial period during which the radiation is due to the changing mass distribution as the star collapses, followed by a phase of damped oscillations as the neutron star bounces or the black hole "rings" at its quasi-normal mode frequencies (e.g. Detweiler 1979). For a neutron star, the ringing frequency will be ~1kHz with a damping time of ~0·1s, while a black hole will have a characteristic frequency of $\sim 10(M/M_\odot)^{-1}$kHz and a damping time of $\sim 0\cdot3(M/10M_\odot)$ms (though this depends on the angular momentum). This radiation will probably have a frequency spread $\Delta f/f \sim 0\cdot1$ (Eardley 1983).

While the predicted radiation occurs at frequencies which are quite convenient for ground-based detectors (section 1·3), the possibility of detection depends critically on how often such events occur. This remains, however, uncertain. Fig. 1·4 shows (after Blair 1983), an

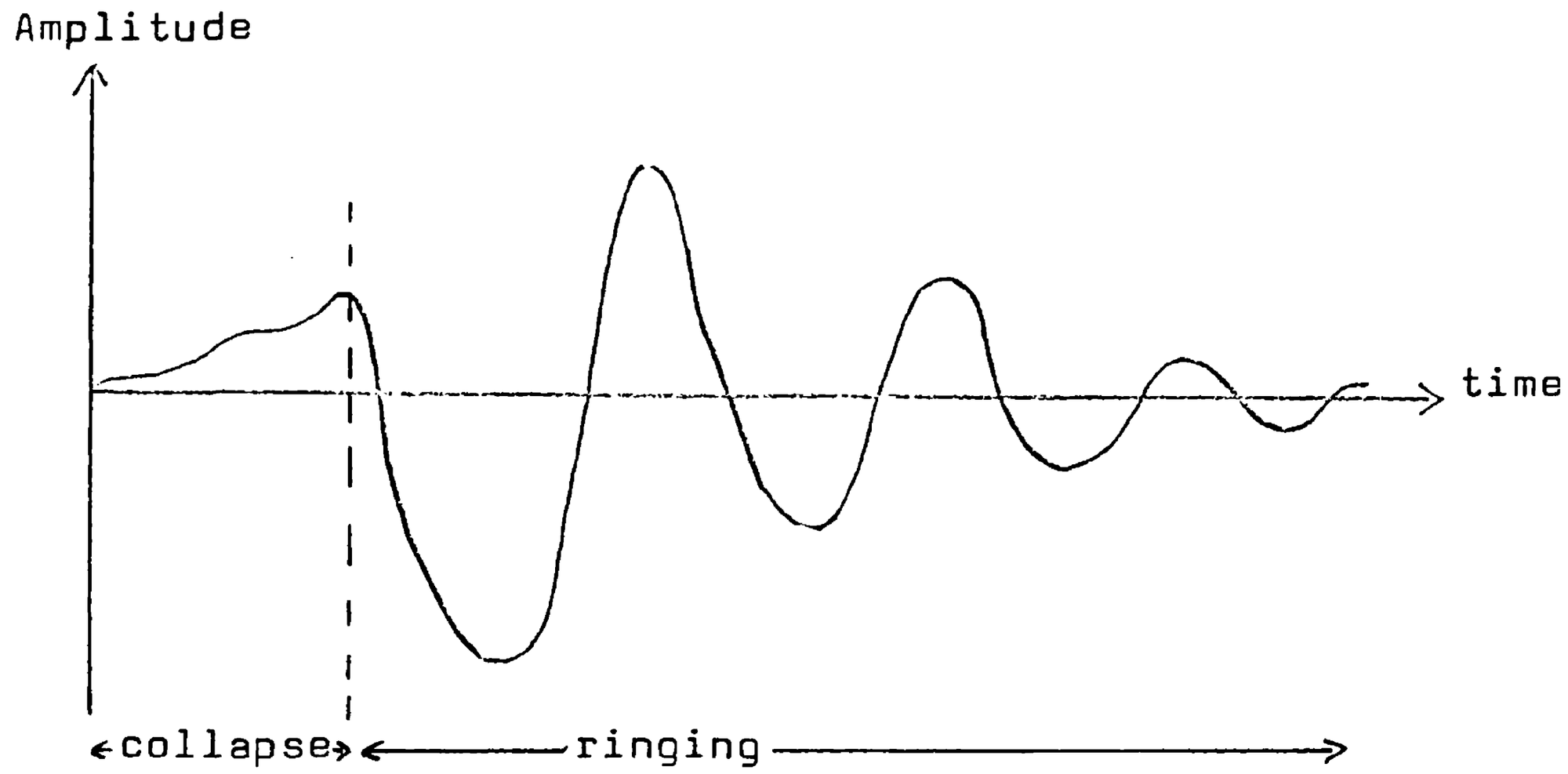

Fig.(1·3): Possible gravitational radiation from a stellar collapse.

estimate of event rate as a function of distance, hence amplitude h (assuming $\epsilon \sim 0{\cdot}1\text{-}1\%$). In order to detect 10 events per year, a sensitivity of at least $h \sim 10^{-21}$ must be achieved.

The gravitational radiation emitted by the anisotropic neutrinos emanating from a supernova may also be significant (Epstein and Clark 1979), of order

$$h \sim 10^{-21}(e_\nu/1)^2(r/10\text{Mpc})^{-1}(E_\nu/0{\cdot}1M_\odot c^2)$$

where e_ν is the eccentricity of the neutrino-emitting ellipsoid and E_ν is the energy of the neutrinos. This radiation will probably occur at 100 Hz or less.

While core collapse probably provides the mechanism for supplying the largest amount of energy to neutron star oscillations, rather more frequent emissions may be due to corequakes or phase changes. Events with an energy

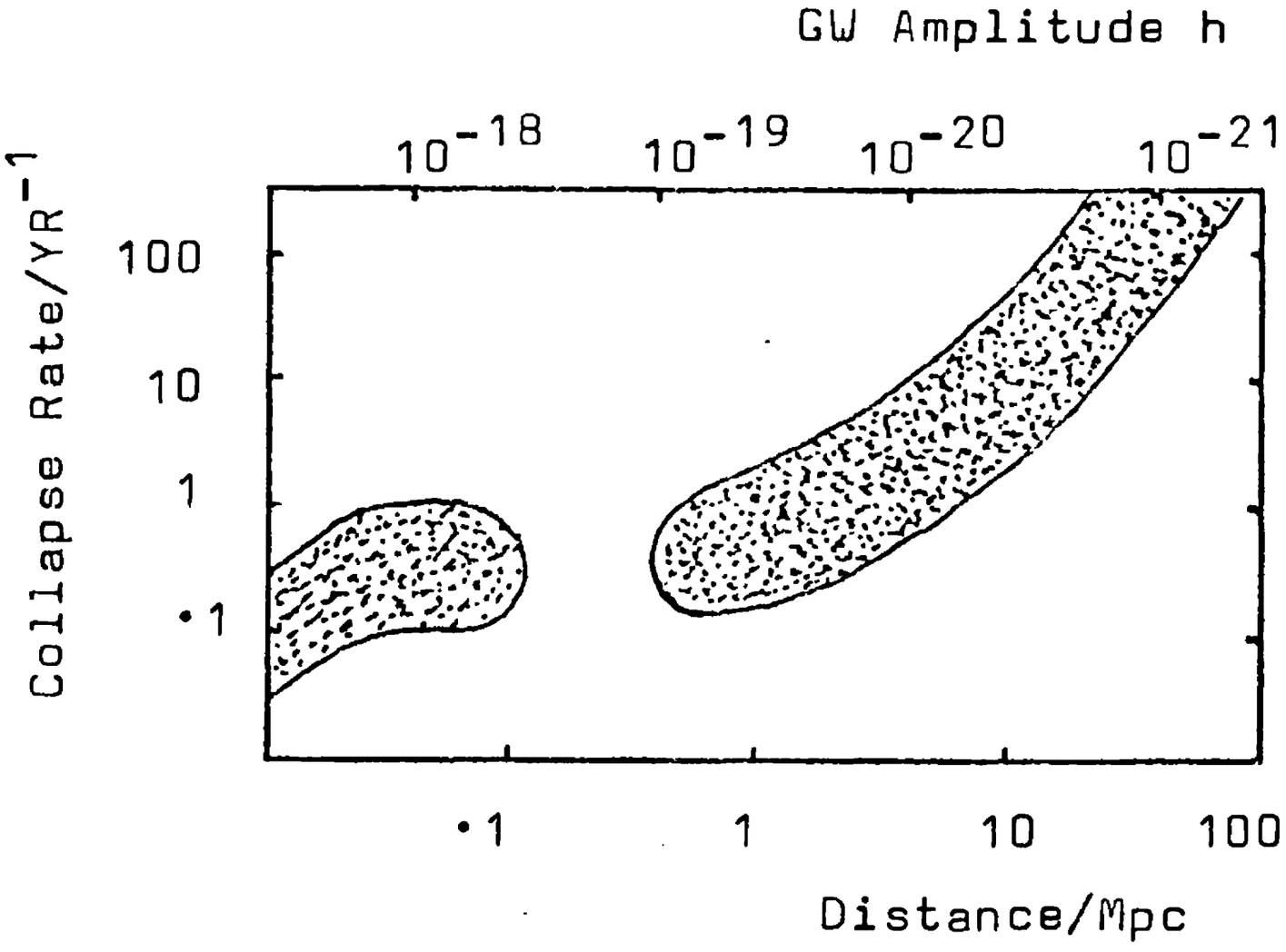

Fig.(1·4): A plot of the estimated rate of occurrence of stellar core collapses against the gravitational-wave amplitude they might produce at the Earth (after Blair 1983).

release of $\Delta E \sim 10^{38}$J might occur once a year within 1kpc (Epstein and Clark 1979), giving a gravitational-wave amplitude of

$$h \sim 3\times10^{-23}(\Delta E/10^{38}\mathrm{J})^{\frac{1}{2}}(f/3\mathrm{kHz})(\tau/1\mathrm{s})^{-\frac{1}{2}}(r/1\mathrm{kpc})^{-1}(\zeta/1)^{\frac{1}{2}}$$

where τ is the damping time (~1s) and ζ the fraction of the energy ΔE deposited in torsional oscillations.

Quite a promising source of gravitational radiation is the collision of compact objects (neutron stars or black holes). Such collisions might result from the orbital decay of binary systems, or take place in a binary formed by the collapse of a rapidly rotating stellar core, or in a very dense star cluster. The attractive feature of these collisions is their relatively high efficiency of conversion of rest mass into gravitational radiation -

probably about 2% (Clark and Eardley 1977, Clark 1979). The radiation is emitted in the form of a "chirp", the signal frequency increasing (to ~1kHz) as the objects spiral together, then decreasing again. Excitation of the neutron star or black hole normal modes will also occur. Again, events occurring in the Virgo cluster will give $h \sim 10^{-21}$, with the rate being highly uncertain. Clark(1979) estimates one event per year for $h \sim 10^{-21}$.

Bond and Carr (see Rees 1983) have considered the coalescence of postulated Population III binaries in the galactic halo. These bursts would occur with a frequency of less than $10(M/10^2 M_\odot)^{-1}$ per year and amplitude

$$h \lesssim 10^{-16}(M/10^2 M_\odot)(R_{halo}/60kpc)^{-1}$$

Zel'dovich and Polnarev (1974) estimated that gravitational bremsstrahlung from close encounters in a postulated dense stellar cluster of $\sim 10^9 M_\odot$ in the galactic centre might produce bursts of $h \sim 10^{-20}$ at frequencies below 1kHz, occurring perhaps once a year.

(1.2(ii))Periodic Sources of Gravitational Radiation

Perhaps the most obvious sources of periodic gravitational radiation are binary star systems. If the two components have masses M_1, M_2 (in $M_\odot$), then the expected amplitude of gravitational radiation is (Douglass and Braginsky 1979)

$$h \approx 2{\cdot}4\times10^{-20}(f/1Hz)^{2/3}(10kpc/r)M_1M_2(M_1+M_2)^{-\frac{1}{3}}g_n^{\frac{1}{2}}(e) \quad ;(1{\cdot}11)$$

where $g_n(e)$ is a function (order unity) of the eccentricity. Some examples of predicted amplitudes are shown in Table 1·1.

TABLE 1·1: The Gravitational Radiation Produced By Some Binary Systems

Nama	$f_g/10^{-6}$Hz	GW Luminosity/10^7W	Distance/pc	GW Amplitude $h/10^{-22}$
i Boo	86	1·1	11·7	51
VW Cep	83	0·7	16·7	30
YY Eri	72	0·4	29	15
RZ Com	68	2·3	64	17
UV Leo	38	0·5	75	13
RT And	37	0·4	54	16
YY Gem	28	0·02	11·7	22
μ Sco	16	51	109	210
V Pup	16	59	520	46
β Per	8·1	0·01	30	21

(After Douglass and Braginsky 1979)

The energy loss due to gravitational radiation causes the orbit of the binary to decay, though this effect is small except in compact binary systems. The good agreement between the predicted and observed orbital changes in the binary pulsar PSR 1913+16 (Taylor and Weisberg 1982) provides impressive indirect evidence for the existence of gravitational radiation.

Rotation of neutron stars or white dwarfs may be a way of generating significant quantities of gravitational radiation. This requires a component of the quadrupole moment not aligned with the spin axis, possibly due to a non-axial magnetic field. The apparent shape may then change (thus generating gravitational radiation) at both the rotational and twice the rotational frequency. If a neutron star has ellipticity ϵ, moment of inertia I and rotational frequency f, the expected amplitude is approximately (Douglass and Braginsky 1979)

$$h \sim 8\times10^{-28}(I/3\times10^{34}\text{kgm}^2)(\epsilon/10^{-6})(100\text{pc}/r)(f/10\text{Hz})^2$$

The value of ϵ is highly uncertain.

Zimmermann (1978,1980; Zimmermann and Szednits 1979) has attempted to calculate the gravitational radiation from the Crab and Vela pulsars, finally concluding that most energy would be radiated at the rotational frequency. Estimates for the Crab were $h_{max}\sim10^{-25}$, $h_{prob}\sim2\times10^{-27}$, $h_{min}\sim10^{-29}$ at 30Hz; for Vela, $h_{max}\sim2\times10^{-24}$, $h_{prob}\sim3\times10^{-26}$ and $h_{min}\sim5\times10^{-28}$ at 11Hz. It is also predicted that the frequency of emission of the gravitational radiation will differ from that of the radio pulses by the pulsar precessional frequency. This may severely handicap the detection of the radiation by high Q tuned bars (section 1·3(ii)).

The upper limits arise from the presumption that no more energy is being radiated than is being lost by the decrease in the spin rate of the pulsar, i.e.

$$L_{GW} \lesssim 4\pi^2 f^2 I(\dot{f}/f) \qquad (1\cdot12)$$

This may be used to place a limit on the radiation emitted by the millisecond pulsar PSR 1937+214 (Backer et al 1982). While it might be expected that this object would be a strong gravitational-wave emitter, it has an exceptionally low slowdown rate of $\dot{P}/P = \dot{f}/f \sim 10^{-19} s^{-1}$ (Ashworth et al 1983, Backer et al 1983). If it is assumed that the pulsar has a mass of $1\cdot4M_{\odot}$, radius R ~10km, uniform density and a distance of 2kpc, the relations (1·9) and (1·12) may the be used to limit the amplitude at the Earth to

$$h \sim \left(\frac{2GMR^2}{5c^3r^2}(\dot{P}/P)\right)^{\frac{1}{2}} \sim 10^{-28} \qquad (1\cdot13)$$

Neutron stars rotating faster than ~1·5ms may not, however, radiate mainly at harmonics of the rotation frequency. For in this circumstance, radiation reaction may cause travelling wave modes in the neutron star, which rotate in <u>opposite</u> senses with respect to inertial space and the star, to <u>grow</u> with respect to the star(Papaloizou and Pringle 1978). It is then these modes which radiate most strongly; for example, a star with rotational period P ~1·5ms would have its gravitational radiation peaked at f ~6kHz.

(1·2(iii))A Stochastic Background of Gravitational Radiation

A stochastic background of gravitational radiation may be produced by the superposition of many uncorrelated sources. One likely source population consists of galactic binaries; in particular, the large class of close binaries known as W Ursae Majoris stars. Mironovskii (1966) estimated the flux from the $\sim 10^8$ such stars in our galaxy as producing an amplitude spectral density of

$$h \sim 10^{-17}\ \mathrm{Hz}^{-\frac{1}{2}}$$

in a bandwidth $\Delta\nu \sim 5\times10^{-5}$Hz around $\nu \sim 8\times10^{-5}$Hz.

A substantial number of stars may have formed early in the history of the Universe; these would now constitute a Population III in the galactic halo (White and Rees 1978). Production of a stochastic gravitational wave background might then occur via stellar collapse, emission in binaries or compact binary coalescence (Rees 1983). If the objects formed at a redshift z_f and have a mass M, then the radiation would have a frequency of

$$\nu \sim (M/10^4 M_\odot)^{-1}(1+z_f)^{-1} \qquad (1\cdot14)$$

If Ω_r is the fraction of the critical density in Population III remnants, then the resultant fraction in broad band ($\Delta\nu\sim\nu$) gravitational waves is

$$\Omega_g = \Omega_r \varepsilon/(1+z_f) \qquad (1\cdot15)$$

The corresponding wave amplitude is

$$h = 5\times10^{-19}\Omega_g^{\frac{1}{2}}(\nu/\mathrm{Hz})^{-1} = 5\times10^{-19}(\nu/\mathrm{Hz})^{-1}\left(\frac{\Omega_r\varepsilon}{1+z_f}\right)^{\frac{1}{2}} \quad ;(1\cdot16)$$

Some of the constraints on the value of $\Omega_r(M)$ are shown in fig 1·5 (from Rees 1983).

As an example, consider a population of $10M_\odot$ remnants forming at $z_f \sim 10$ with $\Omega_r \sim 10^{-3}$ and $\varepsilon \sim 0\cdot1$; the resultant

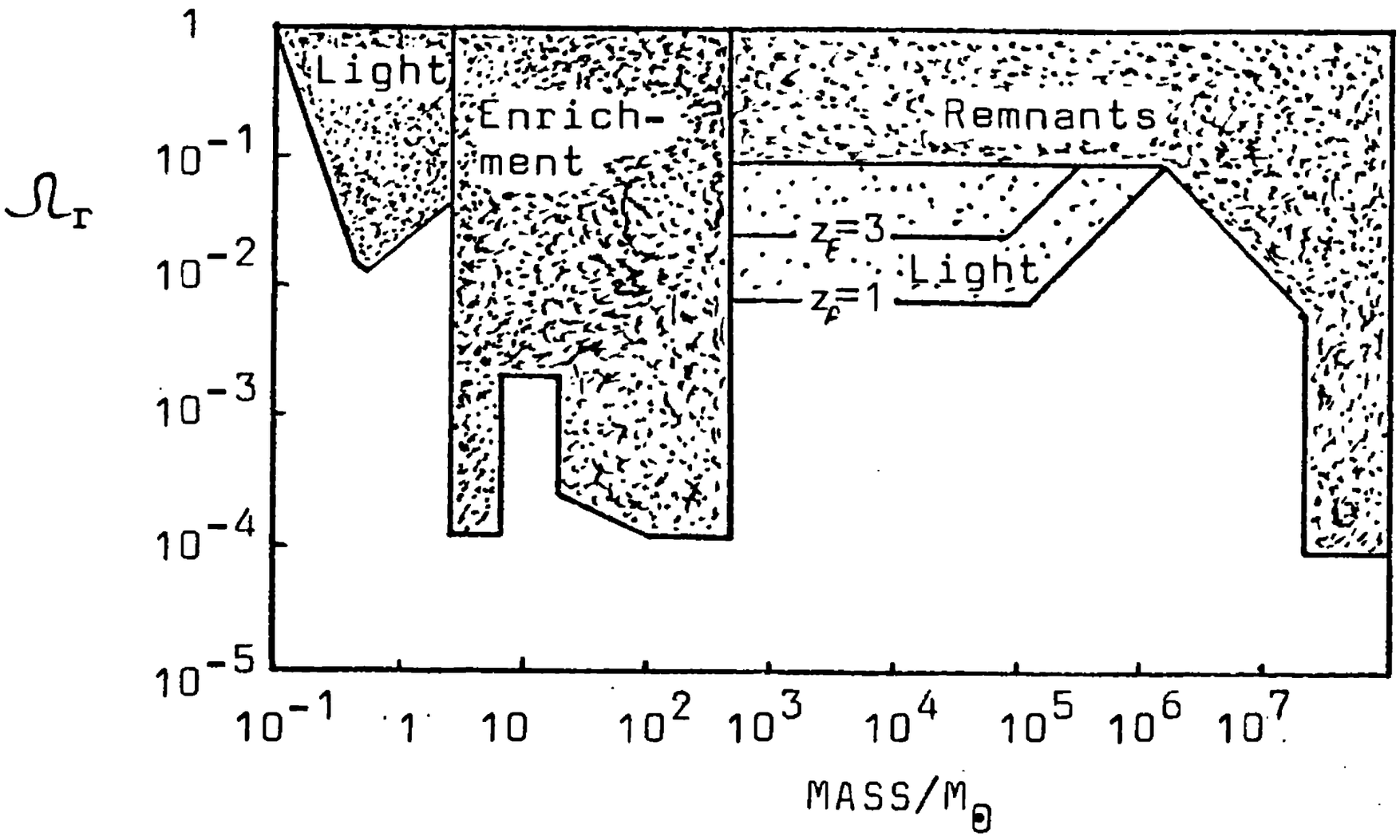

Fig 1·5: Constraints on the density Ω_r of Population III remnants, as a function of the mass of the remnants. The basis for each limit is indicated (Rees 1983).

amplitude would be $h \sim 10^{-23}$, peaked at ~100Hz. If $10^3 M_\odot$ remnants formed at the same redshift with $\Omega_r \sim 10^{-2}$, the radiation might have $h \sim 5\times10^{-21}$ at 1Hz.

A background of gravitational radiation may also be produced by inhomogeneities in the very early universe. The spectrum would not, in general, be thermal but would depend on the fluctuation spectrum, equation of state and subsequent history. Grishchuck (1977) considered early quantum fluctuations while Starobinsky (1979) analysed the effect of an inflationary phase, predicting a spectrum of form

$$h \sim 3\times10^{-21} s/\nu \qquad (1\cdot17)$$

where s is a parameter of the Grand Unified Theories involved. So the primordial gravitational-wave background,

unlike the microwave background, may not be restricted to very short wavelengths. Its detection would provide information about early stages of the universe.

Quite a strong limit may be placed on the possible strength of a primordial gravitational-wave background by requiring its energy density not to be sufficiently large to affect the expansion rate, hence the helium abundance, at the time of nucleosynthesis. This limits Ω_g to $\sim 10^{-4}$, or $h \sim 5\times10^{-21}(\nu/\mathrm{Hz})^{-1}$. Carr (1980) reviews the constraints in detail.

Some of the likely source strengths are summarised in fig 1·6, taken from Thorne (1980).

(1·3)Detectors of Gravitational Radiation

(1·3(i))Principles

It was seen in section 1·1 that the action of a gravitational wave is to flex the spacetime between different masses, thus changing their separation. This effect may also be regarded as the production of a force F^j, a viewpoint especially useful when the masses are not free. The force between masses m separated by a distance x^j which is small compared with a wavelength is just (cf. 1·1)

$$F^j = m\ddot{x}^j = \tfrac{1}{2}m\ddot{h}_{jk}x^k \qquad (1\cdot18)$$

It is the change in apparent dislacement produced by these forces that all detectors of gravitational radiation hope to detect. The difficulty of the task is indicated by the likely sizes of h discussed in section 1·2.

There are at least two different approaches to the

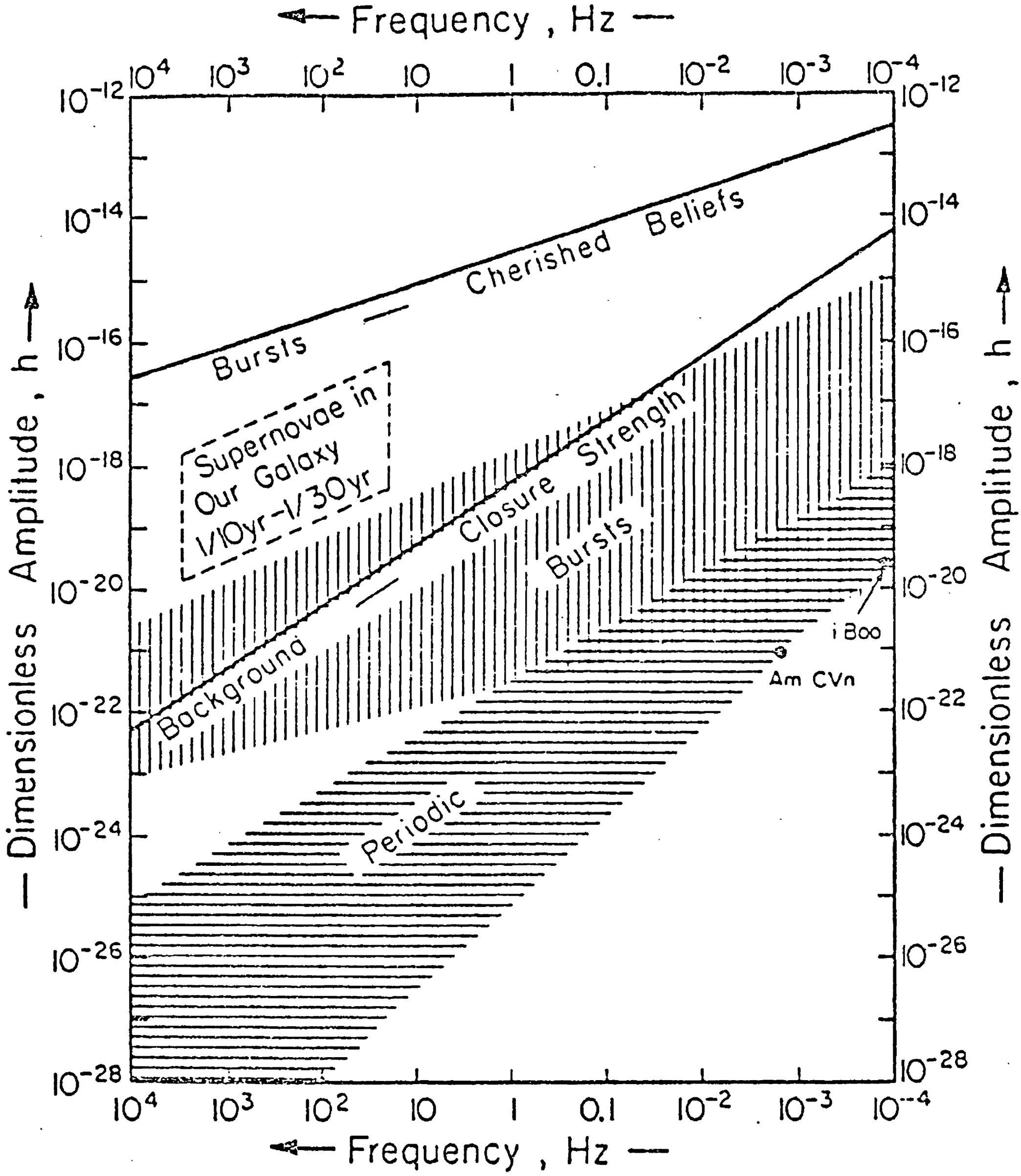

Fig 1·6: A summary of the likely strength of gravitational radiation from various astrophysical sources, taken from Thorne (1980).

construction of a gravitational wave detector. One, perhaps the most obvious, is to attempt to monitor the separation of free masses. This has the advantage of possibly being sensitive to a broad range of gravitational wave frequencies, with an associated increase in the probability of finding narrow-band sources and in the information concerning the shape of the waveform; it would be possible to accurately time the arrival of pulses. The separation of free masses may be made large, enhancing the effect of the gravitational wave. The other approach is to make the detector resonant by effectively joining the test masses with a spring. A continuous gravitational wave at the resonant frequency then produces a larger displacement, while the effect of an impulse persists for much longer. Both of these effects would seem to facilitate the achievement of a high sensitivity, at the cost of narrowing the bandwidth. The size of a resonant detector is limited by the speed of sound in the spring (for a given resonant frequency); furthermore, losses in the spring may limit the performance. It seems probable that the two approaches are complimentary. Examples of each type of detector are discussed in sections 1·3(ii)-1·3(v), where it will be seen that the quest for high sensitivity is a battle against competing noise sources which threaten to overwhelm the gravitational-wave signal.

If it is assumed that a detector (with a given sensitivity and bandwidth) has been constructed, the ways in which particular types of gravitational radiation might be detected (and source information extracted) must be

considered. For example, while the minimum detectable size of a periodic signal may be decreased by increasing the integration time of the measurement ($h_{min} \propto \tau_{int}^{-\frac{1}{2}}$), such integration must take account of the changing frequency of the signal due to the Doppler shift as the Earth revolves and rotates (see,also, Appendix 1). Conversely, if a periodic signal is detected, then observation of the annual variation of its frequency will enable the source position to be determined (for the pulsar case see e.g. Smith 1977). The determination of the direction of origin of bursts of gravitational radiation requires a comparison of arrival times by at least three separated detectors. A stochastic background of gravitational radiation could be detected by cross-correlating the outputs from two or more different detectors, thus rejecting any noise not common to the detectors ($h_{min} \propto (\Delta f \tau_{int})^{-\frac{1}{4}}$; see Hough et al 1975 for an example of the application of this technique).

(1·3(ii))Weber Bars

The first laboratory detectors for gravitational radiation, proposed and constructed by Joseph Weber (1960, 1970a,b,c), were large cylindrical bars of aluminium with piezoelectric crystals glued to their surface in order to sense their vibrations. The ensuing controversy over whether his reported detection of gravitational wave pulses was real stimulated the rapid development of gravitational wave detectors. The status of bar detectors has been reviewed by Weiss (1979) and Blair (1983), from where much of the material in this section has been taken.

A gravitational wave of amplitude h incident on a massive cylinder will excite its odd normal modes (order n):

$$(\Delta l/l)_{bar} \approx Ch/3n^2 \qquad (1\cdot19)$$

The proportionality constant C is approximately unity for a short burst of radiation (but depends on the pulse shape) and of order of the quality factor Q of the resonance for continuous radiation (e.g. Braginsky 1983). The motion may be sensed with a transducer, followed by an amplifier and filter to increase the resultant electrical signal. A gravitational wave will only be detectable if the final signal it produces is larger than that due to amplifier noise or motion of the bar produced by thermal noise, back-reaction of the amplifier noise via the transducer, acoustic or seismic noise, cosmic rays or electromagnetic pulses. If the bar is suspended in a vacuum chamber with appropriate low-pass acoustic filters (e.g Blair 1983, Michelson 1983) then only the fluctuations due to thermal and transducer/amplifier noise should remain.

Each normal mode of the antenna contains a thermal energy kT. Energy exchange between modes occurs at the damping timescale τ_d, which for a mode of angular frequency ω is $\tau_d = 2Q/\omega$. If the energy of the mode is measured in a time τ_m which is short compared with the damping time, the change in energy expected from thermal noise is

$$\Delta E = kT(\tau_m/\tau_d)$$

So a long damping time (high Q) and short measuring time minimise the effect of thermal noise.

Series amplifier noise produces an (energy) output which increases linearly with <u>decreasing</u> measuring time (i.e.

increased bandwidth), while parallel amplifier noise acts back to the bar through the transducer, producing an output which increases with <u>increasing</u> measuring time. There is thus an optimum measuring time τ_{mo}, determined by the relative magnitudes of the thermal plus backreaction and series amplifier noises.

An important measure of the coupling between the bar and the transducer is the parameter β, the proportion of the acoustic energy that can be extracted electrically in one cycle (Gibbons and Hawking 1971). If β is small, the gravitational wave signal takes a long time to appear in the transducer, increasing the importance of thermal fluctuations. If a detector is dominated by thermal noise (as all current detectors are), the optimum integration time for pulses of gravitational radiation is (e.g. Weiss 1979)

$$\tau_{mo} = (T_a Q/2T\beta\omega^2)^{\frac{1}{2}} \qquad (1\cdot20)$$

where T_a is the amplifier noise temperature. The resultant strain sensitivity, for unpolarised incident radiation is

$$\begin{aligned}\Delta l/l &= \pi(15/16Mv^2)^{\frac{1}{2}}(32kT.kT_a/\beta Q)^{\frac{1}{4}} \\ &= 3.2\times10^{-17}(M/1\ \text{ton})^{-\frac{1}{2}}(T_{eff}/1K)^{\frac{1}{2}}(v/5\text{kms}^{-1})^{-1} \\ &\qquad \times(\beta/10^{-3})^{-\frac{1}{4}}(Q/10^6)^{-\frac{1}{4}} \qquad (1.21)\end{aligned}$$

Here M is the mass of the bar, v is the velocity of sound in the bar and $T_{eff} = (T_a T)^{\frac{1}{2}}$. Attainment of a good sensitivity thus requires a large antenna with a high Q and sound velocity, cooled to a low temperature and used in conjunction with a high β transducer and low-noise amplifier.

If the factor $Q\beta/T$ is made sufficiently large for

backreaction noise to dominate over thermal noise, the optimum integration time for pulses becomes (Giffard 1976, Weiss 1979)

$$\tau_{mo} = 1/\sqrt{2}\beta\omega \qquad (1\cdot22)$$

and the minimum detectable energy is

$$\Delta E = 4\sqrt{2}kT_a \qquad (1\cdot23)$$

Now quantum mechanics (via spontaneous emission) places a lower limit on the noise temperature of a linear amplifier (Heffner 1962):

$$T_a \gtrsim 2\pi\hbar f/k\ln 2$$

So a quantum-limited amplifier would enable detection of an energy change (Giffard 1976)

$$\Delta E = 8\pi\sqrt{2}\hbar k f/\ln 2 \qquad (1\cdot24)$$

corresponding to a minimum detectable strain

$$\Delta l/l \approx (\hbar\omega/Mv^2)^{\frac{1}{2}}$$

$$= 2\times10^{-20}(M/1\ \text{ton})^{-\frac{1}{2}}(v/5\text{kms}^{-1})^{-1}(f/1\text{kHz})^{\frac{1}{2}} \qquad (1\cdot25)$$

This latter result is equivalent to the "standard quantum limit" on an observable displacement set by the Heisenberg uncertainty principle (see, for example, Thorne et al 1979). Bearing in mind likely pulse strengths of $h\sim10^{-21}$, this limit appears to be very severe. It does seem, however, that higher sensitivies may be achieved by the use of "quantum non-demolition techniques"—so-called because they attempt to measure the amplitude of vibration of the bar without "demolishing" its quantum state (Caves et al 1980). For example, "back-action-evading" measurements attempt to monitor only one phase of the bar's oscillation, the uncertainty resulting from the measurement appearing in the other phase. The amplitude of one phase may therefore, in principle, be measured with arbitrary

accuracy. The practical implementation of such a technique will probably be necessary if pulses of gravitational radiation are to be detected by Weber bars.

For continuous gravitational radiation, the minimum detectable amplitude is (Weiss 1979)

$$h \gtrsim \left[(2/\tau_m M\omega^3 l^2)(4kT/Q + 4kT_a\beta + 8kT_a/\beta Q^2)\right]^{\frac{1}{2}} \qquad (1\cdot26)$$

In this case, a weakly coupled transducer ($\beta \approx \sqrt{2}/Q$) minimises the combined effect of backreaction and series amplifier noise. The sensitivity always improves with increasing Q, since this increases the signal size (as long as the gravitational radiation remains within the bandwidth of the detector). The optimum sensitivity of the detector is achieved when

$$T = T_a(QL) = 2\pi hf/k\ln 2$$

Since $T_a(QL) \sim 7\times10^{-8}$K at 1kHz, this does not look practical within the near future.

If the output from two detectors is to be cross-correlated in a search for a stochastic background of gravitational radiation, it is most efficient to include a filter to counteract (or "whiten") the resonance in order to increase the bandwidth. The resultant sensitivity is (Weiss 1979)

$$\Delta l/l \gtrsim \left\{\left[ml^2\omega^3(\Delta f\tau_m)^{\frac{1}{2}}\right]^{-1}\left[4kT/Q + 4kT_a + 8kT_a/\beta\right]\right\}^{\frac{1}{2}}; \qquad (1\cdot27)$$

This also places a severe demand on the performance of the transducer-amplifier combination, the reason why Hough et al (1975) used a split bar with high β (as suggested by Gibbons and Hawking 1971) for their search using this technique.

All of the currently operating Weber bar detectors

are a long way from achieving a quantum-limited sensitivity; they are all limited by thermal noise.

There have been two contrasting approaches to the problem of improving the thermal noise-limited sensitivity (cf. 1·21). One, typified by the detector at Stanford (Michelson 1983), is to build very large (~5 tonne) bars from aluminium, which has a modest Q (~5×10^6 for Al 6061 or ~7×10^7 for Al 5056) and speed of sound (5kms^{-1}). The alternative (e.g. Braginsky 1977) is to much smaller (~30kg?) crystals of sapphire or silicon which can have very high Q (~3×10^9) and sound velocity (~9kms^{-1}). Both types of bar are cooled to as low a temperature as possible — 4K at present and perhaps 0·1K in the near future.

Their performances when limited by thermal noise may not be too dissimilar if large enough high Q crystals can be grown, but the large detectors have the advantage of having a smaller quantum limit.

It is evident from the material discussed here (cf. 1·21) that the attainment of a high sensitivity with a bar detector requires an excellent transducer-amplifier combination. Weber used piezoelectric transducers (PZTs) and FET amplifiers, but PZTs are lossy and spoil the Q of the resonance, whilst FET amplifiers are some 10^4 times noisier than the quantum limit. Indeed, the poor matching of the transducers and "high" noise of the amplifiers seems likely to remain a severe problem with bar detectors.

An example of a modern passive transducer, which has no power gain, is the superconducting inductive readout coupled to a SQUID amplifier; such a system is used at Stanford (Michelson 1983). Here, the motion of the bar

modulates the inductance L of a superconducting coil carrying a persistence current I; since flux is conserved, LI is constant and I changes. The SQUID then acts as a current amplifier.

Another class of transducers may be called active or parametric (e.g. Blair 1983). These have an external power source and intrinsic power gain. Most parametric transducers use a resonant cavity, the characteristic frequency of which is modulated by the movement of the bar, producing sidebands around this (high)frequency which are then further amplified. This technique allows the use of high frequency, low noise amplifiers. A great similarity between these microwave transducers and the laser interferometers will become apparent.

The most sensitive currently operating bar detector is that at Stanford, a 5 ton aluminium bar cooled to 4K, which has a noise temperature of 20mK — equivalent to $h \sim 10^{-18}$ for pulses (Michelson 1983). All other bars are still at earlier stages in their development, attempting to overcome considerable technological problems. Improvement of this sensitivity will require further cooling, higher transducer coupling and lower noise amplifiers. If an improvement by a factor of over a hundred can be acheived, then the quantum limit will have to be bypassed.

Much of the sensitivity of a bar detector is bought at the cost of narrowing the bandwidth ($\Delta f \sim \pi\omega/Q$) and so losing information on the waveform shape or pulse arrival time. This does not matter, however, when observing a continuous sine wave. Tuned, high Q bar detectors are therefore appropriate for searching for gravitational

radiation from pulsars. The Tokyo group have placed a limit of $h \gtrsim 10^{-19}$ on the radiation at 60·2Hz from the Crab pulsar (Hirakawa et al 1977), whilst Hough et al (1983) at Glasgow found no radiation at $h \sim 10^{-20}$ from the millisecond pulsar PSR 1937+214 (see Appendix 1). The discovery of more fast pulsars (Boriakoff et al 1983) will further encourage such experiments.

It is clear that problems with thermal noise, narrow bandwidth and the quantum limit will severely hamper the detection of gravitational radiation with Weber bars.

(1·3(iii))Laser Interferometers

A promising technique by which gravitational waves might be detected by monitoring their effect upon nearly free masses is that of laser interferometry (reviewed by Weiss 1979 and Drever 1983). The apparent change in the separation of two masses caused by a gravitational wave is converted into a fluctuation of the phase of a laser beam, which in turn changes the intensity of an interference pattern (see fig 1·7). It is desirable to make a differential length measurement between two perpendicular arms since this retains the sensitivity to gravitational waves propagating normally to the plane of the interferometer (cf. fig 1·1) while reducing the effect of various changes in the laser beam, especially frequency fluctuations. These other noise souces will be discussed in Chapters 2 and 3.

The phase change in each arm may be increased (as in the original Michelson-Morley experiment) by reflecting

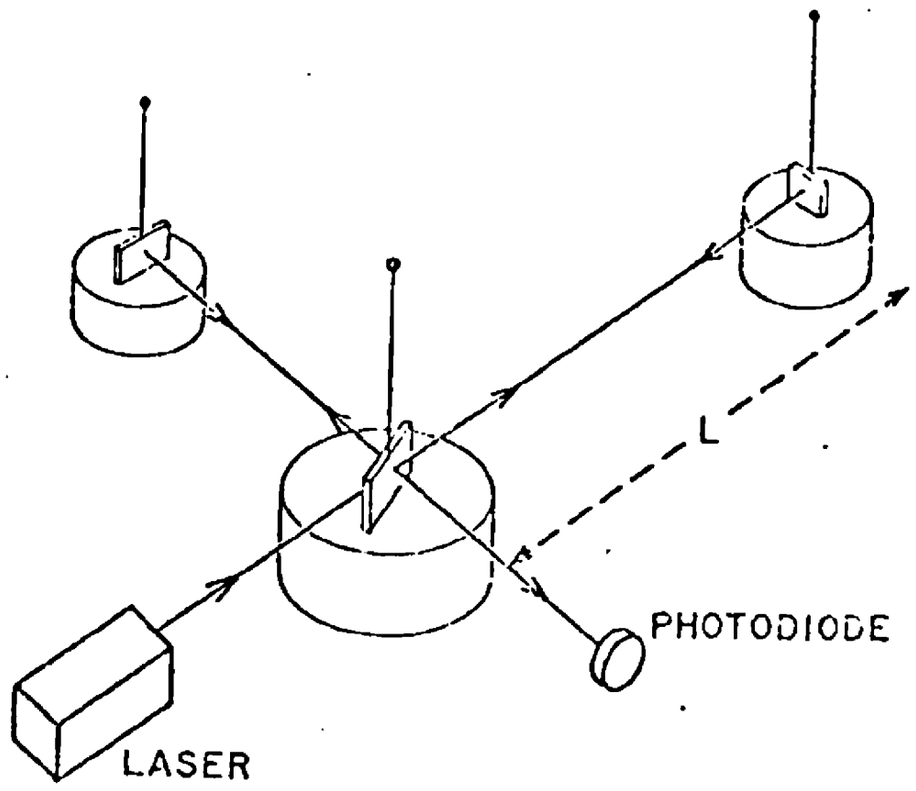

Fig 1·7: An illustration of the principles of a laser interferometer gravitational-wave detector. Test masses are suspended so that they appear nearly free to a gravitational wave, the effect of which is then to cause opposite length changes in the two arms of the interferometer. The relative phase fluctuation of the laser beams in the two arms then changes the light intensity seen by the photodiode.

the beam backwards and forwards many times. If the total time spent in bouncing by a beam is τ_s (the storage time) and the incident gravitational wave is

$$\Delta l/l = \tfrac{1}{2}h\exp(i\omega_g t)$$

then the resultant phase change is

$$\Delta\phi = \tfrac{1}{2}ckh\int_{t-\tau_s}^{t}\exp(i\omega_g t)\,dt$$

$$\Delta\phi = (k\lambda_g h\exp(i\omega_g t)/4\pi i)(1-\exp(-i\omega_g\tau_s)) \qquad (1.28a)$$

$$\Delta\phi = (k\lambda_g/2\pi)h.\exp(i\omega_g(t-\tau_s/2))\sin(\pi\tau_s/\tau_g) \qquad (1\cdot28b)$$

where $k = 2\pi/\lambda$ and τ_g is the period of the gravitational

wave. For storage times much smaller than τ_g, this reduces to

$$\Delta\phi = \tfrac{1}{2}hk\lambda_g(\tau_s/\tau_g)\cos\omega_g t = hkNl\cos\omega_g t \qquad (1\cdot29)$$

where l is the length of one arm of the interferometer and N is the number of bounces (there and back) of the beam. So for effective arm lengths small compared with the wavelength of the gravitational radiation, the optical phase change increases linearly with the storage time. It does not, however, increase indefinitely, but is a maximum when the storage time is equal to half a gravitational wave period. In this case, the phase change produced in one arm is

$$\Delta\phi(\text{opt}) = (hk\lambda_g/2\pi)\sin\omega_g t = h(\lambda_g/\lambda)\sin\omega_g t \qquad (1\cdot30)$$

If no modulation techniques are used (see Chapter 2), the intensity change produced by this phase change when the beams from the two arms interfere is a maximum half way up a fringe; in this case, since the phase difference is $2\Delta\phi$,

$$\delta I/I_{max} = 4\Delta\phi \qquad (1\cdot31)$$

Now the smallest detectable intensity change is fundamentally limited by the counting statistics of the detected photons: if N photons are detected, the uncertainty is $\sqrt{N}$ (e.g. Caves 1981). If the signal produced by the gravitational wave is to be larger than that due to this shot noise in the photodiode current,

$$4\eta I_{max}\Delta\phi > (e\eta I_{max}\Delta f)^{\frac{1}{2}} \qquad (1\cdot32)$$

where $\eta = e\lambda\xi/2\pi\hbar c$ is the power to current efficiency and ξ is the quantum efficiency of the photodiode, with e being the electronic charge. This gives the result

$$\Delta\phi > \left(\frac{\pi\hbar c\Delta f}{8\lambda\xi I_{max}}\right)^{\frac{1}{2}} \qquad (1\cdot33)$$

For example, if $\lambda = 5\times10^{-7}$m, $\zeta = 0{\cdot}4$ and $I_{max} = 1$W,

$$\Delta\phi_{min} \sim 2{\cdot}5\times10^{-10}\,\text{rad}/\sqrt{\text{Hz}}$$

So the minimum detectable gravitational-wave amplitude is

$$h_{min} = \frac{(\lambda/\lambda_g)(\pi\hbar c\Delta f/8\lambda\zeta I_{max})^{\frac{1}{2}}\exp(i\pi\tau_s/\tau_g)}{\sin(\pi\tau_s/\tau_g)} \qquad (1{\cdot}34)$$

If $\tau_s \ll \tau_g$, this reduces to

$$h_{min} = (\lambda\hbar c\Delta f/32\pi\zeta I_{max}N^2l^2)^{\frac{1}{2}} \qquad (1{\cdot}35)$$

The final light intensity and the number of bounces are evidently not independent of each other: if the mirrors have reflectivity R^2, the intensity after n reflections is $I_n = I_0R^{2n}$, where I_0 is the incident power. The sensitivity (1·34) is then optimised when

$$\tan(\pi\tau_s/\tau_g) = \tan(\pi l(n+1)/c\tau_g) = 2\pi l/c\tau_g(1-R^2) \qquad (1{\cdot}36)$$

In the case of $\tau_s \ll \tau_g$, this gives

$$(n+1)_{opt} = 2N_{opt} = 2/(1-R^2) \qquad (1{\cdot}37)$$

The final intensity is then $1/e^2$ of that incident, giving an (optimum) sensitivity of

$$h_{min} = \left(\frac{e^2\lambda\hbar c\Delta f}{32\pi\zeta I_0(n+1)^2l^2}\right)^{\frac{1}{2}} = e(1-R^2)\left(\frac{\lambda\hbar c\Delta f}{32\pi\zeta I_0l^2}\right)^{\frac{1}{2}} \qquad (1{\cdot}38)$$

As an example, consider the case of a detector of length l = 10 m, with an incident power I_0 = 1W and mirrors of reflectivity $R^2 = 99{\cdot}7\%$; the minimum sensitivity is then

$$h_{min} = 1{\cdot}6\times10^{-20}\,/\sqrt{\text{Hz}}$$

On the other hand, if losses are negligible then the optimum storage time is just $\frac{1}{2}\tau_g$, giving

$$h_{min} = (\lambda/\lambda_g)\left(\frac{\pi\hbar c\Delta f}{8\lambda\zeta I_0}\right)^{\frac{1}{2}} = f_g\left(\frac{\pi\lambda\hbar\Delta f}{8\zeta cI_0}\right)^{\frac{1}{2}} \qquad (1{\cdot}39)$$

With I_0 = 1W, the resultant sensitivity at f_g = 1 kHz is

$$h_{min} = 4\times10^{-22}\ /\sqrt{Hz}$$

For observation of pulses of gravitational radiation, the bandwidth Δf might be ~1 kHz; this would give

$$h_{min} = 10^{-20}$$

This storage time limit could be attained with 300 bounces if the arm length is 1 km. Some possible ways of further improving the potential sensitivity are discussed in Chapter 6.

The laser beam may be regarded as an active transducer, with the fluctuations in the photon number playing the role of series noise. Backreaction noise is provided by the radiation pressure fluctuations due to the random nature of the paths taken by the photons at the beamsplitter. As for bars, minimisation of the total noise leads to the quantum limit (Edelstein et al 1978; Caves 1981):

$$h_{min} = (8\hbar\tau_m/Ml^2)^{\frac{1}{2}} \qquad (1\cdot40)$$

with M the mass of the test masses and τ_m the measuring time. With τ_m = 1 ms, l = 1 km and M = 10 kg, this gives

$$h_{min}(QL) = 3\times10^{-22}$$

The incident power required to achieve this sensitivity is

$$I_0 = Mc\lambda/\pi(n+1)^2\tau_m^2 \qquad (1\cdot41)$$

With the same parameters as before, the required incident power is $I_0 \approx 3$ kW. Since this is beyond current technology, the fundamental limit to the sensitivity of such interferometers will be set by photon counting statistics. It should be emphasised that there are many other noise sources present, which may be larger than the photon noise

(just as transducers/amplifiers for bars are not quantum limited). The identification and reduction of these other noise sources is a major task, and constitutes a large part of this thesis. All of these other noise sources are practical rather than fundamental: they can be suppressed by appropriate design and construction of the detector.

Pioneering work on laser interferometers for the detection of gravitational radiation was carried out by Forward (Moss et al 1971, Forward 1978) and Weiss (1972). The former demonstrated, with a low power He-Ne laser, the possibility of attaining a sensitivity near the photon noise limit. The first serious attempts, however, at constructing a gravitational wave detector were started at Munich (e.g. Billing et al 1981) and Glasgow (e.g. Drever et al 1981) in 1975, followed by Caltech in 1979; there is also a group at MIT. These detectors all use Ar^+ lasers which, while noisy, give the largest power output of available CW lasers: an unaltered commercial laser may give several watts of single-line power at 514·5 nm.

While all of these prototype detectors are fundamentally similar, there are also significant differences in approach. Perhaps the most obvious is the nature of the optical system for arranging multiple reflections in each arm of the interferometer. The system proposed by Weiss (1972) and implemented at MIT and Munich is to use an optical delay line in which the beam simply bounces backwards and forwards between spherical mirrors, entering and emerging through a hole in one mirror (see fig 1·8). This has the merit of simplicity. It does, however, require large mirrors, for the spots are all separate - if

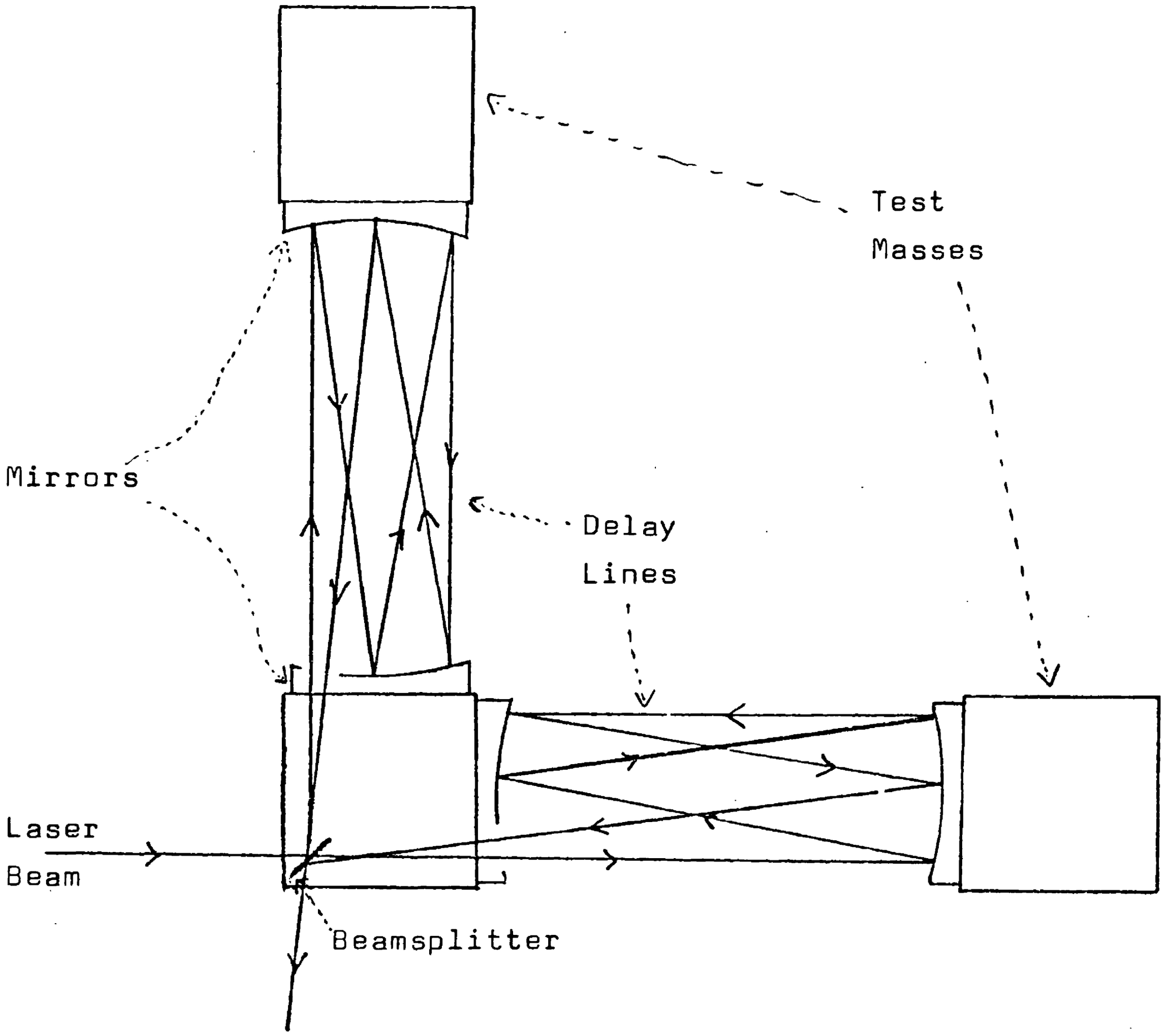

Fig 1·8: A schematic diagram of an interferometer for the detection of gravitational radiation which uses optical delay lines to increase the storage time. The light may be reflected many times in each arm of the interferometer before emerging through the hole in the entrance mirror of the delay line.

the total optical path length is to be 100 km, the minimum mirror diameter is 0·75 m (Rudiger et al 1982). The alternative system, developed at Glasgow (Drever et al 1980, Drever 1983) and also adopted at Caltech, is to use resonant optical cavities in the arms of the interferometer (see fig 1·9). The laser beam enters each arm through a mirror of finite transmission, bouncing up and down with the spots coincident on the two mirrors. On each traverse, a fraction of the beam emerges from the cavity and may be interfered with either the beam reflected directly off the input cavity mirror or with the beam from the other cavity. The cavity system is not only more complicated to analyse than the delay lines, it is also more difficult to operate, for the relative lengths of the laser light and the cavities must be accurately adjusted so that the cavities resonate. Conversely, the cavities provide a convenient length standard against which to stabilise the laser. Their great advantage, however, is that they enable relatively small mirrors to be used: with an arm length of 1km, mirrors of diameter 10cm would give diffraction losses of less than one part in 10^5. The performance of a detector based on resonant optical cavities is extensively analysed in Chapter 2.

The great feature of laser interferometers is that they allow the test masses to be separated by a large distance, thus reducing the importance of stochastic forces on each mass and allowing a broad-band detector of potentially good sensitivity to be constructed. Since the mechanical resonances of the test masses may be arranged to lie at a frequency outside the range of interest for the detector,

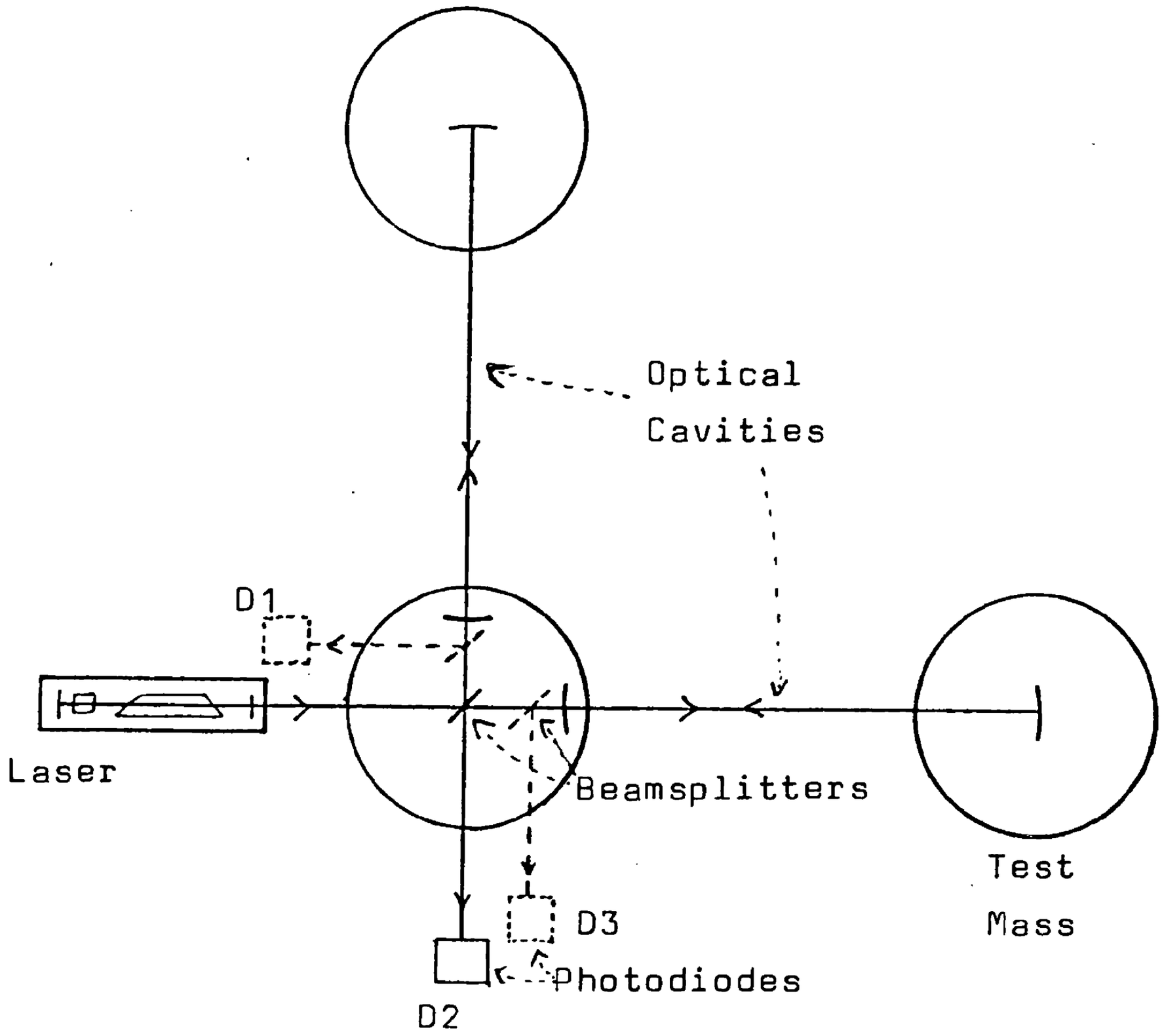

Fig 1·9: Diagram of an optical cavity gravitational wave detector. The multiple beams in the two arms are coincident, with a fraction leaking out of the input mirror at each pass. The phase of the beam emerging from one of the cavities may be determined by interfering either the two beams from the cavities (diode 2) or the cavity beam with the light directly reflected off the input cavity mirror (at diodes 1 and 3). The beamsplitters for diodes 1 and 3 would typically sample 10% of the light intensity.

the effect of thermal noise may be further reduced and the need for cryogenic systems avoided. They have great potential as detectors of gravitational radiation.

(1·3(iv))Electromagnetically-Coupled Detectors in Space

At low frequencies, $f \lesssim 30$ Hz, it becomes difficult to isolate ground-based detectors from seismic noise and other noise sources such as gravity-gradient fluctuations become important (see Chapter 2). These problems would be avoided if the test masses of the detector were widely separated spacecraft.

The only such experiments so far carried out have used microwave Doppler tracking of spacecraft such as Voyager I (Hellings 1983). A microwave signal referenced to a hydrogen maser clock is sent from Earth to the spacecraft, where it is coherently transponded and returned to Earth; the beat frequency, hence the Doppler shift, is obtained by comparison with the hydrogen maser. It is straightforward to show (e.g. Hellings 1983) that this Doppler shift should be

$$\Delta\nu/\nu = \tfrac{1}{2}\Big[(1-\cos\theta)h(t) - 2\cos\theta\, h(t-l/c - \cos\theta\cdot l/c) - (1+\cos\theta)h(t-2l/c)\Big] \qquad (1\cdot42)$$

where $h(t)$ is the amplitude of the gravitational wave at time t, propagating at an angle θ to the line of the tracking signal; l is the separation of the spacecraft. So a single gravitational-wave pulse of duration small compared with the light travel time l/c will produce a characteristic three-pulse signature in the output.

The major problem with these observations was noise from phase fluctuations in the interplanetary plasma. This was equivalent (Hellings 1983) to a stochastic gravitational wave background of amplitude

$$h \sim 3\times10^{-14} f^{-\frac{1}{2}} /\sqrt{Hz}$$

in the region $f \sim 10^{-2}$–5×10^{-4} Hz. While simultaneous tracking at two different microwave frequencies may reduce this further, a major advance will probably require optical position sensing. The technological problems involved, however, are formidable: not only would such an optical detector face most of the problems of a ground-based interferometer (e.g. fluctuations in laser frequency, intensity, angle etc.), it would do so with added difficulty of operation and additional constraints such as inadequate power supply and dissipation, the necessity to shield from the solar wind and radiation, and increased noise from cosmic rays (e.g. Weiss 1979, Decher et al 1980).

If the spacecraft were relatively close (either ~10km on a frame or ~1000km free) an interferometer might still be feasible. The factor limiting the sensitivity might be the cosmic ray proton flux (Weiss 1979), which would give

$$h_{min} \sim 10^{-22} /\sqrt{Hz}$$

in the region $f \sim 10^{-3}$–10^{2} Hz. Larger baselines would be necessary to reduce this noise at lower frequencies, when optical Doppler ranging would become advantageous. If laser powers of ~1W could be attained with spacecraft of mass ~1 ton separated by 1AU, a sensitivity of $h_{min} \sim 10^{-22} /\sqrt{Hz}$ might be achieved down to 10^{-6}Hz.

The difficulties involved in this programme are immense.

The potential rewards are great, also: for such systems should be able to detect gravitational radiation from binaries, the only sowces whose strengths may be predicted with confidence. The experience gained in developing ground-based interferometers may well be valuable in enabling space-borne optical detectors to fulfill their potential.

(1·3(v))Other Detectors

A considerable number of alternative designs for gravitational wave detectors have been proposed. Many of these are variants of the detectors already discussed. Thus, the proposed "microwave cavity detector" (Braginsky et al 1974, Caves 1979, Pegoraro and Radicati 1980) in which gravitational waves deform the walls of a microwave cavity, pumping microwave quanta from one mode to another, is essentially a mechanical detector with the microwave cavity acting as a transducer. The sensitivity is therefore likely to be similar to that of the Weber bars.

A rather different approach is enshrined in the "heterodyne detectors" of Braginsky (Braginsky et al 1969, Braginsky and Nazarenko 1971, Braginsky and Menskii 1971). These use the property that circularly polarised gravitational waves have a force diagram that rotates at twice the gravitational-wave frequency (cf. fig 1·2). A detector co-rotating with this force diagram will always "see" the same phase of the gravitational wave, the effect of which will therefore be cumulative. The detector beats

down the gravitational wave. Such a detector may be mechanical — two rotating rods oriented at right angles to each other, with the gravitational wave producing a relative angular acceleration. Or it may be electromagnetic — two counter-rotating light (or microwave)beams with a rotational period half that of the gravitational wave. In this case, a gravitational wave of the correct polarisation produces a cumulative phase change in one beam, while that induced in the other beam averages out to zero in one cycle. Such an electromagnetic heterodyne detector might be a suitable design for a space detector, perhaps in the form of a single-pass ring cavity; this would have the advantage that the two beams would automatically travel the same distance, making the interferometer insensitive to frequency fluctuations of the light.

A possible variant of the laser interferometer detectors places an active laser medium between the test masses. The change in length of this laser cavity due to a gravitational wave results in a frequency change of the light which may be detected by a suitable frequency discriminator. This may consist of an optical resonance filter using either saturated absorption or two-photon Doppler-free spectroscopic techniques; alternatively, heterodyning with another laser may be used (Bagayev 1981, Weksler et al 1980, Brillet and Tourrenc 1983). The attraction of using such an active interferometer is its relative simplicity. Some of the drawbacks are fairly obvious: for example, there is no way of distinguishing between a frequency fluctuation due to a gravitational wave and that due to a refractive index fluctuation or vibration

in the medium. The only way to avoid this confusion is to use a low density medium and try to keep it as quiet as possible; but this means low power and so poor sensitivity. Spontaneous emission noise means that the sensitivity of an active system can never be better than that of a passive system (Brillet and Tourrenc 1983). Thus, active systems may be relatively easy ways of achieving a poor sensitivity, but do not seem capable of reaching $h_{min} \sim 10^{-21}$.

It is also possible to use naturally-occurring objects as gravitational-wave detectors. Thus a limit may be placed on the background gravitational-wave flux by observation of the vibrations of the Earth during seismically quiet periods (Weber 1967); at the Earth normal mode frequency of 3×10^{-4}Hz, this is equivalent to $h \sim 10^{-14}/\sqrt{Hz}$ (or $\Omega_g \lesssim 10$). Another interesting possibility is to use pulsars as the clocks in Doppler-tracking searches for gravitational radiation (Hellings 1983, Rees 1983). These studies have already placed the interesting limit of $\Omega_g < 10^{-3}$ at $f \sim 10^{-8}$Hz; longer observation should enable this to be improved. The relatively recently discovered binary and millisecond pulsars, which are very good clocks, should enable a limit of $\Omega_g \lesssim 10^{-4}$ to be set for $f \sim 10^{-1}$–10^{-4}Hz. These studies may be able to <u>detect</u> gravitational radiation as well as set an upper limit on it by correlating Doppler shifts from different pulsars (Rees 1983).

A limit to the gravitational-wave background may also be set by observations of the perturbations of planetary orbits. Mashhoon, Carr and Hu (1981) claim that current knowledge of the orbit of Mars places a limit of $\Omega_g \lesssim 0{\cdot}1$ at $f \sim 3 \times 10^{-8}$Hz.

CHAPTER TWO

CAVITY INTERFEROMETERS

(2·1(i))Sensitivity: Storage Time, Modulation and Visibility

In section 1·3(iii) it was seen that laser interferometers have the potential of reaching interesting gravitational-wave sensitivities. There are, however, many other noise sources which must be eliminated before this can be acheived. To appreciate the nature of this excess noise, it is first necessary to gain a more detailed understanding of the interaction of a gravitational wave with the interferometer. This is especially true in the rather more complex case of a detector, such as that at Glasgow, whish uses optical cavities to enhance the phase change produced by the gravitational wave.

Consider a laser beam incident on a cavity such as that shown in fig 2·1. The beam reflected back from the cavity consists of the superposition of the component directly reflected off the input mirror and of the (infinite) number of beams emerging from the cavity. If N is the number of traverses of the cavity (there and back) made by a beam, the corresponding emerging field E_N is

$$E_0 = A_0 R_1 \exp(i\omega t) \qquad (2\cdot1)$$

and

$$E_N = -A_0 T_1^2 R_2 (R_1 R_2)^{N-1} \exp(i\omega t + i\phi_N) \qquad (2\cdot2)$$

where $\phi_N+\pi$ is the phase difference between the original and Nth beams produced by traversal of the cavity. It is useful to consider ϕ_N to be made up of two components: one of arbitrarily large size but which changes slowly compared with storage time of the cavity (the meaning of

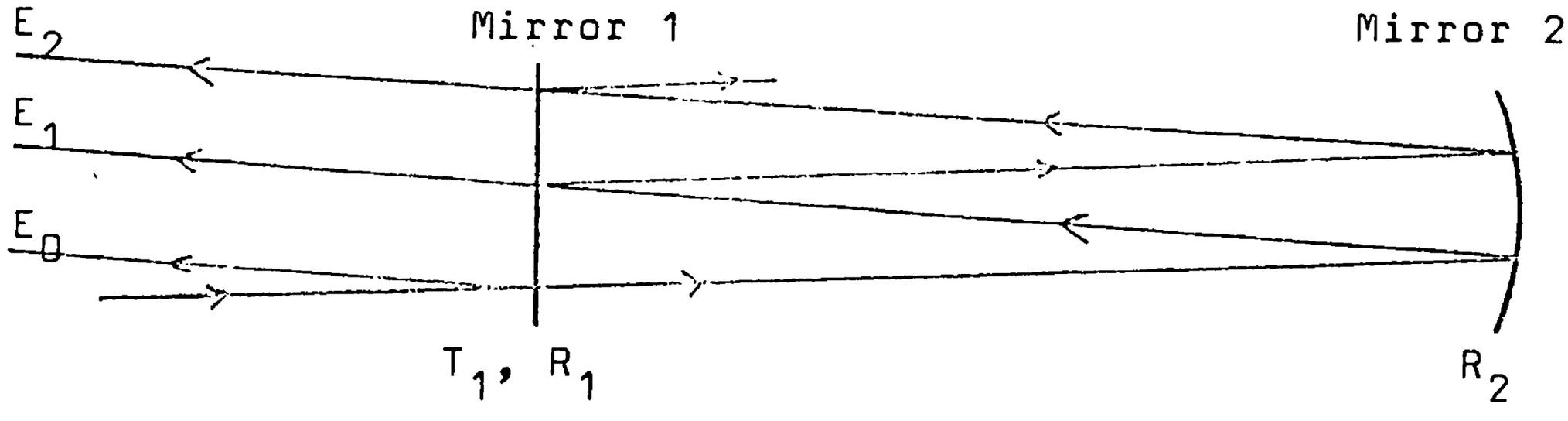

Fig 2·1: Schematic diagram of an optical cavity, with the beams shown separated for clarity. The mirrors have amplitude transmission and reflection coefficients T and R respectively.

which will be defined precisely later); and one of arbitrary frequency but whose magnitude is small compared with unity. Thus,

$$\phi_N = N\delta + \beta(\exp(i\eta N) - \alpha) \qquad (2\cdot3)$$

Here δ is the "static" offset of the cavity; if the "fast" change is due to a gravitational wave then (cf. 1·28a)

$$\beta = -(ihk\lambda_g/4\pi)\exp(i\omega_g t) = -(ih\omega/2\omega_g)\exp(i\omega_g t) \qquad (2\cdot4)$$

$$\alpha = 1 \qquad (2\cdot5)$$

$$\eta = 4\pi l/\lambda_g = 2l\omega_g/c \qquad (2\cdot6)$$

Alternatively, the phase difference may be due to a frequency fluctuation of the laser ($\omega = \omega_0 + \Delta\omega\exp(i\omega_n t)$).

It will be seen in section 2·1(ii) that in this case,

$$\beta = -(i\Delta\omega/\omega_n)\exp(i\omega_n t) \qquad (2\cdot7)$$

$$\alpha = 0 \qquad (2\cdot8)$$

$$\eta = 2l\omega_n/c \qquad (2\cdot9)$$

This formalism is therefore quite general.

The total reflected field is

$$E_R = A_0 \exp(i\omega t)\left\{ R_1 - T_1^2 R_2 \sum_{N=1}^{\infty} (R_1 R_2)^{N-1} \exp(iN\delta) \exp(i\beta(e^{i\eta N} - \alpha)) \right\}; \quad (2.10)$$

Since β is assumed to be small, the last exponential in 2·10 may be expanded:

$$\exp(i\beta(e^{i\eta N} - \alpha)) \approx 1 + i\beta(e^{i\eta N} - \alpha) \quad (2·11)$$

Using the standard expression for the sum of a geometric progression,

$$\sum_{N=1}^{\infty} (R_1 R_2)^{N-1} \exp(iN\phi) = \frac{\exp(i\phi)}{1 - R_1 R_2 \exp(i\phi)} \quad (2·12)$$

the field may be written as

$$E_R = A_0 \exp(i\omega t)\left\{ R_1 - \frac{T_1^2 R_2 (1 - i\alpha\beta)\exp(i\delta)}{1 - R_1 R_2 \exp(i\delta)} - \frac{i\beta T_1^2 R_2 \exp(i(\delta + \eta))}{1 - R_1 R_2 \exp(i(\delta + \eta))} \right\} \quad (2·13)$$

Or,

$$E_R = A_0 \exp(i\omega t)\left\{ R_1 - \frac{T_1^2 R_2}{(1 - R_1 R_2)^2}\left[\frac{(e^{i\delta} - R_1 R_2)(1 - i\alpha\beta)}{1 + F' \sin^2(\delta/2)} + \frac{i\beta(e^{i(\delta+\eta)} - R_1 R_2)}{1 + F' \sin^2((\delta+\eta)/2)} \right] \right\} \quad (2·14)$$

where F' is the coefficient of finesse:

$$F' = \frac{4R_1 R_2}{(1 - R_1 R_2)^2} = 4F^2/\pi^2 \quad (2·15)$$

and F is the finesse. If the cavity is on resonance, $\delta = 0$ and the field is

$$E_R(o) = A_0 e^{i\omega t}\left\{R_1 - \frac{T_1^2 R_2}{1-R_1R_2}\left[(1-i\alpha\beta) + \frac{(e^{i\eta}-R_1R_2)}{(1-R_1R_2)(1+F'\sin^2(\eta/2))}\right]\right\} \quad (2\cdot16)$$

For $\eta \ll 1$ (but $F'\sin^2(\eta/2)$ still unrestricted), this is simply

$$E_R(o) = A_0 e^{i\omega t}\left\{R_1 - \frac{T_1^2 R_2}{1-R_1R_2}\left[1 - \frac{\beta(F/\pi)\sin\eta}{1+F'\sin^2(\eta/2)} - i\beta\left(\frac{(\alpha-1)+\alpha F'\sin^2(\eta/2)}{1+F'\sin^2(\eta/2)}\right)\right]\right\} \quad (2\cdot17)$$

Having obtained this general expression, it is convenient to specialise once more to the case of a gravitational wave. Using (2·4) – (2·6), the field is

$$E_R(0) = A_0 e^{i\omega t}\left\{R_1 - \frac{T_1^2 R_2}{1-R_1R_2}\left[1 + \frac{ik\lambda_g h\exp(i\omega_g t)}{4\pi}\left(\frac{(F/\pi)\sin(4\pi l/\lambda_g)}{1+F'\sin^2(2\pi l/\lambda_g)} + \frac{iF'\sin^2(2\pi l/\lambda_g)}{1+F'\sin^2(2\pi l/\lambda_g)}\right)\right]\right\} \quad (2.18)$$

The imaginary part of the field gives the phase shift due to the gravitational wave. For low storage times ($Fl/c \ll \tau_g$), this phase shift is just

$$\Delta\phi = (F/\pi)lkh\cos(\omega_g t) \quad (2\cdot19)$$

Comparison with the form of (1·29) reveals that a cavity with a finesse F has an effective number of traverses of

$$N = F/\pi \quad (2\cdot20)$$

If a storage time is defined by

$$\tau_s = 2N_{eff}l/c = 2Fl/\pi c \qquad (2\cdot21)$$

then τ_s is also the time for the intensity of the emerging beam to drop to $1/e^2$ of its initial value if the incident beam is suddenly cut off.

As the storage time of the cavity becomes comparable with the period of the gravitational wave, the last term in (2·18) becomes important, giving a phase lag for the observed gravitational wave signal of

$$\theta = \arctan(2\pi\tau_s/\tau_g) \qquad (2\cdot22)$$

So very long storage times lead to a 90^o phase lag. The magnitude of the optical phase shift is

$$|\Delta\phi| = \frac{\frac{1}{2}kc\tau_s h}{(1+(2\pi\tau_s/\tau_g)^2)^{\frac{1}{2}}} \qquad (2\cdot23)$$

For large τ_s/τ_g, this gives

$$\Delta\phi(max) = (kh\lambda_g/4\pi)\sin(\omega_g t) = \tfrac{1}{2}(\lambda_g/\lambda)h\sin(\omega_g t) \quad ;(2\cdot24)$$

Comparison with (1·30) shows that this maximum phase shift is half the size of that of the beam emerging from a delay line of optimum storage time. This reduction in sensitivity may be explained by the fact that, while the beam emerging from a delay line has its phase shifted in the same direction throughout its passage, the light from the cavity is inevitably composed of many beams, none of which has a greater phase shift than the beam from the delay line and some of which will have spent a long time in the cavity and have the wrong sign of phase shift. This averaging also smooths out the oscillation of the phase shift with gravitational-wave frequency embodied in (1·28).

Equation (2·18) gives a convenient expression for the fringe visibility V:

$$V = \frac{I_{max} - I_{min}}{I_{max}} = 1 - \left[R_1 - \frac{T_1^2 R_2}{1-R_1R_2}\right]^2 \qquad (2\cdot25)$$

In terms of the visibility, the amplitude of the beam emerging from the cavity is (assuming perfect mode-matching – see Appendix 4)

$$A_c/A_o = 1 \pm (1-V)^{\frac{1}{2}} \qquad (2\cdot26)$$

The phase change produced by a gravitational wave is detected by the change in intensity that results when the beam emerging from the cavity is interfered with either the beam off the input cavity mirror or the beam from the other cavity. The latter arrangement has the advantage of being more symmetrical (so reducing the size of various noise sources) and of giving good fringe visibility ($V \approx 1$). In either case, it is necessary to use some technique to reduce the effect of laser intensity fluctuations at gravitational-wave frequencies, which would otherwise swamp the signal. It will be seen that such a technique, first suggested at Glasgow (Drever et al 1981, Drever et al 1983) is to phase modulate the incident laser beam at a frequency well above $1/\tau_s$. This provides a measure of the gravitational-wave amplitude or the laser-cavity frequency noise by mixing up the intensity changes produced by the low frequency phase fluctuations to a frequency where the laser intensity noise is limited by photon counting statistics. At the same time, low frequency intensity noise is not mixed up if the interfering beams are accurately in antiphase (see section 2·3(iii)).

Consider a phase modulation of the incident light:

$$E = A_0 \exp\left[i(\omega t + \phi_0 \sin\omega_m t)\right] \qquad (2\cdot27)$$

This phase modulation produces sidebands:

$$\mathrm{Re}(E) = A_0\Big\{J_0(\phi_0)\cos(\omega t) + J_1(\phi_0)\Big[\cos[(\omega+\omega_m)t] - \cos[(\omega-\omega_m)t]\Big] + J_2(\phi_0)\Big[\cos[(\omega+2\omega_m)t] - \cos[(\omega-2\omega_m)t]\Big] + \ldots\Big\} \quad (2\cdot28)$$

$$\mathrm{Im}(E) = A_0\Big\{J_0(\phi_0)\sin(\omega t) + J_1(\phi_0)\Big[\sin[(\omega+\omega_m)t] + \sin[(\omega-\omega_m)t]\Big] + \ldots\Big\} \quad (2\cdot29)$$

where $J_n(\phi_0)$ is a Bessel function of the first kind and nth order. If ω_m is well above the linewidth (π/τ_s) of the cavity, the sidebands will be almost totally reflected since they will not be on resonance; this is shown explicitly when the effect of frequency fluctuations is considered. The total reflected field may then be written as

$$E_R(o) = A_0 e^{i\omega t}\Big\{\exp(i\phi_0\sin\omega_m t) - J_0(\phi_0)(A_c/A_0)\Big[1 - \beta/(1+F'\sin^2(\eta/2))\Big((F/\pi)\sin\eta + i[(\alpha-1) + \alpha F'\sin^2(\eta/2)]\Big)\Big]\Big\} \quad ;(2\cdot30)$$

The mixing of the signal contained in β to around the modulation frequency occurs via the product of the first and last terms. The resulting signal is

$$\delta I(\omega_m) = -\frac{2A_0A_cJ_0(\phi_0)J_1(\phi_0)\sin\omega_m t}{1 + F'\sin^2(\eta/2)}\Big\{(F/\pi)\sin\eta\,\mathrm{Im}(\beta) + ((\alpha-1) + F'\sin^2(\eta/2))\mathrm{Re}(\beta)\Big\} \quad ;(2\cdot31)$$

So the demodulated intensity signal produced by a gravitational wave of amplitude h incident on the two arms of the detector is

$$\delta I(\omega_g) = \frac{A_0A_cJ_0(\phi_0)J_1(\phi_0)k\lambda_g h}{(1 + (4Fl/\lambda_g)^2)}\Big\{(4Fl/\lambda_g)\cos\omega_g t + (4Fl/\lambda_g)^2\sin\omega_g t\Big\} \quad (2\cdot32)$$

Or,

$$|\delta I(\omega_g)| = \frac{4I_0(1\pm(1-V)^{\frac{1}{2}})J_0(\phi_0)J_1(\phi_0)kc\tau_s h}{(1+(2\pi\tau_s/\tau_g)^2)^{\frac{1}{2}}} \qquad (2\cdot33)$$

Now the size of the smallest intensity change (2·33) that may be detected will ultimately be set by the photon shot noise. In turn, the magnitude of this will be determined by the intensity at a null, the value of which is set by the visibility V (without modulation) and the modulation depth ϕ_0. An increase in ϕ_0 both reduces the carrier amplitude and puts more energy into the sidebands (which are not interfered out). So the minimum intensity I_{min} is

$$I_{min}/I_0 = (1-V)J_0^2(\phi_0) + 1 - J_0^2(\phi_0)$$
$$= 1 - VJ_0^2(\phi_0) \qquad (2\cdot34)$$

The apparent visibility therefore becomes $J_0^2(\phi_0)V$. The condition that the intensity change due to a gravitational wave must be as least as large as that due to the shot noise then gives a minimum detectable gravitational wave amplitude of

$$h_{min} = h_0(\tau_s, I_0)f(V,\phi_0)$$
$$= \left(\frac{\hbar\lambda\left[1+(2\pi\tau_s/\tau_g)^2\right]\Delta f}{8\pi\zeta I_0 c\tau_s^2}\right)^{1/2}\left(\frac{(1-VJ_0^2(\phi_0))^{\frac{1}{2}}}{\sqrt{2}J_0(\phi_0)J_1(\phi_0)(1\pm(1-V)^{\frac{1}{2}})}\right); \qquad (2\cdot35)$$

For small ϕ_0, the Bessel functions may be approximated by: $J_0(\phi_0) \approx 1 - \frac{1}{4}\phi_0^2$; $J_1(\phi_0) \approx \frac{1}{2}\phi_0$. So, with unit visibility,

$$f(1,\phi_0) \approx 1 + O(\phi_0^2)$$

In this case, the sensitivity is almost independent of modulation depth. This is because the modulation increases the signal and noise at the same rate. For visibilities

at all different from unity, the higher light level will produce more shot noise. There will then be a modulation depth ϕ_0 which gives an optimum signal to noise ratio. The variation of $f(V,\phi_0)$ is shown in fig 2·2 for some typical values of V. A striking feature is the rapid increase in the optimum value of h_{min} as the visibility deteriorates. This may be understood as being due to a decrease in the signal size (A_c/A_0) and an increase in the noise as the visiblity decreases, combined with the consequent requirement to increase the modulation depth and so further increase the noise. This highlights the need for a good visibility if the best potential sensitivities are to be achieved. From fig 2·2 it can be seen that the optimum modulation ϕ_0 is quite a slow function of visibility. For typical values of V ($V \lesssim 0{\cdot}95$), a modulation depth $\phi_0 \approx 0{\cdot}8$rad would be appropriate; this corresponds to the first sidebands having an intensity ~1/5 of that of the central frequency (see fig 2·3).

If the visibility is high ($(1-V)^{\frac{1}{2}} \ll 1$) it is possible to obtain analytic expressions for $\phi_0(\text{opt})$ and $h_{min}(\text{opt})$ by expanding the Bessel functions; this gives

$$\phi_0(\text{opt}) \approx (4\sqrt{2}/3)(1-V)^{\frac{1}{2}} \qquad (2{\cdot}36)$$

$$h_{min}(\text{opt}) \approx h_0(\tau_s, I_0)\left[1 + \frac{5}{2}(1-V)^{\frac{1}{2}}\right] \qquad (2{\cdot}37)$$

Now for low storage times, the best possible sensitivity h_0 is simply

$$h_0 = \left(\frac{\hbar c \lambda \Delta f}{8\pi\xi I_0 (c\tau_s)^2}\right)^{\frac{1}{2}} = \left(\frac{\hbar c \lambda \Delta f}{32\pi\xi I_0 l^2}\right)^{\frac{1}{2}} \frac{\pi}{F} \qquad (2{\cdot}38)$$

This sensitivity is only possible with unit visibility.

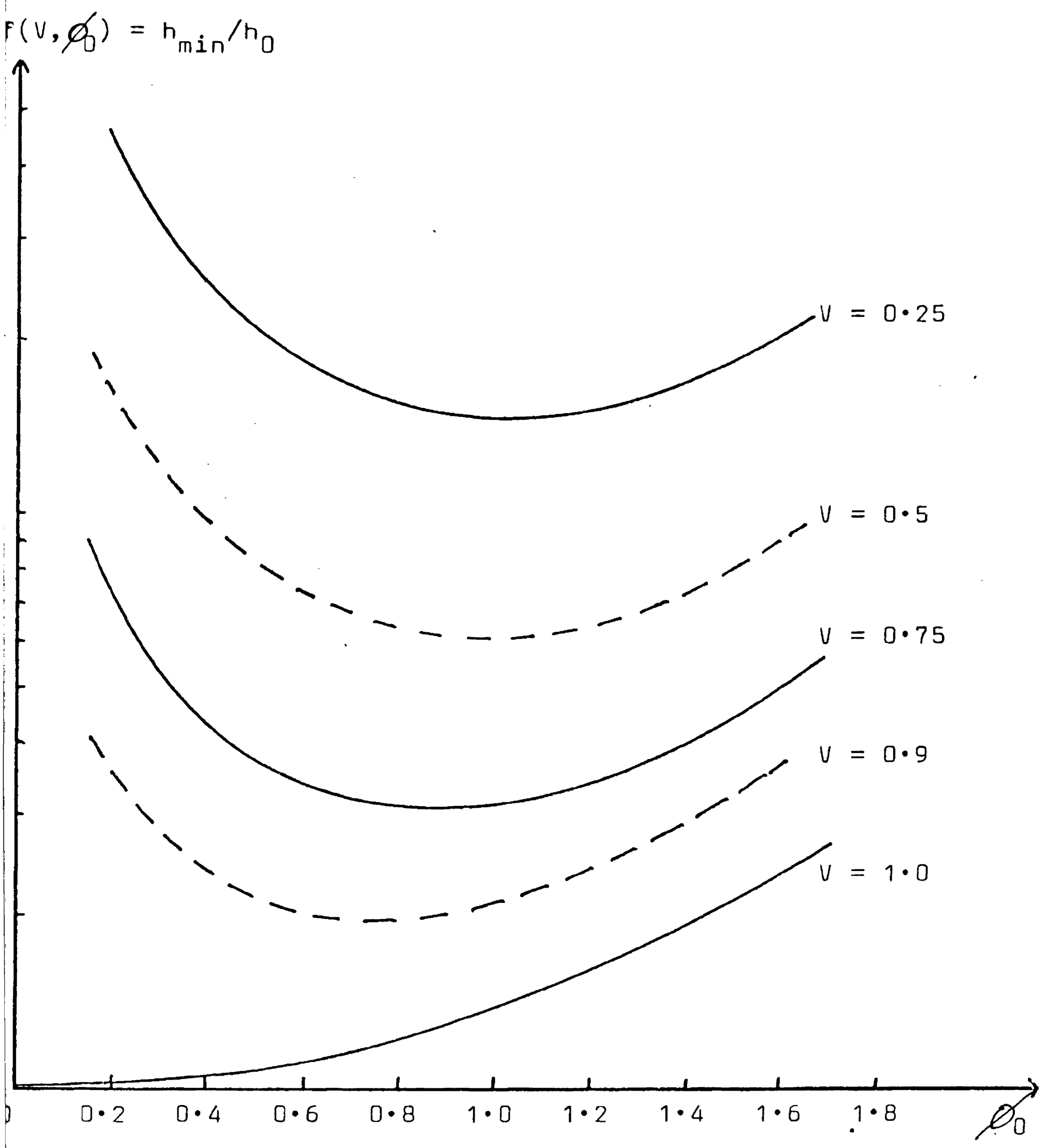

Fig 2·2: A plot of the possible shot noise limited sensitivity h_{min}/h_0 as a function of visibility V and modulation depth ϕ_0. It is apparent that a modulation depth of $\phi_0 \sim 0{\cdot}8$ rad gives the best potential sensitivity for all visibilities less than 95%. It is only for visibilities greater than this that the high-visibility approximation $h_{min}/h_0 = 1$ is valid.

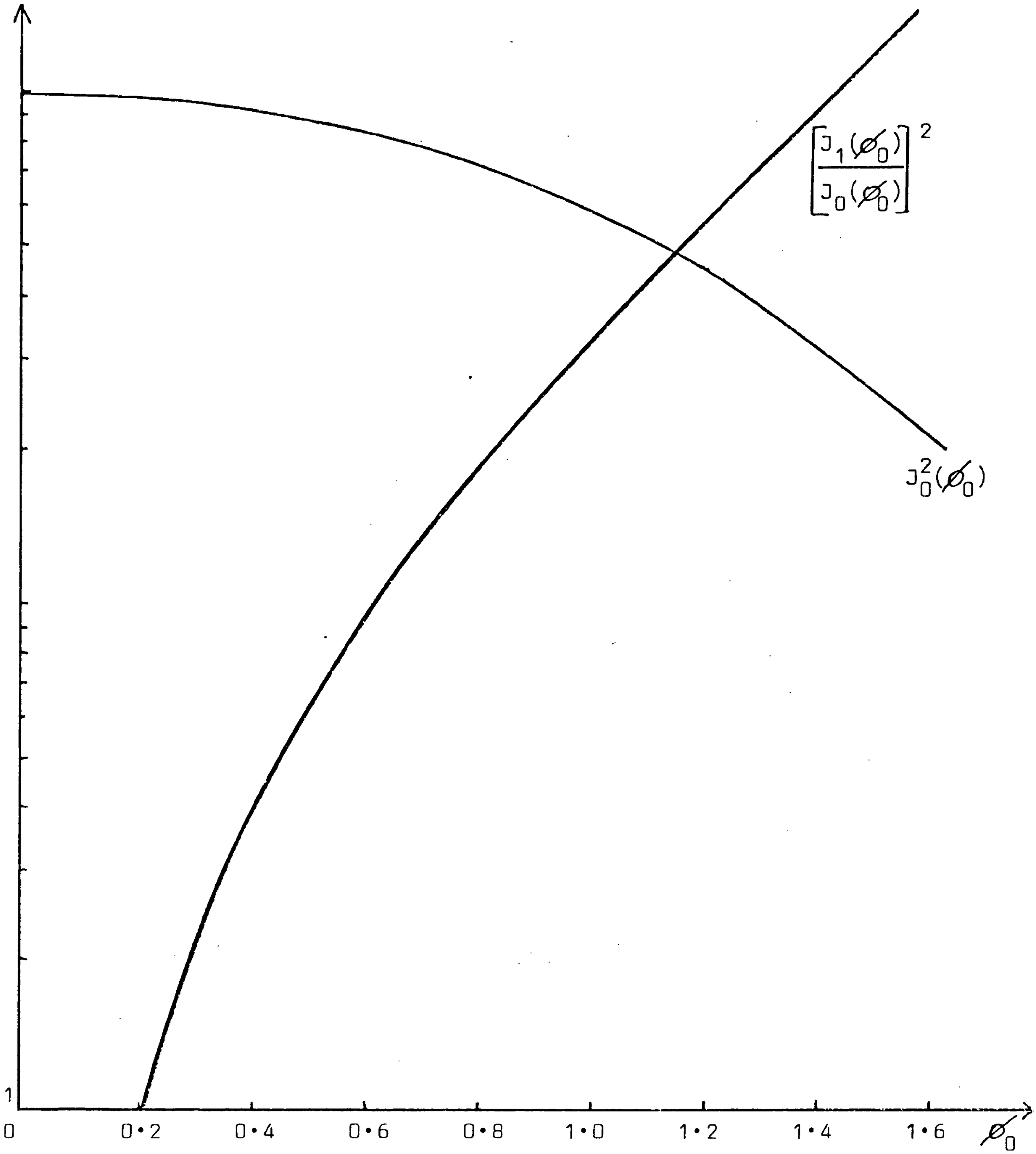

Fig 2·3: A plot of the carrier intensity $J_0^2(\phi_0)$ and relative first sideband intensity $\left[J_1(\phi_0)/J_0(\phi_0)\right]^2$, as a function of modulation depth ϕ_0. Thus, at $\phi_0 \approx 0{\cdot}8$ rad, the first sidebands have an intensity $\sim 0{\cdot}2$ of that of the central frequency. Note that $J_0^2(\phi_0)$ also gives the degradation in apparent visibility.

In this case the light emerging from the cavities has the same intensity as the incident beam. It is therefore not surprising that if absorption is negligible, the shot noise limited sensitivity of a cavity detector is a factor e better than an optimised delay line detector with mirrors of the same reflectivity (cf. 1·38). Note, however, that h_{min} is degraded by a factor of $\sqrt{2}$ by observing the cavities separately.

In practice, absorption is likely to be important; there will then be an input mirror transmission T_1^2 which gives an optimum sensitivity. This optimisation turns out to be the same whether the cavities are observed together or separately:

$$T_1^2(\text{opt}) = A_1^2 + A_2^2 \qquad (2\cdot39)$$

where A_1^2, A_2^2 are the absorption coefficients of the two mirrors. This gives a visibility of unity. When the two cavity beams are interfered, this gives a sensitivity a factor of e/2 better than that of a delay-line detector with equally good high reflectors (equal absorption) and equal incident powers. Since the smaller area of the mirrors required for cavities may enable lower absorptions to be obtained, cavity detectors may have slightly better potential sensitivities in this low storage time regime.

These calculations are consistent with the low storage time regime results of Munley (1982).

An important corollary of the material discussed here (essentially that leading to 2·33) is that if there is phase noise $\delta\phi_{RF}(\nu)$ in the interfered light around the modulation frequency, the equivalent displacement noise δl

noise of one of the masses is

$$\delta l(f) = \delta\phi_{RF}(\nu)/16FJ_0(\phi_0)J_1(\phi_0)\left[1\pm(1-V)^{\frac{1}{2}}\right] \qquad (2\cdot40)$$

For low frequency phase noise $\delta\phi_{LF}(f)$, which has to be mixed up,

$$\delta l(f) = \delta\phi_{LF}(f)/8F\left[1\pm(1-V)^{\frac{1}{2}}\right] \qquad (2\cdot41)$$

These relations will be needed to convert the phase noises predicted later in this Chapter and in Chapter 3 into an equivalent gravitational-wave sensitivity.

If $\phi_0 \approx 0\cdot8$ rad, (2·40) may be rewritten as

$$\delta l(f) \approx \delta\phi_{RF}(\nu)/5F\left[1\pm(1-V)^{\frac{1}{2}}\right] \qquad (2\cdot42)$$

Or,

$$\delta l(f) \approx 10^{-9}(F/100)^{-1}\left[1\pm(1-V)^{\frac{1}{2}}\right]^{-1}\delta\phi_{RF}(\nu) \qquad (2\cdot43)$$

(2·1(ii))Frequency Noise

The relative frequency of the light and the cavities must be stabilised both to maintain the cavities on resonance (maximum sensitivity) and to minimise the detector noise. The RF modulation technique is a way of detecting such frequency fluctuations, providing a good error signal for a stabilising servo (Drever et al 1983).

Consider a frequency fluctuation described by

$$\omega = \omega_0 + \Delta\omega\exp(i\omega_n t) \qquad (2\cdot44)$$

The phase is just the integral of the frequency:

$$\phi = \omega_0 t - i(\Delta\omega/\omega_n)\exp(i\omega_n t) \qquad (2\cdot45)$$

So the phase shift of the Nth beam emerging from a cavity is (cf. 2·3)

$$\phi_N - N\delta = i(\Delta\omega/\omega_n)\exp\left[i\omega_n(t + 2Nl/c)\right] \qquad (2\cdot46)$$

This confirms equations (2·5) – (2·7). The unmodulated

reflected field is then (cf. 2·14)

$$E_R = A_0 e^{i\omega t}\left\{R_1 \exp\left[(\Delta\omega/\omega_n)\exp(i\omega_n t)\right]\right.$$

$$- \frac{T_1^2 R_2}{(1-R_1R_2)^2}\left[\frac{e^{i\delta}-R_1R_2}{1+F'\sin^2(\delta/2)}\right.$$

$$\left.\left. + \frac{\Delta\omega}{\omega_n}\exp(i\omega_n t)\left(\frac{\exp\left[i(\delta+2l\omega_n/c)\right] - R_1R_2}{1+F'\sin^2\left[(\delta+2l\omega_n/c)/2\right]}\right)\right]\right\}; \quad (2\cdot47)$$

Since only imaginary terms are mixed up to around the modulation frequency, the output of the phase—sensitive detector as a function of the offset δ will be

$$dI \propto \frac{\sin\delta}{1+F'\sin^2\delta/2} \quad (2\cdot48)$$

This is the characteristic ∿ shape of the "RF" fringes at the PSD output. Note the bipolar nature, giving the correct sign of error signal.

(2·49)

For a resonating cavity, in which $\delta = 0$, the reflected field (including modulation) may be written (cf. 2·30) as (p.t.o.):

$$E_R = A_0 e^{i\omega t}\left\{\left(1+(\Delta\omega/\omega_n)\exp(i\omega_n t)\right)\exp(i\phi_0\sin\omega_m t)\right.$$

$$\left. - \frac{J_0(\phi_0)A_0}{A_c}\left[1 + \frac{i(\Delta\omega/\omega_n)\exp(i\omega_n t)}{1+F'\sin^2(l\omega_n/c)}\left(\frac{F}{\pi}\sin(2l\omega_n/c) - i\right)\right]\right\} \quad (2\cdot50)$$

The mixed up terms are then

$$\delta I = \frac{2A_0A_cJ_0(\phi_0)J_1(\phi_0)F(\Delta\omega/\omega_n)}{\pi(1+(4F^2/\pi^2)\sin^2(\pi\nu_n/\nu_0)}\left[\sin(2\pi\nu_n/\nu_0)\cos\omega_n t\right.$$

$$\left. + (4F/\pi)\sin^2(\pi\nu_n/\nu_0)\sin\omega_n t\right] \quad (2\cdot51)$$

For fluctuations occurring at low frequency ($\nu_n < \nu_0/F$), this is just

$$\delta I/I_0 = 4(A_c/A_0)J_0(\phi_0)J_1(\phi_0)\tau_s\Delta\omega\cos\omega_n t \quad (2\cdot52)$$

So the intensity changes around the modulation frequency produced by slow changes in the laser frequency are simply proportional to, and in phase with, these frequency fluctuations. On the other hand, the cavity cannot follow changes occurring on timescales less than the storage time. This is reflected in the dominance of the last term in (2·50) at frequencies $\nu_n > \nu_0/F$, where the intensity changes are

$$\delta I/I_0 = 4(A_c/A_0)J_0(\phi_0)J_1(\phi_0)(\Delta\omega/\omega_n)\sin\omega_n t \quad (2\cdot53)$$

So fast frequency fluctuations produce intensity changes proportional to the <u>phase</u> difference between the incident light and that emerging from the cavity.

The phase lag θ between the frequency fluctuation and the resulting intensity change is given by

$$\tan\theta = \frac{(4F/\pi)\sin^2(\pi\nu_n/\nu_0)}{\sin(2\pi\nu_n/\nu_0)} \quad (2\cdot54)$$

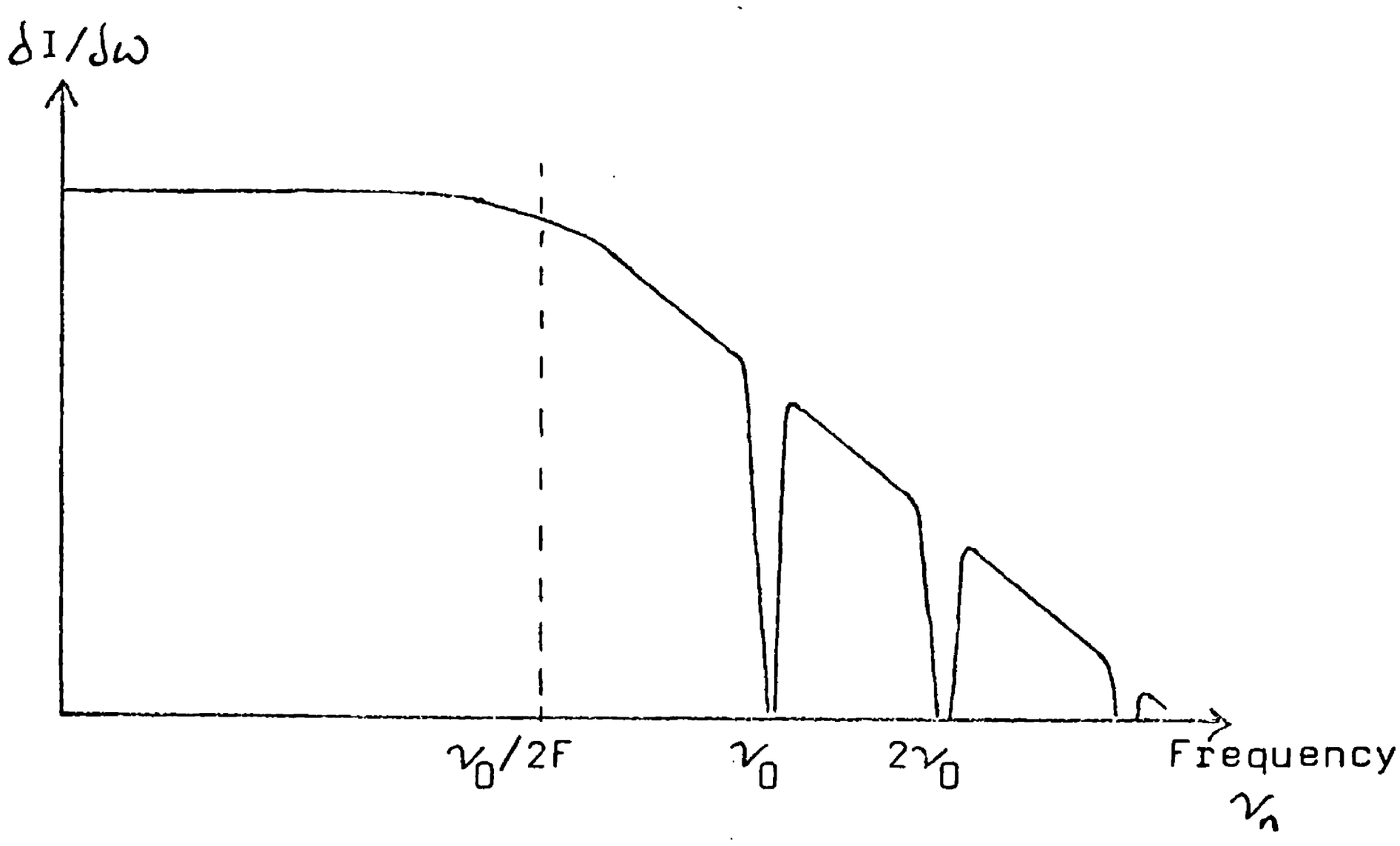

Fig 2·4: A schematic indication of the response of a cavity to a frequency fluctuation $\delta\omega$ occurring at a frequency ν_n. The resultant intensity change δI is constant out to the cavity line width, where it begins to roll off at 6dB/octave. At multiples of the free spectral range ν_0, however, the response of the cavity drops to zero.

The phase lag θ is thus zero at low frequencies, while for $1 \ll 2F\nu_n/\nu_0 \ll F$, θ is about 90^0. In this regime, the cavity acts as an integrator with a time constant of τ_s.

This simple behaviour breaks down at higher frequencies, when the fluctuation frequency is equal to multiples of the free spectral range ν_0 of the cavity. At these frequencies, the sidebands have their original amplitude and phase and so produce no changing intensity signal. There is therefore a dip in the response of the cavity at these frequencies, as indicated in fig 2·4. This is also shown in the form of (2·50): the first term is negligible for $\nu_n - n\nu_0 > \nu_0/F$ (being zero at $\nu_n = n\nu_0$) whilst the second term also becomes zero at $\nu_n = n\nu_0$.

The corresponding phase lag is given by (2·54): it is 180^{o} at $\nu_n = \nu_0$.

This complicated transfer function must be taken into account when designing a feedback system. It is especially significant in a long detector: for 1 km cavities, the free spectral range is 150 kHz.

Comparison of (2·52) with (2·33) in the low storage time limit confirms that a frequency fluctuation produces an equivalent apparent change in the length of a cavity:

$$\Delta l/l = \Delta\nu/\nu \qquad (2\cdot55)$$

If the cavities are observed separately, any residual frequency noise appears as noise; if $\Delta\nu \sim 10^{-2}\,\mathrm{Hz}/\sqrt{\mathrm{Hz}}$, for example (good stabilisation), the equivalent gravitational wave signal would be $h \sim 10^{-17}/\sqrt{\mathrm{Hz}}$. It seems likely that some additional means of reducing the effect of frequency fluctuations must be found. Indeed, the existence of this problem is the primary reason why a two-arm interferometer is used, for if the path lengths are equal in the two arms a frequency fluctuation will produce no <u>relative</u> phase fluctuation. If the apparent optical lengths of the two cavities are L_1, L_2 respectively, the size of the displacement noise is

$$\delta L = (\Delta\nu/\nu)(L_1 - L_2) \qquad (2\cdot56)$$

This subtraction of the frequency noise may be achieved in two different ways. The reflected outputs from each cavity may be observed separately and the subtraction performed electronically. This has the advantage that the effective lengths of the two arms may be readily adjusted electronically to give good subtraction. Alternatively,

the beams from the two cavities may be optically interfered. While this ensures good optical symmetry and high fringe contrast, it means that L_1 and L_2 are determined solely by the optics:

$$L_1 = 2F_1 l/\pi \qquad (2\cdot57)$$

The displacement noise is then

$$\delta l/l = \frac{(F_1-F_2)}{F}(\Delta\nu/\nu) \qquad (2\cdot58)$$

So reasonable matching of the cavity finesses gives a substantial reduction in the effect of frequency noise.

If the gain of the frequency stabilisation system can be made sufficiently high for the residual frequency noise to be limited by the photon shot noise in light power I_s (i.e. $\Delta\nu/\nu = (\Delta l/l)_{\text{shot noise on } I_s}$), then the condition for the interfered output not to be limited by frequency noise is just

$$\Delta F/F < (I_s/I_{int})^{\frac{1}{2}} \qquad (2\cdot59)$$

where I_{int} is the power in the interfered output (remember that shot noise scales as the square root of the power).

The degree of frequency stabilisation required is very high and provides a major experimental challenge. Some experimental implications are considered in more detail in section (2·2).

(2·1(iii)) Intensity Noise

The effects of low frequency changes in the laser intensity may be calculated by the same method as that used for frequency fluctuations. Just as for frequency

noise, the cavity acts as an integrator with time constant τ_s: the internal field is of form

$$A_c \propto 1 + (\delta A/A)\left[1 + (\omega_n \tau_s)^2\right]^{-1} \qquad (2\cdot60)$$

Since only imaginary terms are mixed up, low frequency intensity changes do not appear in the demodulated intensity signal for $\delta = 0$. If the cavity is slightly off resonance, the ratio of the signal caused by a gravitational wave to that due to low frequency intensity noise is

$$S/N = (\Delta\phi_{GW}/\delta)(\delta I/I_0)^{-1} \qquad (2\cdot61)$$

If a sensitivity of $\Delta\phi \sim 10^{-9}$rad$/\sqrt{Hz}$ is desired and $\delta I/I_0 \sim 10^{-5}/\sqrt{Hz}$, it is therefore necessary to keep the phase offset δ to less than 10^{-4}rad. This requires a high loop gain servo system.

Some reduction of $\delta I/I$ may be obtainable by use of an approp riate feedback system (e.g. the Coherent "Noise Eater"). The further loss in light, increase in complexity and possible introduction of beam distortion by such a system means that such a solution should be avoided if possible.

(2·1(iv))Scattering

Another way in which frequency noise may cause significant phase noise is via scattered light (Drever et al 1980, Billing et al 1981). If light is scattered, perhaps at a mirror surface, with a fractional amplitude σ arriving at the photodiode and a phase angle θ relative to the main beam, the resultant phase change is

$$\Delta\phi = \sigma\sin\theta \qquad (2\cdot62)$$

Noise may be introduced by the variation of σ (see section

3·3(ii) for further discussion) or of θ. If the main beam and the scattered light have travelled distances differing by L, then

$$\theta = 2\pi L/\lambda = 2\pi\nu L/c \qquad (2\cdot63)$$

A change $\Delta\nu$ in the frequency then produces a phase change

$$\Delta\phi = (2\pi\sigma L/c)\cos\theta.\Delta\nu \qquad (2\cdot64)$$

Now L might be of order $c\tau_s$, whilst the value of $\cos\theta$ is unpredictable and uncontrollable (this is true even for optical cavities, since the scattered light has a different mode structure and therefore a different phase velocity – see section 3·2). So $\Delta\phi$ might be as large as

$$\Delta\phi = 2\pi\sigma\tau_s\Delta\nu \qquad (2\cdot65)$$

The noise from scattering could swamp the phase change produced by a gravitational wave unless

$$\sigma \lesssim \Delta\phi_{GW}/2\pi\tau_s\Delta\nu \qquad (2\cdot66)$$

$$\text{Or,} \quad h_{min} = 2\sigma(\Delta\nu/\nu) \qquad (2\cdot67)$$

This is of the same form as (2·58); so frequency noise coupling via scattered light will only be important if σ is larger than $\Delta F/F$. Such a situation is certainly conceivable: it would seem that there is little point in trying to match the finesses to better than 1%.* Further reduction of the noise produced by frequency fluctuations would then require better stabilisation.

That the condition $\sigma \lesssim \Delta F/F$ is so weak reflects the fact that the use of optical cavities forces a high degree of stabilisation. Scattering may be relatively much more important in a delay line system (unless comparable frequency stabilisation is achieved). The MIT group are planning to impose a random phase modulation on the light entering their delay line interferometer in order to

* Assuming scattered intensity $\sigma^2 \sim 10^{-4}$

spoil the coherence. The effect of the scattered light would then be proportional to its intensity rather than its amplitude.

Man et al (1978) and Schilling et al (1981) suggested the use of a technique in which the light is phase-modulated in such a way that the effect of scattered light with certain path differences averages to zero during the measurement.

(2·1(v))Seismic Noise

An obvious source of possible noise is ground vibration, the natural amplitude of which is considerably larger than the motions induced by a typical gravitational wave (Weiss 1972):

$$\Delta x \sim 2\times10^{-9}/f^2 \quad m/\sqrt{Hz}$$

It is, however, relatively easy to make acoustic filters which attenuate this motion at frequencies of interest. Thus, suspending the test masses as simple pendulums of low resonant frequency f_0 and high Q provides isolation, for frequencies $f \gg f_0$, of (Weiss 1972)

$$\Delta x(\text{bottom})/\Delta x(\text{top}) \propto (f_0/f)^2 \qquad (2\cdot68)$$

If $f_0 \sim 1$ Hz, the motion at 1 kHz therefore attenuated by a factor of $\sim10^6$. This is almost sufficient. Further attenuation may be obtained by using stacks of alternating lead (or steel) and rubber. Each layer acts as a single pole acoustic filter ($f_0 \sim 10$ Hz). This should provide adequate isolation above ~100 Hz, though at the cost of increasing the size of low frequency motions and thereby introducing possible dynamic range problems. A lead and

rubber stack should also ensure reasonable vibration isolation even at the resonant frequencies of the suspension wires. Suppression of seismic noise below ~100 Hz will probably require an active system (e.g. Robertson 1981).

(2·1(vi))Thermal Noise

Thermal motions of the test masses may confuse the signal from a gravitational wave. Unlike Weber bars, however, laser interferometer detectors do not work at the resonant frequency of the test masses. Since most of the thermal motion occurs near the normal mode frequencies, its effect being further reduced by the increase in detector size, laser interferometers may be made less susceptible to thermal noise.

The thermal noise acting on a mechanical system with mass m, resonant frequency ω_0 and a damping time $2Q/\omega_0$ effectively produces a stochastic driving force (e.g. Weiss 1972) of

$$\Delta F^2(f) = 4kTm\omega_0\Delta f/Q \qquad (2\cdot69)$$

The resultant motion is evidently concentrated near the resonant frequency ω_0. If $Q \gg 1$ and $\omega \gg \omega_0$, the motion is

$$\Delta x^2(f) = \frac{4kT\omega_0\Delta f}{mQ\omega^4} \qquad (2\cdot70)$$

An example of such a situation is the pendulum mode of the test masses, where $\omega_0 \approx 6$ rad/s and Q may be as high as 10^6 (in vacuum). With masses of 10 kg at 300 K, this would give

$$\Delta x \approx 2\times10^{-21} \text{ m}/\sqrt{\text{Hz}} \quad \text{at 1 kHz}$$

On the other hand, for modes well above the frequency of interest, the thermal motion will be

$$\Delta x^2(f) = \frac{4kT\Delta f}{mQ\omega_0^3} \qquad 2\cdot71)$$

Thus, minimisation of the effects of internal resonances of the test masses requires that they be of high natural frequency and high Q. For example, if f_0 = 5 kHz, m = 10kg and $Q \sim 10^5$, the motion at 1 kHz would be

$$\Delta x \sim 7\times10^{-21} \text{ m}/\sqrt{\text{Hz}}$$

A complicated test mass will, however, have many resonances. It will be difficult to ensure that all of these will have high Qs and resonant frequencies. It may be necessary to keep the masses containing the cavity mirrors very simple and rigid.

A disadvantage of cavity interferometers compared to delay line detectors is the apparent necessity to use a cavity mirror mounted on a piezoelectric transducer (PZT) in order to acquire and maintain resonance of the cavities. While this may have a resonant frequency of $f_0 \sim$ 20kHz, it may also be highly damped, with $Q \sim 1$. For an effective mass of 0·2 kg, this would give thermal motion of

$$\Delta x \sim 6\times10^{-18} \text{ m}/\sqrt{\text{Hz}}$$

If the mirror was undamped, with $Q \sim 10^3$, the thermal noise might be

$$\Delta x \sim 2\times10^{-19} \text{ m}/\sqrt{\text{Hz}}$$

So the attainment of the best potential sensitivity will require high Q, high resonant frequency and a long baseline.

(2·1(vii))Acoustic Noise and Refractive Index Fluctuations

Fluctuations in the pressure of the residual gas in the vacuum system cause apparent changes in the length of the interferometer both by producing a variable force on the test masses and via fluctuations in the refractive index. At high pressure (collision time < sound wave period), these pressure fluctuations may be caused by acoustic waves. In this regime, there are two effects which determine the size of a pressure fluctuation inside the vacuum system, for a given amplitude of acoustic wave outside. One is the change in the transmission coefficient of the sound waves through the vacuum tank as the acoustic impedance of the gas changes; a gas with density ρ and sound velocity v_s has an impedance Z_a given by

$$Z_a = \rho v_s \qquad (2\cdot72)$$

The transmission coefficient T_a is then, for low Z_a,

$$T_a = Z_a / Z_{\text{vacuum tank}} \propto \rho \qquad (2\cdot73)$$

The transmitted value of a pressure fluctuation $\Delta P/P$ is therefore proportional to the density, hence the pressure. Now ΔP also decreases simply because P decreases; the size of the internal pressure fluctuations $\Delta P_i(P)$ is thus given by

$$\Delta P_i(P) = (P/P_0)^2 \Delta P_i(P_0) \qquad (2\cdot74)$$

So the effect of acoustic vibrations decreases as the square of the pressure.

At atmospheric pressure, the displacement sensitivity of the 10m interferometer is of order $10^{-12} m/\sqrt{Hz}$ (Munley 1982). If this is assumed to be due to sound waves, then the noise at pressure P would be

$$\Delta l \sim 2\times10^{-18}(P/\text{Torr})^2 \quad m/\sqrt{Hz} \tag{2·75}$$

Refractive index fluctuations will also be produced by random density changes. Now the refractive index μ is related to the number density n by

$$\mu - 1 = \gamma n/n_0 \tag{2·76}$$

For air, $n_0 = 2{\cdot}5\times10^{25}\ m^{-3}$ and $\gamma = 3\times10^{-4}$.

If the beam in the cavity has a radius w and length l, the number of molecules of mean velocity $\bar{v}$ entering the beam per second will be

$$N \approx \frac{\pi}{2} n\bar{v}wl \tag{2·77}$$

Purely random fluctuations will produce shot noise of size

$$\Delta N^2 = 2N\Delta f \approx \pi n\bar{v}wl\Delta f \tag{2·78}$$

where Δf is the measurement bandwidth. The equivalent refractive index fluctuation is just

$$\Delta\mu \approx (\gamma/n_0)(2w/\bar{v})(1/\pi w^2 l)(\pi n\bar{v}wl\Delta f)^{\frac{1}{2}} \tag{2·79}$$

which produces an apparent length fluctuation of

$$(\Delta l/l) \approx (\gamma/n_0)(P\Delta f/kTwl\bar{v})^{\frac{1}{2}} \tag{2·79}$$

For cavities of geometry similar to that in present use,

$$w^2 \approx \tfrac{1}{4}\lambda l \tag{2·80}$$

So (2·79) may be rewritten to show the dependence on arm length:

$$\Delta l/l \approx (\gamma/n_0)(2P\Delta f/kT\bar{v}\lambda^{\frac{1}{2}}\ l^{3/2})^{\frac{1}{2}} \tag{2·81}$$

Or,

$$\Delta l/l \approx 9\times10^{-19}(P/1\ \text{Torr})^{\frac{1}{2}}(l/10\ m)^{-\frac{3}{4}}\ \text{per}\sqrt{Hz} \tag{2·82}$$

So a strain sensitivity of $h \sim 3\times10^{-23}/\sqrt{Hz}$ with l = 1 km would require pressures of order 10^{-6} Torr.

Comparison with (2·75) indicates that the refractive index fluctuations will be dominated by $\sqrt{N}$ rather than acoustic fluctuations below pressures of ~0·5 Torr.

(2·1(viii))Optical Isolation

If even a small fraction of the laser light is reflected back from the detector to the laser, a significant amount of noise may be produced. Part of the effect of the return beam is simply to increase the magnitude of the low frequency laser noise; probably more important is the production of noise around the RF modulation frequency. This is a very complex problem, with many possible ways in which noise may be produced. The seriousness of the situation may, however, be indicated by a relatively simple example.

The light reflected from the central mass is Doppler shifted due to the swinging at the pendulum frequency. If the motion is 1μm, the peak frequency deviation is 25 Hz. Some of this reflected light will re-enter the laser, while some will be reflected off the laser output mirror. The latter component will be able to interfere with the main beam and, since it contains the RF phase modulation, produce noise around the modulation frequency. Most of this noise will be in a ~25 Hz bandwidth, but high frequency noise may be produced by the coupling in of intensity fluctuations. This is essentially the same situation as that discussed in section 2·1(iii). If the fractional amplitude of the light returning to the laser is A_R and θ is the phase difference between the interfering beams, then the mixed-up apparent low-frequency phase fluctuation produced by an intensity fluctuation $\delta I/I$ is

$$\delta\phi(\omega) \sim A_R \sin\theta(\delta I(\omega)/I) \qquad (2\cdot83)$$

Now θ is varying due to the Doppler shift:

$$\theta \sim \theta_0 \sin\omega_0 t \qquad (2\cdot84)$$

where θ_0 might be as large as 150 rad/s. Equation (2·83) may be expanded in terms of Bessel functions:

$$\delta\phi(\omega) \sim 2A_R(\delta I(\omega)/I)\sum_{n=0}^{\infty} J_{2n+1}(\theta_0)\sin\left[(2n+1)\omega_0 t\right] \qquad (2\cdot85)$$

So noise components are produced at $\omega\pm(2n+1)\omega_0$, or $f \pm (\lesssim 25\text{Hz})$: the swinging of the mass effectively smooths out the intensity noise spectrum.

If only a quarter-wave plate-polariser combination is used to provide isolation, A_R might be $\sim 3\times10^{-2}$, with $\delta I/I \sim 5\times10^{-5}/\sqrt{\text{Hz}}$ at 1 kHz. Crudely guessing the sum to be of order unity at a particular frequency then gives a phase noise of

$$\delta\phi \sim 3\times10^{-6} \text{ rad}/\sqrt{\text{Hz}} \text{ at } 1 \text{ kHz}$$

This is four orders of magnitude larger than the shot noise on 1 W of light. An acousto-optic modulator, which frequency shifts the return light out of the region of interest, might reduce A_R by a further factor of 30, giving

$$\delta\phi \sim 10^{-7} \text{ rad}/\sqrt{\text{Hz}} \text{ at } 1 \text{ kHz}$$

Excess high-frequency noise may also be produced by fluctuations in the laser gain affecting the size of the RF sidebands on the light re-entering the laser. Since the sidebands will not suffer from the gain saturation produced the main beam, they may have considerably larger amplitudes than might be thought. The gain fluctuations may be intrinsic to the laser (such as those which produce intensity noise) or be the result of geometry fluctuations of the returning beam.

This noise around the modulation frequency sets a limit on how well the laser may be stabilised; it may

therefore appear as noise at the interferometer output if subtraction is not used or is imperfect. If the excess intensity noise is N times the shot noise in the output light power and the detector is to reach a shot-noise limited sensitivity, then some form of subtraction must be used with effective finesses matched to within

$$\Delta F/F < 1/N \qquad (2\cdot86)$$

Thus, even with the figures quoted above, acheivement of a shot-noise limited sensitivity on 10 mW of light would require effective finesses matched to within 3%.

Improvement of the optical isolation is evidently required. This may be achieved by the use of further acousto-optic (or Faraday) isolators in series, at the cost of complexity and loss of light. In addition, application of the phase modulation <u>after</u> a mode cleaning cavity (Chapter 4) of linewidth smaller than the modulation frequency will reduce the sideband amplitude returning to the laser. For the cavity currently in use, the possible improvement factor with 24 MHz modulation is approximately 8.

(2·1(ix))Other Noise Sources

Various important noise sources have already been discussed and another, laser beam geometry fluctuations, will be considered in the next Chapter. Other noise sources that have been conceived, while not negligible, are probably less important.

Weiss (1972) pointed out that fluctuating gravitat-

ional gradients caused by moving objects or atmospheric density changes would produce arm-length fluctuations. This has been analysed by Saulson (1982), who found that the displacement noise might be of order

$$\Delta l \sim 10^{-16}/f^{7/2} \quad m/\sqrt{Hz}$$

for $f \lesssim 20$ Hz. With a detector of arm-length 1 km, gravity gradient noise would limit the attainment of $h \sim 10^{-23}/Hz$ to above 10 Hz.

Collision of cosmic rays with the test masses might produce occasional impulsive changes to the detector length. Weiss (1972) estimated that cosmic ray muons might produce events with $\Delta l \sim 10^{-19}$ m once a year with 10 kg test masses. So $l > 100$ m or $m > 10$ kg is desirable if events of $h \sim 10^{-21}$ are being searched for. Monitoring of the arrival of cosmic ray showers will probably be needed during searces for pulses of gravitational waves. Magnetic monopoles may also be able to produce significant pulses (Michelson 1983).

Weiss (1972) also considered the effect of low frequency electromagnetic pulses, perhaps generated by ionospheric storms. While it seems unlikely that these would be of significant size, monitoring would be desirable. Such storms do, in principle, have the ability to generate coincident pulses at separated detectors.

(2·2)Design and Operation of the Glasgow Detector

This section will attempt to describe the design, construction and operation of the 10 m optical cavity

gravitational-wave detector at Glasgow. The material described is therefore the work of the whole Glasgow group.

The construction of a prototype gravitational-wave detector using a laser interferometer of arm length 10 m was started at Glasgow in late 1978, with the first investigations into its performance becoming possible in 1980 (see Munley 1982 for details). This first version used three-mirror ring cavities in the interferometer arms to avoid optical feedback to the laser and contained no facility for optically recombining the beams from the two cavities. A typical sensitivity of this interferometer is shown in fig 2·5. This experience emphasised the need for very good seismic and acoustic isolation to reduce noise below 1 kHz, excellent frequency stabilisation (and possible subtraction)to reduce noise at higher frequencies together with the possibility of reducing beam positional fluctuations. These improvements were incorporated in a major reconstruction which lasted from late 1981 to early 1983.

Each test mass is suspended as a pendulum using steel wire, providing seismic isolation while allowing the mass to respond freely to a gravitational wave. In addition, the point of suspension of the pendulums is now the top of a five-element lead and rubber stack of resonant frequency ~10 Hz. This provides further seismic and acoustic isolation. The suspension is shown in fig 2·6; the development of the suspension system and orientation controls by the Glasgow group is described by Robertson (1981) and Munley (1982). It can be seen that the test mass itself is suspended by three wires from a triangle, which in

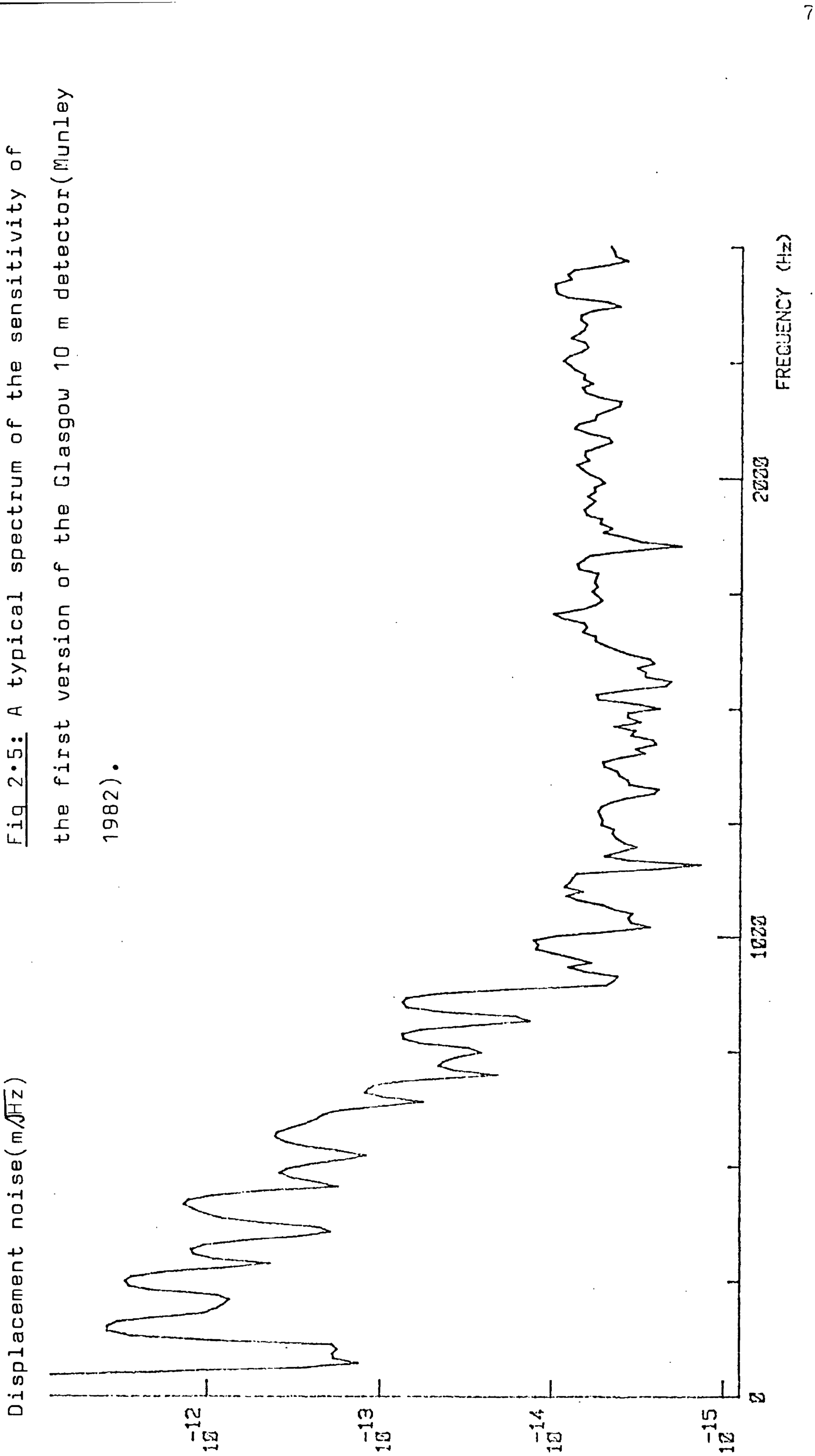

Fig 2·5: A typical spectrum of the sensitivity of the first version of the Glasgow 10 m detector(Munley 1982).

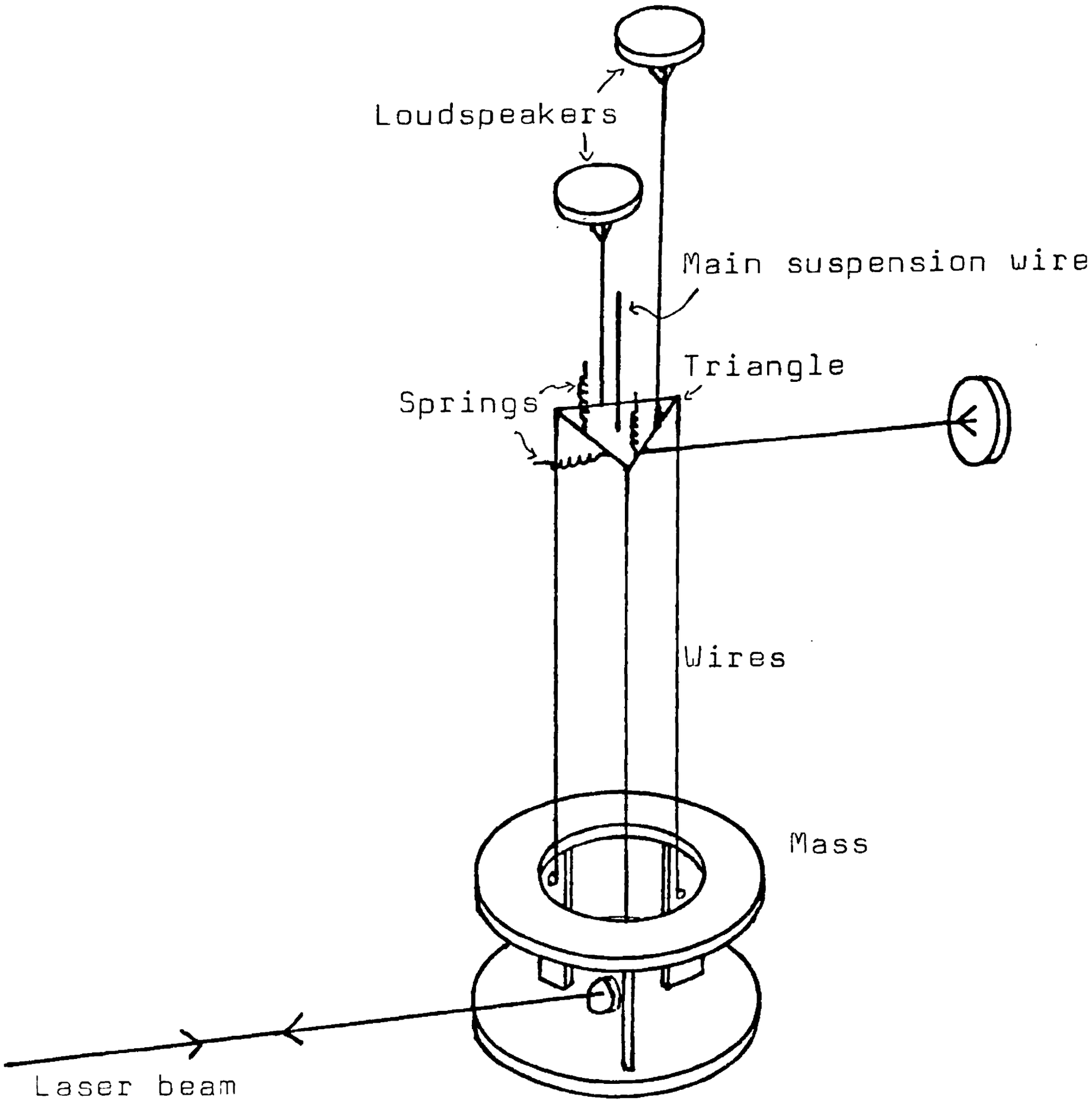

Fig 2·6: Diagram of the suspension of one of the test masses.

turn is suspended from the top of the stack by a single wire. The triangle may be rotated or tilted by varying the current flowing in the loudspeakers, which are tensioned via springs. This enables the orientation of the masses to be controlled. Now if the cavities are to remain resonant, the orientation of the masses must be stable to within an angle of (cf. 3·15)

$$\delta\theta \ll \lambda/\pi w \qquad (2\cdot88)$$

where w is the beam size in the cavity. For the 10 m cavities, $w \approx 1$ mm so $\delta\theta \ll 10^{-4}$ rad. Maintenance of such pointing accuracy requires the use of servo systems. The orientation of a test mass is monitored by using a resistive-sheet position-sensitive photodiode to detect the change in position of a He-Ne laser beam reflected off a mirror on the mass. Deviations from the set position are then minimised by feeding back onto the loudspeakers. This set position is conveniently adjusted by using a FET as a variable load resistor for the photodiode current. The feedback signal is arranged to include some differentiated position signal to provide damping. These orientation control servos are arranged to work only at low frequencies: they are rolled off very strongly above ~30 Hz to ensure that no noise is produced at gravitational-wave frequencies. It will become apparent that servo systems which only function within a certain frequency region are a common feature of the detector.

The orientation control servos have a loop gain, hence a suppression factor for the fluctuations, of about 30 dB at 1 Hz. This gives a final pointing accuracy of $\delta\theta \sim 10^{-5}$ rad, which seems perfectly adequate. The loud-

speakers give a dynamic range of $\sim 10^{-2}$ rad. While this is sufficient for normal operation, drift of the rubber in the stacks when the system is evacuated produces rather larger motions. This problem is overcome by designing the top of the stack so that it may be rotated or tilted by DC motors, controllable from outside the vacuum system (this idea originated at Caltech).

All wires leading to the top of the stack were made as light as possible and looped loosely between successive lead elements: the resulting acoustic impedance mismatch minimises the transmission of sound along the wires.

The present interferometer uses two-mirror optical cavities, with a one inch diameter plane mirror on the central mass and mirrors of radius of curvature 15 m on the end masses (giving good mode separation – see Chapter 3). Two-mirror cavities involve the minimum number of reflections, hence the minimum losses, giving the best potential sensitivity. Their property of giving a reflected beam which is exactly coincident with the incoming laser beam produces, however, isolation problems for the laser and necessitates the use of some additional technique if the reflected beam is to be observed. The method adopted at Glasgow (e.g. Drever 1983) utilises the phase change on reflection which converts an incident left-handed circularly polarised beam into a right-handed circularly polarised reflected beam; the two polarisations may then be separated by a quarter-wave plate-polariser combination (see fig 2·7).

It can be seen that the optical arrangement on the central mass allows the beams from each cavity separately,

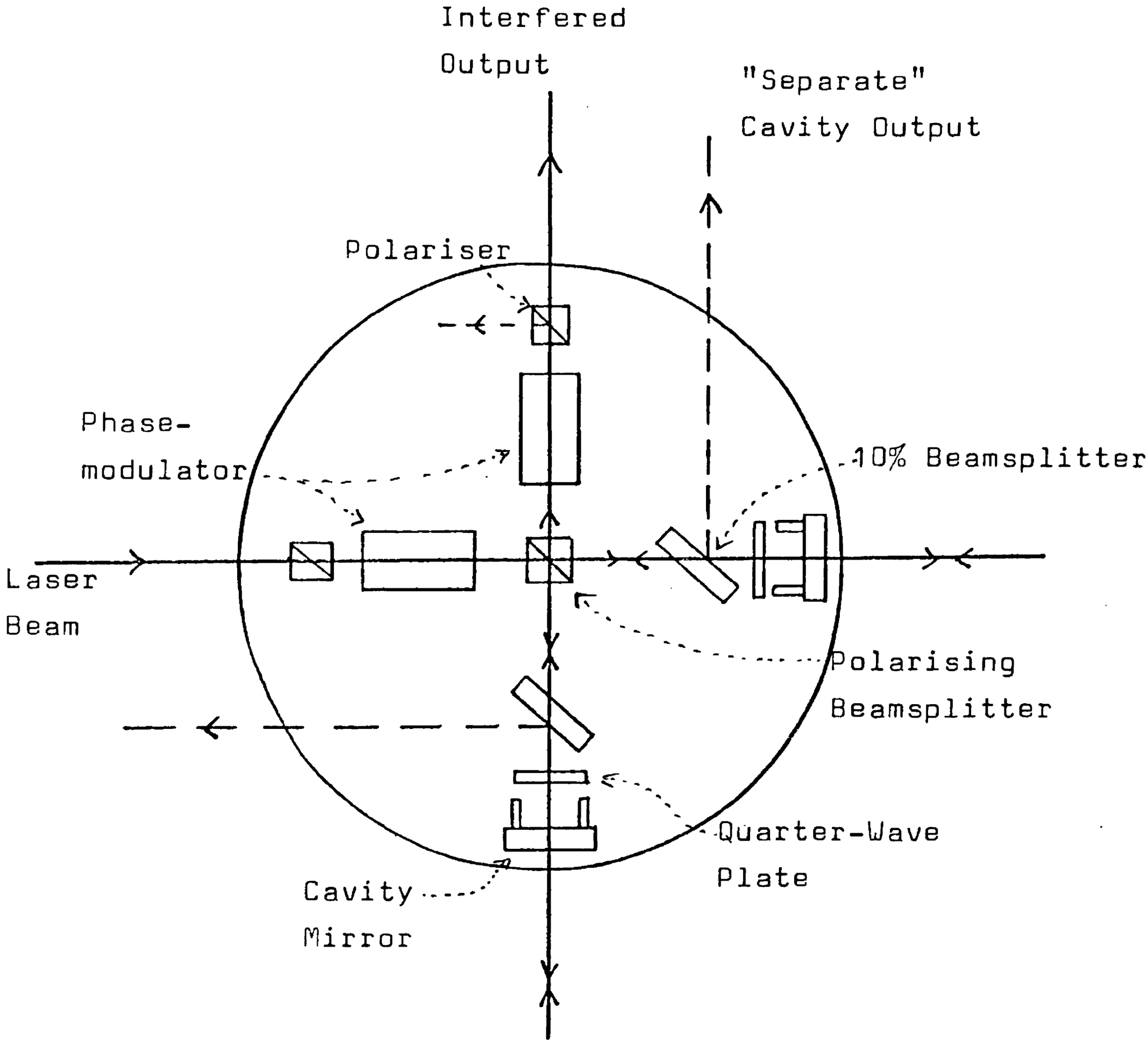

Fig 2·7: An indication of the optical arrangement on the lower tier of the central mass.

or the interfered beams, to be observed. The first phase modulator provides the signal for the frequency stabilisation. Since this modulation is effectively removed from the intra-cavity beams (the sidebands are not on resonance), a second phase-modulator is necessary if the beams are to be interfered. This second Pockels cell may provide both modulation and control of the relative phases of the two combining beams.

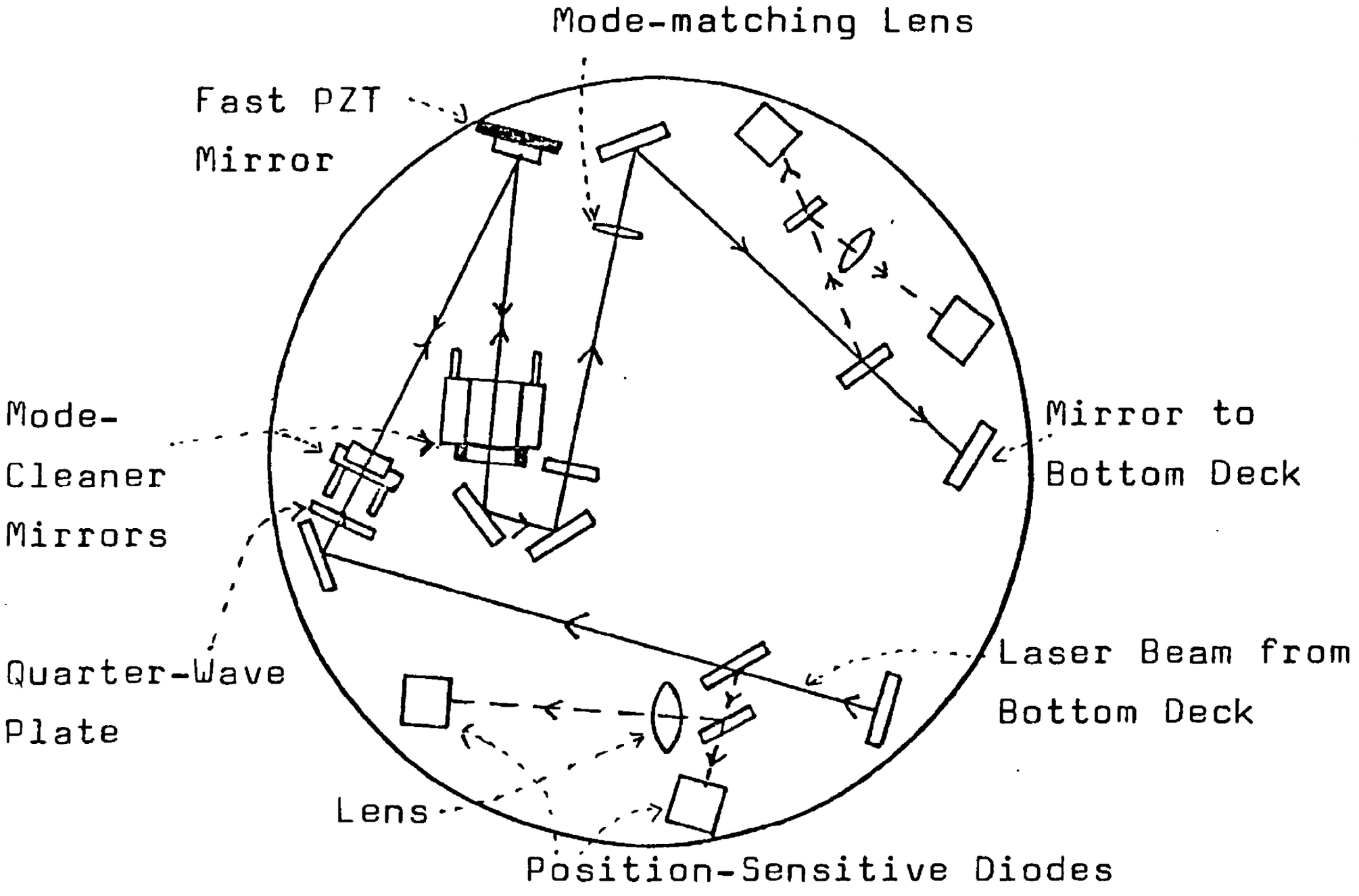

Fig 2·8: An indication of the optical arrangement on the upper tier of the central mass.

The central mass is composed of two tiers: the lower contains the optical arrangement shown in fig 2·7, while the upper, shown above in fig 2·8, supports the mode-cleaning cavity (section 4·2) and the position-sensitive photodiodes for the beam steering system (section 4·3). With both sections in use, the incident beam is steered onto the top deck, passes through the mode-cleaner and, via beam handling mirrors and mode-matching lenses, is returned to the lower deck and the interferometer. Alternatively, the beam may enter the lower tier directly,

with a portion of the beam split off to provide light for the position-sensing diodes which enable the beam position to be "locked" with respect to the central mass. In this case, lenses on the optical bench outside the vacuum system are chosen to ensure the correct size and curvature of the beam for efficient coupling into the detector cavities (i.e. proper mode-matching).

Rotation and tilt of the mode-cleaner and interferometer cavity mirrors, together with rotation of the beam-splitter, are adjustable via DC motors. This allows remote alignment of the cavities. Information about the motor to be selected, the amplitude and direction of its motion is carried on a pulsed infra-red signal which is received and decoded on the central mass, a system designed by H. Ward.

The cables that connect the items on the central mass to the top of the stack are made as light as possible, to avoid both damping and acoustic transmission. Signals from the quadrant diodes use twisted pairs of 44 gauge copper wire, whilst the RF modulation is transmitted via 50Ω co-axial cable of diameter 8×10^{-3}inch.

In operation, the frequency of the laser is controlled to maintain its resonance with one cavity and the length of the second cavity is adjusted to keep on resonance with the laser light. The amount of this required adjustment (within a certain frequency range) is the gravitational-wave signal.

It has already been seen that the technique of phase modulating the incident light at a high frequency and then

observing the light reflected off the input cavity mirror provides a good measure of the frequency difference between cavity and light. The aim of the stabilising system is thus to minimise this error signal. The laser frequency is controlled by means of a Pockels cell in the laser cavity — a voltage applied to the Pockels cell alters its optical length, hence the length (frequency) of the laser cavity. The great advantage of such a system is the possibility of acheiving a wide bandwidth in the feedback system, for Pockels cells are not plagued by resonances in the same way as piezoelectric transducers. Large bandwidth is vital if high loop gain and so a high degree of stabilisation is to be achieved. It also helps in the acquisition of lock, when the system is non-linear (see Appendix 3).

The present intra-cavity Pockels cell consists of two crystals, each with Brewster windows to minimise losses and balanced to avoid deflecting the beam. The change in the length of the laser cavity is 0·4 nm/V, equivalent to 2 nm/V in the 10 m cavities. While this is sufficient to compensate for the noise above a few hertz, it is not large enough to enable the laser frequency to track slow drifts or 1 Hz pendulum motions of the cavity. At these low frequencies, the length of the cavity is forced to follow changes in the laser frequency by means of feedback onto bimorph PZTs pulling on the suspension wires. Driven by 100 V amplifiers, these PZTs have a considerable range ($\sim 40\lambda$), enabling resonance to be maintained for long periods of time.

Fig 2·9 shows the feedback circuit for the PZT wire

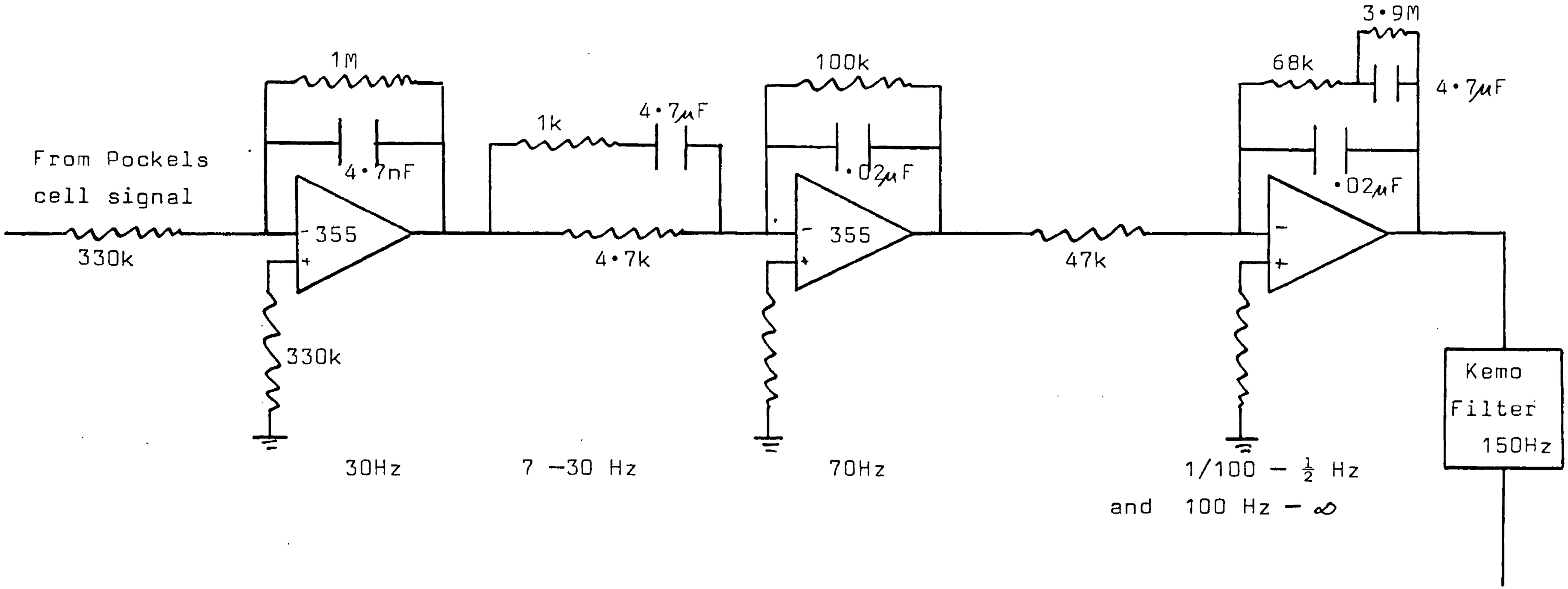

Fig 2·9: The feedback circuit to the wire pullers in the primary cavity. The Kemo is a multi-pole low-pass filter. The characteristic frequencies of the various filters are indicated.

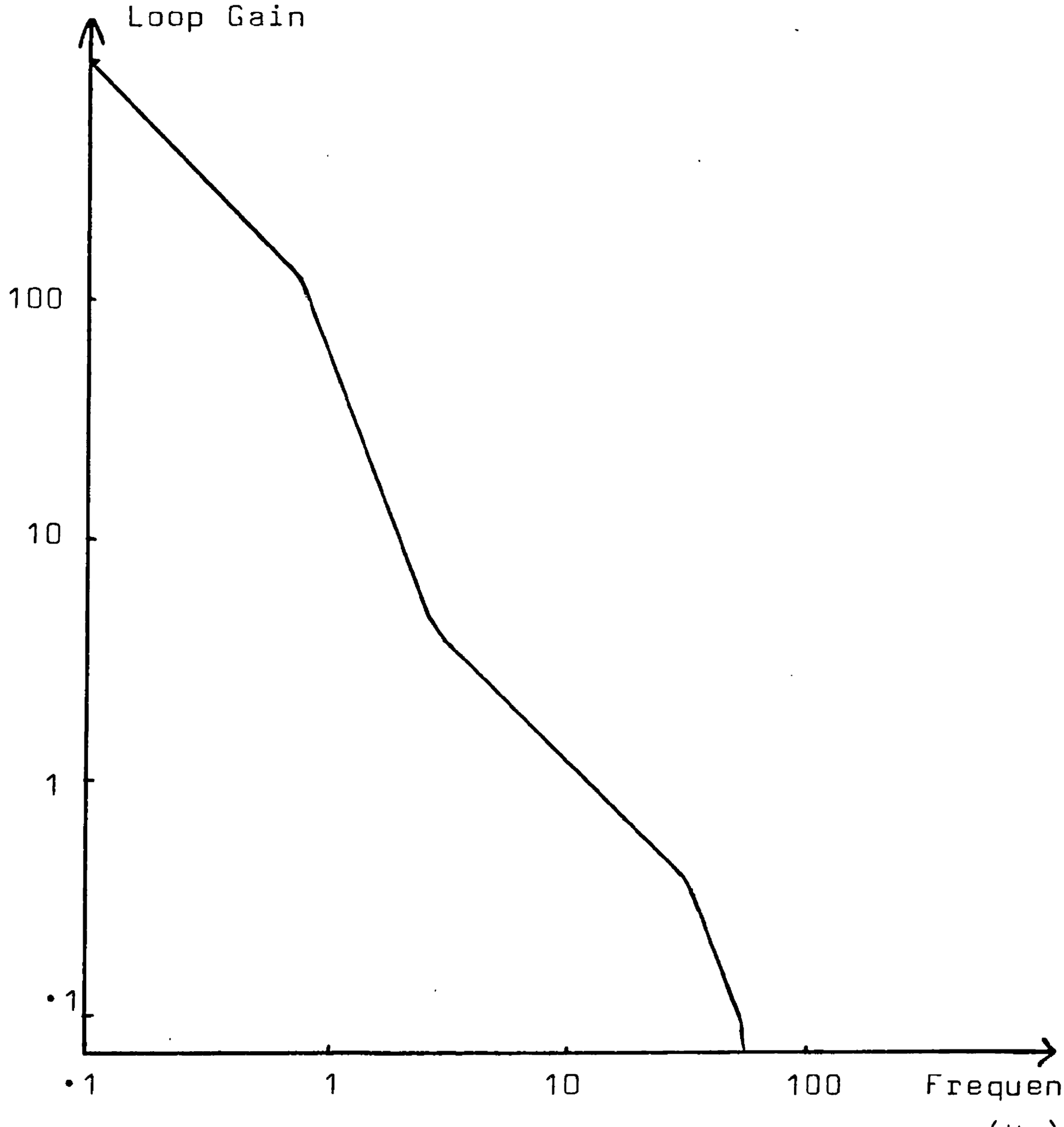

Fig 2·10: An approximate indication of the variation of the gain of the PZT wire-pulling feedback system with frequency. The values of loop gain shown are typical of normal operation.

pulling system, while fig 2·10 indicates the corresponding frequency response (including the double integration of the pendulum suspension). The unity gain frequency may be as high as 30 Hz, limited by a (mechanical) resonance at just above 100 Hz. The numerous integrations above 100 Hz are to avoid exciting the wire resonances at 640 Hz. In principle, higher loop gain at low frequency could be

acheived by raising the lower frequency of the differentiation. This is not practically possible, however, without exciting resonances (perhaps in the stack) at 10 and 15 Hz. So, considering the mechanical problems, the filtering is probably not far from being optimum. At least for the primary cavity, to which the laser is locked, the performance of the PZT wire pullers seems quite adequate.

The feedback circuit to the Pockels cell in the laser is indicated in fig 2·11. It will be seen that two sets of amplifiers are used in parallel to acheive the combination of high dynamic range at low frequency and high overall bandwidth (Helmcke et al 1982). This enables loop gains of $\sim 10^5$ to be achieved at ~100Hz (see Chapter 5).

Thus, the combination of Pockels cell and PZTs maintains the primary cavity on resonance with the laser light. While the laser frequency is absolutely stable at high frequencies, the motion of the cavity means that the frequency still fluctuates considerably below a few Hz. This, together with the independent motions of the secondary cavity at low frequencies, produces a requirement for some means of controlling the length of the second cavity so that it, too, resonates with the laser light. Because of the highly non-linear nature of the fringes,a reasonable bandwidth is required for this length controlling system even if the motion to be corrected is only low frequency (see Appendix 3). Thus, PZTs pulling on the suspension wires alone are not sufficient, even though their range is adequate. This problem is currently solved by mounting the cavity mirror (of the secondary cavity end mass) on a tubular PZT. This has a first resonance

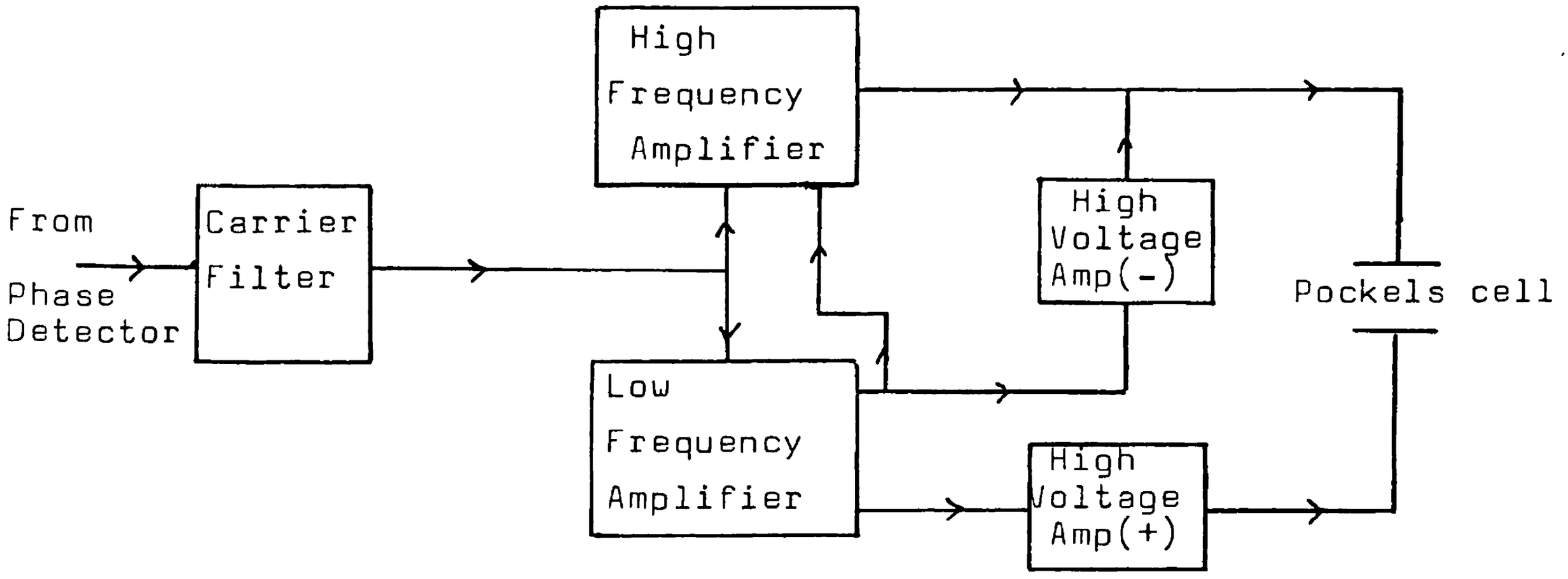

Fig 2·11: A block diagram of the fast feedback system to the Pockels cell in the laser.

at 22 kHz, damped by a rubber compound; sufficient gain and bandwidth may (just) be achieved to give reasonable operation (see fig 2·12 for a diagram of the feedback system). Use of such a PZT produces potential problems with thermal noise (section 2·1(vi)) and electrical pick-up, but these may not be insuperable.

The operation of the detector thus consists of locking the laser frequency to the first cavity via the Pockels cell (helped by the PZTs) and then locking the second cavity to the stabilised laser light by adjusting its length with the PZTs pulling the suspension wires and moving the mirror. Well below the unity-gain frequency of this secondary cavity stabilisation loop (~5 kHz), the measure of the detector sensitivity, or gravitational wave amplitude, is just the motion of the PZT-driven mirror.

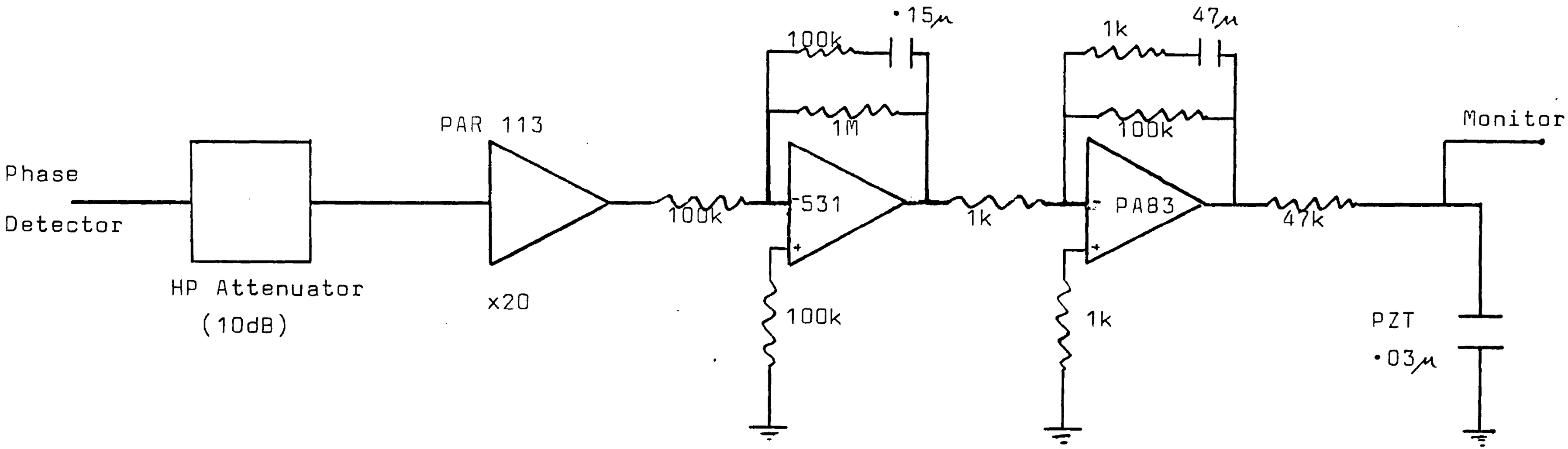

30kHz Low pass	1Hz – 10Hz	30Hz – 3kHz	100Hz – ∞

Fig 2·12: Circuit diagram for the secondary cavity stabilisation loop. The gain is rolled off so that it reaches unity by about 5 kHz, to avoid exciting the 22 kHz resonance of the PZT. The final stage (PA83) has a range of ±100V.

At higher frequencies, the output of the phase-sensitive detector observing light from the second cavity provides a measure of the changes in length of the cavity. These observed noise levels will be discussed in detail in Chapter 5. Before then, it is necessary to consider the significance and suppression of laser beam geometry fluctuations.

CHAPTER THREE

LASER BEAM GEOMETRY FLUCTUATIONS — IMPORTANCE, MEASUREMENT AND SUPPRESSION

(3·1)Introduction

Laser beam geometry fluctuations are changes in the size, shape and position of a laser beam. Preliminary work, both at Glasgow and at Munich (Rüdiger et al 1981), indicated that these fluctuations may cause phase changes in the interfered light, setting a serious limit to the sensitivity of the gravitational wave detector. A considerable fraction of my work has gone towards investigating this problem: elucidating the coupling mechanisms and significance of the geometry fluctuations to the interferometer, measuring the positional fluctuations and developing various techniques for suppressing them by large factors ($\gtrsim 100$). It will be seen that for much of this work it is appropriate to consider laser beam geometry changes as fluctuations in the radial mode content of the beam, a point of view which is discussed in the next section.

(3·2)Laser Beam Modes

A laser beam is formed by optical resonance in a cavity formed by two (usually spherical) mirrors. Any cavity with spherical mirrors may reduced to an equivalent confocal cavity (e.g. Kogelnik and Li 1966) such as that shown in fig 3·1 .

Now the field distribution which will result when

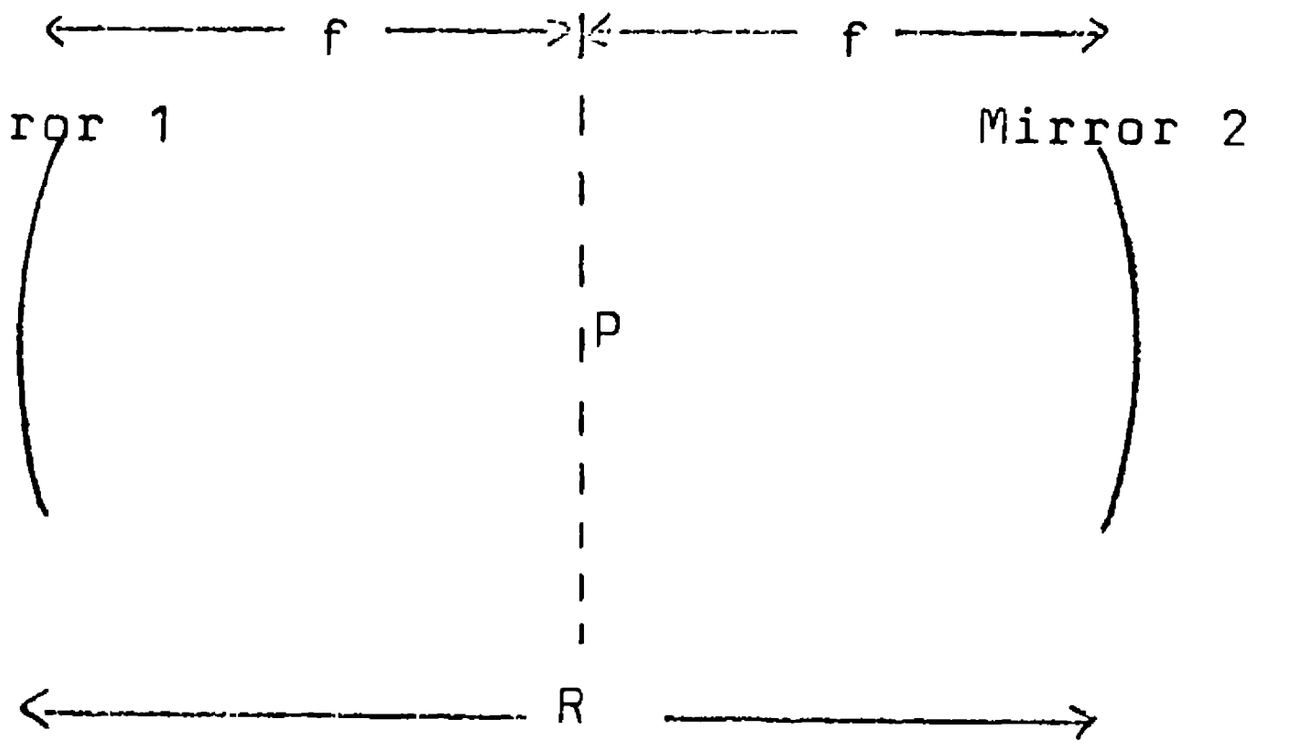

Fig 3·1: A confocal cavity consisting of two equal mirrors of radius of curvature R and focal length f. Both focal points lie in the plane P.

the material in the cavity lases will be determined by the necessity for it to resonate inside the cavity — it must be self-reproducing on a transit of the cavity. A set of such resonating field distributions exists — the normal modes of the cavity. For mirrors which are large compared with the beam size, it can be seen straightforwardly that the normal modes must be the set of functions which are their own Fourier transform. For consider an initial field distribution in the central plane P, travelling to the right. Since P is the front focal plane of mirror 2, the reflected field distribution back in P will just be the Fourier transform of the initial field

distribution, but travelling to the left. For resonance, however, the field distribution travelling in both directions must be the same. The set of resonant field distributions is therefore composed of those which are their own Fourier transforms. In rectangular Cartesian co-ordinates (x,y,z) aligned along the cavity axis, the modes are thus Hermite-Gaussian functions (Boyd and Gordan 1961); the field distribution E(x,y) is

$$E(x,y) = \sum_n \sum_m A_m h_m(x) A_n h_n(y) \qquad (3\cdot1)$$

with A_m, A_n amplitude coefficients and $h_m(x)$, $h_n(y)$ the normal modes. It is convenient to work in normalized co-ordinates $X = \sqrt{2}x/w$, $Y = \sqrt{2}y/w$ (w is the beam size) in which

$$h_m(X) = \frac{\Gamma(\frac{1}{2}m+1)}{\Gamma(m+1)} H_m(X) e^{-X^2/2} \qquad (3\cdot2)$$

where $H_m(X)$ is a Hermite polynomial:

$$H_m(X) = (-1)^m e^{X^2} (d/dx)^m e^{-X^2} \qquad (3\cdot3)$$

For example, $H_0(X) = 1$, $H_1(X) = 2X$ and $H_2(X) = 4X^2-2$; some low order mose are illustrated in fig 3·2.

Now the modes are orthogonal; this means that the mode structure (i.e.the value of the amplitude coefficients A_m, A_n) is independent of the distance along the beam axis, even after the beam has "leaked" out of the cavity. This is one reason why it is so useful to express beam geometry fluctuations as changes in the mode amplitude coefficients. As the beam propagates, the relative <u>phase</u> of the modes does, however, change; if ϕ is the phase change of the laser light relative to a plane wave then (e.g. Kogelnik and Li 1966)

$$\phi = (m+n+1)\arctan(\lambda z/\pi w_0^2) \qquad (3\cdot4)$$

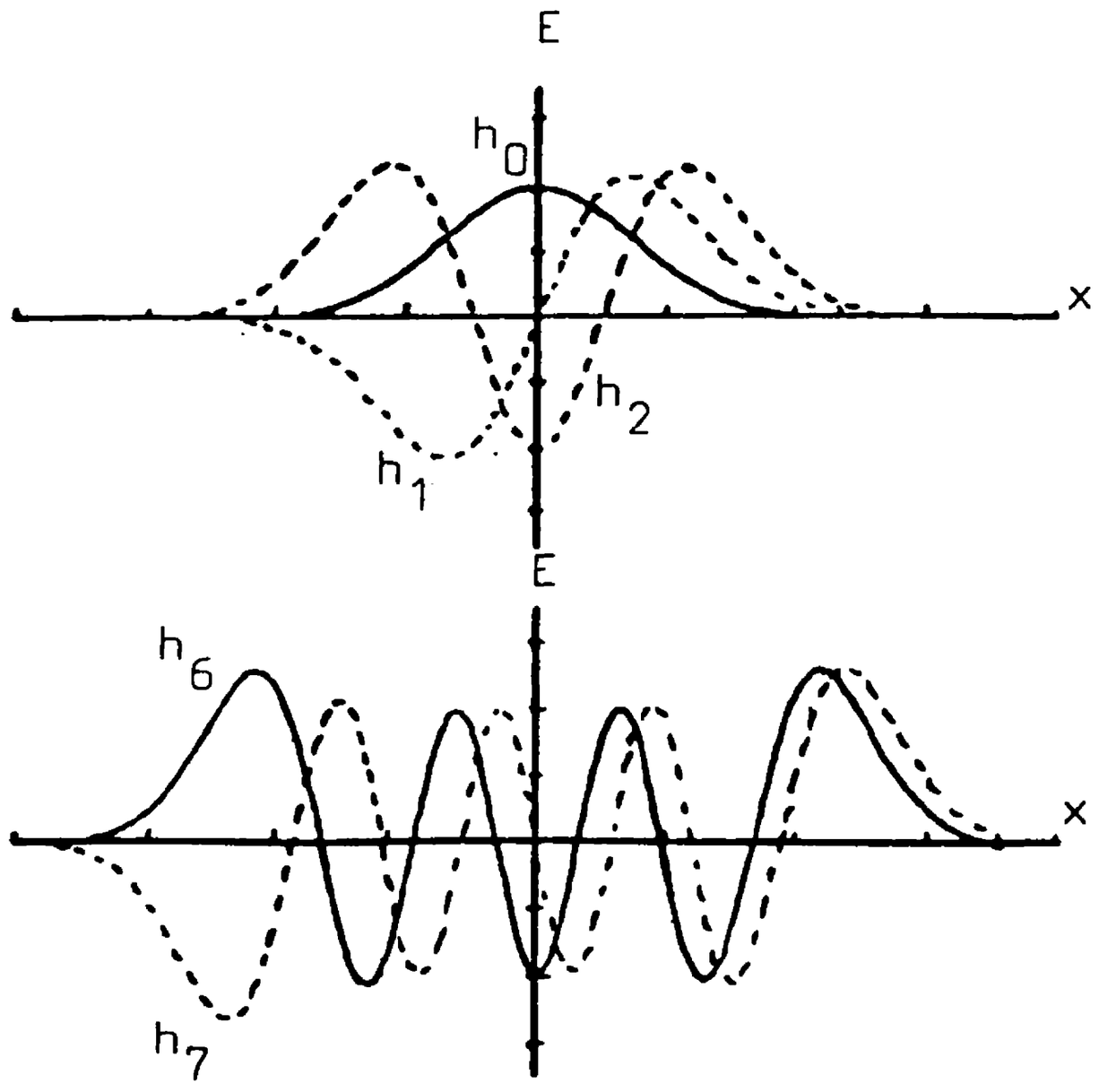

Fig 3·2: The field distribution E(x) corresponding to some low order laser beam modes (after Rüdiger et al 1981).

Here λ is the wavelength and z the axial distance travelled away from a beam waist of size w_0. Thus, the modes have different phase velocities; in turn, this means that they have different resonant frequencies in an optical cavity. The frequency difference $\Delta\nu$ of modes separated by Δq in longitudinal mode order and $\Delta(m+n)$ in radial mode order is (Kogelnik and Li 1966)

$$\Delta\nu = \nu_0(\Delta q + C\Delta(m+n)) \qquad (3\cdot5)$$

where ν_0 is the free spectral range (c/2d) and C is a constant depending on the geometry of the cavity: if a cavity has mirrors of radii of curvature R_1, R_2 separated by a distance d, then

$$C = \frac{1}{\pi}\arccos\sqrt{(1-d/R_1)(1-d/R_2)} \qquad (3\cdot6)$$

For the present 10 m cavities, C = 0·304.

Now the transmitted <u>amplitude</u> of any mode through

an optical cavity is just

$$\left|\frac{A_m(\delta)}{A_m(0)}\right| = (1 + F'\sin^2\delta/2)^{-\frac{1}{2}} \qquad (3\cdot7)$$

where F' is the coefficient of finesse ($F' = 4F^2/\pi^2$) and δ is the phase difference for one round trip in the cavity (cf. section 2·1(i)). But this phase difference is

$$\delta = 2d\Delta k = 4\pi d\Delta\nu/c = 2\pi\Delta\nu/\nu_0 \qquad (3\cdot8)$$

Thus,

$$\left|\frac{A_m(\Delta\nu)}{A_m(0)}\right| = \left[1 + (4F^2/\pi^2)\sin^2(\pi\Delta\nu/\nu_0)\right]^{-\frac{1}{2}} \qquad (3\cdot9)$$

So if a cavity is of a length that the fundamental mode h_0 is on resonance, other mode amplitudes will be suppressed by a factor

$$S_m = \left[1 + (4F^2/\pi^2)\sin^2(\pi\Delta\nu/\nu_0)\right]^{\frac{1}{2}} \qquad (3\cdot10)$$

To completely describe a field distribution E(X)E(Y) it is necessary to specify the (complex) mode amplitudes A_m, A_n. Since $h_m(X)$ are orthogonal, the amplitudes are just given by

$$A_m = \frac{\int_{-\infty}^{\infty} E(X)h_m(X)dX}{\int_{-\infty}^{\infty} h_m(X)h_m^*(X)dX} \qquad (3\cdot11)$$

Or,

$$A_m = \frac{(2/\pi)^{\frac{1}{2}}}{\sqrt{(\frac{1}{2}m+1)2^m}} \int_{-\infty}^{\infty} E(X)H_m(X)e^{-X^2/2}dX \qquad (3\cdot12)$$

The corresponding power in each mode, relative to that in the fundamental, is given by

$$I_m/I_0 = \frac{A_m^2\int_{-\infty}^{\infty} h_m(X)h_m^*(X)dX}{A_0^2\int_{-\infty}^{\infty} h_0(X)h_0^*(X)dX} \qquad (3\cdot13)$$

Or,

$$I_m/I_0 = \left[\frac{A_m}{A_0}\right]^2 \left[\frac{\Gamma(\frac{1}{2}m+1)}{\Gamma(m+1)}\right]^2 2^m m! \qquad (3\cdot14)$$

An important example of the application of (3·12) is the excitation of higher modes when a beam, initially containing only the fundamental, moves sideways by δX; the mode amplitudes are then

$$A_m/A_0 = \frac{\exp(-\delta X^2/4)}{\Gamma(\frac{1}{2}m+1)} (\delta X/2)^m \qquad (3\cdot15)$$

For an angular change $\delta\theta$, which requires a phase gradient across the beam, this expression is multiplied by i^m and δX is replaced by $\sqrt{2}\pi w\delta\theta/\lambda$. It can be seen from (3·15) that small positional fluctuations (δX, $\sqrt{2}\pi w\delta\theta/\lambda \ll 1$) may be regarded as consisting of changes in the amplitude solely of the first order mode $m = 1$. Note that $\Gamma(N+\frac{1}{2}) = (\sqrt{\pi}/2^N)(2N-1)!!$, so that $\Gamma(\frac{1}{2}+1) = \sqrt{\pi}/2$.

It is not immediately obvious how to reconcile this picture of, say, an angular change in the beam as a fluctuation in the first order mode 90^o out of phase with the fundamental with the requirement that the lateral displacement of the beam must increase linearly with distance along the beam. That the two viewpoints are equivalent is shown in Appendix 7.

A beam size change δw implies, via (3·12), a change in the amplitude coefficients of all even modes. For small fluctuations, it is only necessary to consider the second order mode:

$$\delta A_2/A_0 = \tfrac{1}{2}\delta w/w \qquad (3\cdot16)$$

Similarly, a ripple on the intensity of form $\cos\Omega X$ will excite mode amplitudes

$$A_m \propto (\Omega\sqrt{2})^m \exp(-\Omega^2/2) \qquad (3\cdot17)$$

This is a maximum when $m = \Omega^2$.

We have seen that laser beam geometry fluctuations are readily expressible in terms of changes in the amplitudes of beam modes. It will become apparent that this facilitates the analysis of the effect of such fluctuations on the gravitational wave detector, as well as suggesting ways in which the geometry fluctuations might be reduced.

(3·3)The Importance of Beam Geometry Fluctuations

Laser beam geometry fluctuations will be a noise source in the gravitational wave detector if they produce relative phase fluctuations between the two interfering light beams. There are at least two basic mechanisms by which this may occur (each of which is discussed below): coupling throwgh a static phase difference between the recombining beams (as suggested by Rüdiger et al 1981) and a modulation by the geometry fluctuations of the amplitude of scattered light.

(3·3(i))Coupling Through a Static Phase Difference

Consider the case of two interfering beams, each with an intensity distribution $I(x,y,t)$, having a static phase difference $\phi(x,y) + \pi$. The measured phase difference between the two beams is then, for small $\phi(x,y)$,

$$\Delta\phi = \frac{\int_{-\infty}^{\infty}\int_{-\infty}^{\infty} I(x,y,t)\phi(x,y)\,dxdy}{\int_{-\infty}^{\infty}\int_{-\infty}^{\infty} I(x,y,t)\,dxdy} \qquad (3\cdot18)$$

If the intensity profile fluctuates by $\delta I(x,y,t)$ around an average value of $I_0(x,y)$, then the resultant phase

fluctuation is

$$\delta\phi = \frac{\int_{-\infty}^{\infty}\int_{-\infty}^{\infty}\delta I(x,y,t)\phi(x,y)\,dxdy}{\int_{-\infty}^{\infty}\int_{-\infty}^{\infty}I_0(x.y)\,dxdy} \qquad (3\cdot19)$$

One of the most important examples of this is the situation of the two beams recombining at a small angle α, so that $\phi(x,y) = k\alpha x$, with a lateral beam jitter $\delta x(t)$ at the point of interference. The spurious phase signal is then simply

$$\delta\phi = k\alpha\delta x(t) \qquad (3\cdot20)$$

The relative angle of the two beams might arise, for example, from a misalignment of the beamsplitter, which can only be adjusted easily to within $\sim 10^{-5}$rad. It will be seen in section 3·4(i) that the positional fluctuations of the Ar^+ laser beam are of the order of $5\times10^{-9}\,m/\sqrt{Hz}$ at 1 kHz, implying a phase noise of $\sim 6\times10^{-7}\,rad/\sqrt{Hz}$. This is a factor of approximately 2000 worse than the shot noise on 1 W of light; with a finesse of 200 and visibility of 40%, it is equivalent to a displacement noise of $1\cdot5\times10^{-15}\,m/\sqrt{Hz}$. The seriousness of this noise is evident.

At first sight one might think that this noise would only arise in that component of the light which was directly reflected off the input mirror of the interferometer cavities, for the component emerging from the cavities has its positional fluctuations suppressed (cf. 3·10). The relative phase of the light <u>entering</u> the cavities still fluctuates, however. If the visibility is poor, this phase noise on the intra-cavity beam <u>will</u> produce slightly less equivalent displacement noise than that on the directly reflected component, simply because of the

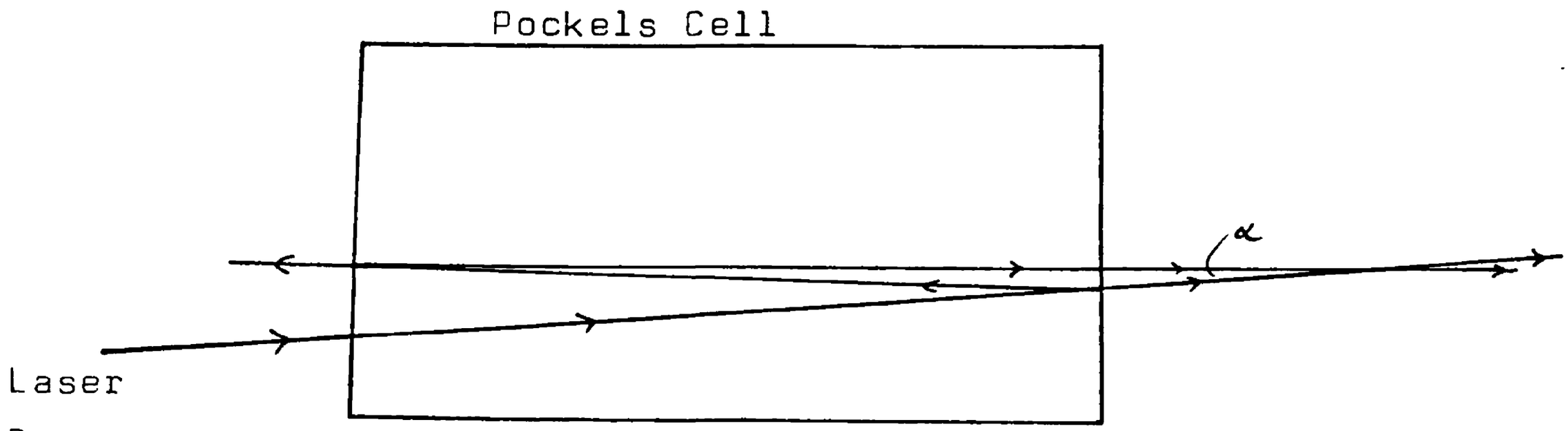

Fig 3·3: An indication of how internal reflections within a Pockels cell may lead to two beams interfering at a small angle α, if the two faces of the Pockels cell are not perfectly parallel.

smaller size of the intra-cavity beam.

Another way in which the interference of two misaligned beams may arise is by multiple reflections inside a phase-modulating Pockels cell (see fig 3·3). The angle α is determined by the angular offset (wedging) between the two faces of the Pockels cell. If a fraction η of the intensity is reflected at each end of the Pockels cell, then the weak beam will have have an amplitude η relative to that of the main beam (typically $\eta \sim 10^{-2}$). For small α, when the two beams still overlap, the phase noise will be (cf. 3·20)

$$\delta\phi \sim \eta \alpha k \delta x$$

Now α might be as large as 1 min, or 3×10^{-4}rad, which gives, for $\delta x \sim 5\times10^{-9}$ m/$\sqrt{\text{Hz}}$, a phase noise of

$$\delta\phi \sim 10^{-7} \text{ rad}/\sqrt{\text{Hz}}$$

For larger α, the beams do not overlap, effectively reducing η. Thus, with the size of this effect being considerable, either a very large or a very small value of the offset α is desirable.

It is possible to consider a more general static phase difference, such as that produced by mirror or polariser imperfections, as being made up of a Fourier series; examination of the effects of a single component of this series allows a determination of the most critical spatial frequencies in the optical components. Thus, taking

$$\phi = \phi_0 \sin \Omega x$$

in (3·19) leads, via integration by parts and use of a standard integral, to the phase fluctuation $\delta\phi$ corresponding to a positional fluctuation δx:

$$\delta\phi = \phi_0 \Omega \exp(-\Omega^2/2)\delta x \qquad (3·21)$$

This expression has a maximum at $\Omega = 1$. So the phase noise coupled by flatness asymmetries in the two arms of the interferometer is largest if these asymmetries occur at a spatial period of about $\sqrt{2}\pi$ times the beam radius w, or ~4 mm for the 10 m cavities. If the mirrors or polarisers are flat to within $\lambda/20$ on this scale and $\delta x \sim 5\times10^{-9}$ m/$\sqrt{Hz}$, the resultant phase noise is $\sim5\times10^{-7}$ rad/$\sqrt{Hz}$.

Another way in which an effective static phase difference (i.e. a position-variable weighting in (3·19)) may arise is by non-uniformities in the detecting photodiode (e.g. Meyer et al 1983). A $\lambda/20$ mirror non-uniformity corresponds to a variation of about 30% in the diode efficiency. The scale dependence is the same as that in equation (3·21). While an initial judgement might be that this coupling mechanism is considerably less important

than others, care must be exercised: for a detecting diode outside the vacuum system will not benefit fully from any system to reduce the size of the beam positional fluctuations.

Positional fluctuations, being changes in the amplitude of an odd mode (m=1), require an <u>odd</u> static phase difference $\phi(x,y)$ between the interfering beams for phase fluctuations to be produced. Size fluctuations, on the other hand, are coupled in via <u>even</u> static phase differences, such as a curvature mismatch between the combining beams. There are several possible ways of approaching the problem of the origin, magnitude and significance of such static phase differences.

One obvious and fairly simple approach is to assume a static phase difference $\phi = \phi_0 \cos\Omega x$ and calculate the resultant phase noise for a "reasonable" value of ϕ_0, in a similar fashion to the calculation for positional fluctuations above. For beam radius fluctuations δw, this gives

$$\delta\phi = \phi_0 \Omega^2 \exp(-\Omega^2/2)(\delta w/w) \qquad (3\cdot22)$$

This has a maximum at $\Omega = \sqrt{2}$. So if the mirrors and polarisers are flat to within $\lambda/20$ on a scale of ~3 mm (for 10 m cavities) and $\delta w/w \sim 2\times10^{-6}/\sqrt{Hz}$ (see section 3·4(ii)), the phase noise might be as large as 3×10^{-7} rad$/\sqrt{Hz}$.

Beam size fluctuations may also be coupled in by a curvature difference between the interfering beams. This might be due to an asymmetry in the curvature of the mirrors in the two arms of the interferometer, or in their distances. It is evidently desirable to investigate the likely magnitude of the noise resulting from such mismatches, and to gain some idea of how critical are differences in

mirror curvature and placement.

With the present optical arrangement, as indicated in fig 2·7, there are two places where phase fluctuations due to beam geometry changes may enter: at the light sampled by the 10% splitters (to lock each cavity) or at the interference of the cavity output beams. In the first case, beam size fluctuations may cause phase changes if the incoming laser beam does not have the same size or curvature as the beam in the cavity. A signal mimicking a phase change will then appear in the secondary arm if the cavity lengths or mirror curvatures are different; alternatively, the distances from the beamsplitter to the cavities may differ. If the cavity output beams are interfered, only differences in the beamsplitter-cavity distance and cavity sizes allow beam size changes to produce noise.

Consider the case of two interfering beams, of radius of curvature R_1 and R_2 respectively; the phase difference between the two beams is, as a function of the radial distance r,

$$\phi(r) = (1/R_1 - 1/R_2)\pi r^2/\lambda \qquad (3\cdot23)$$

Application of (3·19) using cylindrical co-ordinates then yields the relative phase change produced by a beam size fluctuation δw:

$$\delta\phi = (2\pi w^2/\lambda)(1/R_1 - 1/R_2)(\delta w/w) \qquad (3\cdot24)$$

Now the curvature difference $\delta(1/R)$ may be due to either a difference in the effective distance of propagation to the waist Δz_p of the beams or a difference in waist size Δw_0:

$$\delta(1/R) = \partial(1/R)/\partial z.\Delta z + \partial(1/R)/\partial w_0.\Delta w_0 \qquad (3\cdot25)$$

This, together with (3·24) and the relations describing the propagation of a laser beam (e.g. Kogelnik and Li 1966):

$$R(z) = z\left[1 + (\pi w_0^2/\lambda z)^2\right] \qquad (3\cdot25)$$

$$w(z) = w_0\left[1 + (\pi w_0^2/\lambda z)^2\right] \qquad (3\cdot26)$$

gives the relative phase fluctuation of the interfering beams:

$$\delta\phi = \frac{2\pi w_0^2\left[1 + (\lambda z/\pi w_0^2)^2\right](\delta w/w)}{\lambda z\left[1 + (\pi w_0^2/\lambda z)^2\right]^2}\left\{\left[1 - (\pi w_0^2/\lambda z)^2\right]\Delta z/z - (2\pi w_0^2/\lambda z)^2\Delta w_0/w_0\right\} \qquad (3\cdot27)$$

For small cavities, i.e. $(\lambda z/\pi w_0^2)^2 \gg 1$ (or confocal parameter $b = 2\pi w_0^2/\lambda \ll z$), this reduces to

$$\delta\phi = (2\lambda z/\pi w_0^2)(\delta w/w)\left[(\Delta z/z) - (2\pi w_0^2/\lambda z)^2(\Delta w_0/w_0)\right] \qquad (3\cdot28)$$

In the case of large cavities ($b \gg z$), the phase noise is approximately

$$\delta\phi = -(2\lambda z/\pi w_0^2)(\delta w/w)\left[(\Delta z/z) + 4(\Delta w_0/w_0)\right] \qquad (3\cdot29)$$

It can be seen from (3·28) and (3·29) that small cavities are more susceptible to beam size fluctuations than are large ones (their wavefront curvature is greater).

Remember that the shot noise on 1 W of light corresponds to $\sim 3\times10^{-10}$ rad/$\sqrt{\text{Hz}}$.

Optically recombining the beams helps reduce $\Delta w_0/w_0$ and $\Delta z/z$; the limitation will be any asymmetry in the

cavity mirror curvature or placement. If the optical paths of the two beams in the present detector were different by 5 mm, the resultant phase noise would be, again taking

$\delta w/w \sim 2\times10^{-6}/\sqrt{Hz}$ at 1 kHz,

$$\delta\phi \sim 5\times10^{-9} \text{ rad}/\sqrt{Hz}$$

The beam waist size w_0 in a plane-concave cavity of mirror separation d and curvature R is (Kogelnik and Li 1966)

$$w_0^4 = (2\lambda/\pi)^2(R-d)d \qquad (3\cdot30)$$

So, if the cavities are not identical:

$$\Delta w_0/w_0 = (\lambda/\pi w_0^2)^2\left[d\Delta R + (R-2d)\Delta d\right] \qquad (3\cdot31)$$

Taking asymmetries in the curvature (15m) and separation (10m) to be of the order of 1cm gives a phase noise of

$$\delta\phi \sim 10^{-3}(\delta w/w) \sim 2\times10^{-9} \text{ rad}/\sqrt{Hz} \text{ at 1 kHz}$$

Overall, it thus seems likely that fluctuations in beam size will produce phase noise at the detector output which is at least one order of magnitude larger than the shot noise on 1W of light.

Fluctuations of higher order modes will produce phase fluctuations if a static phase difference of appropriate symmetry exists. The magnitude of such fluctuations, however, is difficult to predict.

(3·3(ii))Coupling Through Scattering

Any light scattered out of the main laser beam may alter its phase. Beam geometry fluctuations can modulate the amount of scattering, thus producing phase fluctuations.

Consider the case of N scattering centres distributed randomly across the beam profile; this might occur on a mirror surface or within a phase modulator. If the nth centre scatters light with amplitude and phase a_n and θ_n respectively (relative to the main beam), then the total phase difference due to the scattering is, for small a_n,

$$\Delta\phi(N) = \sum_{n=1}^{N} a_n \sin\theta_n \qquad (3\cdot32)$$

If the beam geometry changes, the scattered amplitudes a_n will also change; for a small positional change of the laser beam,

$$|\delta a_n| \approx |a_n \delta x/w| \qquad (3\cdot33)$$

The sign of δa_n is random.

As a further simplification, it will be assumed that the phases θ_n are random (due, for example, to a variation in size of small scattering centres) and the amplitudes a_n are uniform (a_0). The randomness of the sign of δa_n effectively reverses the sign of θ_n randomly, leaving it random. The phase noise is then

$$\delta\phi \sim a_0(\delta x/w)\sum_{n=1}^{N}\sin\theta_n = (2a_0\sqrt{N}/\pi)(\delta x/w) \qquad (3\cdot34)$$

The total scattered amplitude $\eta = Na_0$, so the phase fluctuations are just, dropping the factor of order unity,

$$\delta\phi \sim (\eta\sqrt{N})(\delta x/w) \qquad (3\cdot35)$$

Since $\delta x/w \sim 5\times10^{-6}/\sqrt{Hz}$ at 1 kHz, taking $\eta\sqrt{N} \sim 10^{-2}$ gives

$$\delta\phi \sim 5\times10^{-8} \text{ rad}/\sqrt{Hz}$$

A more general way in which to write (3·35) would be

$$\delta\phi \sim (\eta\sqrt{N})(\delta A_m/A_0) \qquad (3\cdot36)$$

where δA_m is the amplitude change of the mth mode. This relation should be approximately true for fluctuations of all low order modes. Thus, they are all potentially dangerous noise sources.

(3·4)The Measurement Of Beam Geometry Fluctuations

(3·4(i))Positional Fluctuations

Movements of the Ar^+ laser beam at kilohertz frequencies are only of the order of $10^{-9}m/\sqrt{Hz}$, placing considerable constraints on possible detection systems. For example, the thermal noise of most resistive-sheet-backed position-sensitive photodiodes is excessive. It was decided to use a quadrant photodiode, taking the current from opposite sides as the position signal. This has the advantage of high sensitivity to positional fluctuations (negligible thermal noise from the diode) and an insensitivity to intensity fluctuations when the beam is well centred. The response of this system is fully analysed in Appendix 5, where it is shown that if a laser beam is close to the centre of the quadrant diode (i.e. offset $r \ll w$), the difference current for a movement δx is

$$\delta i_x = (2\sqrt{2}\eta P/\pi w)\delta x \qquad (3\cdot37)$$

Here η is the power to current efficiency of the diode and P is the total power of the laser beam. If the positional fluctuation is to be detected, this change in current must be greater than the shot noise in the diode current, giving a minimum detectable displacement of

$$\delta x_{min} = \pi w(e/4P\eta)^{\frac{1}{2}} = \pi w(\pi\hbar\nu/2P\xi)^{\frac{1}{2}} \qquad (3\cdot38)$$

where $\xi = (2\pi\hbar\nu/e)\eta$ is the quantum efficiency of the diode ($\sim$0·35). For P = 1mW, w = 0·2mm, this gives a minimum detectable displacement of $\sim 10^{-11}m/\sqrt{Hz}$. If this sensitivity is to be attained, the beam must be centred, in order to null out intensity noise, to within

$$\left[r/10^{-6}m\right] < \left[\delta x/10^{-11}m/\sqrt{Hz}\right]\left[(\delta P/P)/10^{-5}/\sqrt{Hz}\right] \qquad (3\cdot39)$$

For ordinary measurements of the positional fluctuations, it is perfectly possible to achieve this centreing accuracy manually (at least over fairly short time scales). The offset r can be continually monitored by observing the strength of a signal, in the difference current, due to an artificial modulation of the laser intensity. When the size of this signal is drastically reduced relative to the background signal from the quadrant diode, it is known that the sensitivity of the diode to intensity noise has been suppressed and the difference current is a good measure of the positional fluctuations (as long as other noise is not important). Within a certain range, the output signal is then independent of the positional offset.

In situations where greater long-term stability or resolution are required, a servo system may be used to keep the beam centred on the diode. This solution has been adopted in the present version of the gravitational wave detector. The servo system, which also maintains the detector alignment, is described in section 4·3.

To be able to measure a shot noise limited displacement, it is necessary to use a low noise differential amplifier. The circuit that was originally designed and constructed for this purpose is shown in fig 3·3. Similar, though rather more sophisticated, wideband amplifiers are currently in use in conjunction with the diodes on the central mass described in section 2·2.

A typical spectrum of the positional fluctuations of our Spectra Physics 170 Ar^+ laser is shown in fig 3·4. The small size of the artificial intensity peak relative

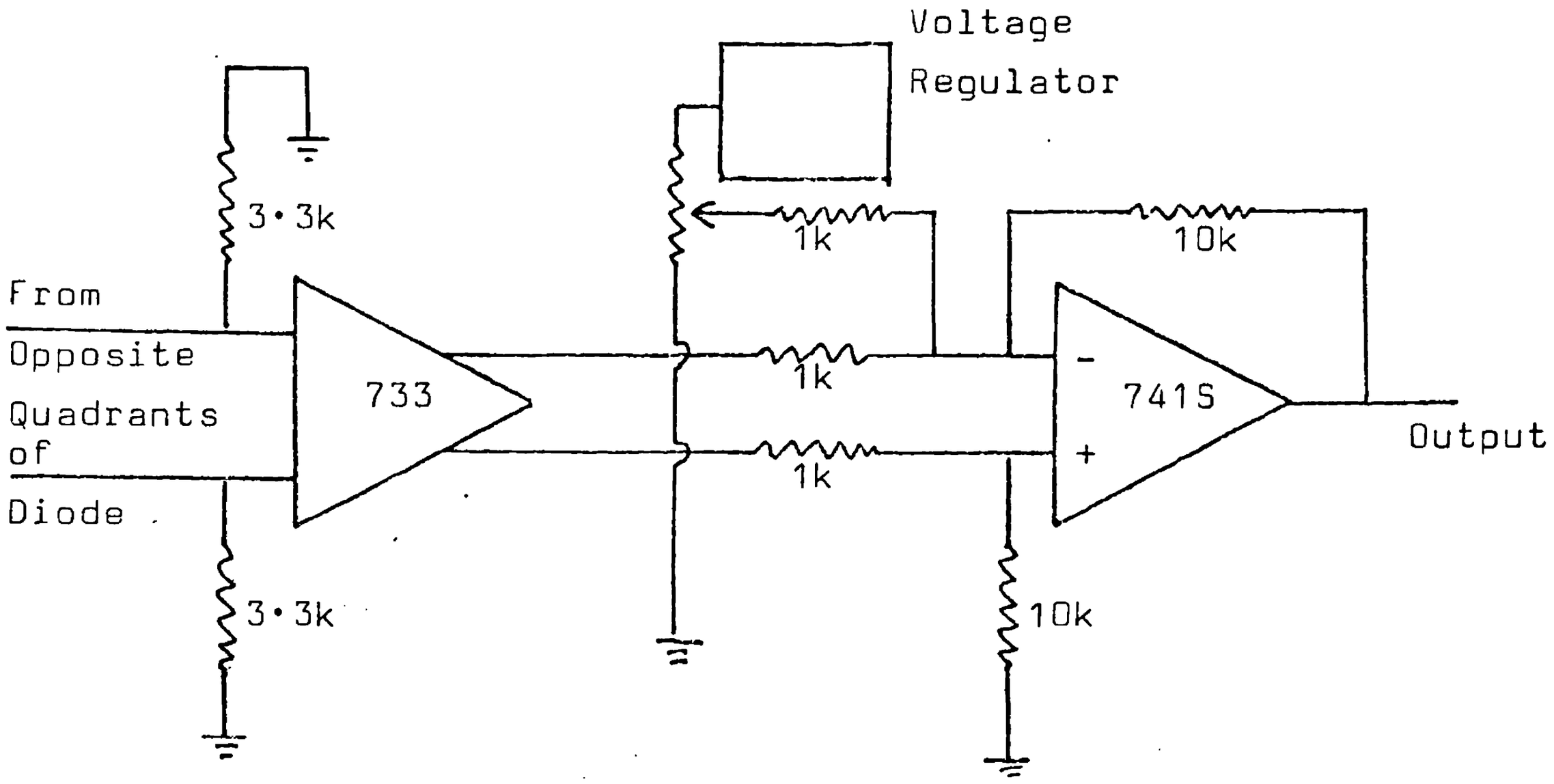

Fig 3·3: Circuit diagram for one half(dimension) of the original beam displacement detector. The 733 is a differential input, differential output amplifier with a bandwidth of 30 MHz at a gain of 10 (as here). Both outputs of the 733 have a DC offset of approximately 3 V; this is subtracted off by the following op amp, which also provides a further factor of ten in gain. Since the offsets are not identical, current is injected from the regulator to balance the 733 outputs.

to its size in the intensity spectrum demonstrates the insensitivity to intensity fluctuations. For comparison, the equivalent spectrum for the smaller Spectra 165 laser is shown in fig 3·5. Both of these spectra were calibrated by using relation (3·37) together with the measured gain of the amplifiers, the measured diode current (ηP) and the beam size w (~1mm and ~0·5mm respectively) as calculated from the known beam parameters in the laser and the

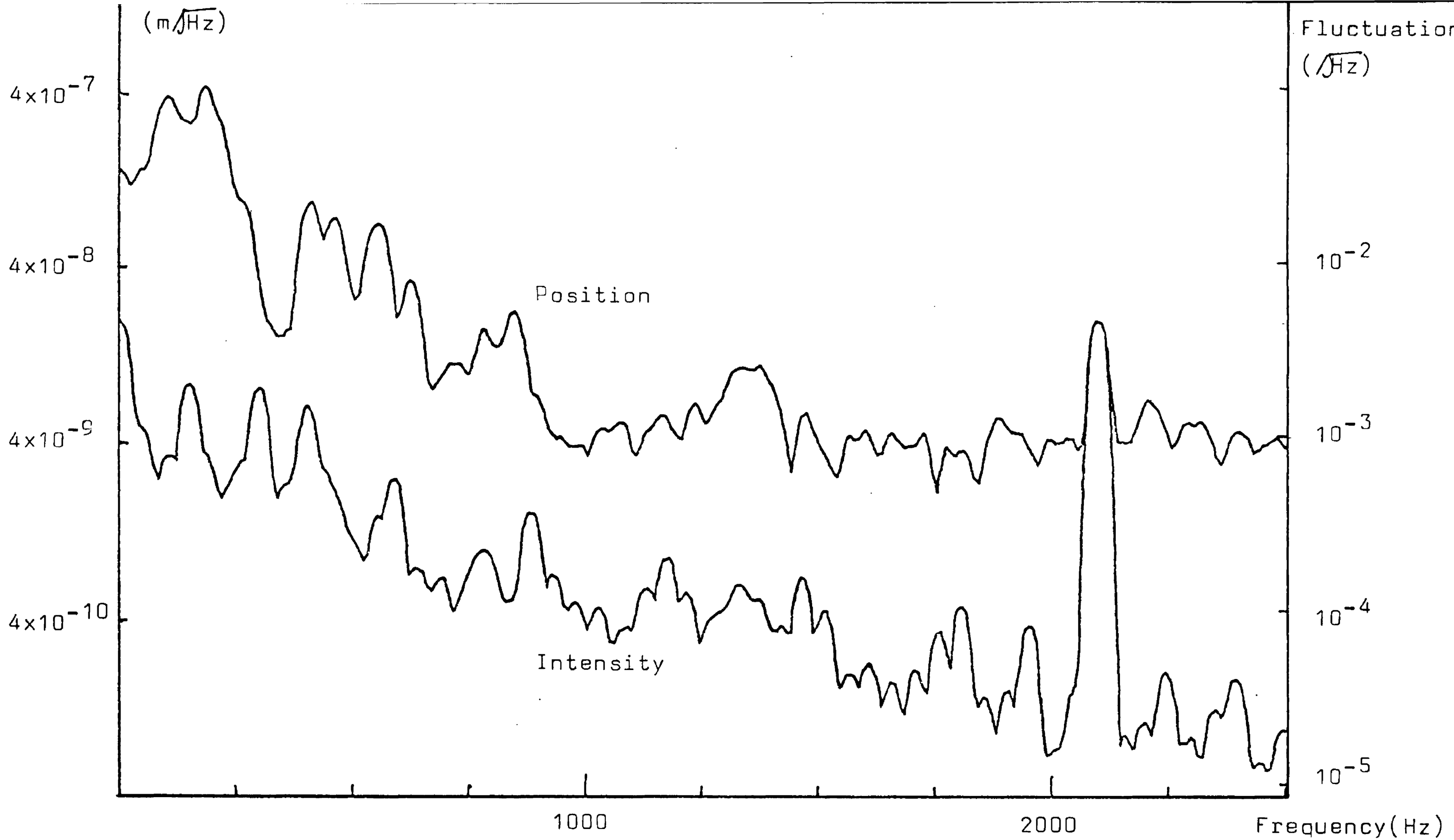

Fig 3·4: A spectrum of the positional fluctuations of the Spectra 170 Ar^+ laser, measured on the central mass where w ~1mm. The effect of a modulation of the intensity at ~2 kHz can be seen, together with a spectrum of the corresponding intensity noise.

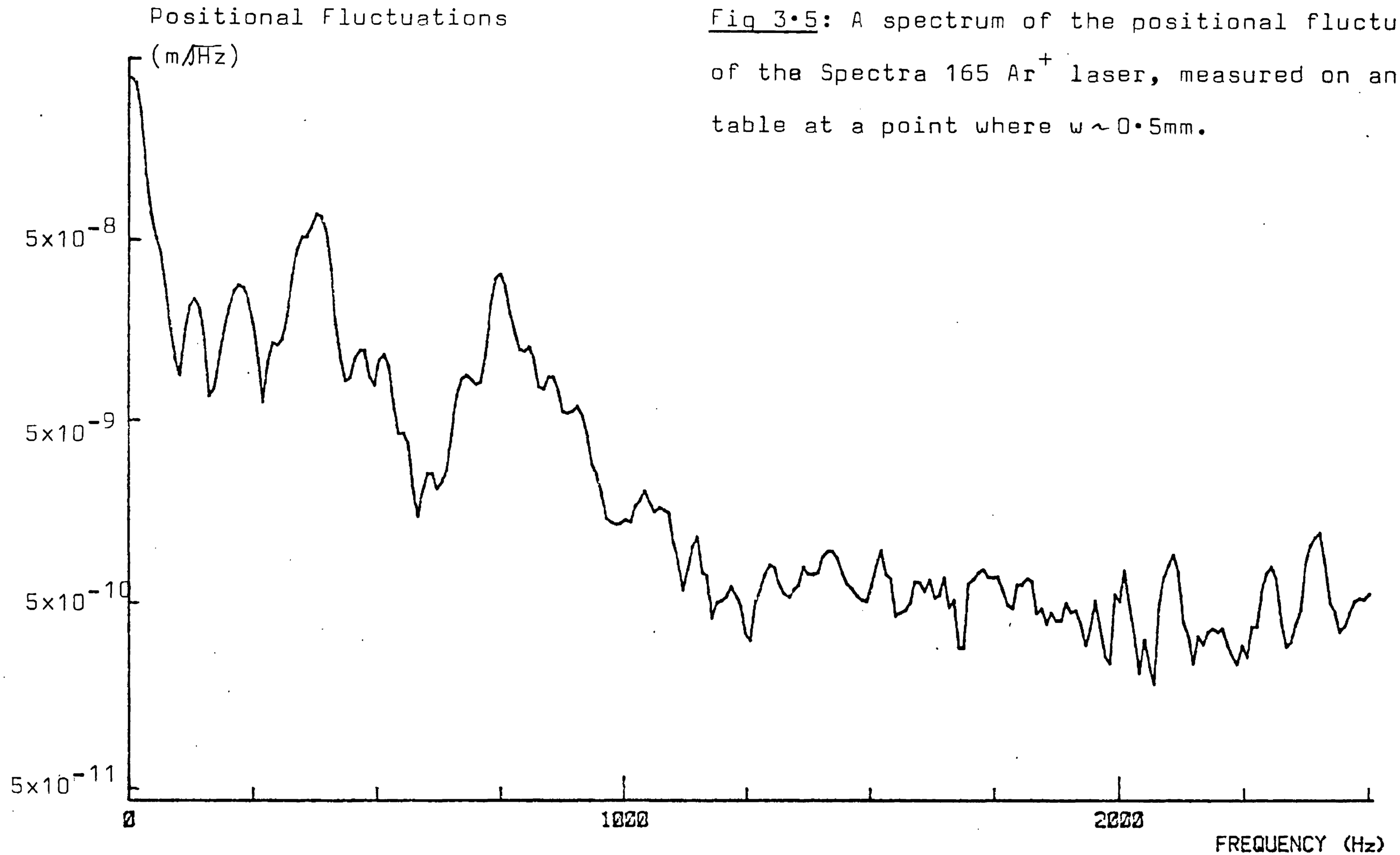

Fig 3·5: A spectrum of the positional fluctuations of the Spectra 165 Ar^+ laser, measured on an optical table at a point where $w \sim 0{\cdot}5mm$.

distance of propagation of the beam. This method has been checked (for other measurements) by displacing the beam with a mirror mounted on piezoelectric legs of known motion per volt; the two methods were found to be consistent.

It can be seen from figs 3·4 and 3·5 that, for both lasers, the positional fluctuations are $\delta x/w \sim 5\times10^{-6}/\sqrt{Hz}$ at 1 kHz, and considerably larger at low frequencies.

The angular fluctuations of the laser beam at a particular point may be measured by placing a quadrant diode in the focal plane of a lens. The resulting spectrum, for an older tube of the Spectra 170 laser, is shown in fig 3·6. These measurements were made on the optical table with a beam size the same as that at the entrance to the interferometer, $w \sim 1$mm. Note that, with this beam size, an angular fluctuation of 10^{-10}rad corresponds to a mode fluctuation which, were it in phase with the fundamental, would produce positional changes of $\sim 6\times10^{-9}$m. These results are therefore consistent with the amplitude of fluctuation of the two quadrature phases of the first order mode being equal.

These measurements of the positional fluctuations of the laser beam provide the justification for the figures quoted in the previous section. Experimental measurements of the magnitude of the noise produced in the gravitational wave detector by the positional fluctuations are described in Chapter 5

(3·4(ii))Other Fluctuations

In principle, beam size fluctuations may be observed

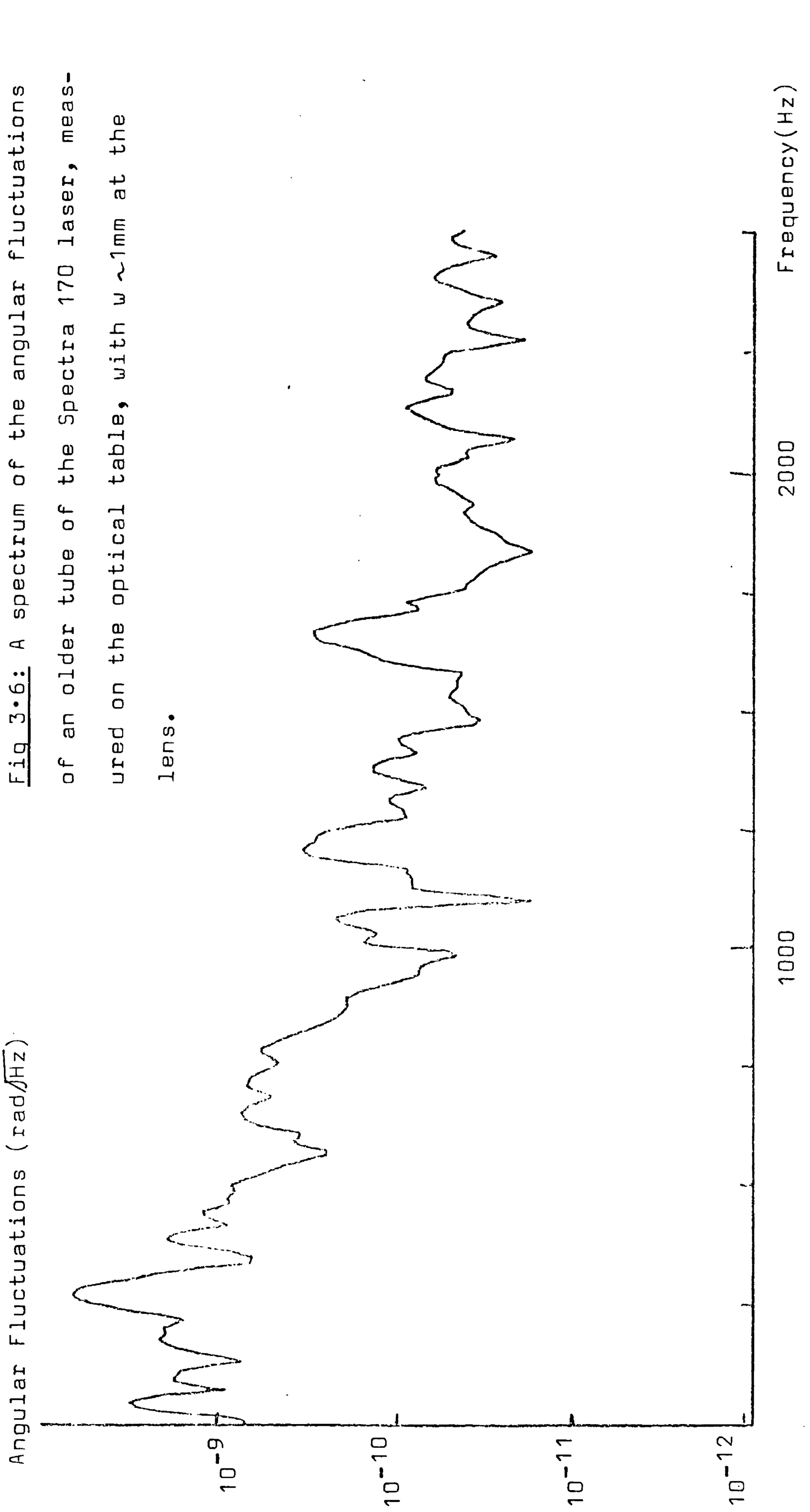

Fig 3·6: A spectrum of the angular fluctuations of an older tube of the Spectra 170 laser, measured on the optical table, with w ~1mm at the lens.

by measuring the intensity fluctuations of the central (circular) portion of the beam, subtracting (or dividing) out the amplitude fluctuations of the whole beam. This is further discussed in Appendix 6. Preliminary experiments have been carried out, but were limited by the combination of light scattered off the aperture used to define the central portion of the beam and laser frequency noise, which produced excess intensity noise.

Similar experiments performed by the Munich gravitational wave group on their Ar^+ laser (Billing et al 1981), which has $\delta x/w \sim 10^{-7}/\sqrt{Hz}$, suggest that $\delta w/w \sim 4\times10^{-8}/\sqrt{Hz}$. If the ratio of positional to size fluctuations is the same for our laser, then we might have

$$\delta w/w \sim 2\times10^{-6}\ /\sqrt{Hz}$$

The situation for other types of fluctuation is even more ill-defined. There is no obvious, easy way to measure small fluctuations and no data is available on their magnitude. It is probably reasonable, however, to expect the fluctuation amplitude to decrease fairly steadily with mode order.

(3·5) Summary

This chapter has discussed the ways in which beam geometry fluctuations may produce phase noise in the interfered light, thus limiting the sensitivity of the gravitational wave detector. It has been seen that, in order for the phase fluctuation to be first order in the geometry fluctuation, there must be some other optical imperfection. This may be a phase mismatch due to asymmetrical optics,

scattering or spatial efficiency variations in the detecting photodiode. Even if these imperfections are minimised, the likely size of the phase noise due to positional fluctuations is greater than 10^{-7}rad/$\sqrt{Hz}$ (compared with a shot noise on 1W of ~3×10^{-10}rad/$\sqrt{Hz}$), demonstrating the need for some way of substantially reducing such fluctuations. These predictions are in general agreement with the observations described in Chapter 5.

The discussion of beam size fluctuations emphasised the need for symmetry in the optical arrangement. Even with care, the resultant phase noise will probably be at least an order of magnitude above the shot noise on 1W. Thus, substantial reduction of beam size fluctuations will also be required. Indeed, it seems likely that moderate suppression of all low order ℓ modes ($m \lesssim 10$) would be very desirable. Ways in which this could be acheived are discussed in Chapter 4.

CHAPTER FOUR

THE SUPPRESSION OF BEAM GEOMETRY FLUCTUATIONS

It is apparent from Chapter 3 that fluctuations in beam geometry must be considerably reduced if the ultimate sensitivity of the gravitational wave detector is to be attained. It is possible to conceive of at least three approaches to this problem, each of which is discussed in this chapter: use of a spatial filter, of a resonant cavity mode-suppressor or of active control of beam position. A fourth possibility, use of a single-mode optical fibre, is being investigated at MIT. Its operation is explained in Appendix 8.

(4·1) Mode Suppression by Spatial Filtering

A spatial filter consists essentially of a pinhole placed at the focal point of a lens: the field distribution in this plane is the Fourier transform of the incoming field distribution, so high spatial frequency components occur at large distances from the optic axis and are cut off by the aperture. It might be thought that any higher order modes which constitute a beam geometry fluctuation would also be cut off; but this will only be partially true, for all modes contain some low spatial frequency components (they are their own Fourier transforms) which will be transmitted. The factor by which higher order modes are suppressed relative to the fundamental will be calculated below. The curvature of the beam will be neglected, a restriction which leaves the results unaltered as long as the condition $z \ll \pi w_0^2/\lambda$ is satisfied

at the aperture, with z the distance from the waist w_0.

In a situation with natural circular symmetry, such as the diffr action of a beam by a circular aperture, it is most convenient to consider the laser beam modes in cylindrical polar co-ordinates (r,ϕ,z) oriented along the beam. The normal modes then become Laguerre-Gaussian functions (e.g. Kogelnik and Li 1966):

$$E(r,\phi) = \sum_l \sum_p A_p^l g_p^l(r) e^{-il\phi}$$

$$= \sum_l \sum_p A_p^l \frac{p!l!}{(p+l)!} (\sqrt{2}r/w)^l L_p^l(2r^2/w^2) e^{-r^2/w^2} e^{-il\phi}; \quad (4\cdot1)$$

where $L_p^l(2r^2/w^2)$ is a generalised Laguerre polynomial:

$$L_p^l(x) = (e^x x^{-l}/p!)(d/dx)^p(e^{-x}x^{p+l}) \quad (4\cdot2)$$

For example, $L_0^1(x) = 1$ and $L_1^1(x) = 1+1-x$. Thus g_0^0 is just the usual fundamental mode, while g_0^1 corresponds to a field distribution

$$E_0^1(r,\phi) = (\sqrt{2}r/w)e^{-il\phi}e^{-r^2/w^2} = (\sqrt{2}/w)(x-iy)e^{-(x^2+y^2)/w^2} \quad (4\cdot3)$$

This is a combination of the Gaussian-Hermite field distributions $E_{10}(X,Y)$ and $E_{01}(X,Y)$; so a small fluctuation in g_0^1 corresponds to a displacement in one direction and a tilt in the other. Similarly, a small change in g_1^0 represents a fluctuation in beam size.

The mode amplitudes A_p^l constituting a general field distribution $E(r,\phi)$ are given by an analogue of (3·11); expression of the mode orthogonality, however, requires use of the co-ordinate

$$s = 2r^2/w^2$$

so that

$$E(s,\phi) = \sum_l \sum_p A_p^l \frac{p!\,l!}{(p+l)!} s^{l/2} e^{-s/2} L_p^l(s) e^{-il\phi} \qquad (4\cdot4)$$

and the mode amplitudes are

$$A_p^l = \frac{\int_0^\infty E(s) e^{il\phi} s^{l/2} e^{-s/2} L_p^l(s)}{\int_0^\infty \left[s^{l/2} e^{-s/2} L_p^l(s)\right]^2 ds} \qquad (4\cdot5)$$

This relation can now be used to determine the mode amplitudes in the plane of the spatial filter (hence everywhere) where $E(s)$ is simply the incoming field truncated at radius $R_a = \sqrt{2} r_a / w = \sqrt{s_a}$.

If the incoming field is taken to be a single (pth order) mode,

$$E_p^l(s) = A_p^l \frac{p!\,l!}{(p+l)!} s^{l/2} e^{-s/2} L_p^l(s) e^{-il\phi} \qquad (4\cdot6)$$

then the emerging field has (qth order) mode amplitudes of

$$A_{qp}^l = A_q^l / A_p^l = \frac{p!}{(p+l)!} \int_0^{R_a} s^l e^{-s} L_q^l(s) L_p^l(s)\, ds \qquad (4\cdot7)$$

The normalising integral in (4·5) is standard (Gradshteyn and Rhyzhik 1965). The integral in (4·7) may be evaluated using repeated integration by parts together with the relations (4·2) and

$$\frac{d(L_p^l(s))}{ds} = -L_{p-1}^{l+1}(s)$$

For an emerging mode of the same order as that incoming, the resultant amplitude transmission factor is

$$A_{qq}^l = 1 - \frac{e^{-R_a^2}}{(q+l)!} \left\{ \sum_{j=0}^{p+l} \frac{(q+l)!}{(q+l-j)!} R_a^{2(q+l-j)} - \sum_{k=0}^{p-1} (q-k-1)!\, R_a^{2(l+k+1)} L_{q-k}^{l+k}(R_a^2) L_{q-k-1}^{l+k+1}(R_a^2) \right\} \qquad (4\cdot8)$$

Now the factor by which a beam geometry fluctuation corresponding to g_q^l is suppressed is

$$S_q^1 = A_{00}^0 / A_{qq}^1$$

Some values of S_q^1 are plotted in fig 4·1, for various aperture sizes.

An incident mode g_p^1 also excites different modes g_q^1 (of the same symmetry) in the emergent beam. For $q > p$, the mode amplitudes are

$$A_{qp}^1 = \frac{p!e^{-R_a^2}}{q!(p+1)!} \sum_{k=0}^{p} (q-k-1)!\, R_a^{2(1+k+1)} L_{p-k}^{1+k}(R_a^2) L_{q-k-1}^{1+k+1}(R_a^2) \qquad (4·9)$$

For $q < p$, expressions inside the sum have p and q interchanged and the $p!/q!$ term disappears.

The intensity of various modes excited by the fundamental is shown in fig 4·2. The power loss in the fundamental and high intensity in other modes evidently limit the extent to which the aperture size may be decreased.

It is evident from fig 4·1 that the suppression factors for low order modes are generally modest. Fluctuations of the important g_0^1 mode (positional changes) are hardly suppressed at all until the hole size is made very small, when the power throughput is tiny and diffraction excessive. Thus, a suppression of g_0^1 by a factor of 6 (at $R_a = 0·6$) requires that only 9% of the power is transmitted in the fundamental, with 6% being transferred to g_1^0 and 4% to g_2^0 (see fig 4·2). Maximum suppression for the g_1^0 mode (size fluctuations) is only about 3, with 65% transmitted power. A single spatial filter does not, therefore, appear to be a good way to suppress low order mode fluctuations.

The suppression factor A_{00}^0 / A_{qq}^1 is always finite, a consequence of the positive-definite nature of

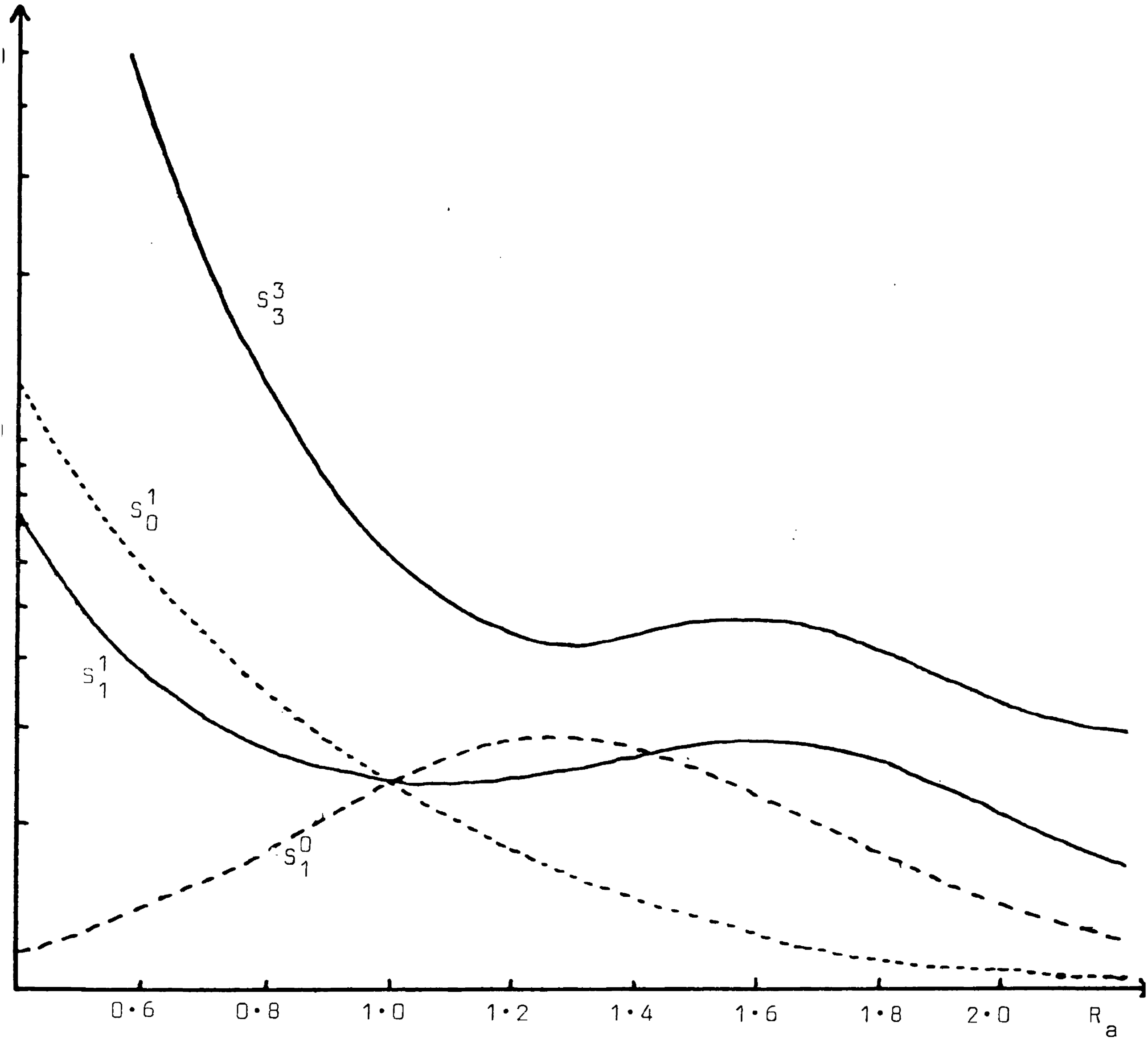

Fig 4·1: Mode suppression factors as a function of hole radius R_a for a single spatial filter.

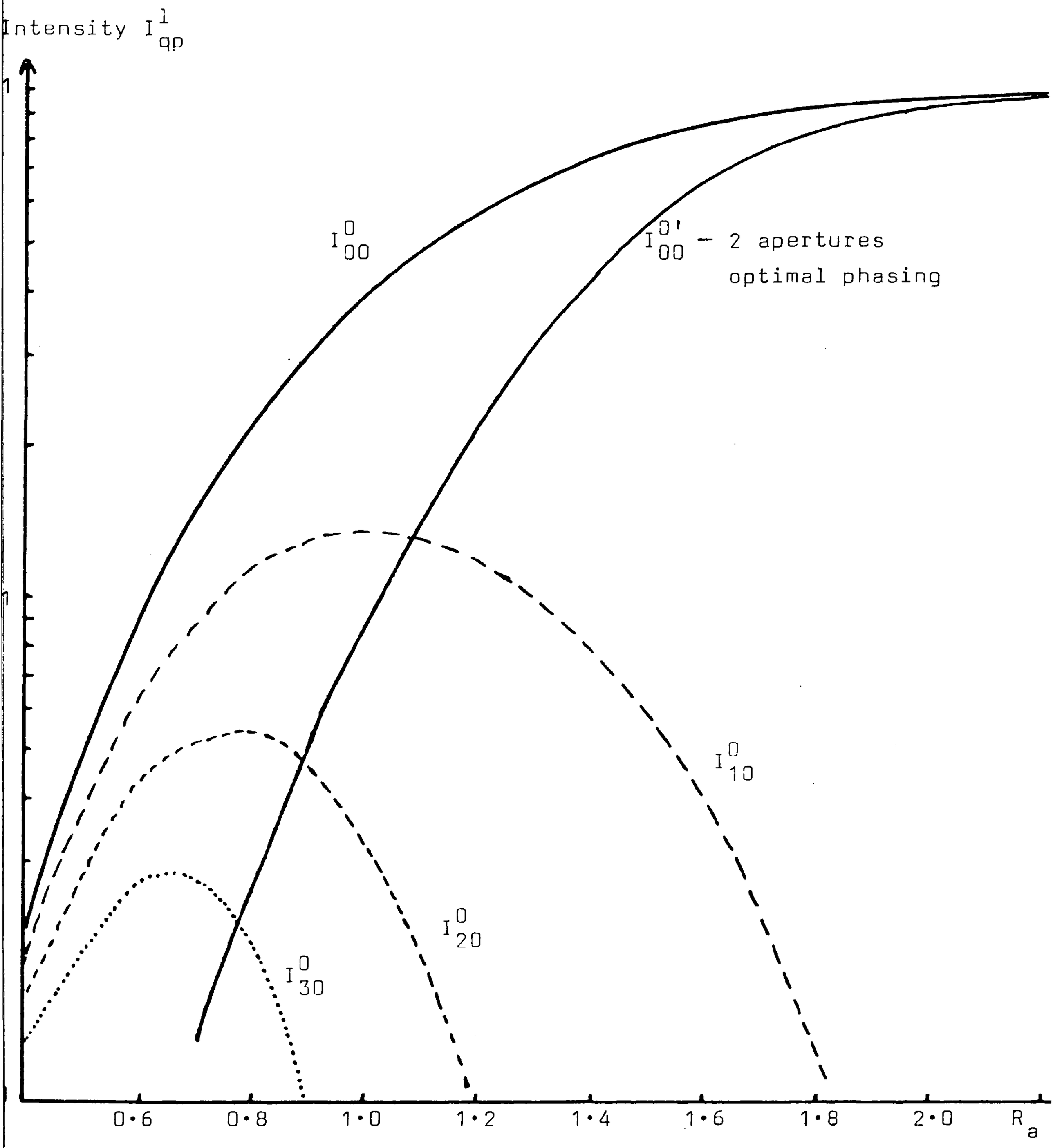

Fig 4·2: qth order mode intensities in the beam emerging from a spatial filter (hole radius R_a) for an incoming beam containing only the fundamental.

$\left[s^{l/2}e^{-s/2}L_q^l(s)\right]^2$ in (4·7). Yet a spatial filter can infinitely suppress a purely sinusoidal field distribution $E = \sin\Omega X$ of sufficiently high spatial frequency Ω. At first sight this seems paradoxical, especially when one notes that the only action of the (necessary) lens is to change the relative phase of the modes constituting the sine wave (cf.3·4) but the suppression factors are independent of phase. The resolution of this paradox lies in the recognition that a sinusoidal initial distribution has mode amplitudes such that the transmitted amplitude A^l_{qq} is precisely cancelled by the amplitudes A^l_{qp} excited by the different incoming modes. The significance of the phase of the incoming modes is now evident. This viewpoint suggests a possible way in which the suppression factors for fluctuations of individual modes might be increased. A spatial filter produces, from an initial mode g^l_p, an infinite collection of modes of the same symmetry whose amplitudes can be varied (within limits) by changing the aperture size and whose relative phase changes with the propagation of the beam. A second aperture placed further along the beam recombines a portion of these different modes with the original (further suppressed) mode, possibly producing total cancellation. The original mode is effectively interfered out.

Fig 4·3 shows some suppression factors, calculated using (4·8) and (4·9), for low order modes passed through two cascaded apertures arranged so that the phases of modes differing by one in the value of p were reversed between the apertures. Such an arrangement is obtained by placing the first aperture immediately in front of the lens of

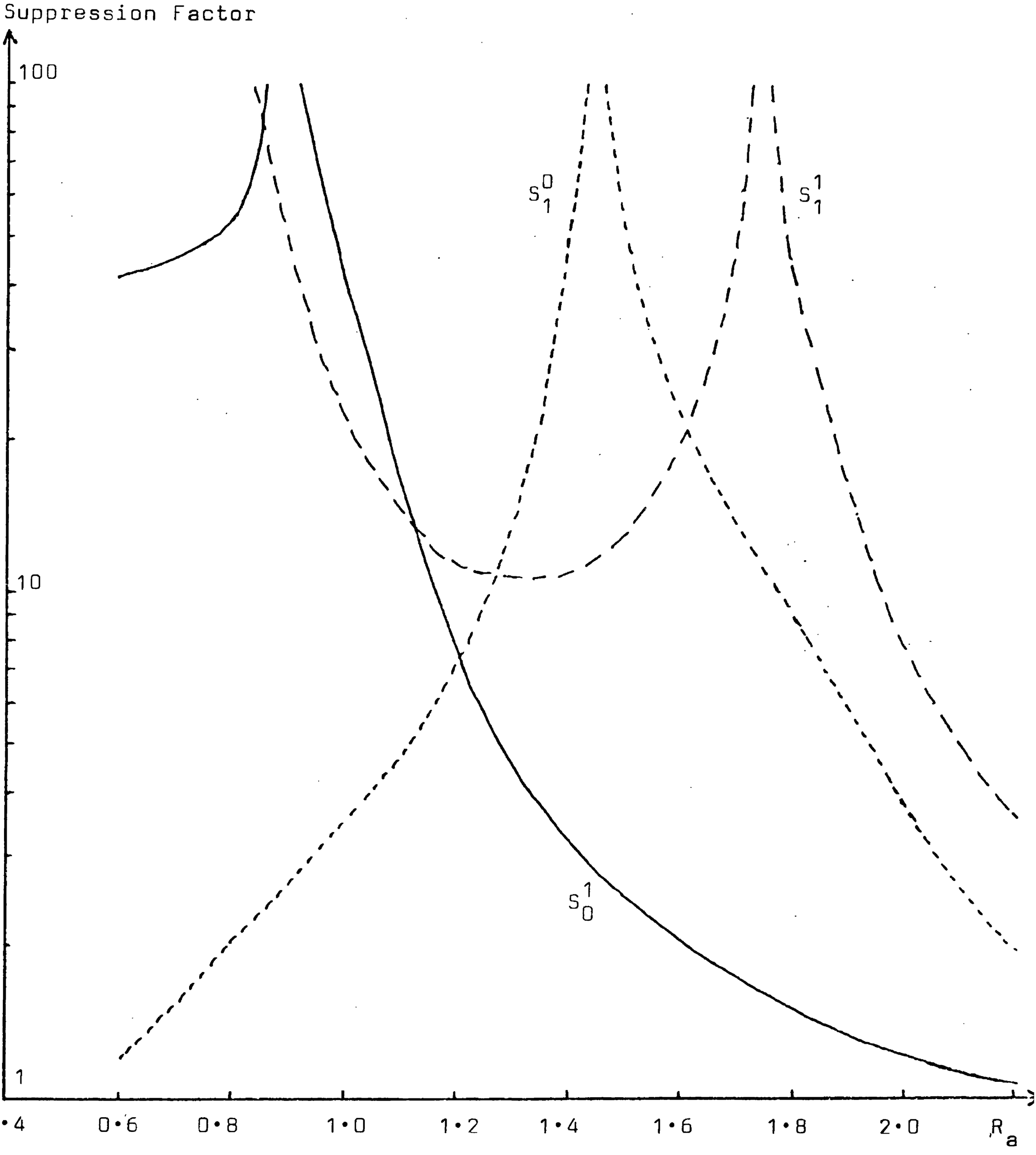

Fig 4·3: Mode suppression factors, as a function of hole radius R_a, for two cascaded apertures with optimal phasing.

a conventional spatial filter (see fig 4·4). Because the relative phase only varies slowly (cf.3·4), the placement is not too critical, the only requirement being $\lambda f/\pi w_0^2 >> 1$, with f the focal length of the lens and w_0 the waist size it produces. This phasing condition is, however, the optimum one and any significant deviation from it will reduce the amount of suppression of higher order modes. Also optimum is equality of size (relative to the beam width) of the two apertures and this was assumed in the calculations. It is evident from fig 4·3 that the suppression factors are considerably increased over those of a single spatial filter and even become infinite at certain hole sizes. Suppression of g_0^1 (positional changes), however, remains poor for reasonable power throughputs (see fig 4·2). For higher modes, the situation is more promising. At an aperture size of $R_a = 1{\cdot}75$, for example, g_1^0 is suppressed by 10 and g_1^1 by greater than 100, yet 80% of the light is transmitted in the fundamental. Such a system of cascaded apertures thus appears to suppress modes of order g_1^0 and higher quite well. This suppression is bought, however, at the cost of transferring power to other modes. For example, a fluctuation in the amplitude of g_1^0 in the input beam results in a (smaller) fluctuation in the amplitudes of g_2^0, g_3^0 etc in the output beam. Similarly, unwanted power in the mode of interest is produced by modes of the same symmetry present in the input beam. Examples of this are shown in fig 4·5, where the amplitude $A_{qp}^{1'}$ of an emerging mode g_q^1 produced by unit amplitude of an incident mode g_p^1, normalised to the transmitted amplitude of the fundamental, is plotted as a function of

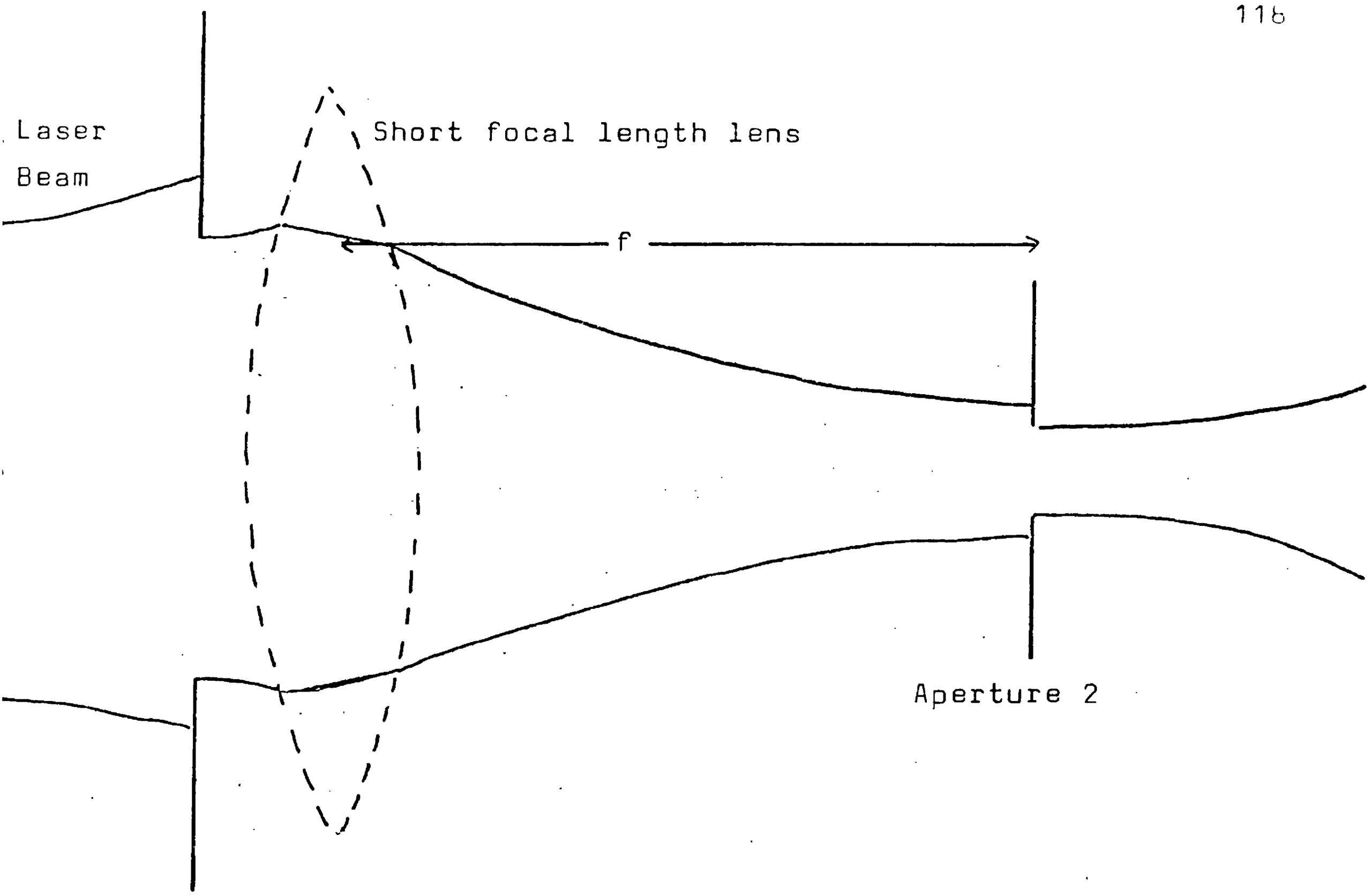

Fig 4·4: Schematic diagram of the arrangement proposed to reverse the relative phase of modes differing by one in order between the apertures. The first aperture is placed in front of a strong lens which produces a beam waist, size w_0, approximately in the focal plane of the lens. Phase reversal occurs if $\arctan(\lambda z/\pi w_0^2) \approx \pi/2$, or $\lambda z/\pi w_0^2 \gg 1$.

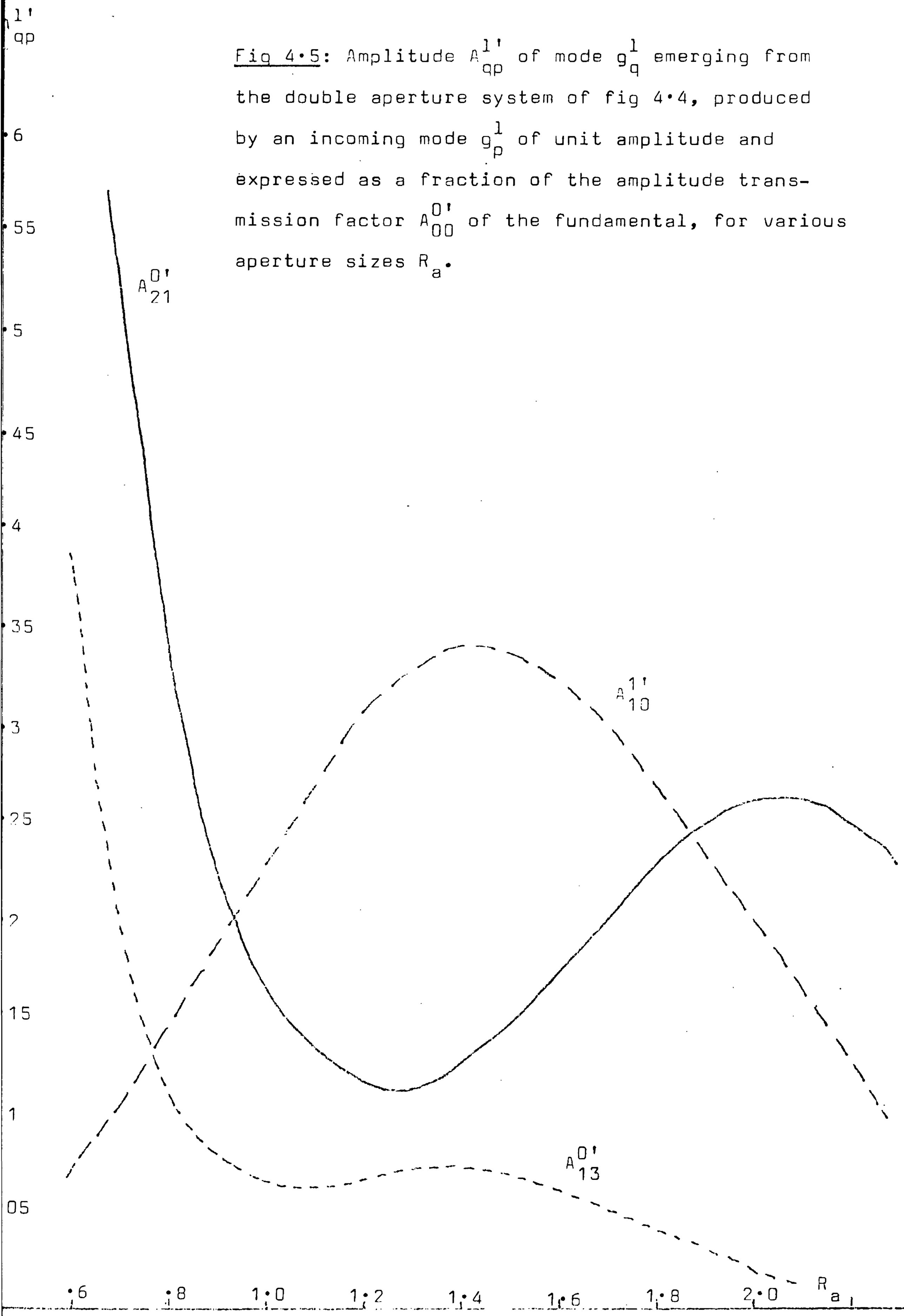

Fig 4·5: Amplitude $A^{l'}_{qp}$ of mode g^{l}_{q} emerging from the double aperture system of fig 4·4, produced by an incoming mode g^{l}_{p} of unit amplitude and expressed as a fraction of the amplitude transmission factor $A^{0'}_{00}$ of the fundamental, for various aperture sizes R_a.

hole size. Thus, at a hole radius R_a = 1·7, some 20% of a size change g_1^0 is transferred to g_2^0, 5% of a fluctuation in g_3^0 is transferred to g_1^0 and about 30% of a positional fluctuation g_0^1 appears in the next highest odd mode g_1^1. It therefore seems unlikely that use of this double aperture system could possibly reduce the overall detector noise by more than a factor of ten.

Overall, spatial filtering does not seem to be a particularly good method of reducing independent fluctuations of laser beam modes. It might be of use if only small, additional suppressions are required or high order modes are a concern, when its simplicity is a great advantage. The spatial filter's property of suppressing modes of order higher than one may make it useful as a method of investigating the sensitivity of the interferometer to high order fluctuations. The need for a system to suppress modes by a large factor remains, however.

(4·2) The Mode-Cleaner

The representation of beam geometry fluctuations as mode amplitude changes, together with the knowledge that higher order modes have different resonant frequencies in an optical cavity, suggests a way of reducing such fluctuations: The laser beam should be passed through an optical cavity (a "mode-cleaner") which is arranged to be resonant for the fundamental mode (Rudiger et al 1981). It was shown in section 3·2 that this would suppress the amplitude of a mode of order m by a factor

$$S_m = \left[1 + (4F^2/\pi^2)\sin^2(\pi\Delta\nu/\nu_0)\right]^{\frac{1}{2}} \qquad (3\cdot10)$$

Well away from resonance, this is approximated by

$$S_m \approx (2F/\pi)\sin(\pi\Delta\nu/\nu_0) \qquad (4\cdot10)$$

The value of $\sin(\pi\Delta\nu/\nu_0)$ for a particular mode is determined solely by the cavity geometry (cf. (3·5) and (3·6)), which must therefore be chosen so that all modes of interest are suppressed. Fig 4·6 shows the variation of $\sin(\pi\Delta\nu/\nu_0)$ with mirror spacing d/R, for several low order modes. It will be seen that a confocal cavity does not suppress even modes at all (they are degenerate), yet is the most efficient suppressor of odd modes. Since it is essential to suppress both positional and size fluctuations of the beam, the choice of geometry d/R ~0·6 or1·4 is the best. This gives about 90% of the maximum suppression for positional fluctuations and about 75% of the maximum for size changes. It also gives reasonable suppression for modes at least up to 6th order.

It can be seen from (4·10) that the acheivement of large suppression factors requires a high valwe for the finesse, but this will be constrained by the power handling capacity of the mirrors (for a small cavity). The power density at the centre of the spot is $I_0 = PF/\pi^2w^2$, and $w \sim 10^{-4}$m for a cavity with mirrors of curvature 50cm and separation 30cm. With commercially available mirrors (CVI Laser Corp., 200 Dorada Pl. SE, Albuqerque NM, USA), which have a quoted maximum power density of 10 kW/cm^2, this would limit the finesse of such a cavity to about 100 for a transmitted power of 100 mW.

Another design consideration is the expected fraction of the power transmitted through the cavity. If the mirrors

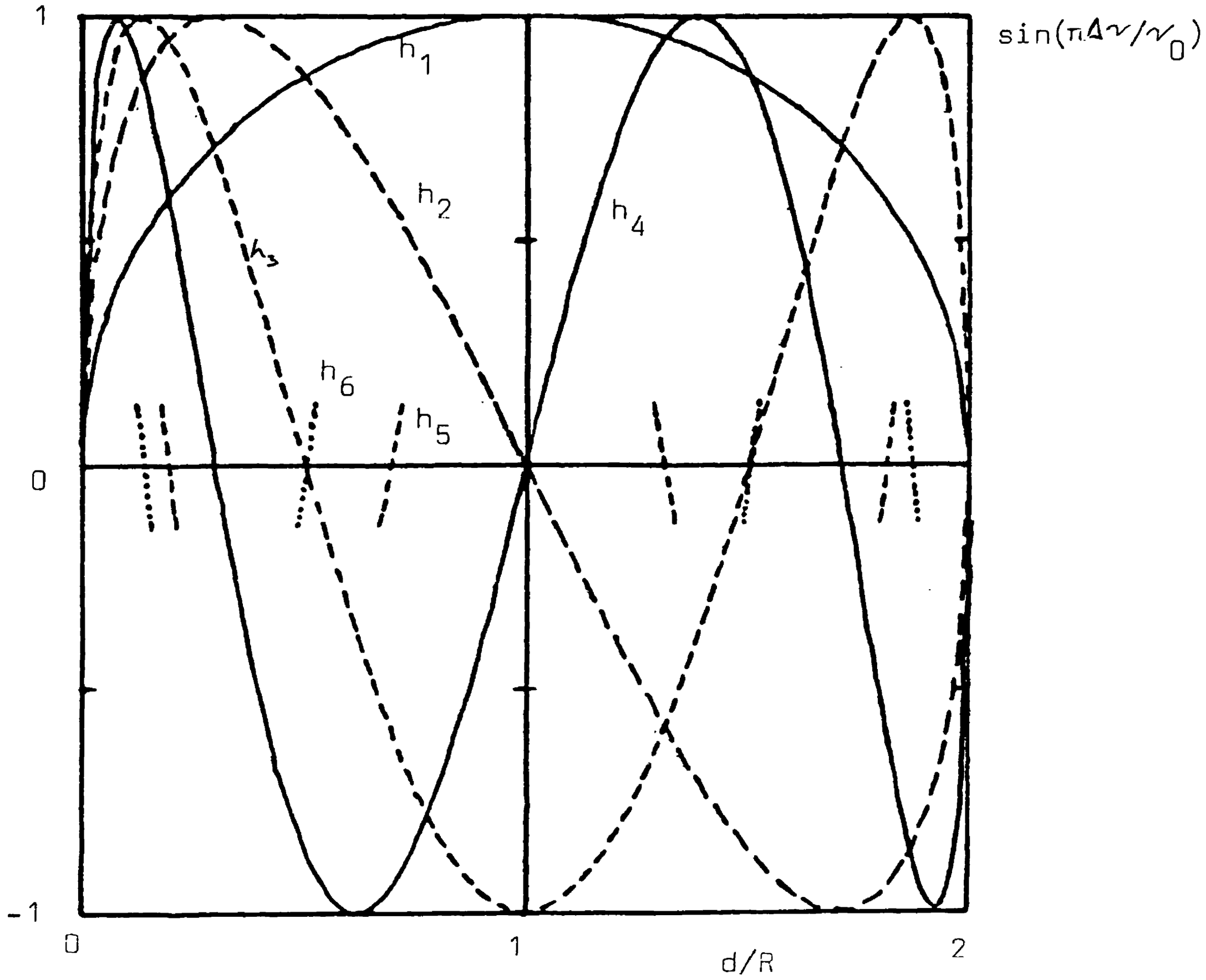

Fig 4·6: Plot of $\sin(\pi\Delta\nu/\nu_0)$, which determines the mode suppression factors (cf. 4·10), for different spacings of the cavity mirrors. d is the separation and R the radius of curvature of the cavity mirrors. The behaviour of different modes h_m is indicated (after Rüdiger et al 1981).

have loss coefficient A^2 and transmission coefficient T^2, this power throughput should be (cf., for example, 2·18)

$$P_T/P_0 = (1 + A^2/T^2)^{-2} \qquad (4·11)$$

With these considerations in mind, a cavity with mirrors of transmission coefficient 4% (finesse ~75), curvature 50cm and spacing 30cm was constructed (see fig 4·7)

A servo system is necessary to keep the incoming light resonating in the cavity. This may take the form of adjusting the cavity length via its PZT-mounted mirrors to follow the laser frequency excursions ("locking the cavity to the laser") or of controlling the laser frequency via its intra-cavity Pockels cell ("locking the laser to the cavity"). The error signal for the servo, the measure of the frequency difference between cavity and laser, may be obtained by phase (or frequency) modulating the light and then coherently demodulating the signal from a photodiode looking at the beam reflected from the cavity.

Fig 4·8 shows an early measurement of the positional fluctuations of the beam with and without the mode-cleaning cavity. A constant artificial modulation of the beam position by a PZT-mounted mirror <u>after</u> the cavity enables comparison to be made between the two cases. It can be seen that the large artificial positional modulation that was also injected <u>before</u> the cavity was suppressed as expected, but the background was hardly reduced at all. Yet this background was found not to be due to intensity noise, but to a combination of frequency noise and a misalignment in the cavity. For either by deliberately mis-

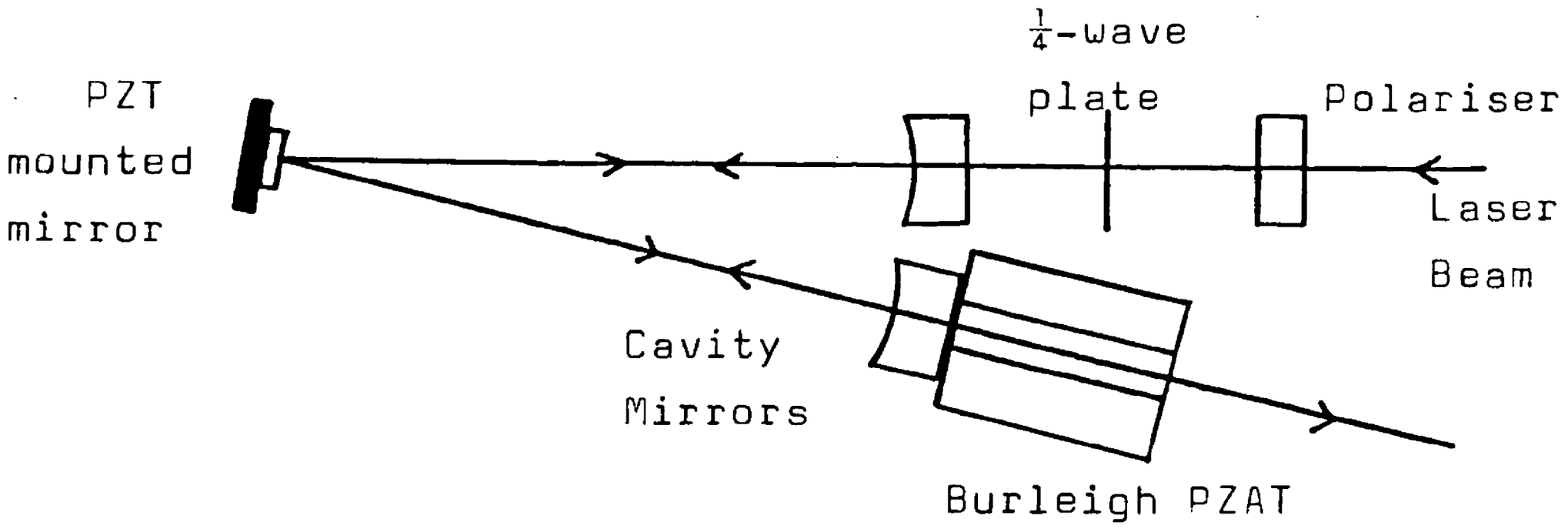

Fig 4·7: A schematic diagram of the mode-cleaning cavity. The cavity mirrors are of radius of curvature 50cm and transmission coefficient 4%, separated by 30cm. The cavity length is folded by reflection off a small, highly reflecting, plane mirror which is mounted on a PZT. With a first resonance of 60 kHz, this provides the fast element in any feedback system which locks the cavity length to the laser light. The folding also reduces the size so that the cavity will fit on the central mass. The slow, large range element of the feedback system is provided by the Burleigh Aligner-Translator, on which one of the 12·5mm diameter cavity mirrors is mounted. The quarter-wave plate-polariser combination both provides isolation for the laser and enables the reflected beam to be observed, thus giving an error signal for locking the cavity. Use of this technique means that the light in the cavity is circularly polarised.

Fig 4·8: An early measurement of the positional fluctuations of the laser beam, with and without the mode-cleaning cavity. It can be seen that the background is reduced much less than the large artificial peak.

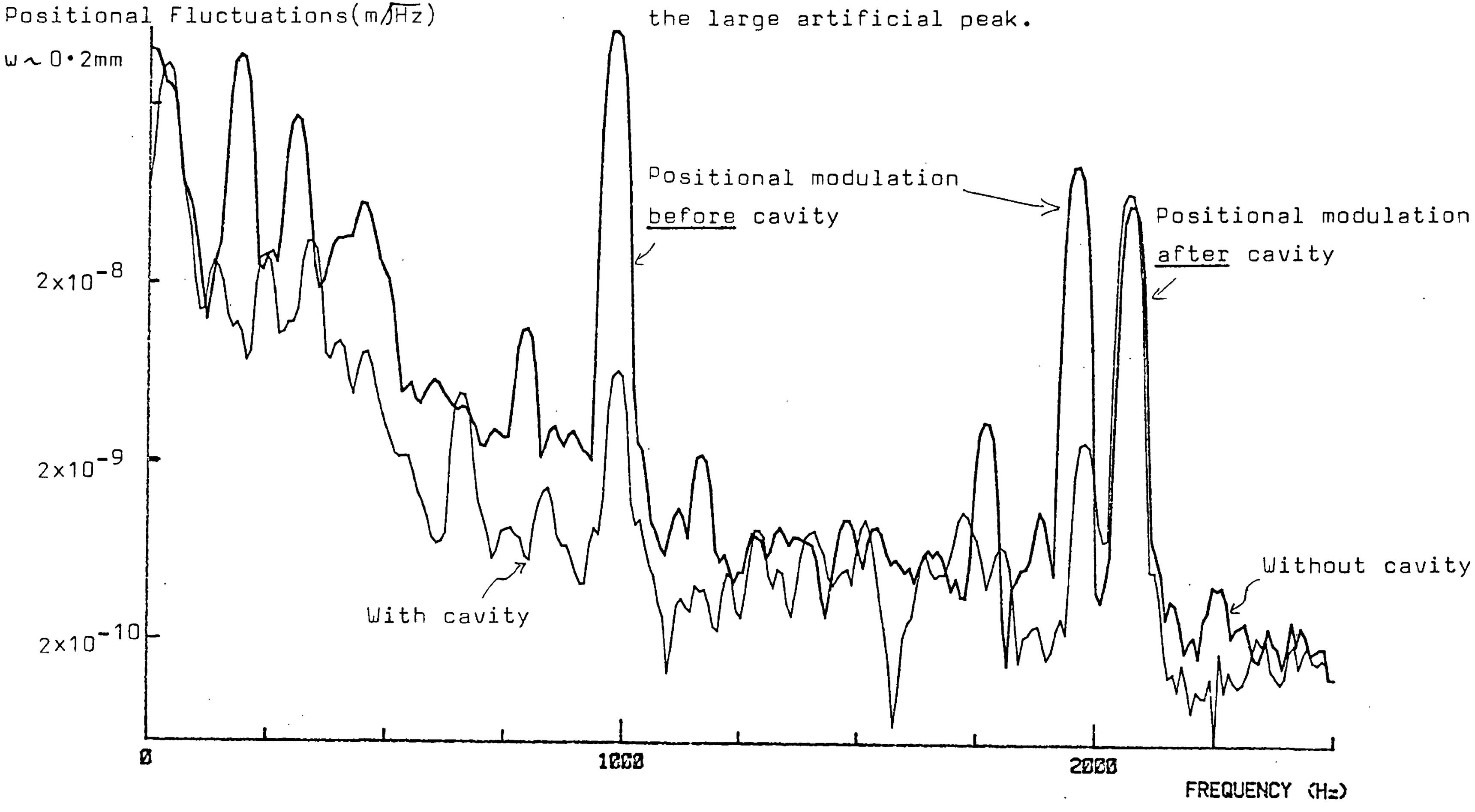

aligning the cavity (see fig 4·9(a)) or by increasing the relative frequency noise of the light and the cavity by decreasing the loop gain of the locking circuit (fig 4·9(b)), this background noise could be increased.

These observations may be explained by a model in which the misalignment produces a certain amplitude of the first order mode in the cavity, this amplitude then being altered by the frequency fluctuations of the incoming laser beam. If the fundamental is on resonance, the fluctuations in its amplitude will be small, so there will be a <u>relative</u> fluctuation $\delta A_1/A_0$. If the misalignment produces a static first order mode amplitude A_1 at the entrance to the cavity, the mode amplitude A_1' inside will be (cf. 3·9)

$$|A_1'/A_1| = [1 + (4F^2/\pi^2)\sin^2(\pi\Delta\nu/\nu_0)]^{\frac{1}{2}}$$
$$\approx (\pi/2F)\sin(\pi\Delta\nu/\nu_0) \qquad (4\cdot13)$$

since the mode is well away from resonance. If the frequency of the light fluctuates relative to the cavity length by $\delta\nu$, the resultant change $\delta A_1'$ in mode amplitude will be

$$|\delta A_1'/A_1| = \frac{\pi^2\cos(\pi\Delta\nu/\nu_0)}{2F\sin^2(\pi\Delta\nu/\nu_0)} \qquad (4\cdot14)$$

For the mode-cleaning cavity already described, this gives

$$\delta A_1'/A_1 \sim 10^{-10}\delta\nu$$

So the beam emerging from the cavity will have mode fluctuations of

$$\delta A_1'/A_0 \sim 10^{-10}(A_1/A_0)\delta\nu$$ required to express offset.

Now a value of $A_1/A_0 \sim 0\cdot1$ would correspond to quite good alignment, with the transmitted intensity in the fundam-

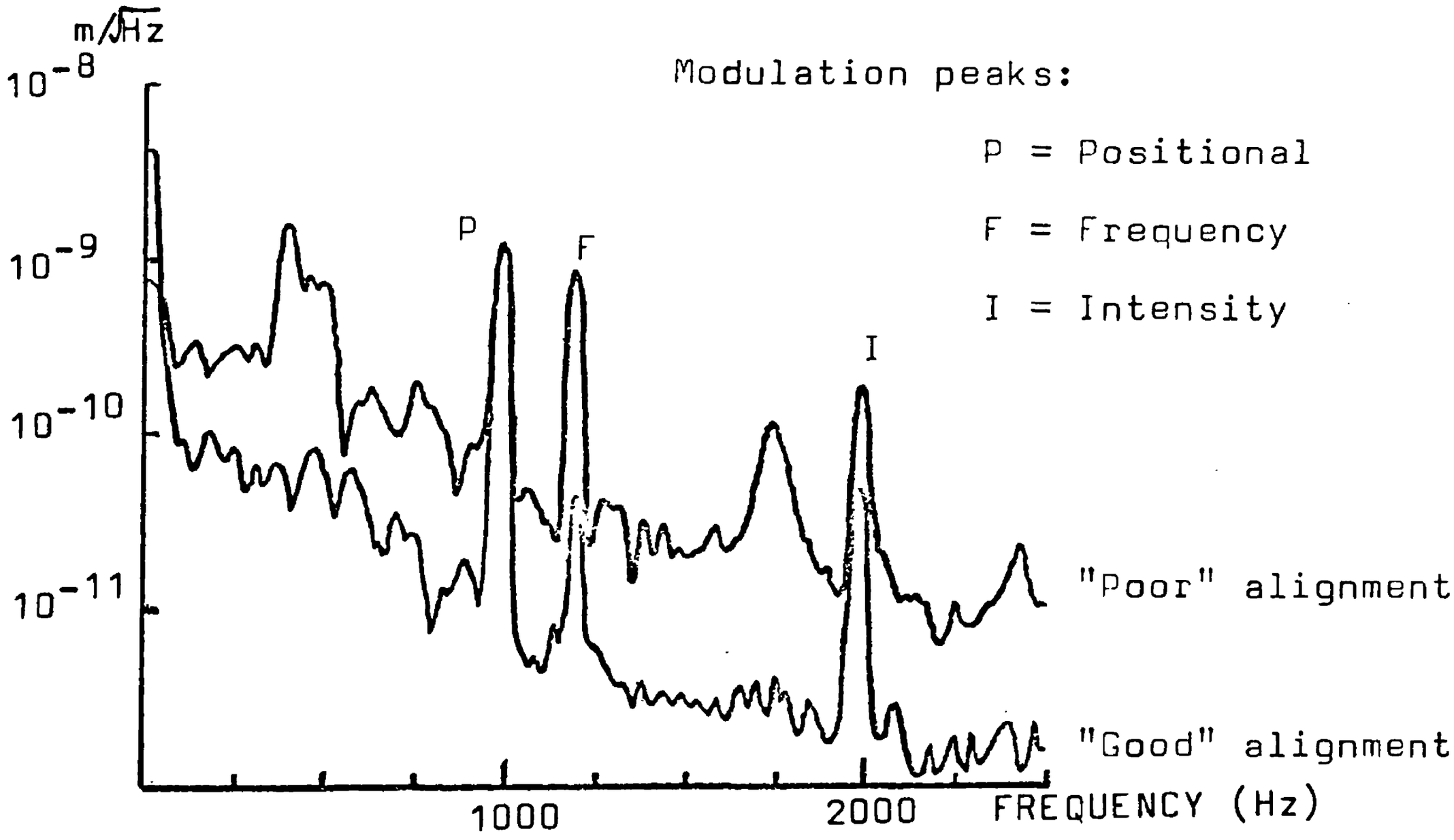

Fig 4·9(a): Beam positional fluctuations after the mode-cleaner, for different alignments of the cavity. Bad alignment allows frequency noise to produce positional changes.

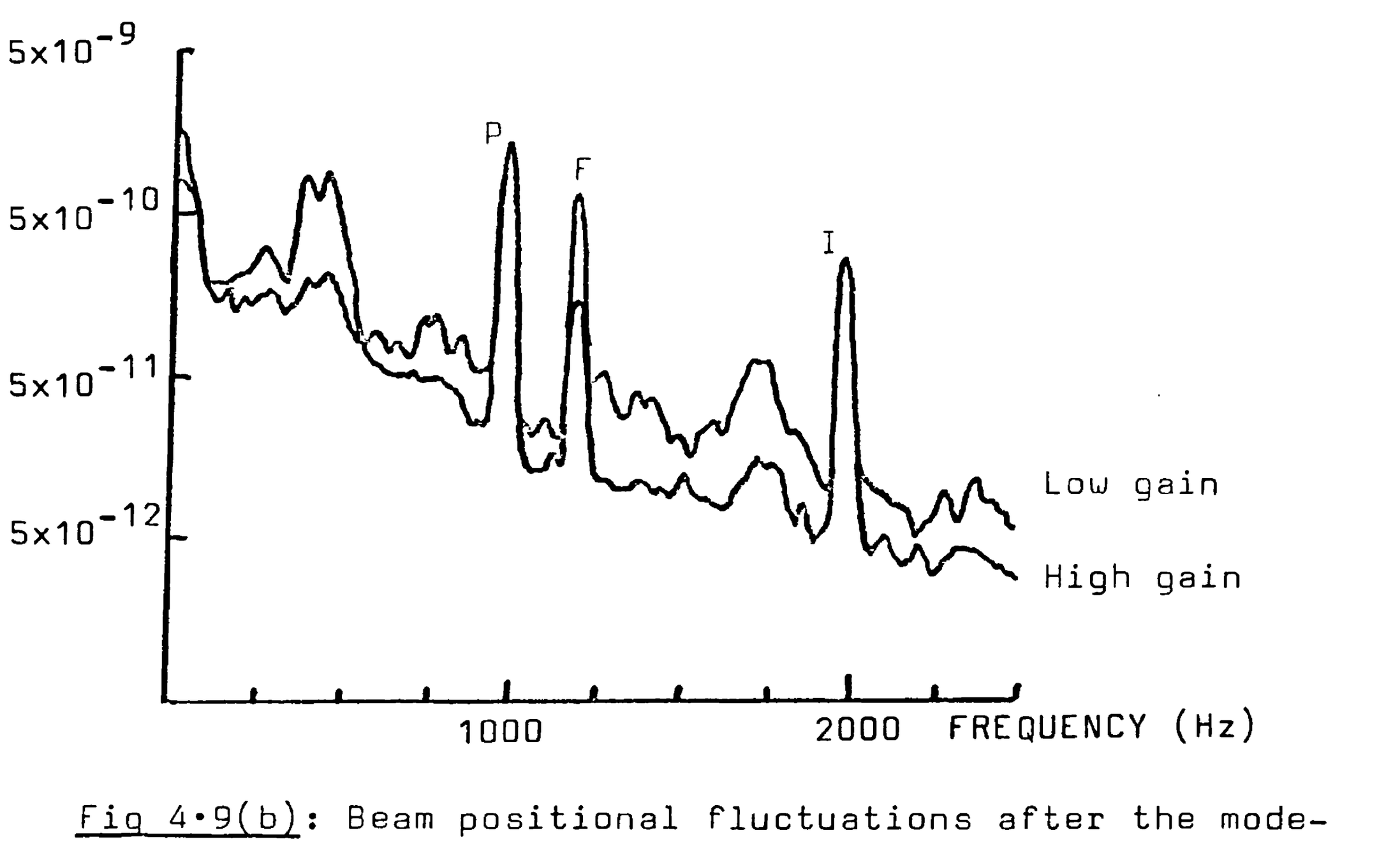

Fig 4·9(b): Beam positional fluctuations after the mode-cleaning cavity ($w \sim 0{\cdot}2mm$), for two different gains (12dB change) of the frequency locking loop. Thus, increasing the relative frequency noise increases the positional fluctuations of the emerging beam.

ental only dropping by 2%. With poor frequency locking, the relative frequency noise might be as high as 5kHz/$\sqrt{Hz}$, giving a fluctuation in beam angle of

$$\delta\theta \sim 5\times10^{-10} \text{ rad}/\sqrt{Hz}$$

The observations are thus explainable. It should be noted that a similar mechanism will produce beam size fluctuations from a combination of frequency noise and incorrect mode-matching.

The elimination of this problem requires both careful alignment of the cavity and very good frequency locking between the cavity and the laser. An increase in the bandwidth of the frequency locking loop achieved by raising the modulation frequency from 80 kHz to 1 MHz and feeding back via the Pockels cell in the laser enabled greater loop gain to be attained, greatly improving the operation of the mode cleaner. The positional fluctuations of the emerging beam were no longer caused by frequency noise, though they were still not reduced by quite as much as a large artificial peak. This was probably due to sound or air currents disturbing the cavity; for once the cavity was placed in a vacuum, both peak and background were reduced by the same factor of about 50 (see fig 4·10). The mode-cleaner thus suppressed positional fluctuations very effectively.

It is evident from (3·14) that the change in transmitted intensity produced by the suppression of higher order modes will be second order in the mode amplitude. It therefore seems that the resultant intensity noise will be completely negligible.

The power throughput achieved with this cavity was

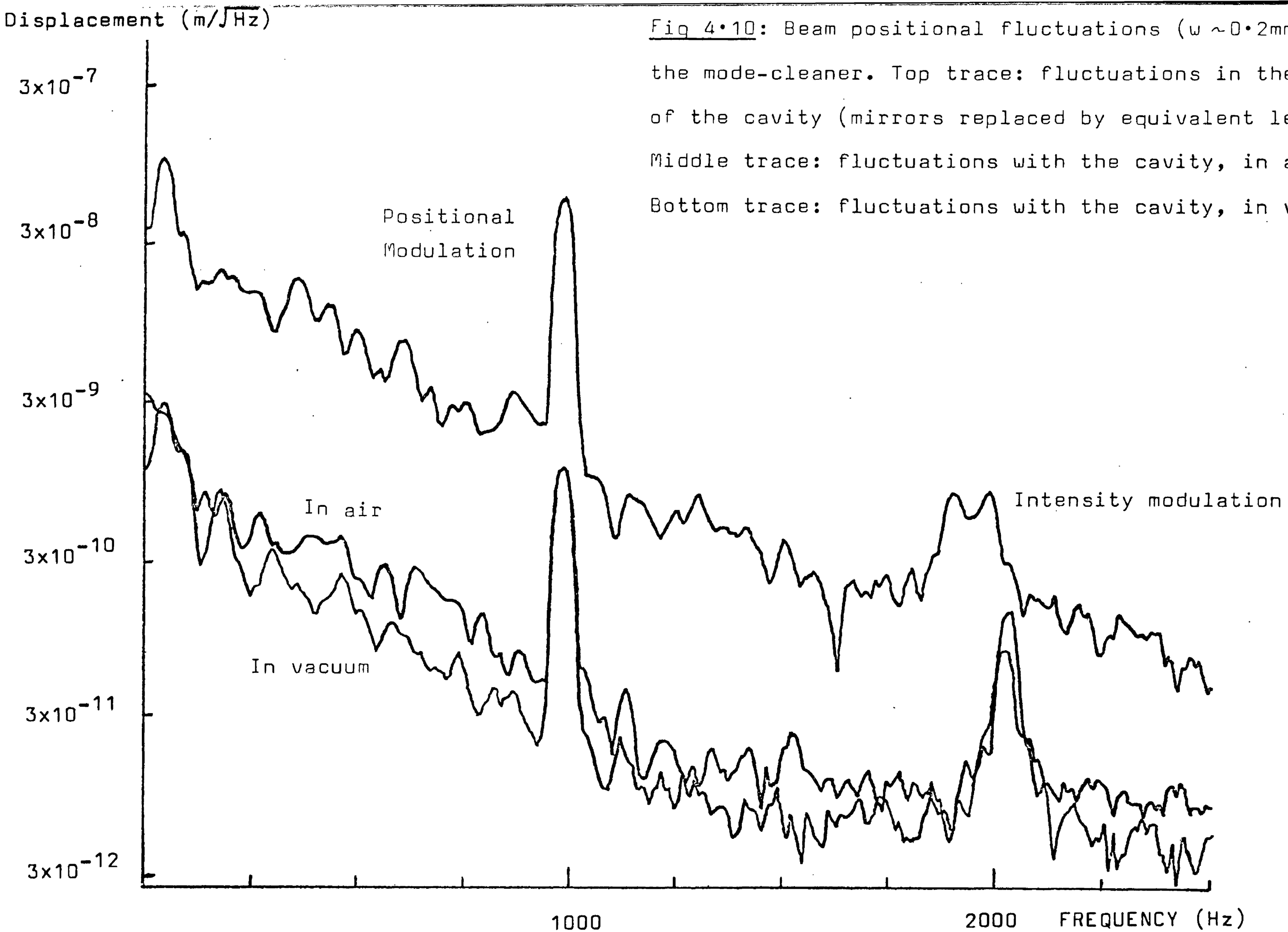

Fig 4·10: Beam positional fluctuations (w ~0·2mm) after the mode-cleaner. Top trace: fluctuations in the absence of the cavity (mirrors replaced by equivalent lenses). Middle trace: fluctuations with the cavity, in air. Bottom trace: fluctuations with the cavity, in vacuum.

only ~45%. It is not clear what limits this, but it is hoped that better mirrors will allow higher efficiencies to be attained.

In the present gravitational wave detector, this same mode-cleaning cavity is incorporated on the central mass. This isolates it from vibration and air currents, and ensures that it stabilises the beam with respect to the correct frame of reference. The linewidth of this mode-cleaner is about 10 MHz, so the RF phase modulation must take place <u>after</u> the cavity. This has the advantage of reducing noise produced by beam positional fluctuations in the Pockels cell (as suggested in Chapter 3 and seen experimentally in Chapter 5). As noted in Chapter 2, the reduction in amplitude of any <u>reflected</u> RF sideband may help to reduce the significance of inadequate optical isolation. In this position on the central mass, the mode cleaner is a good way of reducing beam geometry changes, suppressing beam positional fluctuations by a factor of 50 and (ideally) size fluctuations by a factor of 35. While some additional suppression may ultimately be required, the incorporation of the mode cleaner should certainly greatly reduce the noise due to beam geometry fluctuations.

<u>(4·3)Active Control of Beam Position</u>

An active system for reducing positional fluctuations of the laser beam works by minimising some position signal (e.g. from a quadrant diode) via feedback onto some trans-

ducer (i.e. beam deflector). If both angular and lateral fluctuations (i.e. the two orthogonal phases of the first order mode) are to be suppressed, then two separate detectors and two separate transducers are required for each dimension. The beam may then be stabilised by minimising its positional deviations from each detector independently, using a suitable combination of transducers to do so. With the detectors at different positions, the beam's position in space is defined.

While such a system is complex, it has the advantage that less light may be lost than for a passive system; there are no problems with handling high optical powers; the potential suppression factor is greater (for a noisy laser), being limited by the diode sensitivity; and suitable choice of diode placement enables the beam to be stabilised to any frame of reference. With these considerations in mind, it was decided to construct such a system.

If the diodes and transducers are labelled by subscripts n,m (n,m = 1,2) then the positional signal D_n from a diode, produced by voltages T_m applied to the transducers may be written

$$\begin{pmatrix} D_1 \\ D_2 \end{pmatrix} = \begin{pmatrix} A_{11} & A_{12} \\ A_{21} & A_{22} \end{pmatrix} \begin{pmatrix} T_1 \\ T_2 \end{pmatrix} \qquad (4\cdot15)$$

If the voltages on the two transducers are arranged to be in the ratio $T_2/T_1 = -A_{11}/A_{12}$, then no signal will be produced out of diode 1, while the voltage from diode 2 will be

$$D_2 = T_1(A_{21} - A_{11}A_{22}/A_{12}) \qquad (4\cdot16)$$

So, as long as the optical arrangement is such that $A_{21}A_{12} = A_{11}A_{22}$, a combination of voltages may be found which will minimise the positional deviations on one diode without affecting the other. If the voltages fed-back to the transducers are

$$\begin{pmatrix} T_1 \\ T_2 \end{pmatrix} = \begin{pmatrix} B_{11} & B_{12} \\ B_{21} & B_{22} \end{pmatrix} \begin{pmatrix} D_1 \\ D_2 \end{pmatrix} \qquad (4\cdot17)$$

then the conditions for independent operation are

$$B_{11}/B_{21} = -A_{22}/A_{21} \qquad (4\cdot18)$$

$$B_{12}/B_{22} = -A_{12}/A_{11} \qquad (4\cdot19)$$

These conditions may be achieved in practice using a circuit of the type shown in fig 4·11.

In principle, the beam positional fluctuations may be reduced until they are the same as the noise in the detector (ultimately, the shot noise in the diode current). For 1mW of light, the potential suppression factor is over 100 at 1 kHz for our laser, and larger at lower frequencies. in order to take advantage of this, a high servo bandwidth ($\gtrsim$ 100 kHz) is required. Yet, at the same time, a large dynamic range is needed in order to follow slow drifts of the laser beam position. This latter problem is especially severe when the diodes are placed on the central mass of the interferometer, since the beam steering transducers must then compensate for any motion of this mass, such as occurs when the detector is aligned. The solution adopted was to use two sets of transducers: a large range, low bandwidth (~10 Hz) system consisting of a mirror, the angle of which may be varied (in two dimensions) by small loudspeakers (see fig 4·12); and a

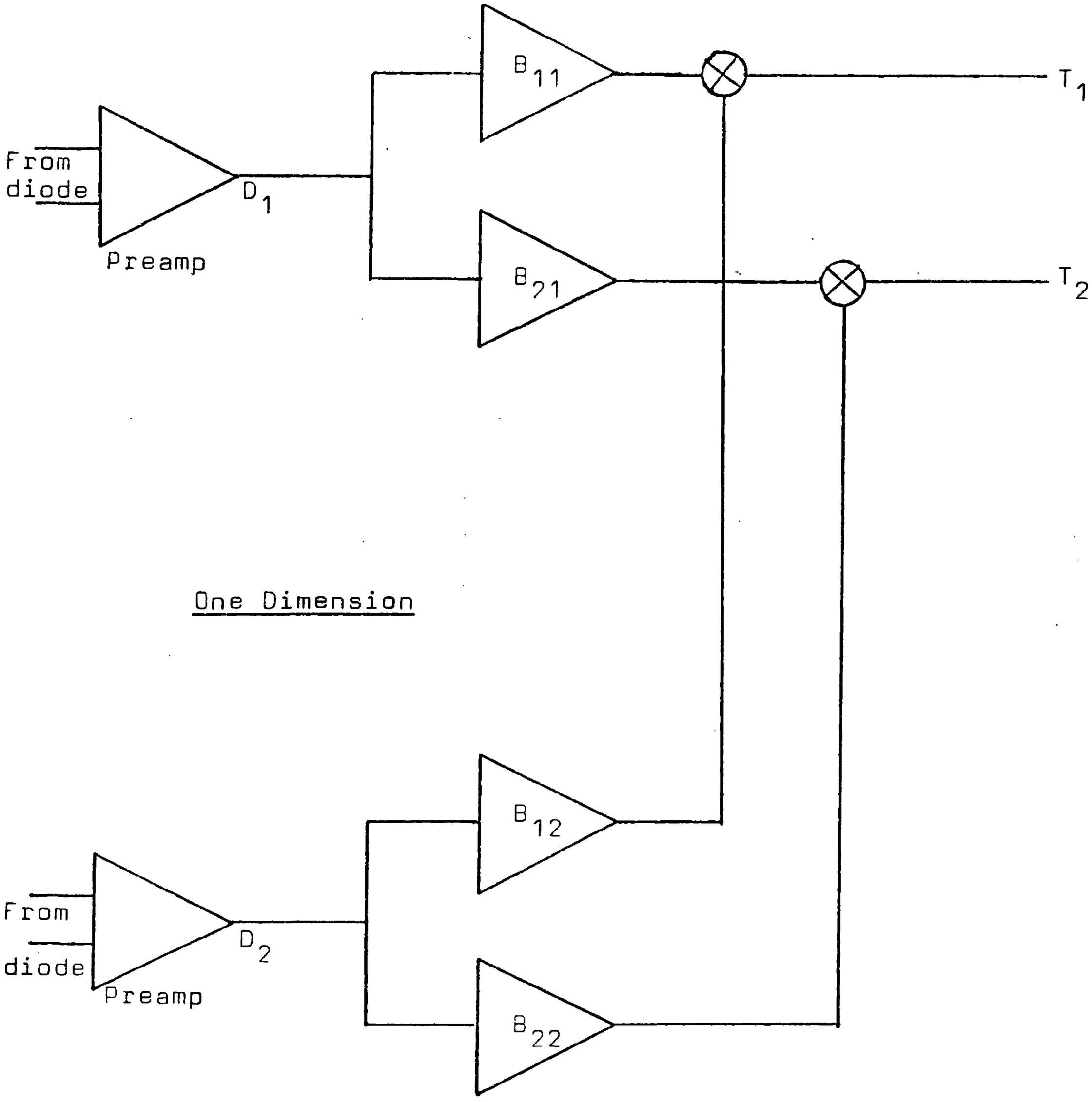

Fig 4·11: Schematic diagram of a system to stabilise the position of a laser beam. The difference signal from each diode, D_n, is split into two and passed through variable gain amplifiers; signals from each diode are added and applied to the transducers T_m. Adjustment of the magnitude and sign of the gains B_{mn} to satisfy (4·18) and (4·19) ensures that a signal applied to the transducers from one diode produces no displacement on the other. The feedback system for each dimension may then be resolved into two independent systems.

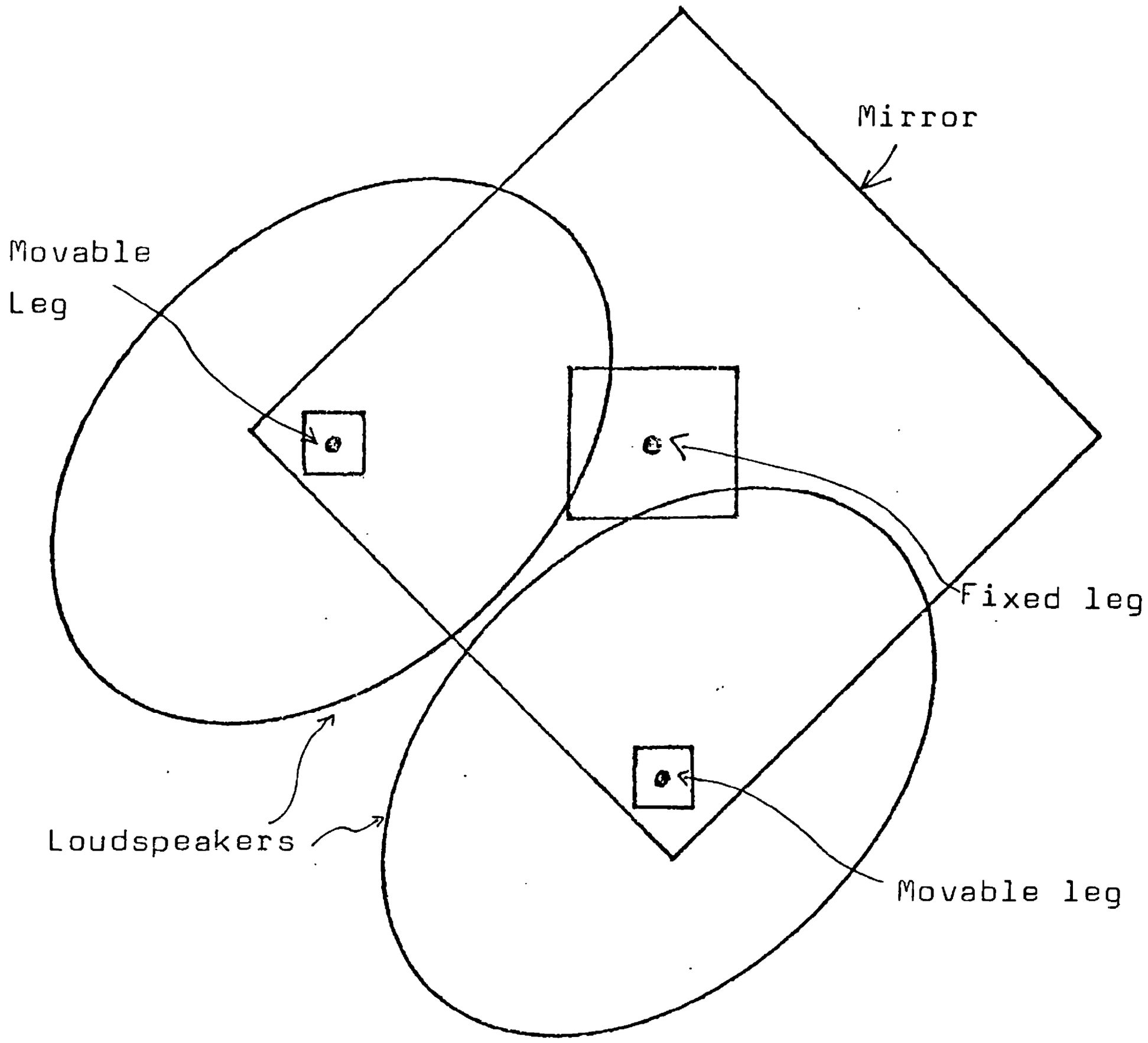

Fig 4·12: Plan view of the large range, low frequency beam steering transducer. The mirror is supported by three legs arranged in a right-angled triangle, two of which are movable by small loudspeakers. The mirror can therefore be tilted in each of the two dimensions.

The transducer is shown actual size.

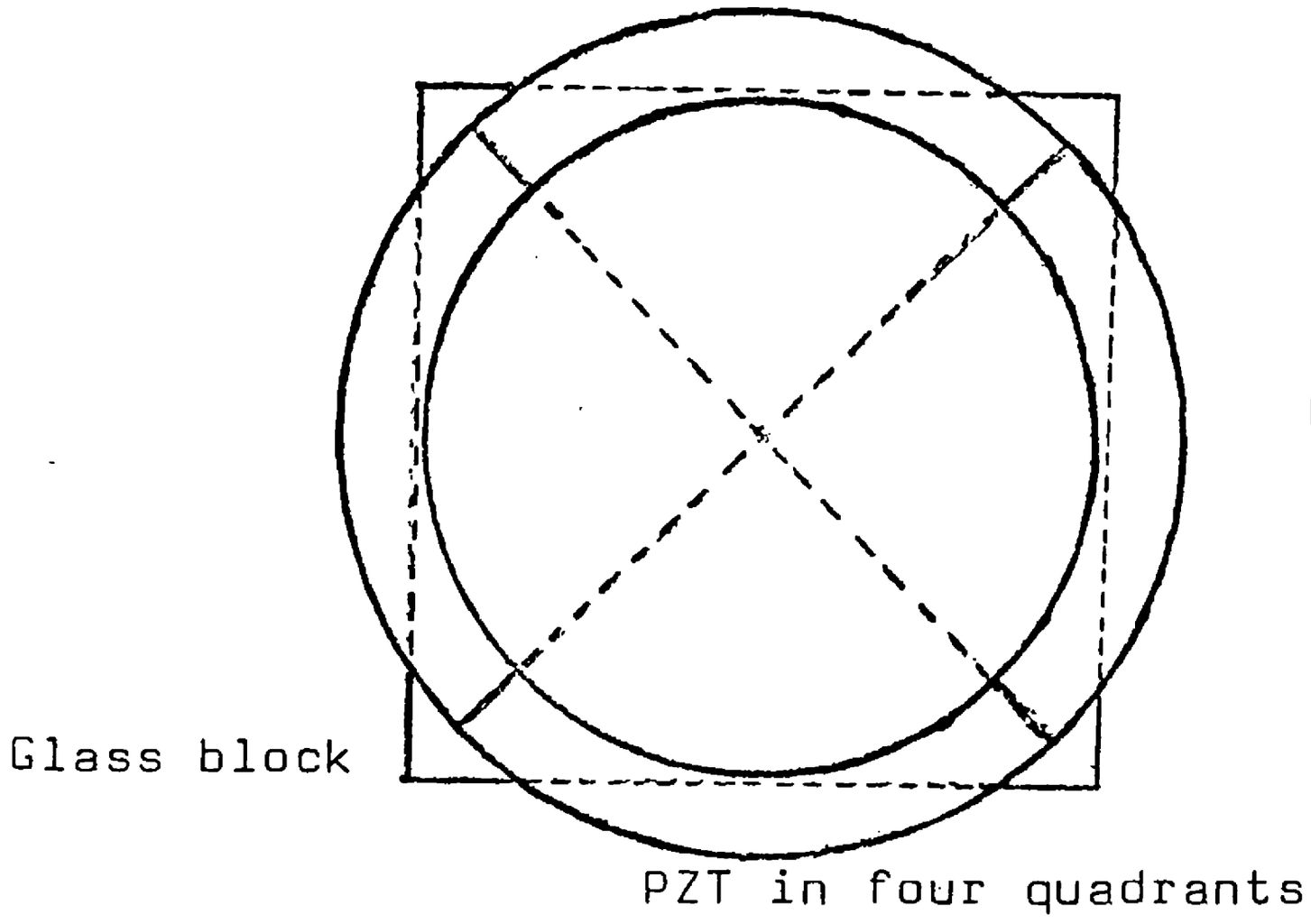

Fig 4·13: Plan view of the high frequency beam steering transducer. A cubic glass block of side 1cm is glued to a lead block, which is both massive and lossy. The glass isolates the PZT which is glued onto it (with epoxy) and allows electrical connections to be made to the underside of the PZT where it overlaps the block. The PZT, which is a 1mm thick disc, is filed into four independent quadrants. Opposite quadrants are driven with opposite volts, so that the mirror glued to the PZT may be tilted in the two dimensions. The mirror used was a Spectra laser back mirror, which conveniently combined high quality and small size.

Electrical connections were made by soldering, epoxy was used throughout and mechanical damping was provided by "Q" compound.

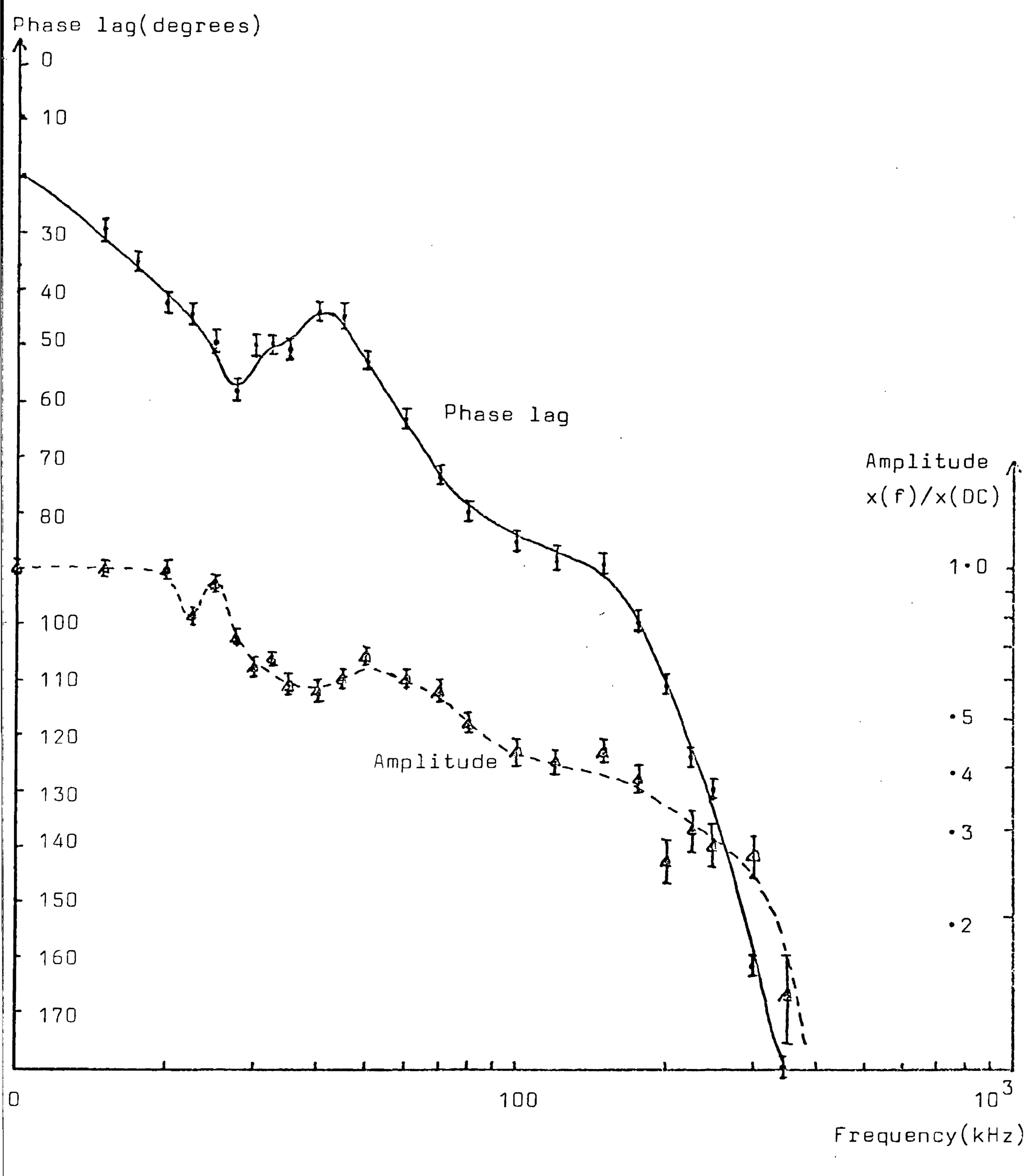

Fig 4·14: The phase and amplitude response of one of the "fast" beam steering transducers. The potential servo bandwidth with such a transducer is about 100 kHz.

small range, high bandwidth system consisting of a mirror mounted on PZTs (see figs 4·13, 4·14). The low bandwidth system has a response of ~0·1 rad/A, with a resonance at 220 Hz. The fast transducers give a movement of $\sim 2\times10^{-7}$ rad/V, or $\sim 4\times10^{-5}$ rad if $\pm$100V amplifiers are used differentially. The frequency response of the better of the two fast transducers is shown in fig 4·14, demonstrating that servo bandwidths of ~100 kHz should be possible. In the other transducer, the resonance at ~35 kHz was more pronounced, limiting the bandwidth, it will be seen, to ~30 kHz.

The final arrangement is indicated in fig 4·15. The two diodes are placed on the central mass of the interferometer, with a lens to effectively separate them (or, equivalently, to change the phase of the first order mode relative to the fundamental). The position signal from each dimension of each diode is then fedback onto either the low frequency transducers only, or both sets together, to keep the laser beam locked onto the centre of both diodes. The ratios (4·18) and (4·19) may be set empirically by injecting a large artificial signal at a point as if it came from one diode and adjusting the potentiometers that determine B_{11}, B_{21} etc until movement is observed on one diode but not the other. It is important to place the transducers as far apart as possible, so that they move the beam differently, as well as having the diodes separated by as large an effective distance as possible.

The low frequency beam steering system uses operational amplifiers to perform the required algebra, with a current booster (I_{out} = 300 mA) as an output driver,

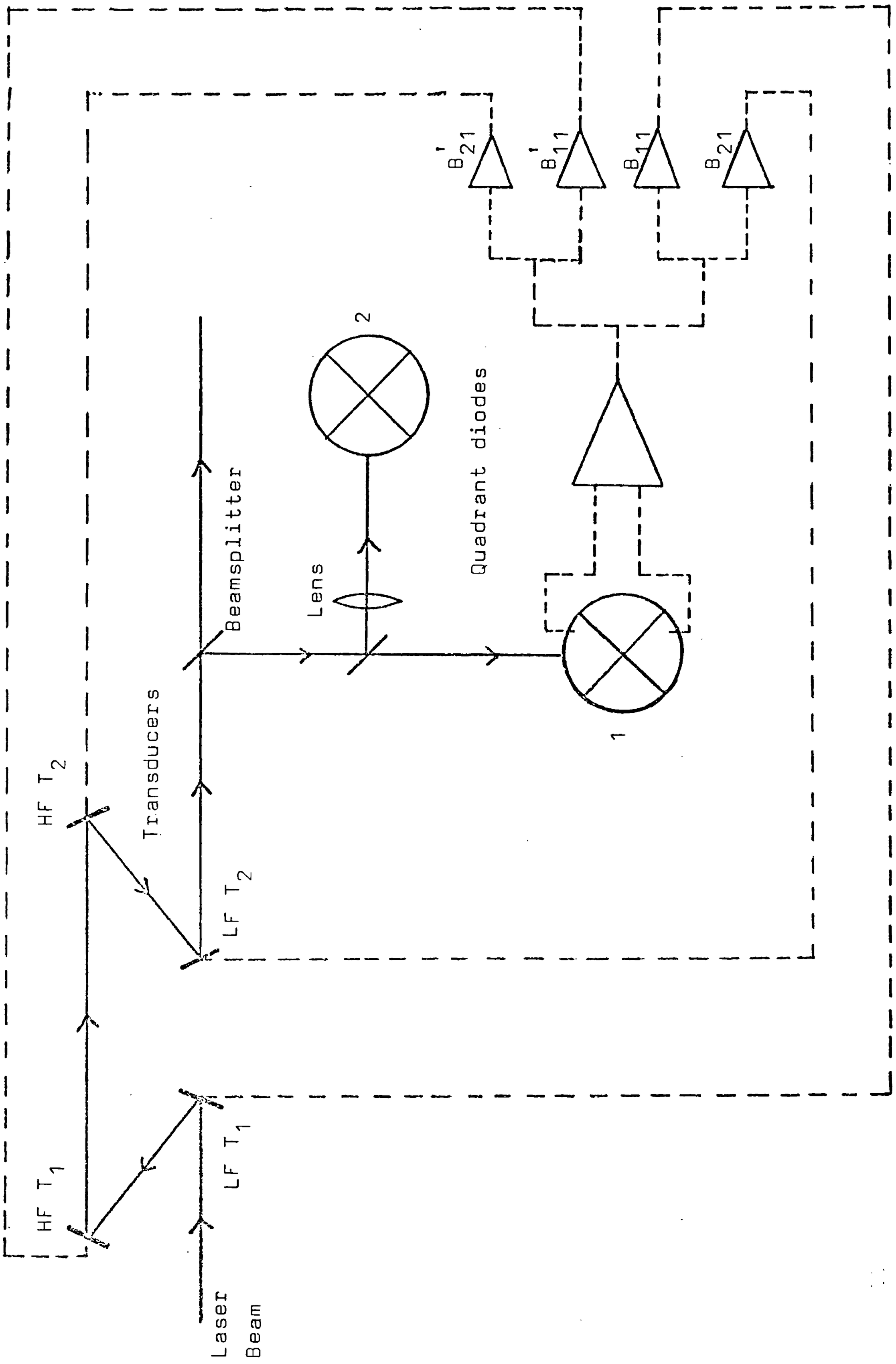

Fig 4·15: Schematic diagram of the current arrangement of the system to stabilise the beam position.

as indicated in fig 4·16. The performance of the low frequency system alone is shown in fig 4·17, where spectra of the signal output from one dimension of the diode with no lens, with the feedback loop open and closed, are compared. The presence of intensity modulation, shown in fig 4·18, demonstrates the insensitivity of the signal to intensity noise. It can be seen that the unity gain frequency is ~10 Hz; the gain increases at lower frequencies (until ~0·25 Hz), where the loop gain is ~40. This bandwidth limit is currently due to the excitation of a high Q loudspeaker resonance at ~220 Hz, which is reduced to an acceptable size by the 270Ω damping resistor and further roll-off at ~50 Hz (fig 4·16). This low frequency servo functions very well on its own as a way of maintaining the alignment of the cavities and providing points at which to monitor the positional fluctuations of the laser beam on the central mass.

The circuit for the high frequency loop is shown in fig 4·19. It was found necessary to drive the two sides of each PZT with opposite volts from two 100 V amplifiers, to provide sufficient range to cope with the natural motions. Note that the feedback network is AC coupled, with a characteristic frequency of ~50 Hz. This is a convenient way of removing the DC offset of the 733 amplifier in fig 4·19 and, more importantly, avoids burdening the loop with the large low frequency motions. Substantial gain remains, however, at a few Hz. Indeed, the achievable loop gain is considerable in the operating range of the detector. This may be seen in figs 4·20 and 4·21,

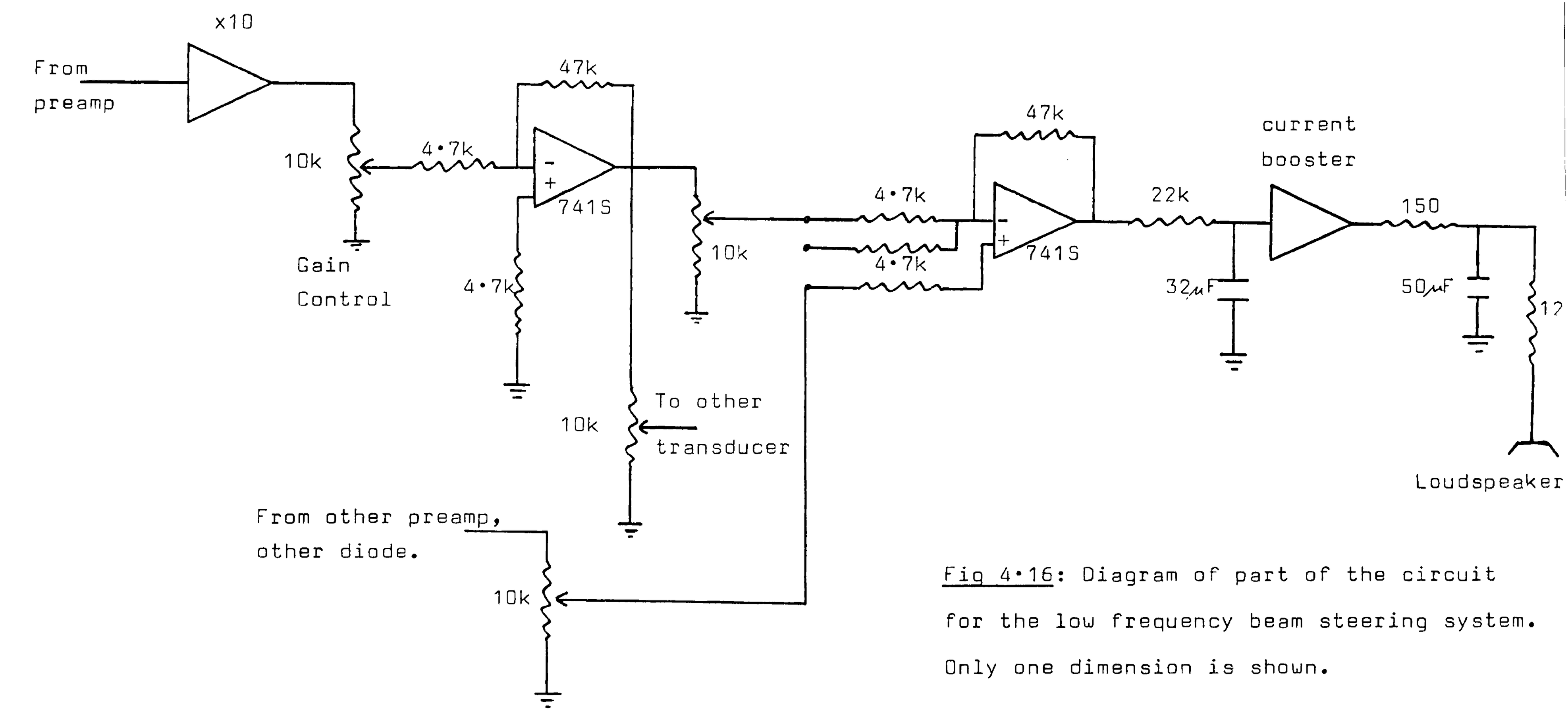

Fig 4·16: Diagram of part of the circuit for the low frequency beam steering system. Only one dimension is shown.

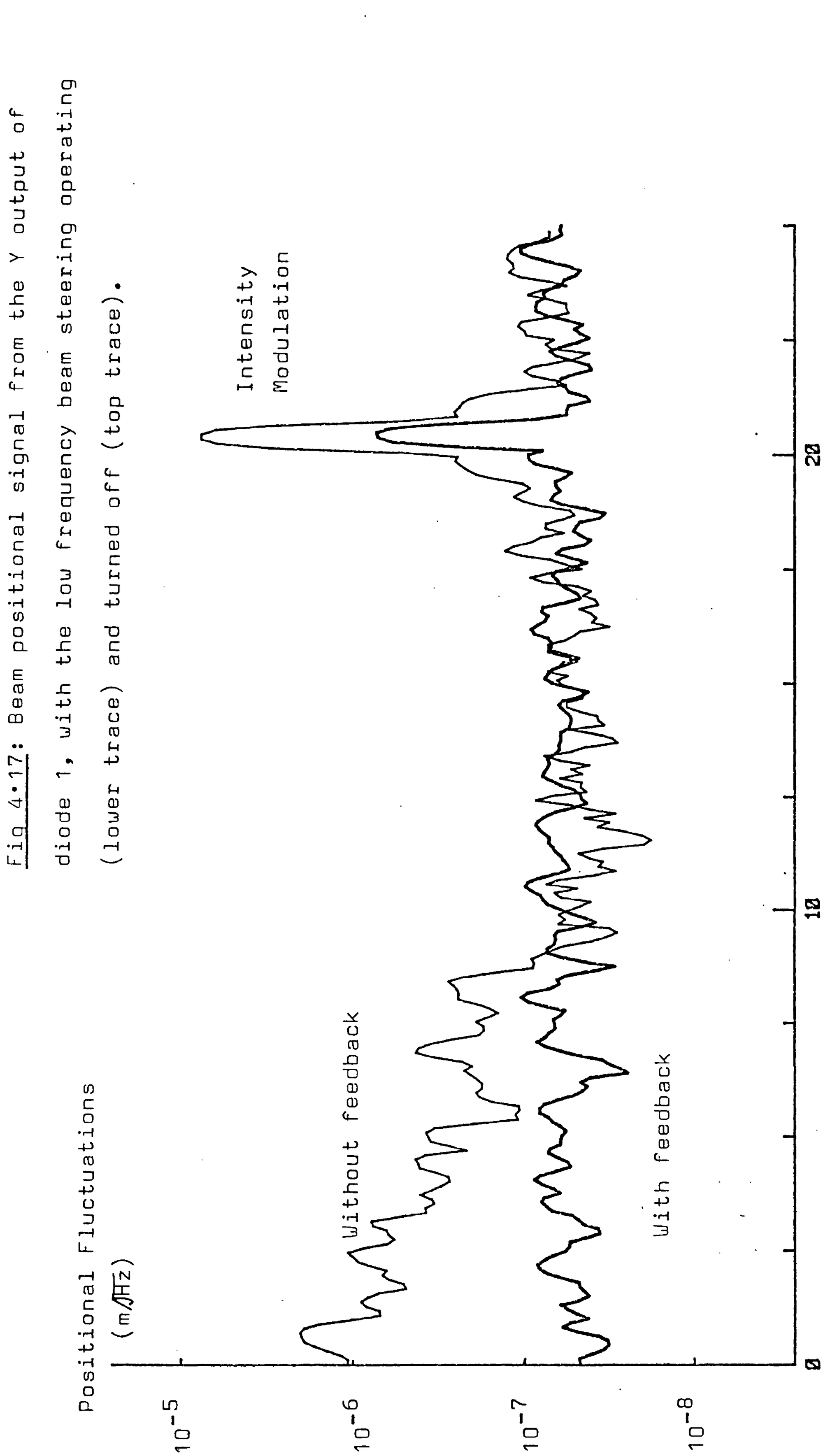

Fig 4·17: Beam positional signal from the Y output of diode 1, with the low frequency beam steering operating (lower trace) and turned off (top trace).

Fig 4·18: The intensity noise of the laser in a 25Hz bandwidth, showing the size of the modulation peak of fig 4·17.

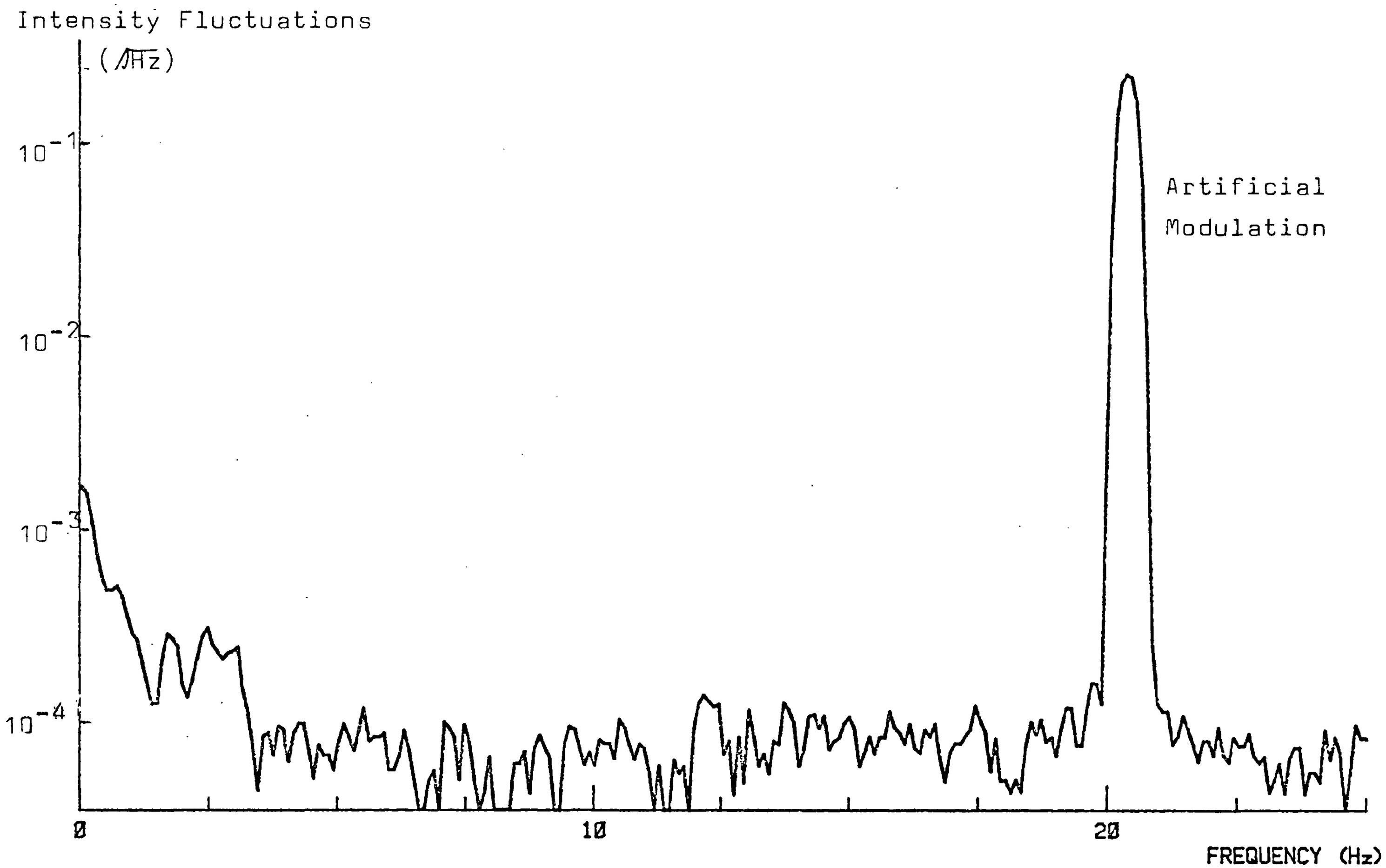

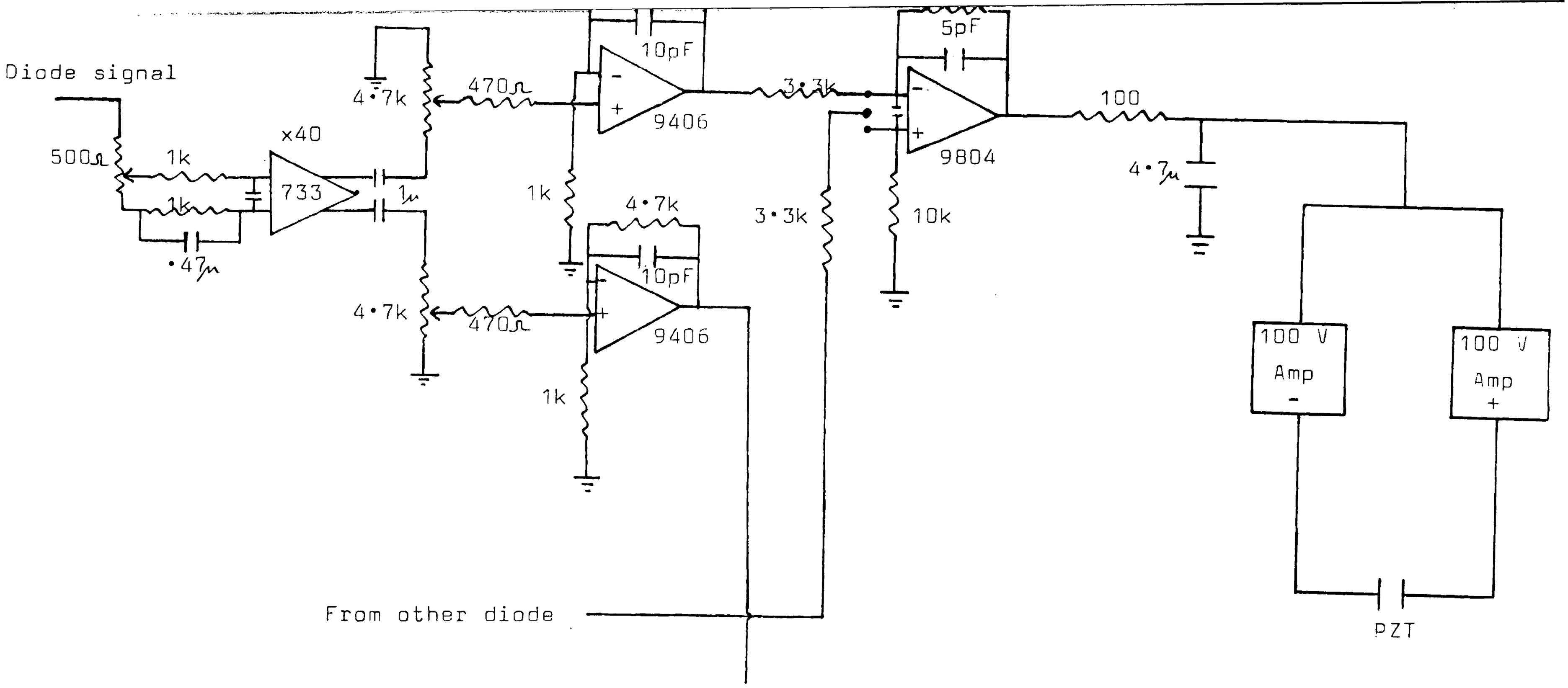

Fig 4•19: Part of the circuit diagram for one dimension, one transducer of the fast beam position stabilisation system.

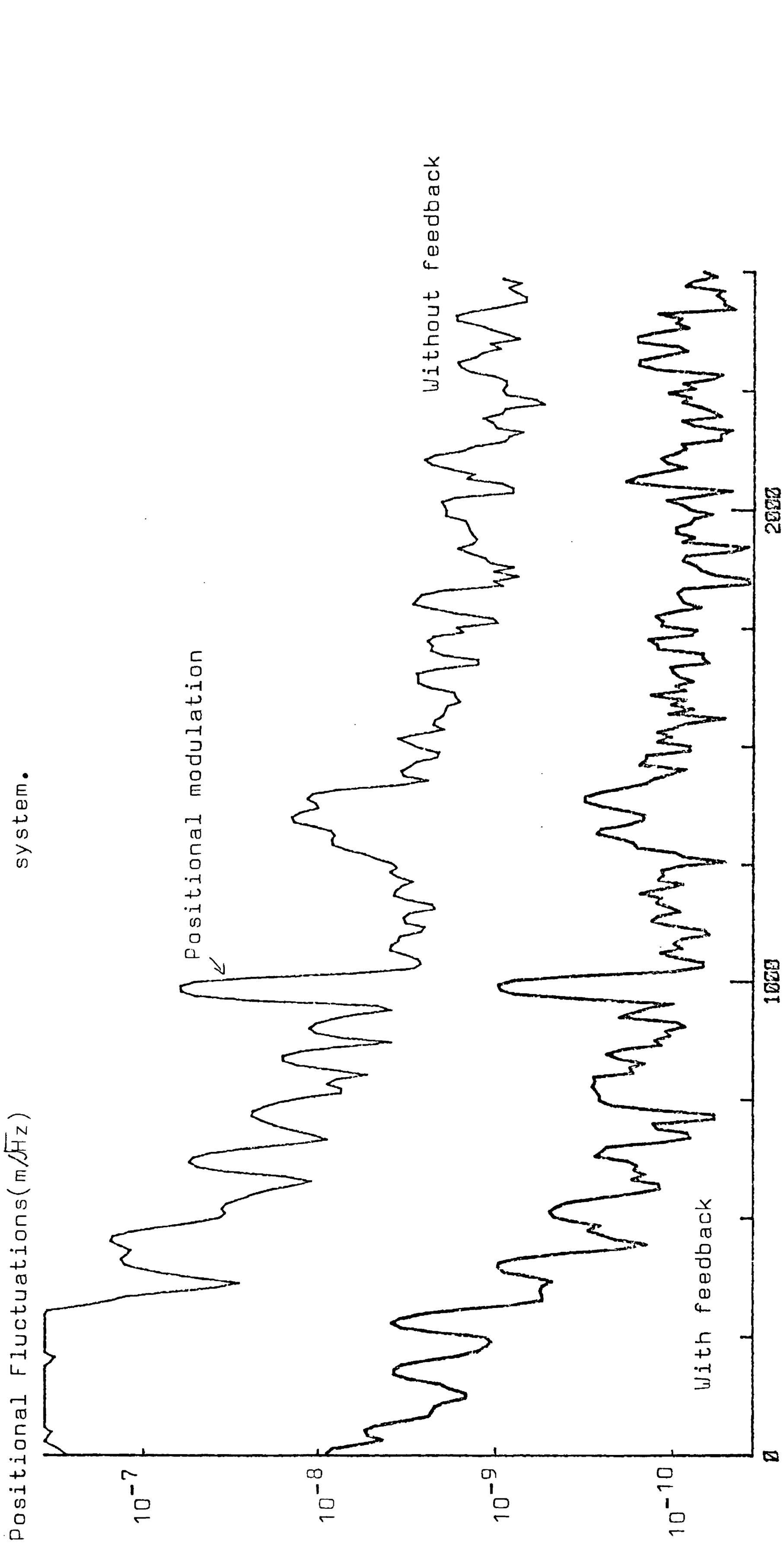

Fig 4·20: Beam positional signal from the Y output of diode 1, with and without the fast beam stabilisation system.

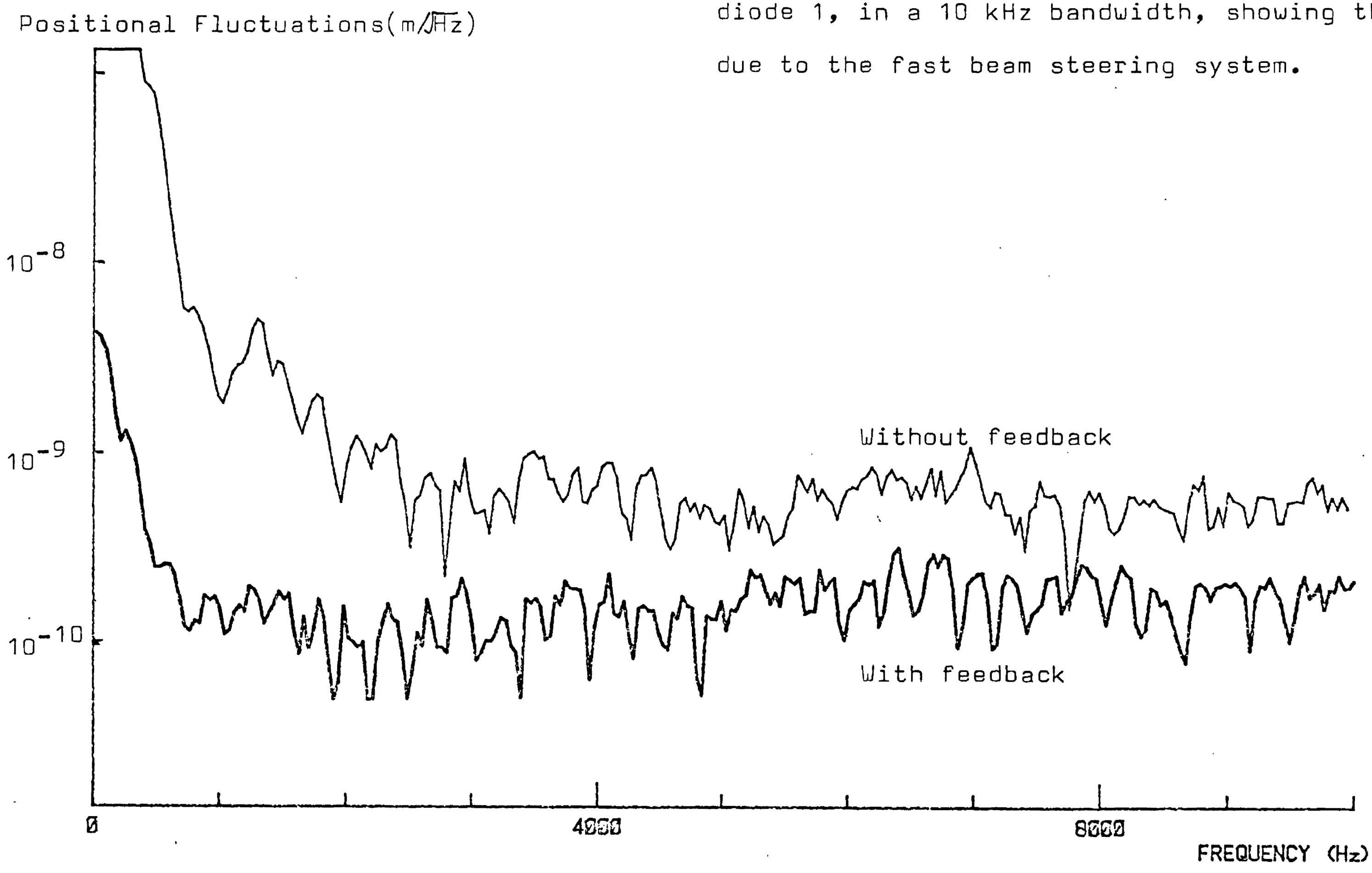

Fig 4·21: Beam positional signal from the Y output of diode 1, in a 10 kHz bandwidth, showing the reduction due to the fast beam steering system.

which demonstrate the reduction by the feedback system of the positional signal from one of the quadrant diodes on the central mass. With a unity gain frequency of ~30kHz, loop gain of ~30dB is attainable at 1kHz and more at lower frequencies.

In the absence of other noise, such as that due to intensity fluctuations or electrical pick-up, the positional fluctuations should be reduced by a factor approximately equal to the loop gain. A lower limit on the importance of intensity noise may be found by measuring the coupling of intensity modulation into the quadrant diode signal with only the low frequency feedback working. This indicates (cf. fig 3·4) that positional fluctuations could be reduced by over an order of magnitude before intensity changes become important. The fast loop will probably also reduce the intensity noise coupling by keeping the beam more accurately centred on the diode.

A serious problem with the present arrangement is electrical pick-up. This is shown in fig 4·22, where the positional signal from one quadrant diode with only the low frequency feedback functioning is compared with the same signal with the incident laser beam blocked. It is evident that beam positional fluctuations are not being measured (and may not, therefore, be suppressed) above 1500 Hz. This pick-up seems to be occurring on the cable from the diodes to the preamplifiers, where the signal levels are low — the peaks correspond to a noise level of ~0·1 $\mu V/\sqrt{Hz}$. This will probably necessitate the replacement of the twisted pairs from the diodes to the stack by proper coaxial cable, such as the microco-ax used for

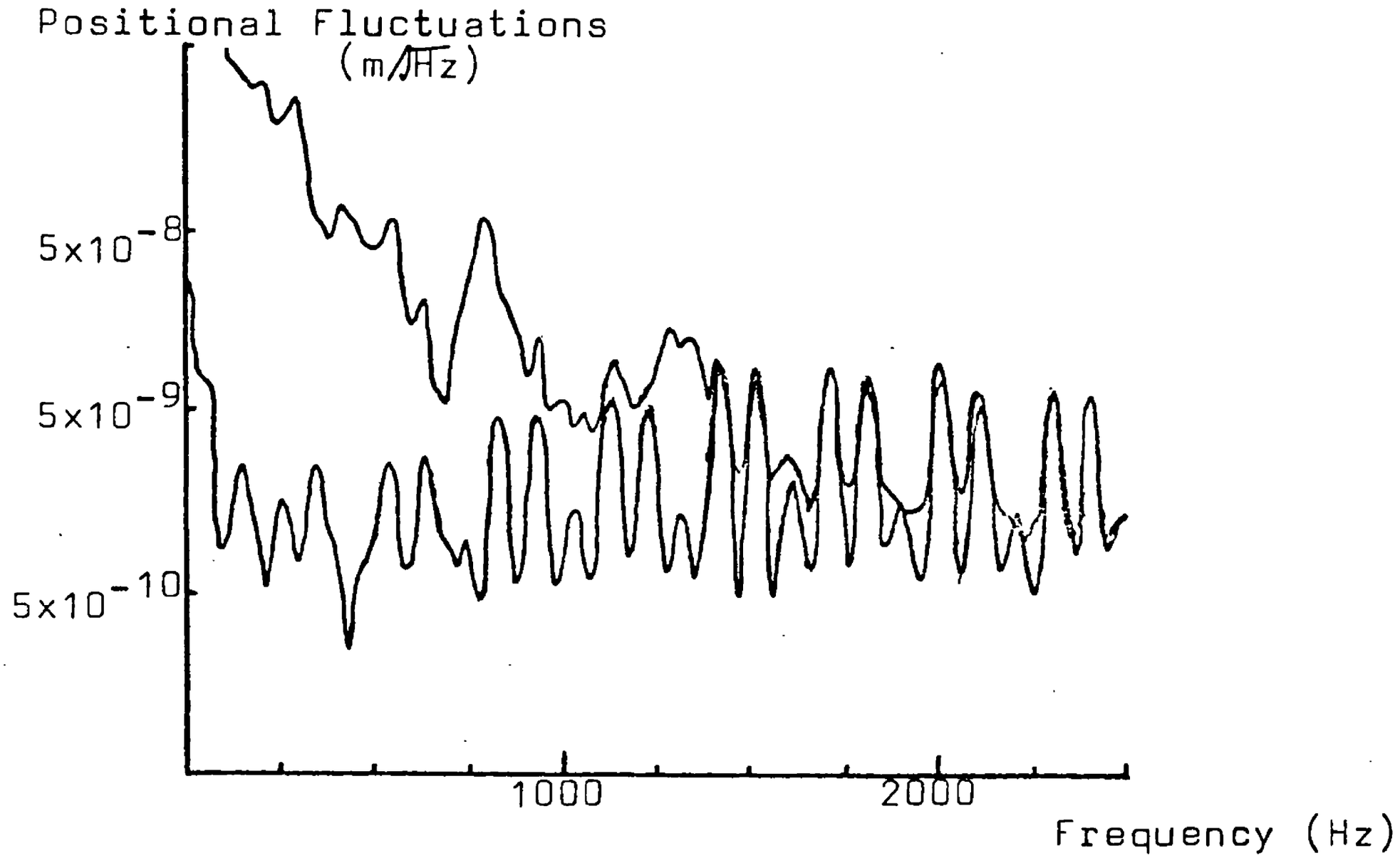

Fig 4·22: Beam positional signal from diode 1 (Y output); top trace: low frequency feedback only functioning bottom trace: no light on diode

the RF modulation. This modification was postponed, however, since it would have disrupted the operation of the whole detector, which took priority. The original arrangement does still provide the possibility of substantially reducing beam positional fluctuations in the important region below 1 kHz.

A proper independent measurement of the functioning of the feedback system would require an additional, independent quadrant diode (or alternative measuring system) actually on the central mass. In view of the practical problems associated with this (such as lack of room), it was decided to attempt a measurement using a quadrant

diode placed on the optical table, with light being split off for it at the entrance to the vacuum system. Even if the beam was perfectly stable with respect to the central mass, it would still produce a fluctuating signal from this diode because of the relative motion of table and mass, together with intensity noise due to imperfect centre-ing. This arrangement is, however, able to put an upper limit on the beam motion, thus a lower limit on the factor by which it is suppressed by the feedback system. The position signal from this independent diode, both with and without the operation of the fast feedback system, is shown in fig 4·23. These measurements were found to be quite repeatable, even though the spot was moving considerably at low frequencies; the lack of dependence on offset suggests that intensity noise was not important. It can be seen that the feedback system suppressed the positional fluctuations of the laser beam by a factor of up to 100 (at ~400 Hz) and typically 10.

While its useful bandwidth is currently restricted, it is evident that the present fast feedback system provides considerable reduction of beam positional fluctuations below 1 kHz. It effectively eliminates the rise in the noise spectrum at low frequencies, a necessity if the interferometer is ever to operate down to 100 Hz. In combination with the mode cleaner, it should allow high gravitational wave sensitivities to be attained.

Fig 4·23: Beam positional signal from the independent measuring diode on the optical table. The reduction of the positional fluctuations by the fast feedback system is shown.

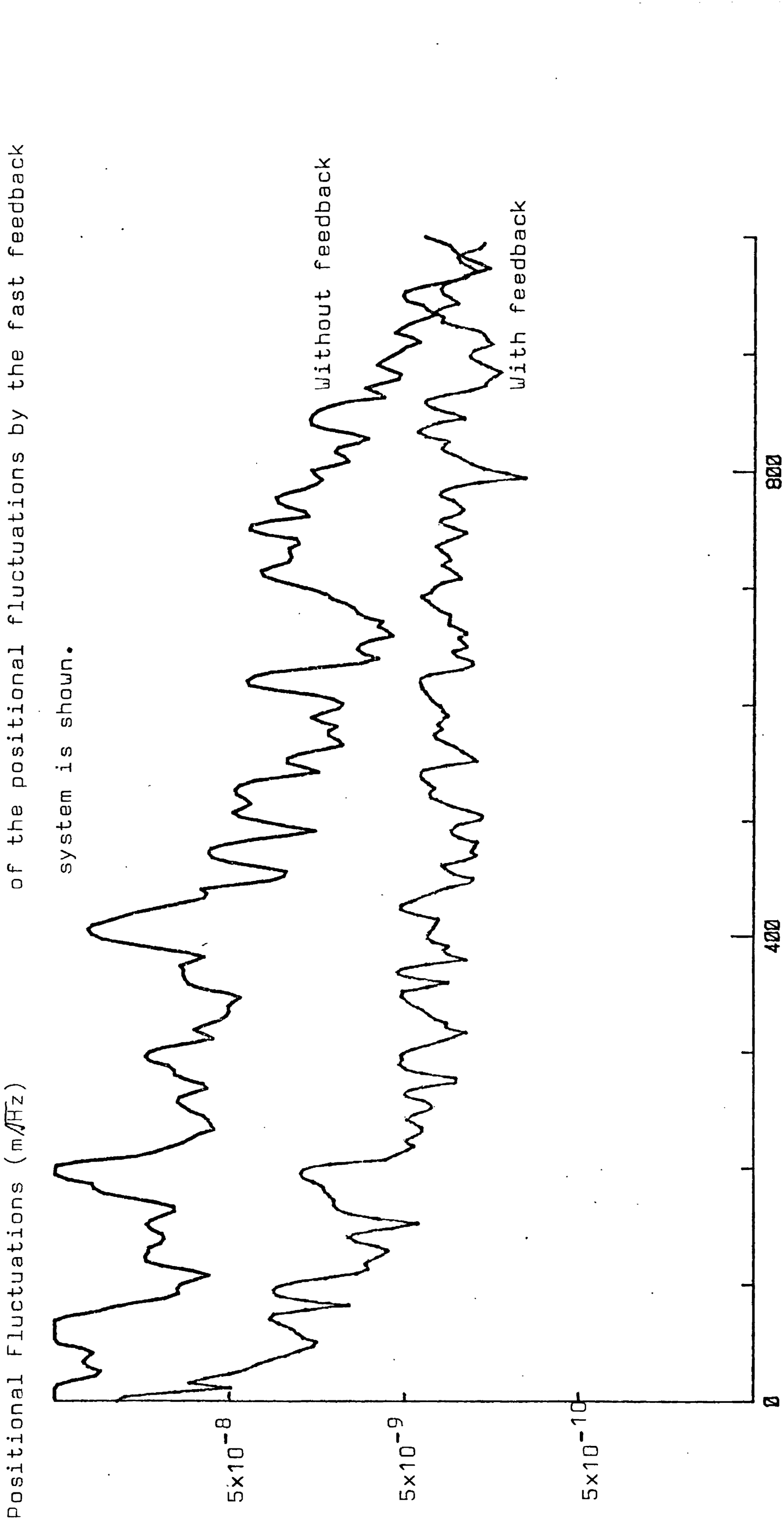

CHAPTER FIVE

DETECTOR PERFORMANCE

(5·1)Preliminary Experiments

When the decision was made to modify the detector to run as a polarisation interferometer wsing two-mirror cavities, it seemed wise to perform some preliminary experiments, which would enable noise sources to be investigated and control experience gained in relatively simple experimental situations. The whole of the group was involved in these investigations.

The first of these experiments, intended to investigate the noise level when recombining two beams, used the simple polarisation interferometer shown in fig 5·1. Linearly polarised light enters a four-crystal Pockels cell at 45° to the optic axis; a signal applied to the Pockels cell thus modulates the relative phase of the two orthogonally polarised components of the incident beam. These two components are then recombined by a polariser followed by a photodiode. Observation of the demodulated intensity signal gives a measure of the low frequency relative phase fluctuations of the two components. The near identity of the paths taken by the two polarisations means that this arrangement is insensitive to some noise sources, notably frequency fluctuations. This system is therefore a good way of testing for the presence of rather more exotic noise sources.

Great care was found to be necessary to avoid scattering as the beam went through the Pockels cell or beamsplitter, since this allowed frequency fluctuations to

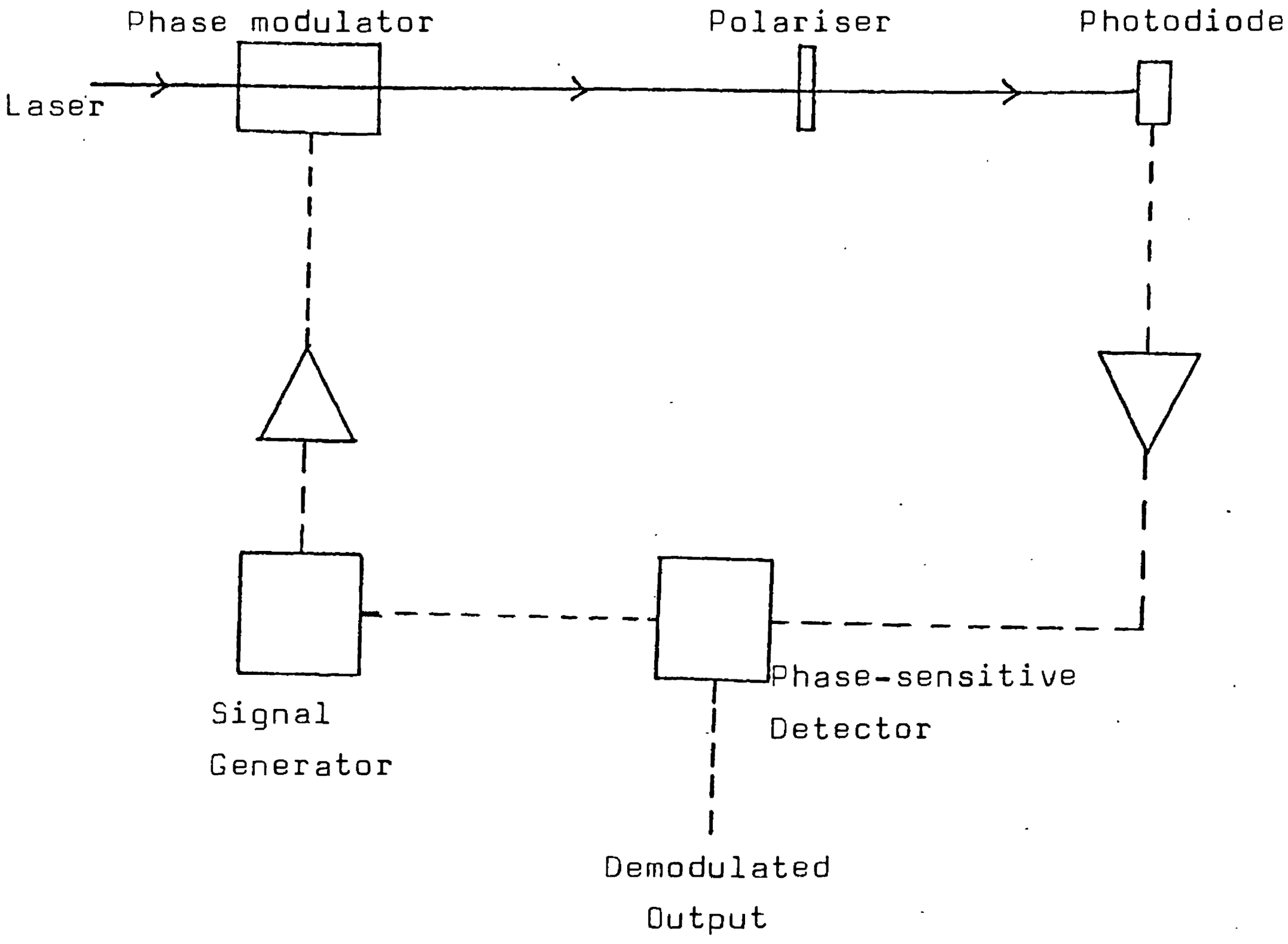

Fig 5·1: Schematic diagram of the simple polarisation interferometer used to investigate noise sources.

produce excessive noise in the final (demodulated) output. Perhaps the greatest surprise at the time, however, was the extreme sensitivity of this interferometer to positional fluctuations of the beam. This can be seen in fig 5·2, which shows the demodulated intensity signal (compared with the photon shot noise), together with a spectrum of the beam positional fluctuations as measured with a quadrant diode ~10cm after the Pockels cell. The shot noise level was measured by shining a torch onto the diode so

(a)

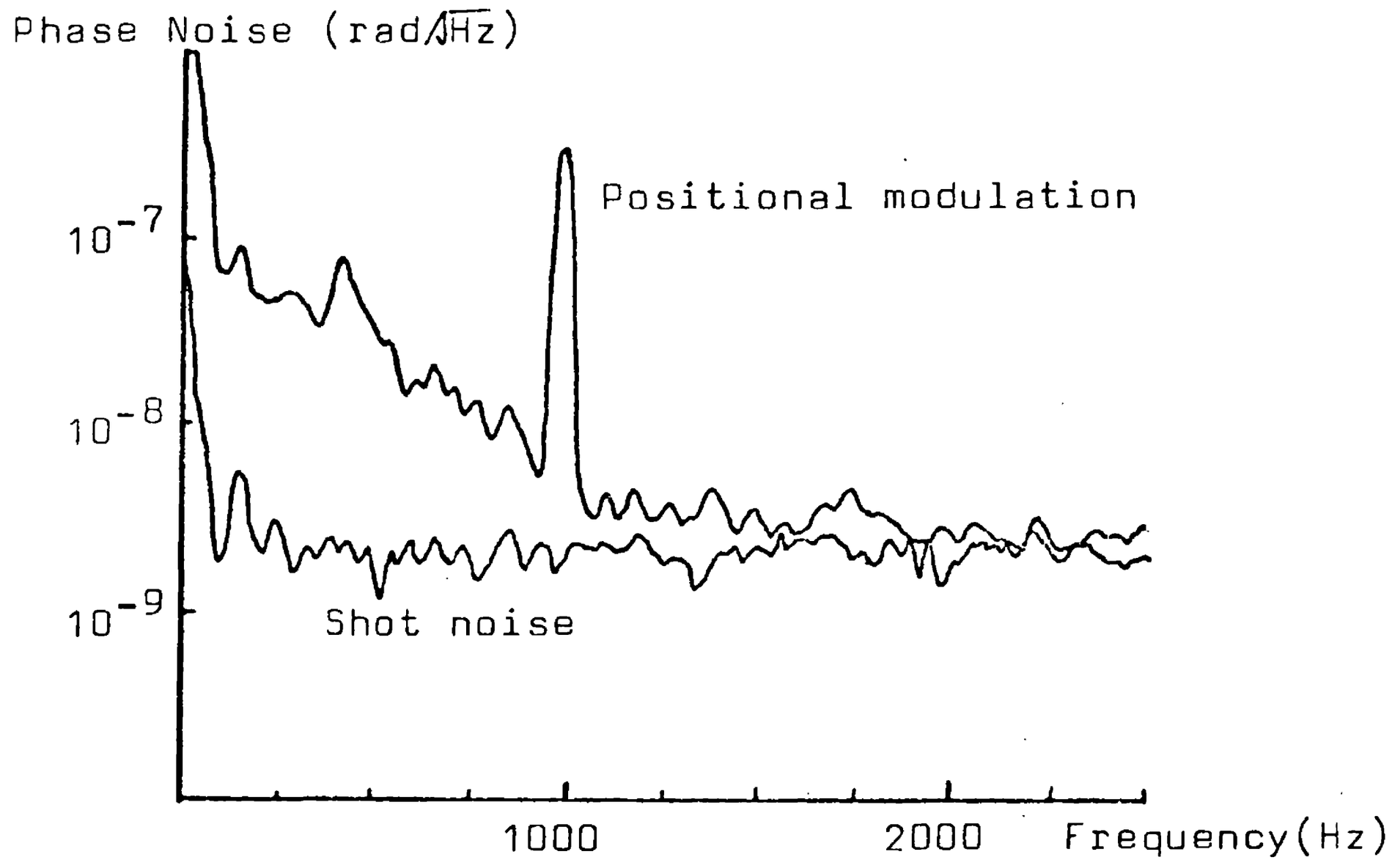

Fig 5·2: Phase noise between the two beams of the polarisation interferometer of fig 5·1, with the shot noise in the same light power indicated in the lower trace. The effect of the positional modulation shown in (b) can be seen.

(b)

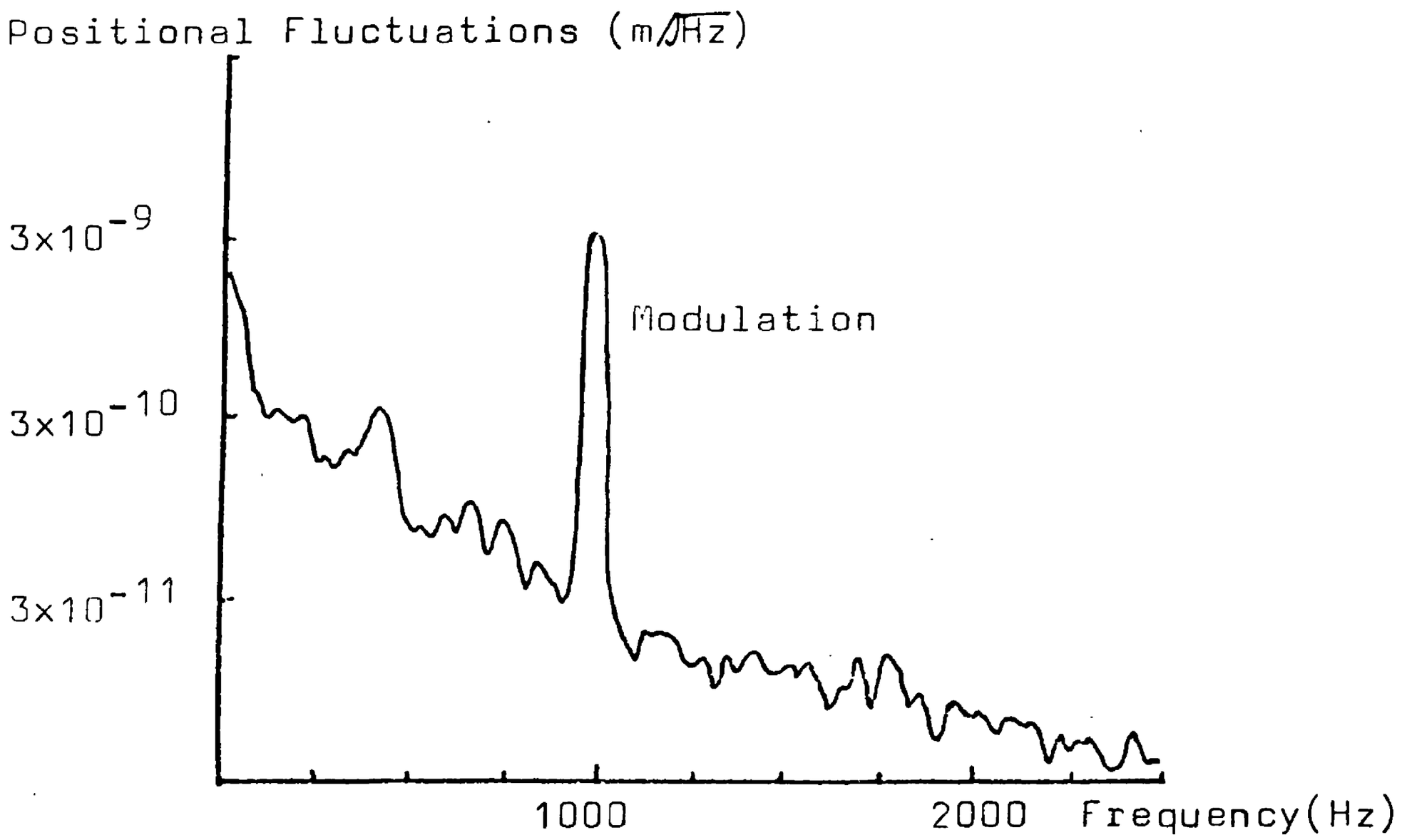

Fig 5·2(b): Beam positional fluctuations ~10cm after Pockels cell. The low level is due the use of the mode-cleaner.

as to give the same DC photocurrent. When these results were taken, a mode-cleaner was in use to suppress beam geometry fluctuations before the polarisation interferometer. The peak at 1 kHz in fig 5·2 is the result of artificial modulation of the beam angle (before the mode-cleaner) by a mirror mounted on PZTs. Whilst the relative heights of peak and background are not quite the same in the two measurements, it must be remembered that only one dimension of one of the orthogonal components of the beam positional changes was being modulated, and the positional fluctuations were monitored at a fairly arbitrary position. These factors, together with the similarity of the two spectra, make it likely that positional fluctuations were producing the observed phase noise. Even in such a simple system, their importance is evident. Indeed, positional fluctuations seem to produce excess high frequency noise whenever Pockels cells are used to modulate the beam. The mechanism for this could be via either scattering or multiple reflections in the Pockels cell, as discussed in section 3·3.

This experiment demonstrated the need for the suppression of beam geometry fluctuations <u>before</u> the phase modulator. It does, however, also demonstrate the possibility of acheiving reasonable sensitivities: the observed noise above 1 kHz is equivalent to a displacement noise of $\sim 10^{-18} m/\sqrt{Hz}$ with cavities of finesse 600. Sufficient encouragement was obtained for the reconstruction described in section 2·2 to go ahead.

Once the new central mass was completed, it was decided to test the noise level in the Michelson interferometer formed by the two cavity mirrors on the central mass. As

well as placing limits on any unexpected noise sources in this relatively simple system, this allowed testing of the low frequency beam steering system, the mode cleaner on the top deck of the central mass, the remote controlled beam handling optics and the optical recombination of the separated beams.

The laser frequency was locked to the mode cleaner, using 1 MHz frequency modulation to obtain an error signal. The usual quarter-wave plate-polariser combination (plus an acousto-optic modulator) provided optical isolation and a rejected beam for the locking. Even with ~35dB of loop gain in this stabilisation system at 1 kHz, it was found necessary to adjust the optical paths of the two arms carefully (to within ~$\frac{1}{2}$mm) to minimise the coupling of frequency noise into the interferometer output. This adjustment also increased the fringe visibility — extinction ratios of ~100:1 were obtained. The resultant low frequency relative phase noise is shown in fig 5·3, compared with shot noise in the same light power (10mW). The observed phase noise above 1 kHz, at ~$1{\cdot}5\times10^{-8}$rad/$\sqrt{\text{Hz}}$, is perhaps a factor of 4 worse than in the simple polarisation interferometer discussed above. While definitive tests of the cause of this noise were interrupted by laser tube failure, the levels are consistent with the noise being due to beam positional fluctuations below ~1 kHz and residual frequency noise above 1 kHz. Since the prospects for improving both of these noise sources in the complete interferometer were good, there seemed little reason to delay tests with the whole interferometer. Again, this experiment demonstrated the possibility of achieving reasonable noise levels.

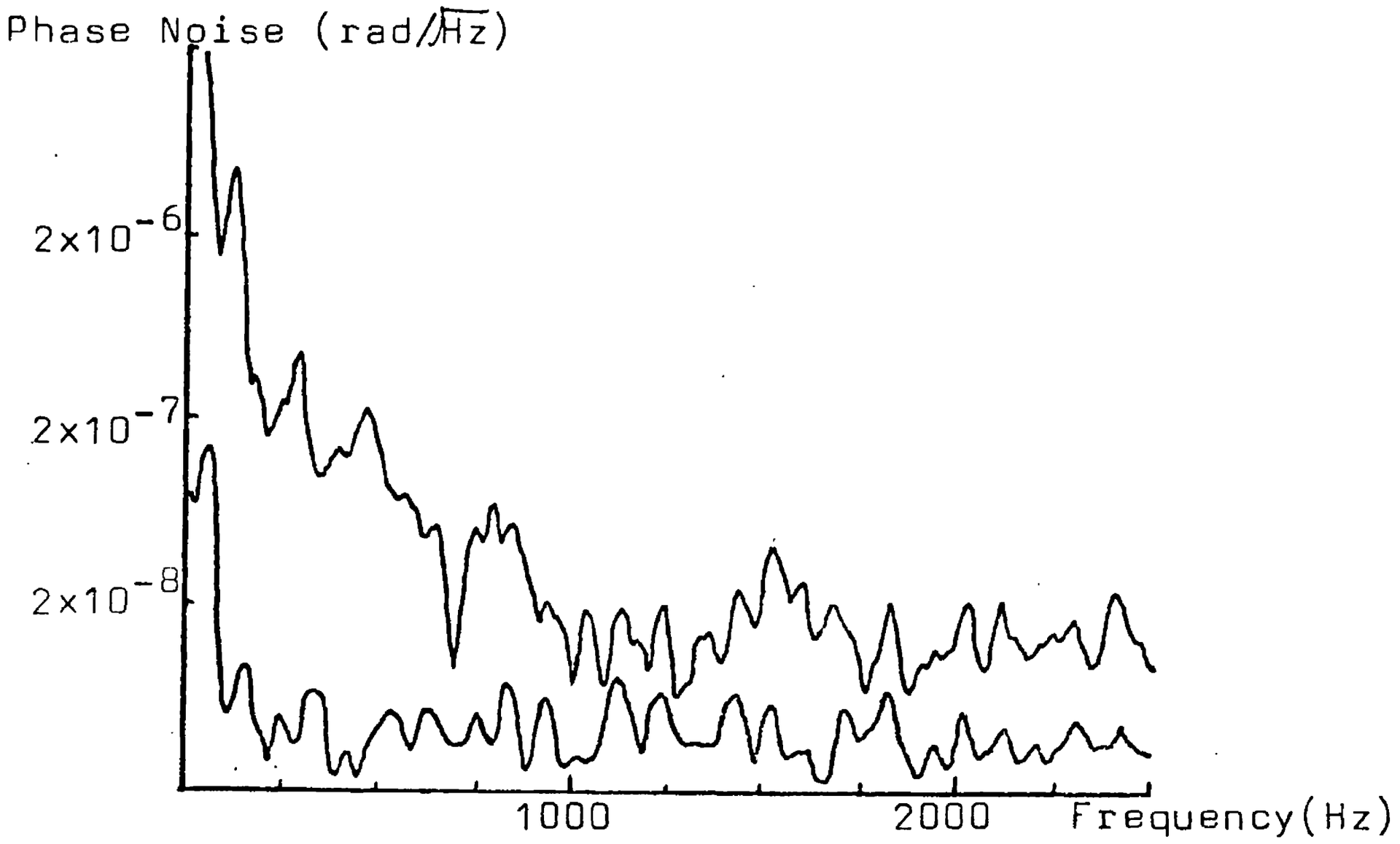

Fig 5·3: The upper trace shows a spectrum of the phase noise observed between the two beams of a Michelson interferometer formed by the two cavity mirrors on the central mass. The lower trace shows the shot noise on the same light power as the output beam (10mW).

(5·2)Interferometer Performance

(5·2(i))Calibration

Before discussing the performance of the 10m interferometer, it is necessary to understand how it is calibrated.

The contents of section 2·2 described how the detector is operated, with secondary arm of the interferometer being maintained on resonance by means of a PZT-mounted mirror on the test mass. At frequencies where the loop gain of this stabilisation system is high (i.e. well below 5 kHz), the motion of this mirror is a good measure of the relative

length changes of the two arms. In this region, the interferometer calibration is known if the motion per volt of the PZT-mounted mirror is determined. At frequencies where the loop gain of the secondary locking loop is negligible, it is the secondary phase-sensitive detector signal which gives the detector phase noise; this, too, must be calibrated.

The calibration of the PZT-mounted mirror used in these experiments was carried out by Munley (1982), who used a two-stage technique. First, the laser was locked to the arm of the interferometer containing the PZT-mounted mirror, by the usual technique. A known signal was applied to the PZT (at $\sim$1kHz) and the resultant signal on the laser intra-cavity Pockels cell measured. This Pockels cell was then calibrated by comparing the frequency deviation produced by the application of a known signal with the free spectral range of a scanning Fabry-Perot spectrum analyser (or with sidebands of a known frequency). The frequency deviation corresponding to a known voltage on the PZT mirror was thus determined, hence the motion of the mirror was known (cf. 2·55). The Pockels cell was found to change its optical length by $0{\cdot}45 \pm 0{\cdot}05$ nm/V, and the PZT mirror to move by $1{\cdot}54 \pm 0{\cdot}15$ nm/V.

When the primary cavity is locked, its phase detector signal provides a measure of the residual frequency noise between laser and cavity, as long as the level does not drop below that of the noise present in the absence of interference fringes (i.e still with laser light). In

the latter case, an increase in loop gain and so a reduction in the error signal only increases the accuracy with which this noise is imposed on the light. The residual frequency noise is then just that represented by the phase detector noise in the absence of interference fringes. This may be calibrated by effectively reversing part of the procedure for calibrating the PZT mirror: with both cavities locked, the laser frequency is modulated at a frequency where the secondary stabilisation loop has a high loop gain, and the resultant signals on both the primary PSD and the secondary PZT mirror drive are measured. The known calibration of the latter enables the primary PSD to be calibrated in $Hz/\sqrt{Hz}$. It would also be possible to calibrate the primary PSD by applying a known voltage to laser Pockels cell.

Once the primary PSD has been calibrated by such a method, the secondary PSD may be calibrated in the region above the unity gain frequency of the secondary loop by modulating the laser frequency and simply comparing the outputs of the primary and secondary PSDs. Even if such a measurement is made at a lower frequency, the calibration in the high frequency regime may be inferred from a measurement of the loop gain — the factor by which the PSD signal is reduced. This, in turn, may be measured by injecting a signal after the error point and measuring the size of the signal at the PZT mirror, first with the loop open, then with it closed. The ratio is the loop gain (plus 1).

The PSD outputs may also be calibrated in terms of <u>phase noise</u> by measuring their noise level when a torch

is shone on the photodiode, a procedure which accurately gives the shot noise on this light level. If the torch power is arranged to give the same DC current from the diode as the laser light and this power is known, then the phase noise in the light may be calculated from (1·33).

Once the PSD outputs have been calibrated, it is possible to deduce the cavity finesses from an observation of the RF fringe height (i.e. the size of the fringes at the PSD output). From equation (2·48) it is straightforward to show that the maximum height of the RF fringes occurs when

$$\delta_m = 2\pi\Delta\nu_m/\nu_0 = \pi/F \qquad (5\cdot1)$$

If ΔV_{pp} is the peak to peak height of the RF fringes and $\partial V/\partial\nu$ is the sensitivity of the PSD to frequency fluctuations when locked ($\delta=0$), then it is evident from (2·47) that

$$\Delta V_{pp}/\Delta\nu_m = \partial V/\partial\nu \qquad (5\cdot2)$$

Or, using (5·1), the finesse is given by

$$F = \frac{\nu_0(\partial V/\partial\nu)}{2\Delta V_{pp}} \qquad (5\cdot3)$$

An alternative method of measuring the cavity finesse is via a determination of the storage time τ_s, the time for the intensity to fall to $1/e^2$ of its value when the incident beam is interrupted. The emerging field a time t after the incident field is removed is

$$E/E_0 = T_1^2\sum_{N}^{\infty}(R_1R_2e^{i\delta})^{N-1} \qquad (5\cdot4)$$

with the notation of section 2·1(i); N = ct/2l. Separating into two sums gives

$$E/E_0 = \frac{T_1^2(R_1R_2e^{i\delta})^{ct/2l}}{1 - R_1R_2} \qquad (5\cdot5)$$

Or $E/E_0 = \exp(\frac{ct}{2l}\ln R_1R_2).\exp(ict\delta/2l)$ (5·6)

For $1-R_1R_2 \ll 1$, the field after time t is

$$E/E_0 = \exp(-\pi ct/2Fl)\exp(it\delta/\nu_0) \quad (5\cdot7)$$

The field is therefore a decaying oscillation, with a time constant

$$\tau_s = 2Fl/\pi c \quad (5\cdot8)$$

Note that this is the same expression for the storage time as that obtained in Chapter 2. So the finesse may be calculated from

$$F = \pi c\tau_s/2l = \pi\nu_0\tau_s \quad (5\cdot9)$$

with τ_s the 1/e time for the field (as measured by the PSD output) or the $1/e^2$ time for the intensity.

(5·2(ii))Interferometer Performance

Early in 1983, the major part of the reconstruction of the detector was completed and the first operational tests could be made. It was decided not to use the upper tier of the central mass initially, since the need to keep the mode cleaner on resonance would complicate the locking of the two detector cavities. This decision was amply justified, for a considerable amount of work was required to acheive proper functioning of the cavity locking systems: in the primary loop, the gain balance of high and low frequency amplifiers had to be adjusted, and more dynamic range found by inserting additional 250V amplifiers to drive the Pockels cell; while the secondary loop required adjustment of its filtering to ensure sufficient gain and

and bandwidth (cf. section 2·2). Both PZT wire-pulling circuits had to be adjusted to try and give maximum gain given the constraints of mechanical resonances; large resonances in the suspension triangles were made unimportant by damping with lead and rubber. Use of only one tier also greatly aided the optical alignment of the system — by no means an easy operation given the need for a 1mm radius beam to pass cleanly through two Pockels cells (7mm diameter, ~12cm long) and quarter-wave plates, as well as resonating in 10m long cavities. Also for simplicity, these initial experiments used separate observation of the signals from the two cavities.

The phase-modulators initially used were Gsänger 4-crystal AD*P Pockels cells. These contain two balanced sets of electro-optic crystals, each of which phase modulates one linear polarisation component. If light linearly polarised at 45^{o} to the crystal axes enters such a modulator (the situation in these experiments), it splits into polarisations parallel and perpendicular to the axes; if a voltage is applied to the electrodes, the two components receive an <u>opposite</u> phase modulation. Such a differential modulation of the incident beam gives the possibility of reducing the sensitivity of the interfered output to noise arising from fluctuations of the components of the beam which do not enter the cavities but are directly reflected from the input cavity mirrors: for by applying exactly the opposite modulation to the output Pockels cell, the modulation would be removed from this component so that any noise would not be detected. The beams from the cavities would be modulated, since their original modulation is

not transmitted by the cavities. A distinct disadvantage of this scheme, however, over one in which both polarisations are modulated equally, is that the effective start of the interferometer is the input to the Pockels cell rather than the beamsplitter. This provides another way of introducing noise. In addition, the required depth of modulation (~0·8rad) at the input is so large that it tends to smear out the output fringes.

One of the first operational findings was the seriousness of optical feedback to the laser, producing excess noise around the RF modulation frequency (cf. section 2·1(viii)). Careful adjustment of the quarter-wave plates (including rotation about all three possible axes) reduced the reflected intensity at the laser to $\sim 10^{-3}$ of that of the main beam. An Isomet acousto-optic modulator was placed ~20cm in front of the laser and arranged so that the beam used for the detector was the first diffracted order. This is Doppler-shifted by the carrier frequency (80MHz). Any return beam should be further Doppler-shifted, so its interference should not produce noise in any frequency region of interest. With careful adjustment, inclusion of this isolator reduced the noise by a factor of ~30 (i.e. it reduced the return intensity by ~1000). This is probably limited by internal scattering.

A spectrum of the noise around the modulation frequency (with the acousto-optic isolator), as measured by the secondary PSD in the absence of interference fringes, is shown in fig 5·4. This compares the noise seen when the input beam followed its usual path (so that the return beam from the cavity mirrors re-entered the laser) with

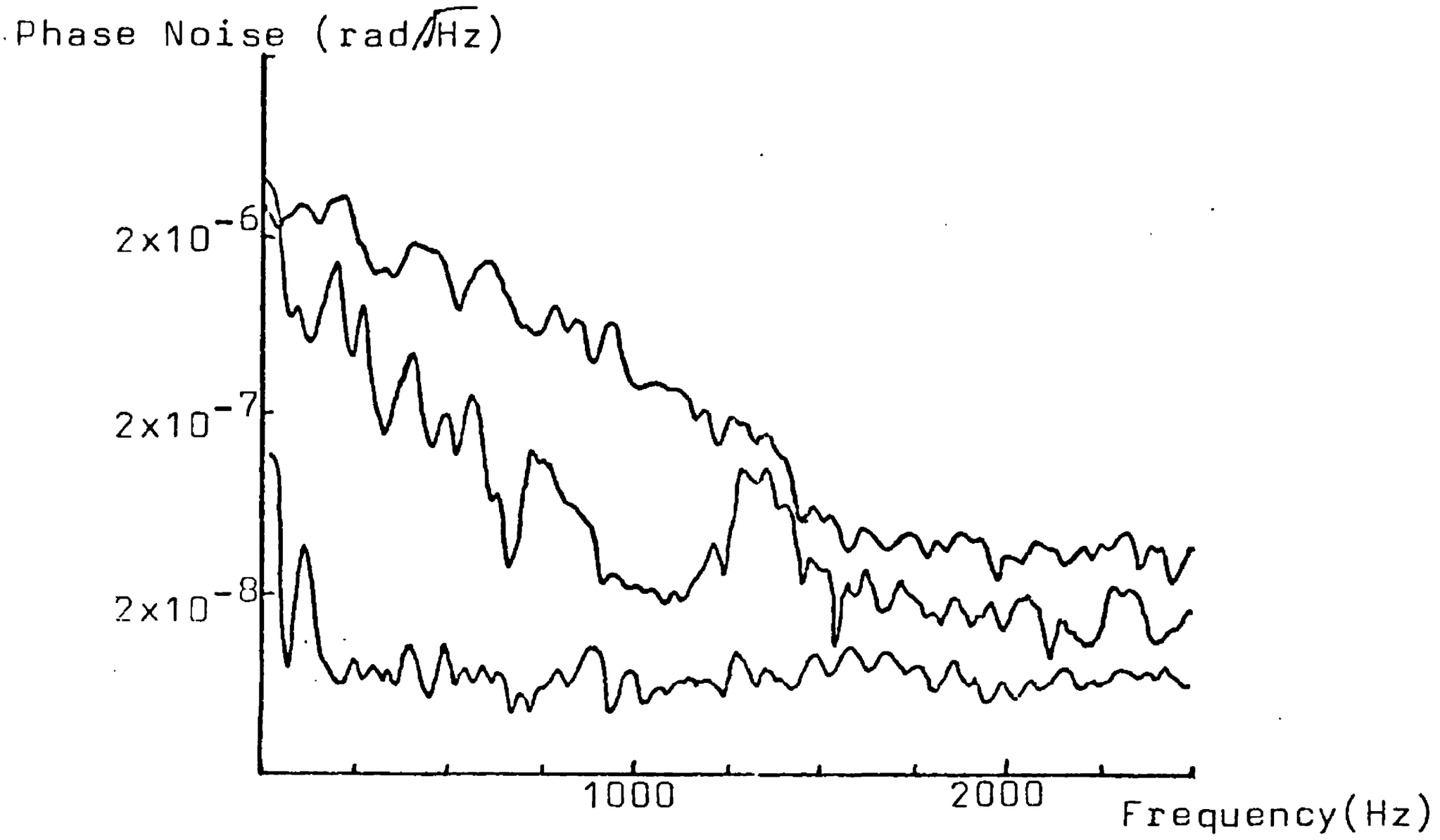

Fig 5·4: Phase noise, in the absence of interference fringes, seen by the secondary PSD. Top trace: beam aligned so that any reflected beam re-enters the laser. Middle trace: beam slightly offset so that the reflected beam misses the laser. Bottom trace: shot noise on the same light power (1·5mW).

that observed when the incident beam was misaligned so that the beam reflected off the cavity mirrors was not coincident with the main beam and did not re-enter the laser. The shot noise level is also indicated. The noise in the intermediate, misaligned case is consistent with being caused by a combination of scattering or internal reflections in the Pockels cell and beam positional fluctuations, as discussed in Chapter 3. It can be seen that the noise resulting from light returning to the laser is a serious problem. In order to further reduce this noise

level, a Coherent acousto-optic frequency shifter (working at 40MHz) was placed in series with the Isomet isolator. Care was taken to ensure that diffracted orders other than the first could not enter either the other modulator or the laser. This required that they be separated by at least 20cm, with irises placed to cut off all but the main beam. The power throughput of this double modulator system was about 50%. That the combination considerably reduces the isolation noise can be seen in fig 5·5, which compares the shot noise in 8mW of light (measured with a torch) with the intensity noise around 24MHz on the same light power, measured on the optical table before the detector to minimise the effects of the noise produced in the Pockels cell. The phase noise is $\sim 6\times10^{-9}$ rad/$\sqrt{Hz}$ at 1 kHz, an improvement by a factor of ~50 being acheived by the use of the additional isolator. The isolation noise had thus been reduced to the point where it was no longer an immediate concern.

The cavity mirrors used in these experiments were all coated by CVI (as were the mode-cleaner mirrors), with "high reflectors" ($R^2 \approx 99{\cdot}7\%$) on the end masses and mirrors nominally of reflection coefficient $R^2 = 99{\cdot}2\%$ on the central mass. This combination should give finesses of approximately 400.

The decay time, hence the finesse, was measured for the primary cavity by observing the PSD output as fringes were swept through. This is shown in fig 5·6: the observed 1/e decay time of ~7μs gives a finesse (from 5·9) of about 330, not far from the expected value. This measurement was made in March 1983, soon after the mirrors were placed in

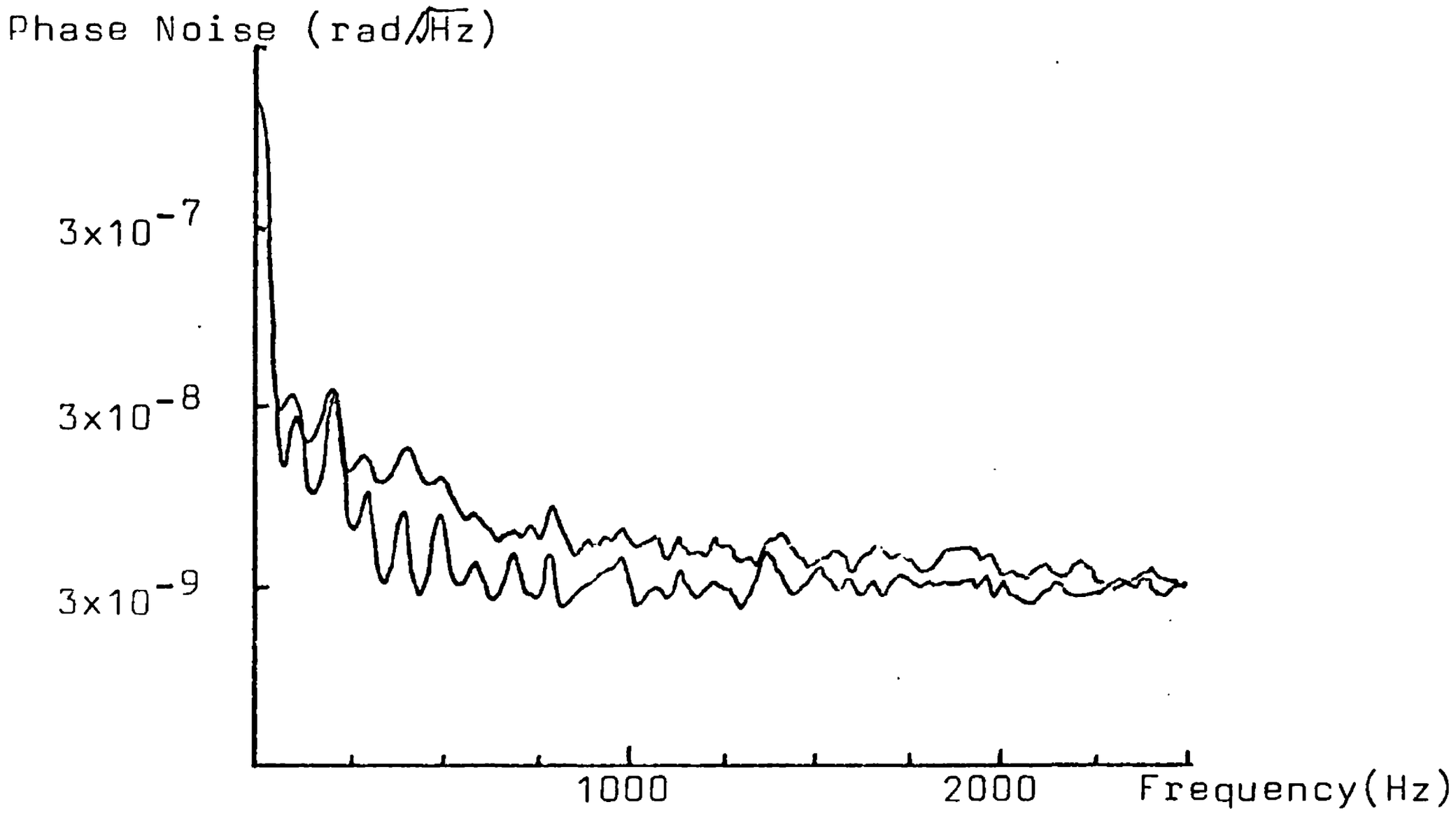

Fig 5·5: Equivalent phase noise in the light around the modulation frequency, measured on the optical table before the detector. The top trace shows the noise in 8mW of laser light, with two acousto-optic isolators, while the bottom trace shows the shot noise level for the same light power.

the detector.

The value of the fringe visibility that was initially obtained was ~50%, unexpectably low. While some of this may be explained by imperfect mode-matching (Appendix 4) and beam shape, it was also found that the fringe visibility steadily degraded over the next few months, becoming less than 10% by late June 1983. This degradation was largely irreversible, with cleaning of the mirrors having only a marginal effect; it will be seen that it was accompanied by a decrease in the finesse. Indeed, it now seems that

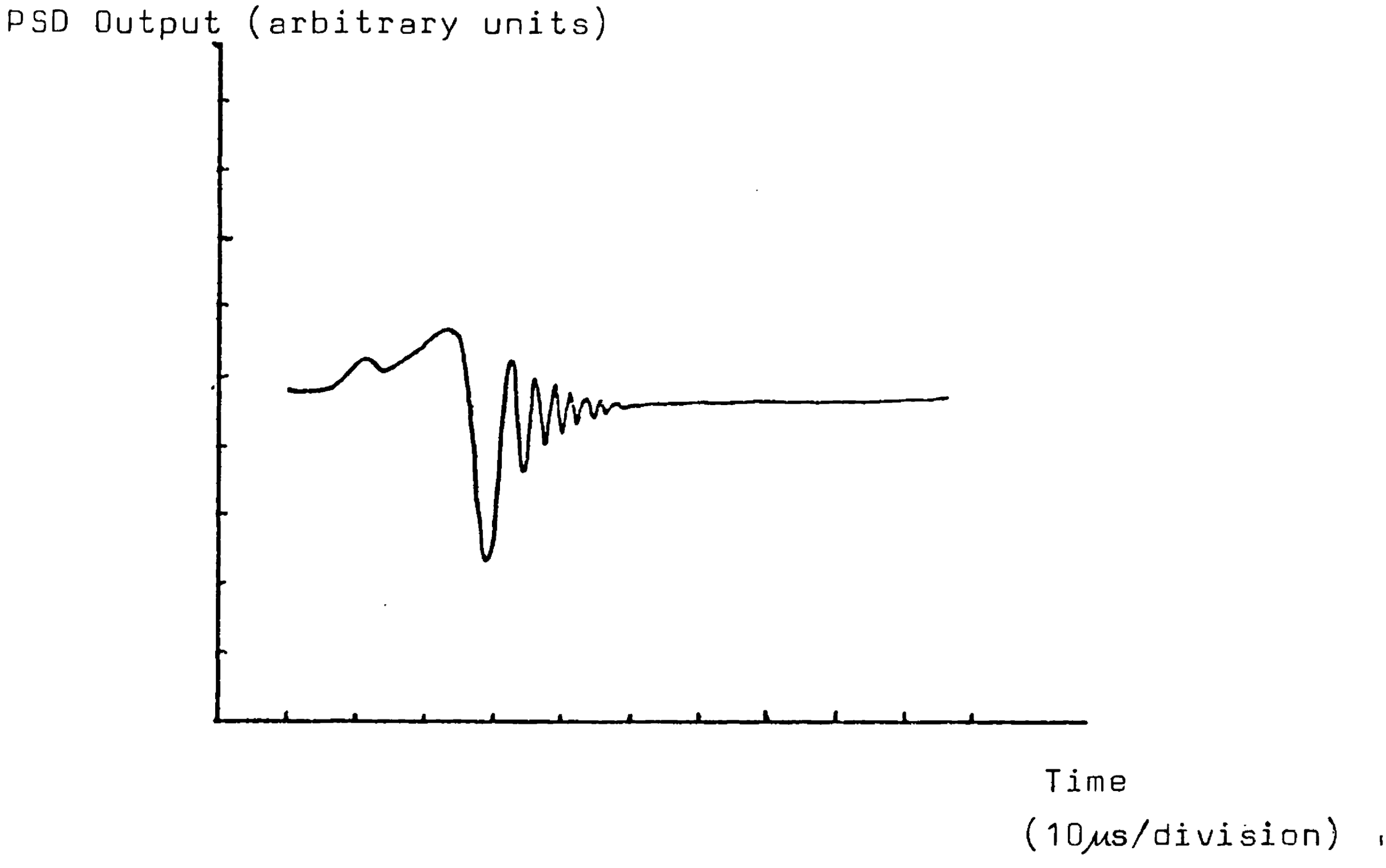

Fig 5·6: Primary PSD output as a fringe sweeps through.

The decay time of the oscillations is the storage time of the cavity.

the absorption of these mirrors steadily increased when left in the vacuum system. This absorption had the effect of degrading the possible shot-noise limited sensitivity of the gravitational wave detector and generally worsening detector performance. It was still possible, however, to make important investigations into the various noise sources of the interferometer.

All of the following spectra were measured using an HP3582A FFT spectrum analyser. This has a dynamic range of 80dB, sufficient for most situations. The drive signal to the secondary PZT mirror, however, contains both very

large low frequency signals (to maintain lock against seismic motion) and very small high frequency signals (ultimately, gravitational waves). In order to be able to observe these high frequency signals, it is necessary to strongly attenuate those at low frequencies. A high pass filter was therefore placed between the PZT drive signal and the spectrum analyser. This filter is shown in fig 5·7, with its measured transfer function shown in fig 5·8. Thus, all of the following spectra of the PZT drive (only) should really be divided by this transfer function: the calibrations given are only strictly true at 1 kHz. For most purposes, however, the effects of the filter may be ignored if attention is restricted to the region above 500 Hz.

A typical spectrum of the detector sensitivity (the PZT drive), obtained soon after the insertion of the double acousto-optic isolator system, is shown in fig 5·9. It can be seen that the displacement noise level is approximately 5×10^{-15} m/$\sqrt{\text{Hz}}$ above 1 kHz.

The claim that the PZT drive signal accurately represents the displacement noise is only justified if the gain of the secondary loop is large compared with unity. This loop gain was measured by injecting an artificial signal into the loop (with a signal generator) and observing the size of this signal on the PZT drive with the loop first open, then closed. Since the action of the feedback system is to reduce the size of the signals, the observed peak size in the closed loop case is smaller by a factor approximately equal to the loop gain of the system. This is shown in fig 5·10. It can be seen that the loop

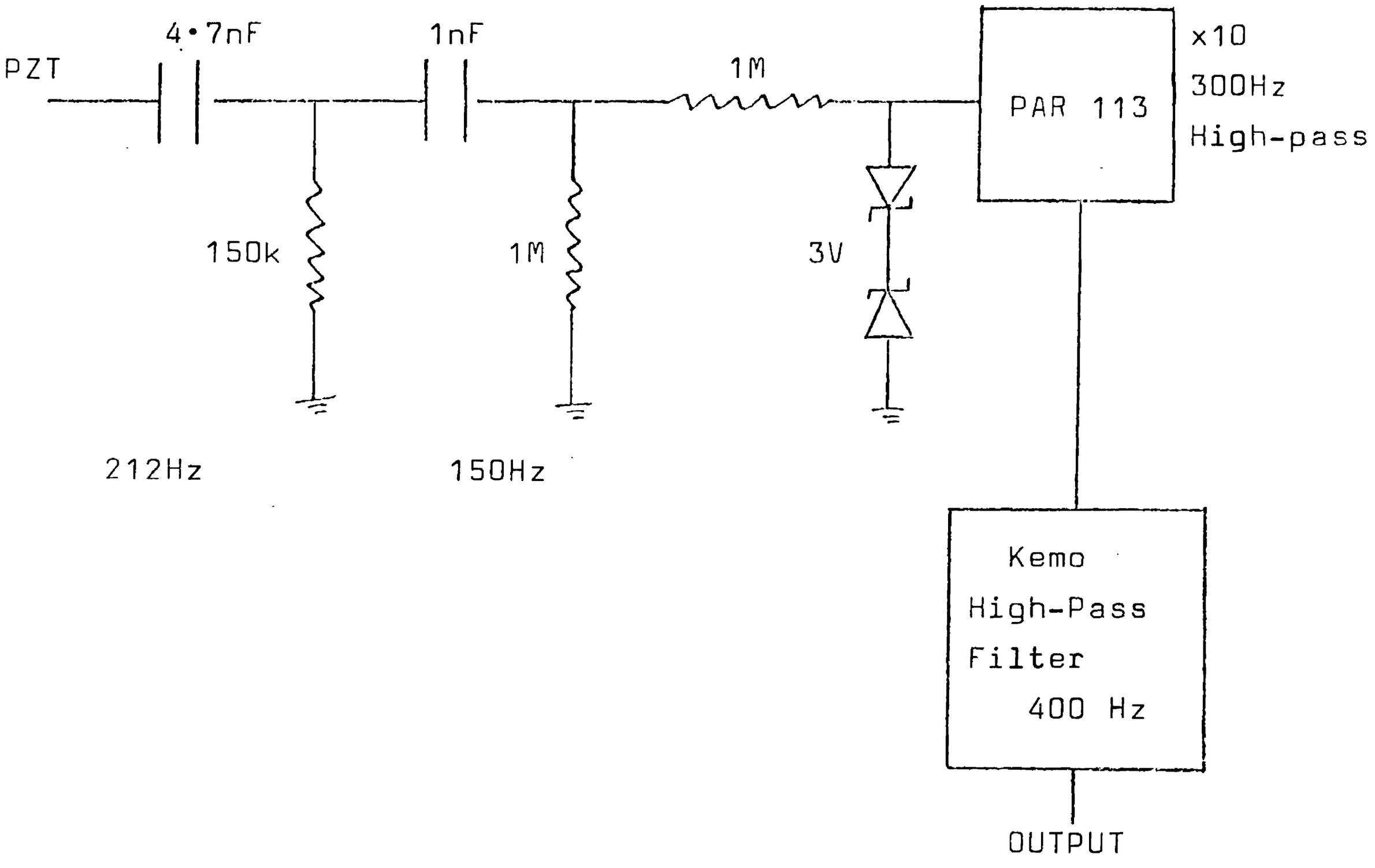

Fig 5·7: The circuit used to monitor the voltage on the secondary PZT. The corresponding transfer function is shown in fig 5·8. The noise in this circuit is equivalent to $2\times10^{-16} m/\sqrt{Hz}$.

gain at 1 kHz is about 15, which is perfectly adequate. The unity gain frequency is about 5 kHz (the filtering is at 12dB/octave between 100 Hz and 3 kHz — see fig 2·12), above which the secondary phase detector output must be used as the measure of sensitivity.

The first noise source investigated during this series of experiments was laser frequency noise. The technique used was to artificially modulate the laser frequency by applying a signal to the Pockels cell in the laser and

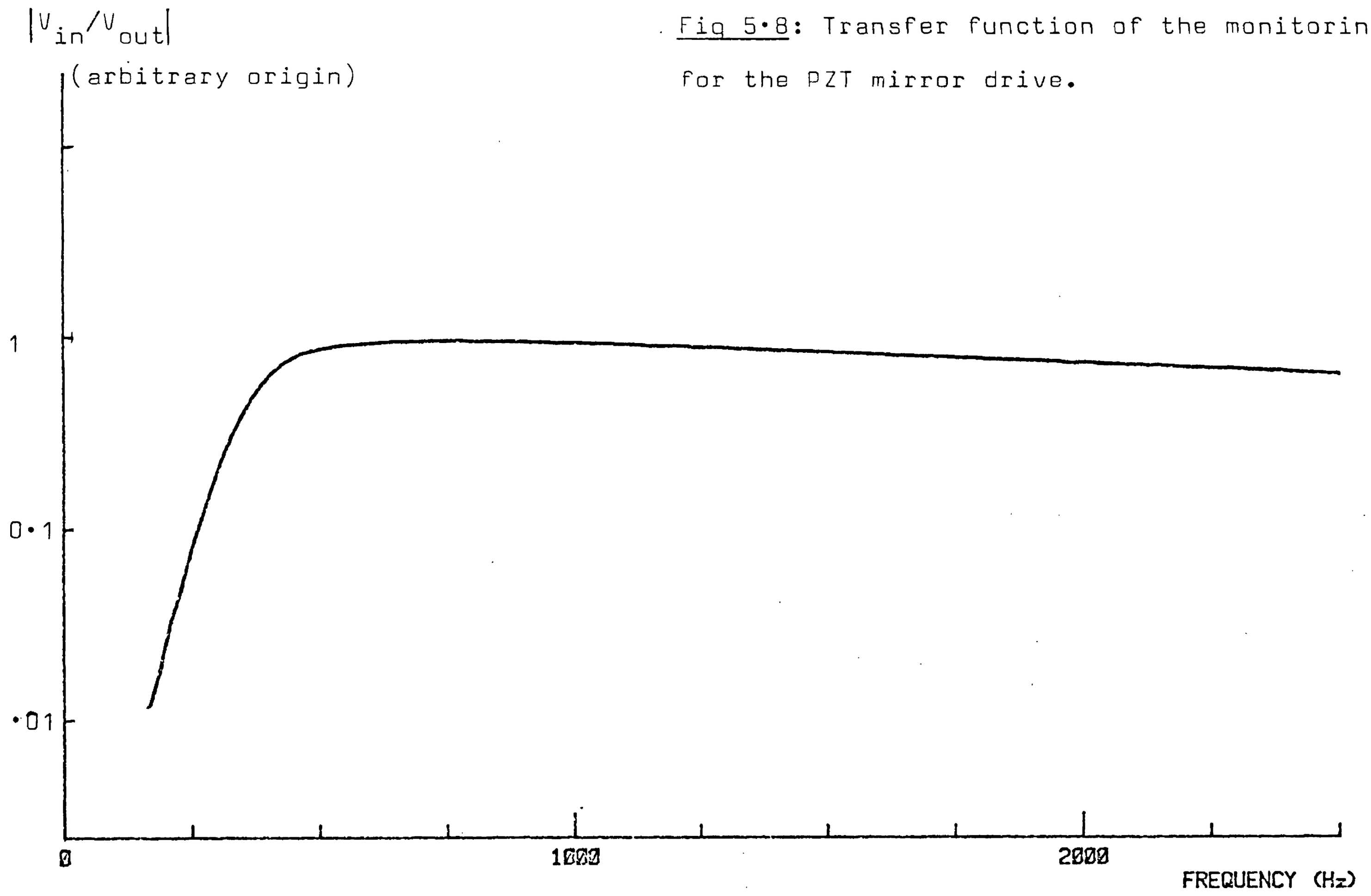

Fig 5·8: Transfer function of the monitoring filter for the PZT mirror drive.

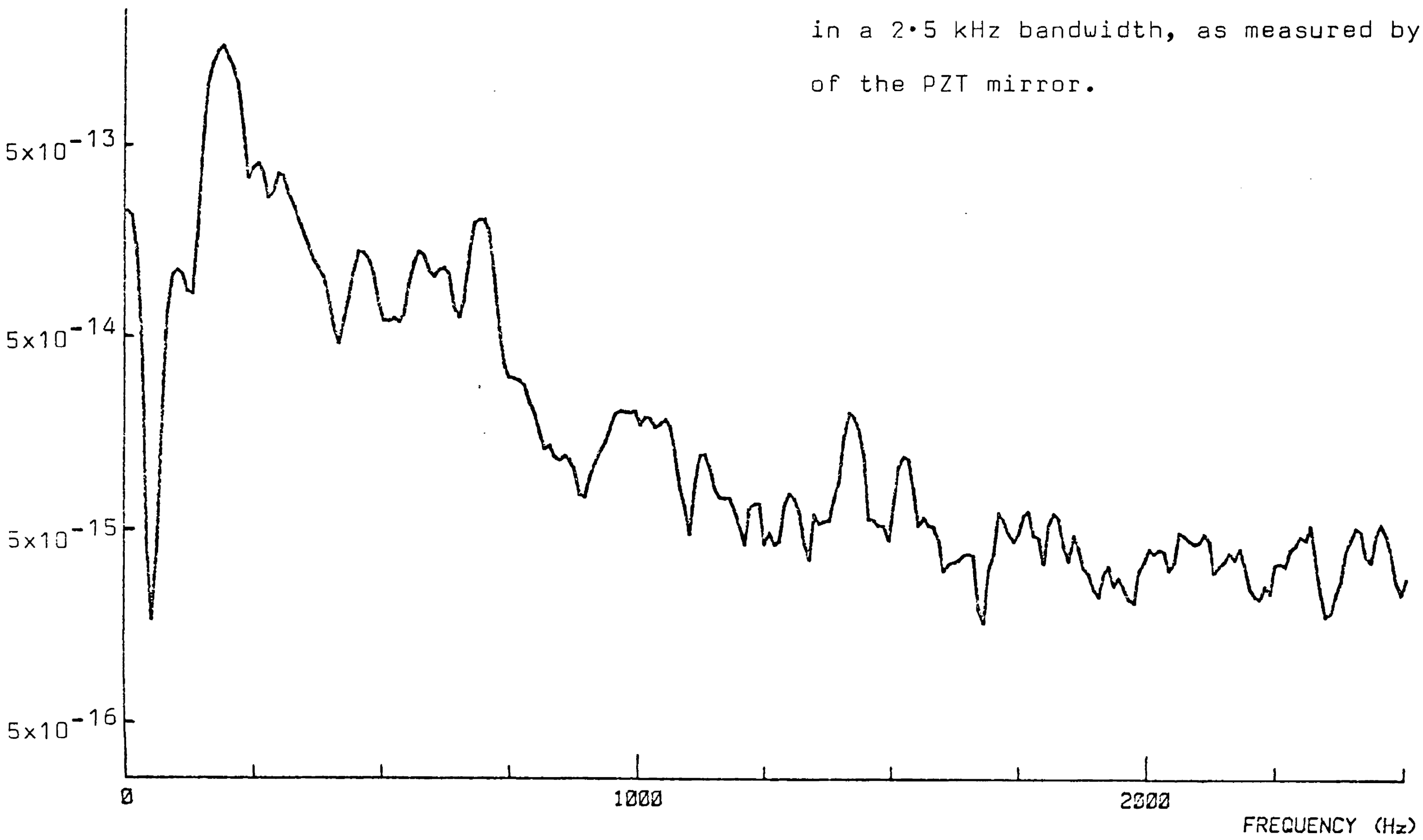

Fig 5·9: Displacement noise of the interferometer in a 2·5 kHz bandwidth, as measured by the motion of the PZT mirror.

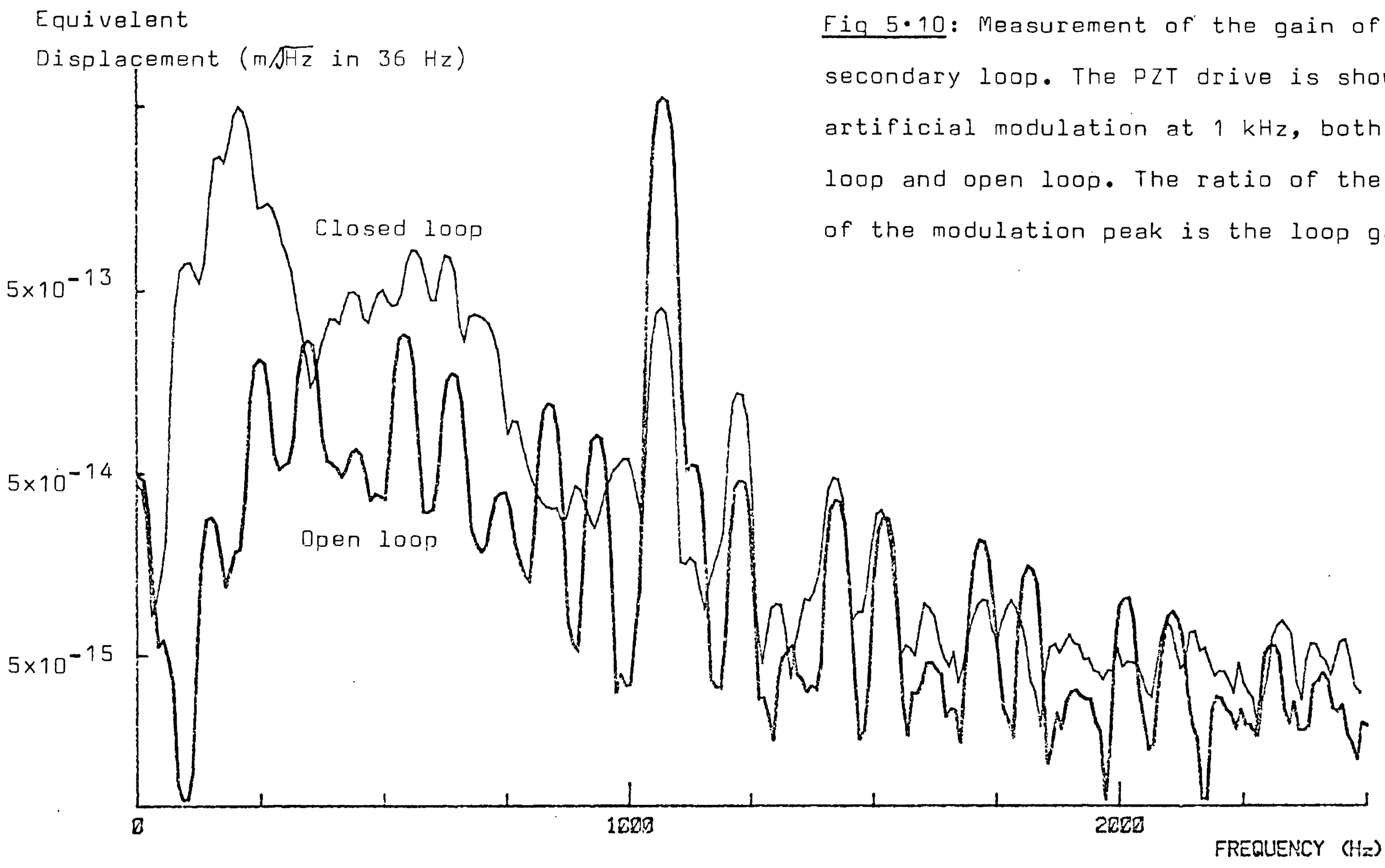

Fig 5·10: Measurement of the gain of the secondary loop. The PZT drive is shown, with artificial modulation at 1 kHz, both closed loop and open loop. The ratio of the heights of the modulation peak is the loop gain.

observe the resultant signals on both the primary PSD (which gives the residwal laser-cavity frequency noise) and the secondary PZT drive. By comparing the relative heights of the injected signal and the background noise in the two cases, the magnitude of the detector displacement noise produced by the residual frequency fluctuations may be inferred. Care must be taken if the error signal is lower than the noise in the absence of fringes, as discussed in 5·2(i). At the same time, the PSDs may be calibrated and the finesses measured. Fig 5·11(a) shows the primary PSD signal when locked, with the signals in the absence of light and the absence of fringes for comparison. Thus, the residual frequency noise is ~0·1 Hz/$\sqrt{\text{Hz}}$ at 1 kHz. This was calibrated using the procedure described in section 5·2(i), i.e. by measuring the corresponding signal on the secondary PZT produced by frequency modulation. This is shown in fig 5·11(b). It can be seen that the artificial frequency modulation peak is slightly smaller on the PZT drive spectrum, compared to the background noise, than it is on the primary PSD spectrum. This indicates that frequency noise alone is not the cause of the detector noise, except perhaps in the region above 1·5 kHz. It is, however, very close to being the limiting factor; if the detector is to be substantially improved, then the importance of frequency noise will have to be reduced. This may be achieved by a combination of better frequency stabilisation and subtraction of the signals from the two cavities.

Part of the reason why frequency noise is so important is the high natural level of the frequency fluctuations in

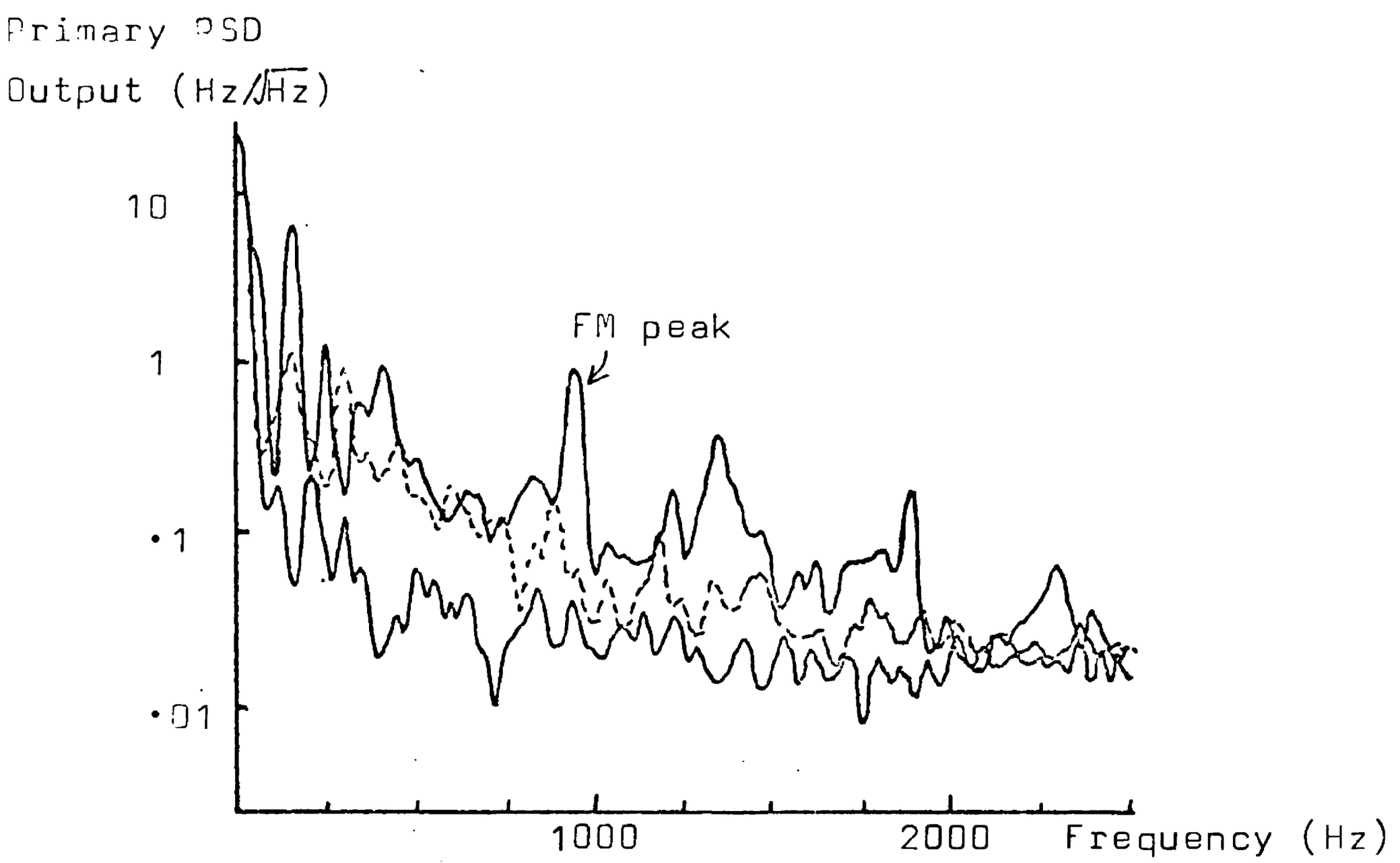

Fig 5·11(a): Primary PSD output; top trace: cavity locked, with modulation at ~1kHz. Intermediate (dotted) trace: no fringes, but still laser light. Bottom trace: light blocked.

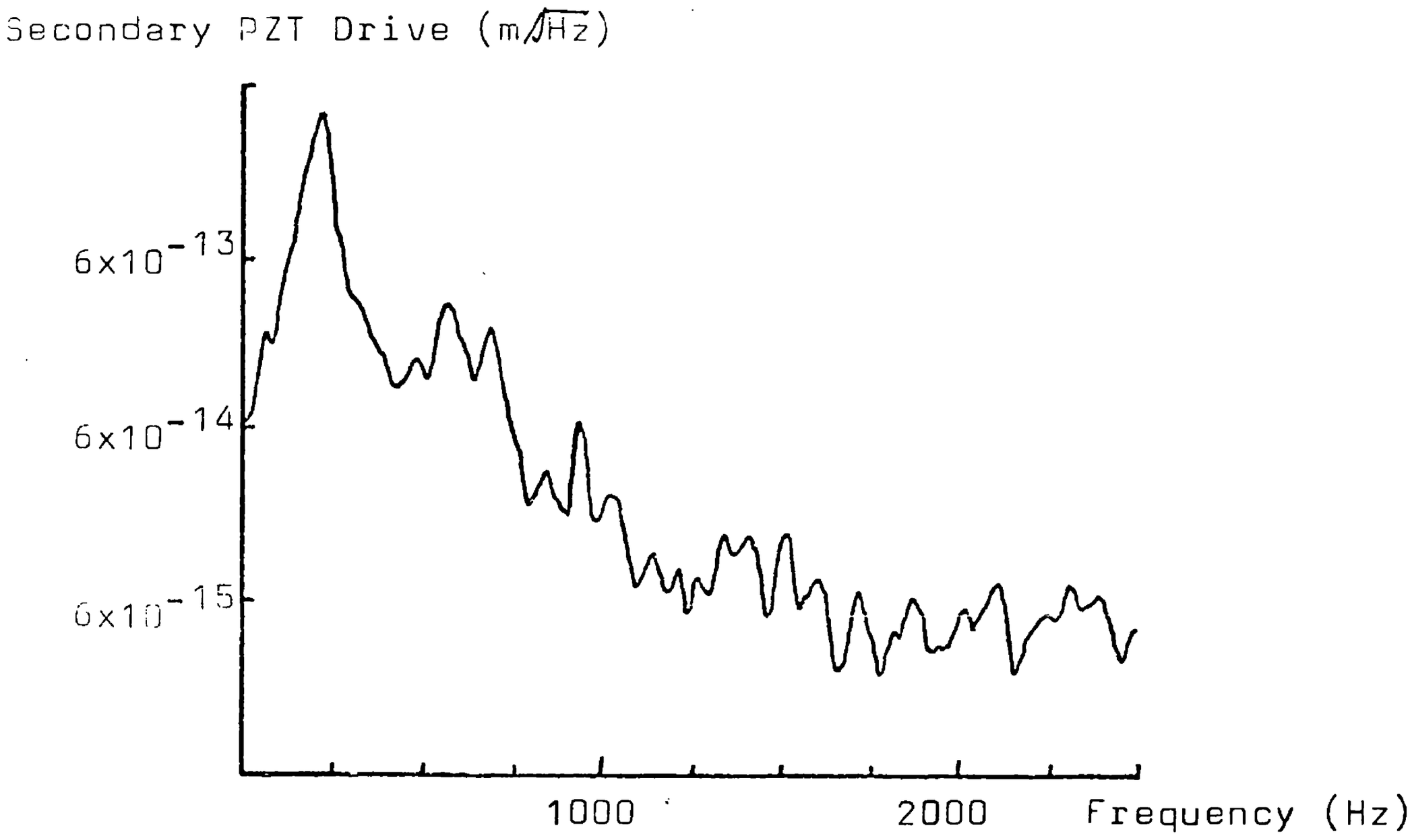

Fig 5·11(b): Secondary PZT drive, with the same frequency modulation as in (a).

our Spectra 170 Ar^+ laser. This can be seen by measuring the voltage applied to the intra-cavity Pockels cell when the laser is stabilised with respect to the primary cavity. The equivalent frequency noise is shown in fig 5·12. The unstabilised frequency noise at 1 kHz was thus about 3 kHz/$\sqrt{Hz}$. Comparison of fig 5·11(a) with fig 5·12 shows that the loop gain of the laser stabilisation system is $\sim 3\times10^4$ at 1 kHz and $\sim 2\times10^5$ at 400 Hz.

It is of interest to note the values of the cavity finesses implied by these measurements (together with observation of the RF fringe heights). The secondary and primary finesses were found to be approximately 300 and 150 respectively. These values are considerably lower than might be expected, but are not totally surprising: for these measurements were made in June 1983, when the fringe visibility had sunk to ~20%.

The importance of laser intensity noise was assessed by modulating the intensity artificially (by driving the laser current) and measuring the size of this signal on the PZT drive. The intensity modulation (measured by a photodiode on the optical table) and resultant sensitivity peak are shown in fig 5·13. The slight increase in the noise level on the PZT drive over that shown in fig 5·9 is due to an earth loop caused by connecting a signal generator to the laser power supply in order to modulate its current. It can be clearly seen, however, that the natural fluctuations in the laser intensity produce noise in the detector output which is about a factor of five less than the observed noise. The significance of intensity noise if the detector performance is to be improved is clear.

Fig 5.12: The natural frequency noise of our Ar^+ laser, measured against the primary cavity.

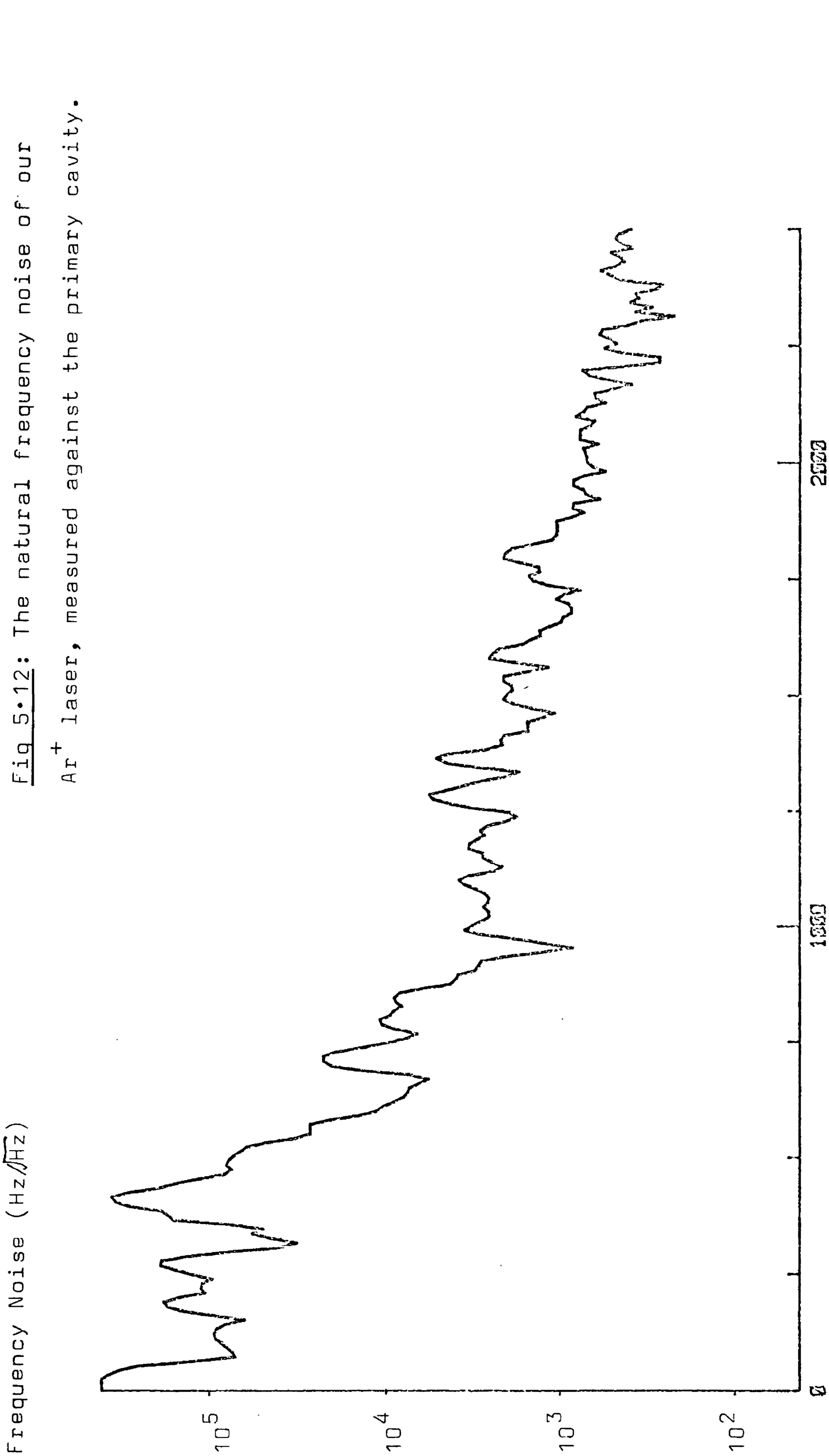

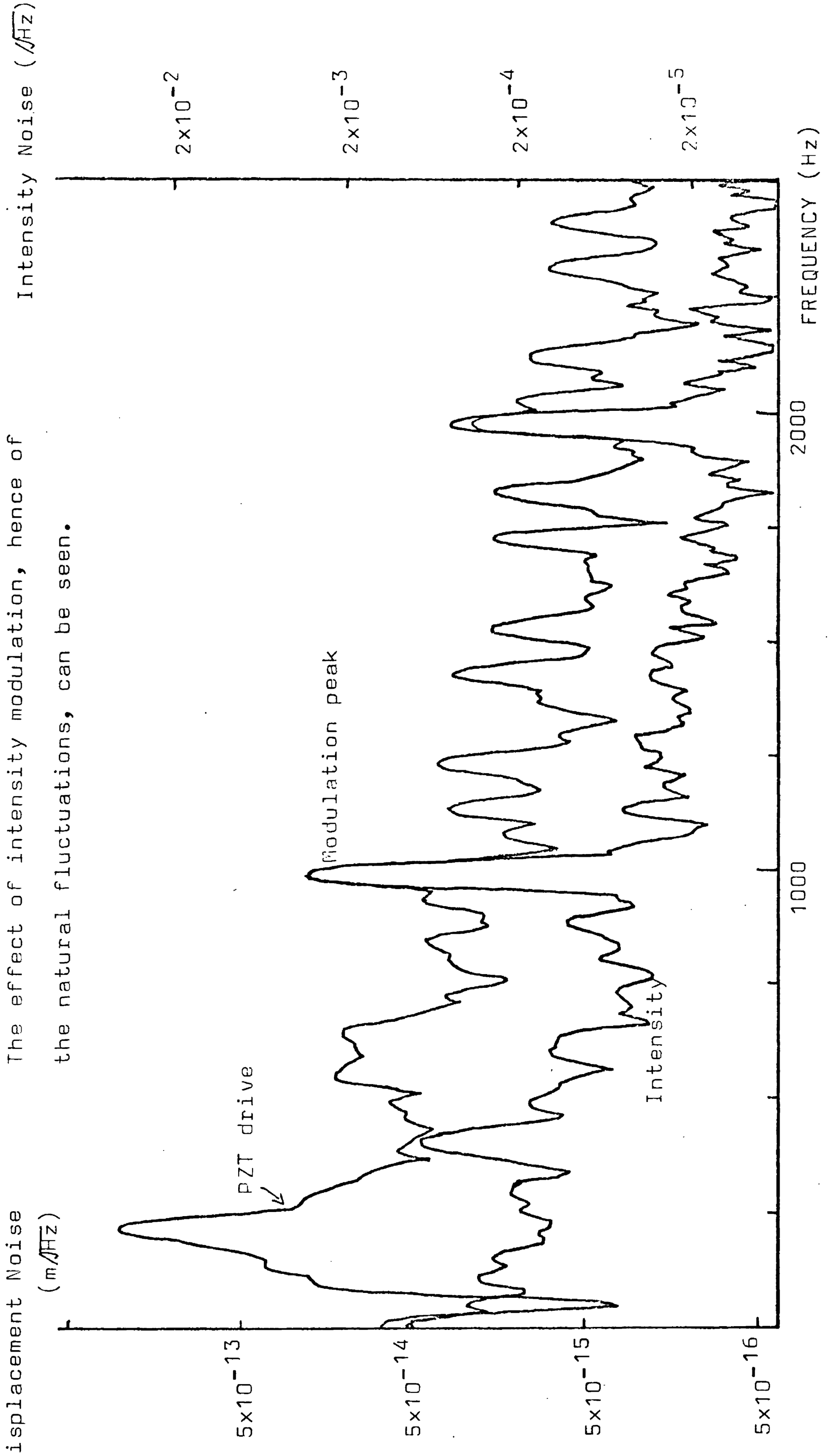

Fig 5•13: The significance of intensity noise.

The effect of intensity modulation, hence of the natural fluctuations, can be seen.

The sensitivity of the detector to positional fluctuations may be evaluated by a similar technique. One of the PZT-mounted mirrors on the optical table may be used to modulate the position of the laser beam (in either dimension), the size of modulation and background fluctuations being monitored by the two position sensitive diodes on the central mass. This is illustrated in figs 5·14 and 5·15, each of which shows the position signals from the relevant dimension of both quadrant diodes, together with the corresponding detector sensitivity, when the two PZT mounted angle-modulating mirrors are driven in turn. It seems that there is little difference in the coupling of different dimensions. Fig 5·16 indicates the equivalent detector displacement noise produced by one component of one dimension of the beam positional fluctuations. It can be seen that this is approximately $10^{-15} m/\sqrt{Hz}$ at 1 kHz. This is almost certainly an underestimate of the noise produced by beam positional fluctuations, for both components (i.e. angular and parallel, in and out of phase) are fluctuating in two dimensions. The true noise level is therefore probably a factor of about 2 higher than that indicated in fig 5·16. The potential importance of beam positional fluctuations is confirmed even though they, alone, did not appear to be the immediate limit to the sensitivity of the detector during these experiments.

The preamplifiers after the photodiodes used in these initial experiments both had a noise equivalent to shot noise in 6mW of light, while the power available from the 10^{-1} splitters was less than 3mW. With the degradation of the fringe visibility and so of the potential sensitivity,

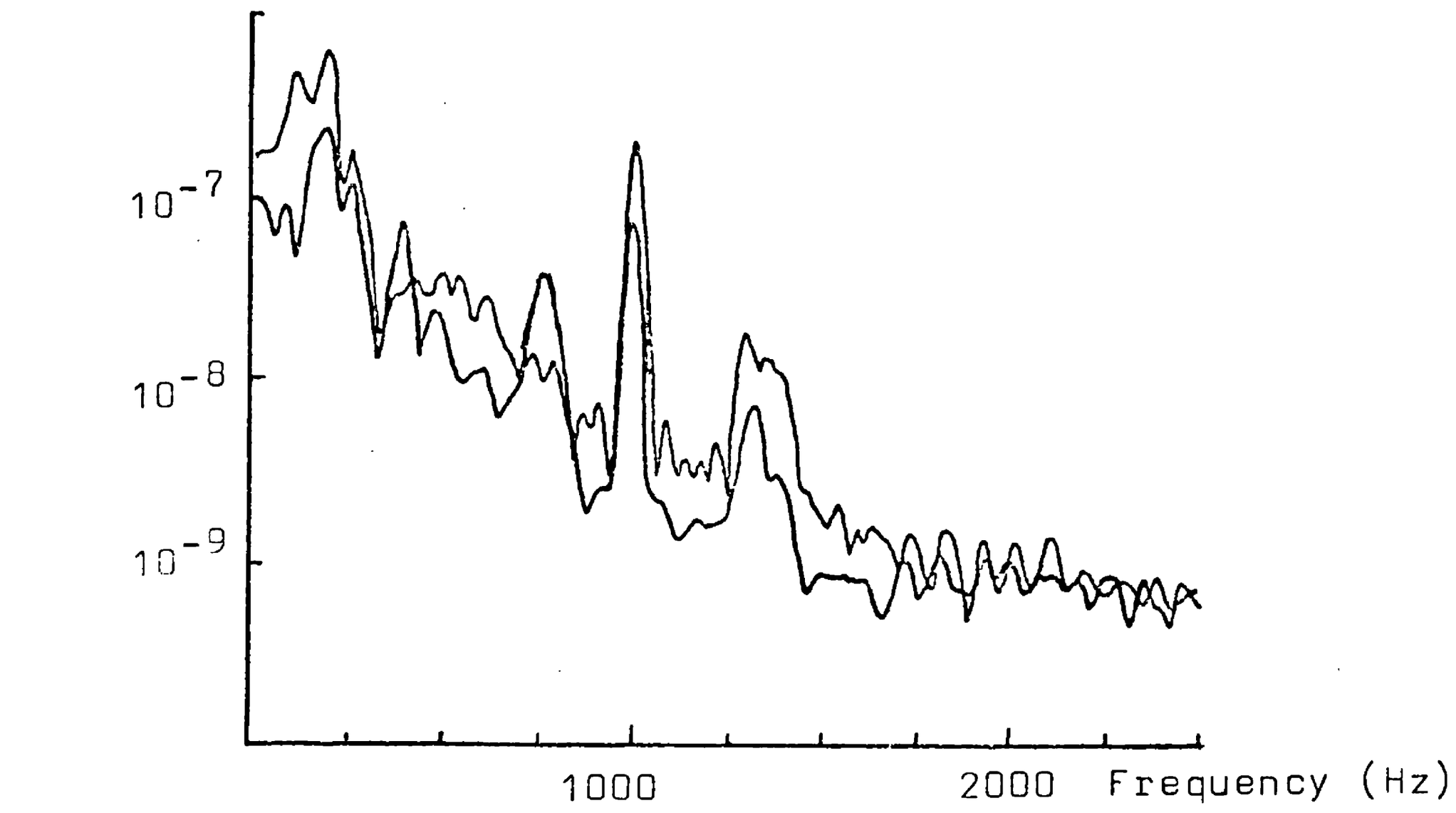

Fig 5·14(a): Y positional signal from the two quadrant diodes, showing positional modulation at 1 kHz. The top trace is diode 1 (no lens, w 1mm), for which the calibration is valid; the bottom trace is diode 2. The Y dimension of transducer 2 was being modulated.

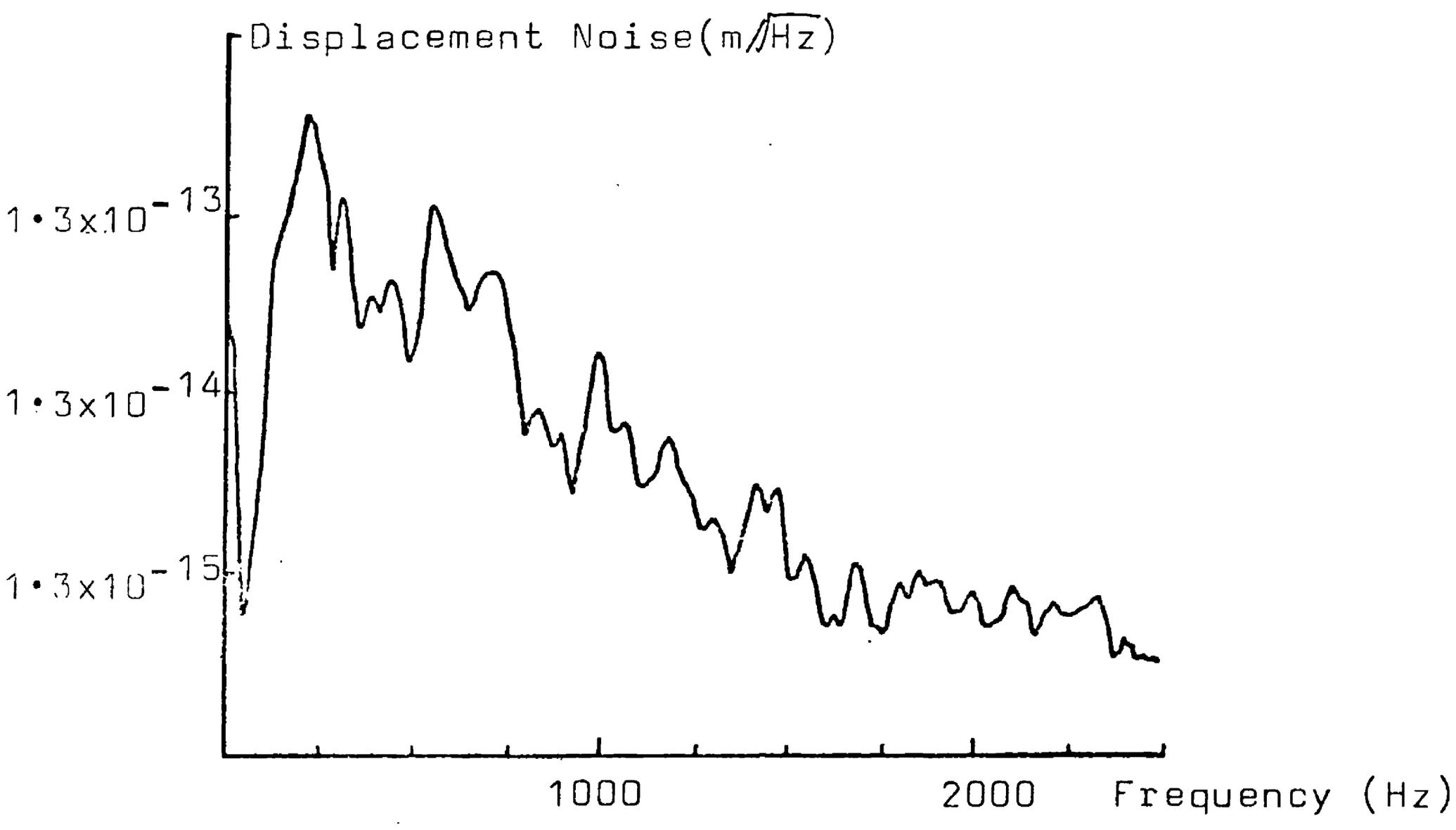

Fig 5·14(b): Detector sensitivity, showing the effect of the modulation in (a).

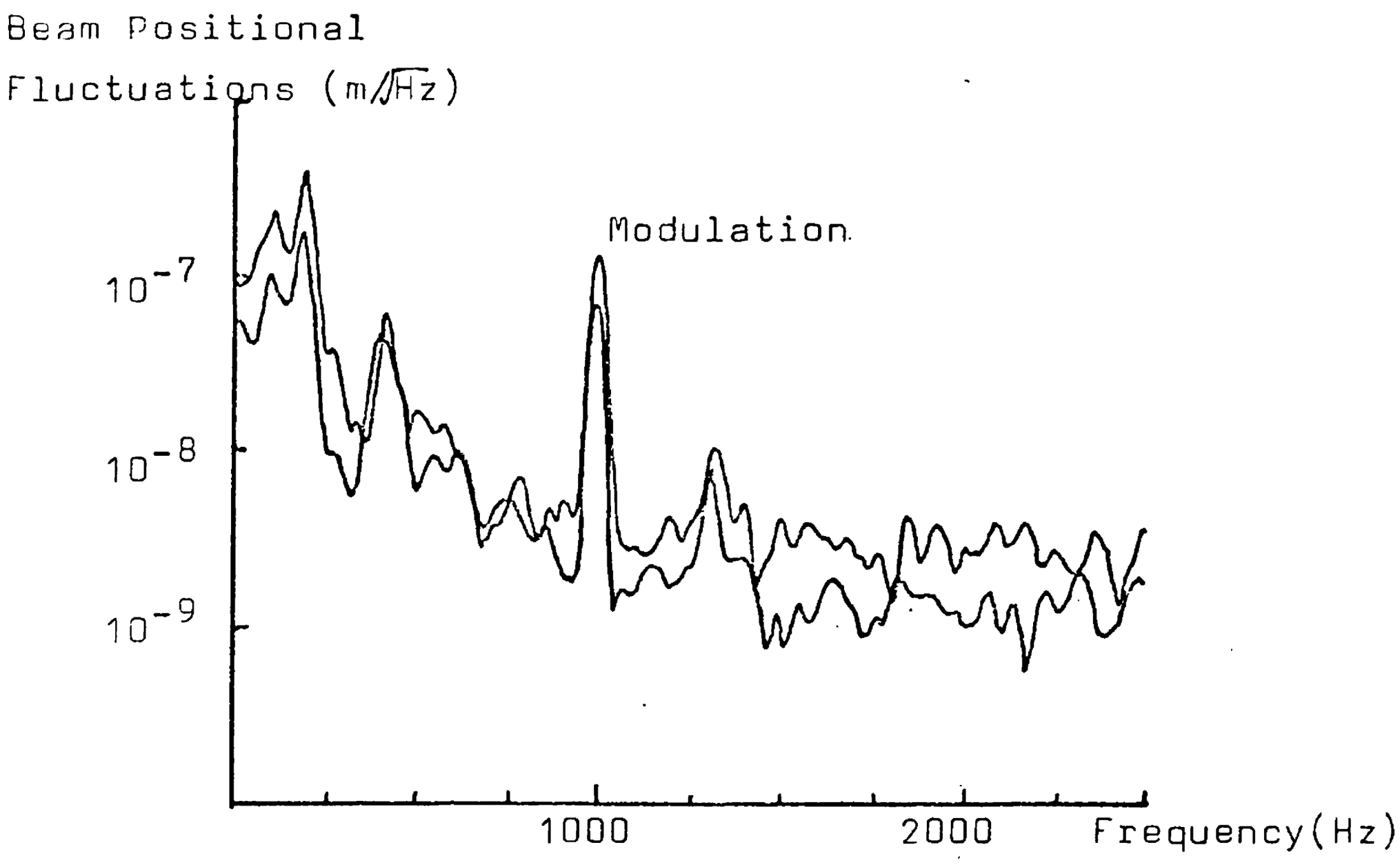

Fig 5·15(a): X positional signal from the two quadrant diodes, modulating the X dimension of transducer 1. Again, diode 1 is the top, calibrated trace.

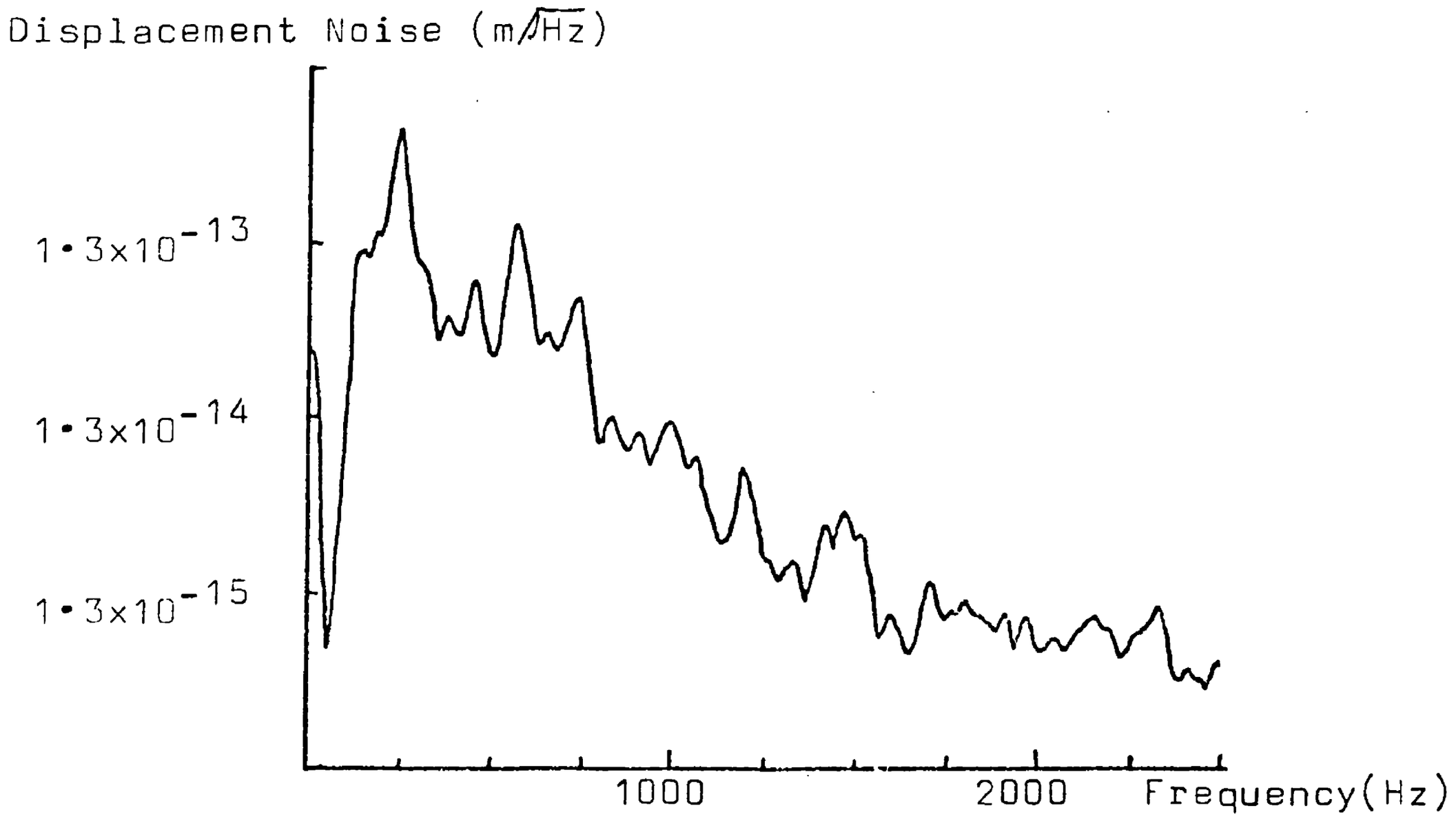

Fig 5·15(b): Detector sensitivity, with modulation as in (a).

Fig 5.16: The displacement noise produced by one component of the beam positional fluctuations.

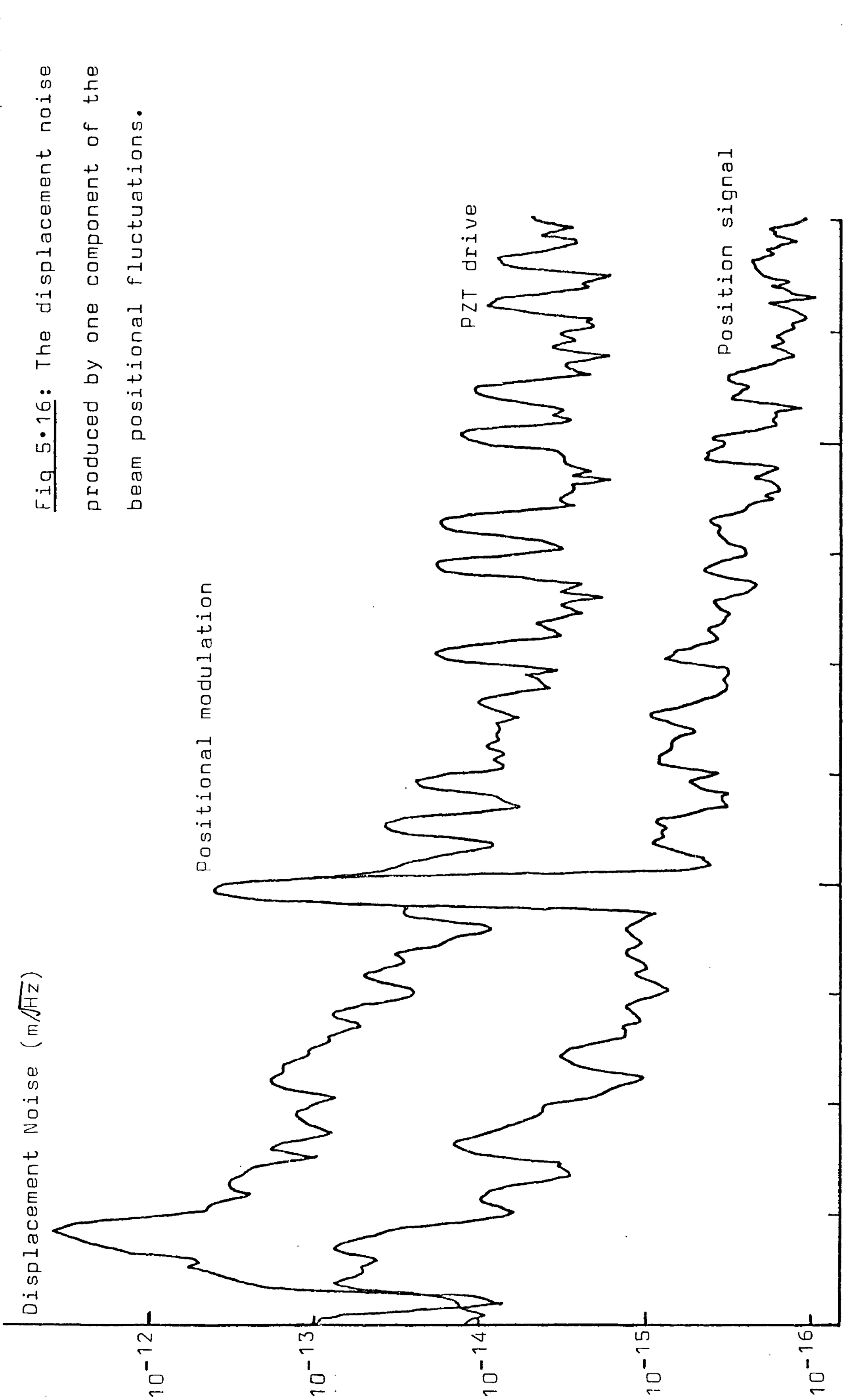

this electronic noise became important. This may be seen in fig 5·17, which compares the size of the PZT drive signal with the detector functioning and with no light on the photodiode: the two signals are near-identical above 1 kHz. While the electronic noise will be reduced by the loop gain, this leaves little margin for error, especially around 2 kHz. Certainly, any substantial improvement in the performance of the detector would require a reduction in this electronic noise. The preamplifiers were therefore replaced with lower noise versions, using smaller photodiodes. Fig 5·18 shows the noise of one of these new preamplifiers, compared with the shot noise in 0·4mW. The noise-equivalent power is therefore about 10μW: since the system was arranged to be front-end limited, amplifier noise was no longer a problem.

The detector sensitivity obtained with these new amplifiers in place is shown in fig 5·19: fig 5·19(a) is a spectrum of the PZT motion up to 2·5 kHz, while fig 5·19(b) displays the noise from the secondary PSD in a 25 kHz bandwidth. It can be seen that the high frequency noise has a flat spectrum at a level of $\sim 10^{-15} m/\sqrt{Hz}$, while the low frequency noise is the same as in the previous measurements. The measured finesses had now decreased to 150 and 120 for the secondary and primary cavities respectively, with the visibility less than 10%. The effect of this decrease in visibility can be dramatically seen in the congruence of shot noise in 3mW (phase noise of $6 \times 10^{-9} rad/\sqrt{Hz}$, bottom trace in fig 5·19(b)) and a displacement noise of $\sim 6 \times 10^{-16} m/\sqrt{Hz}$ — a naive calculation would have suggested that it would have been $\sim 4 \times 10^{-18} m/\sqrt{Hz}$. This

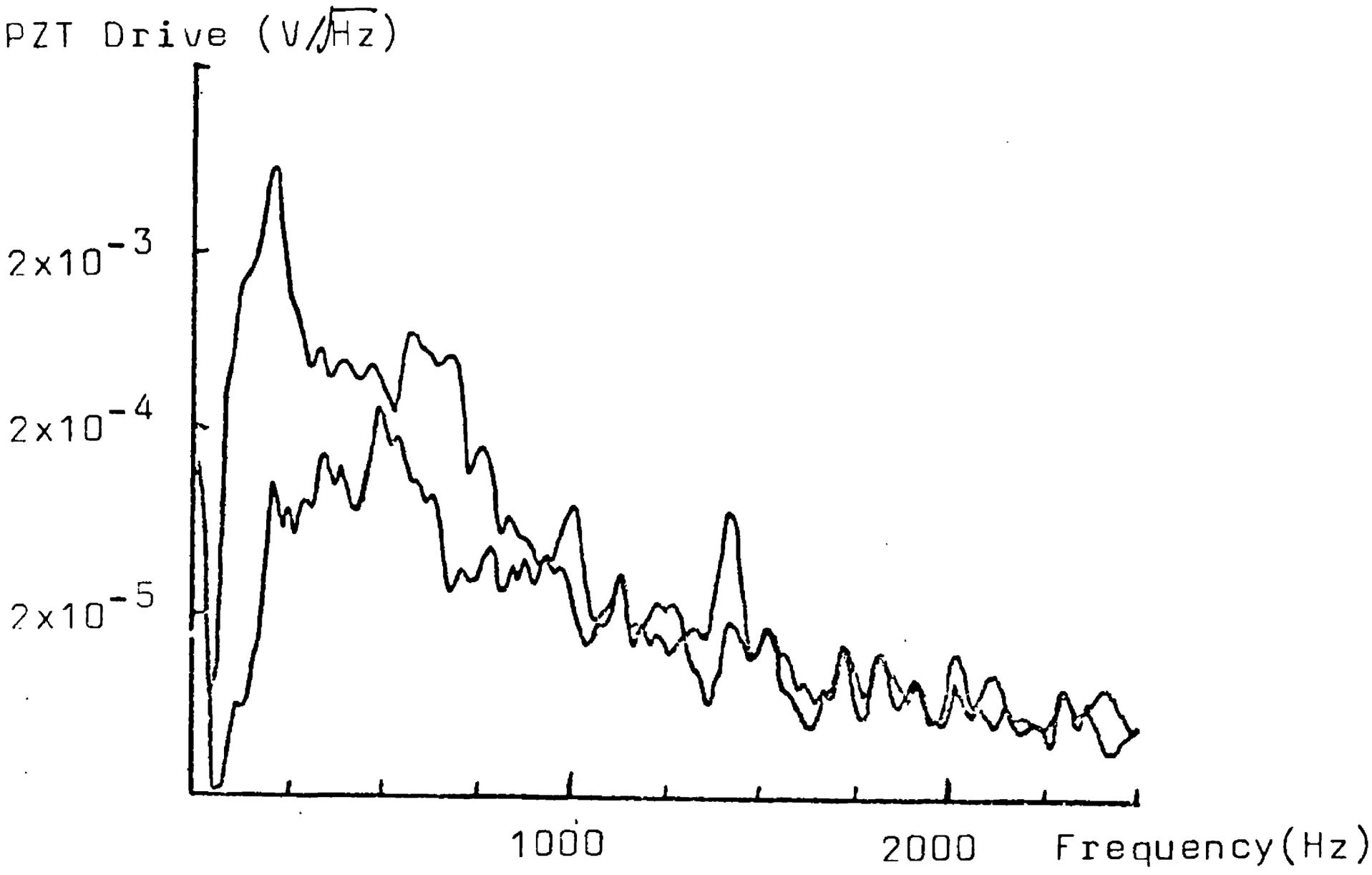

Fig 5·17: PZT mirror drive, with secondary loop closed (top trace) and open – no light on photodiode (bottom trace); original preamplifiers.

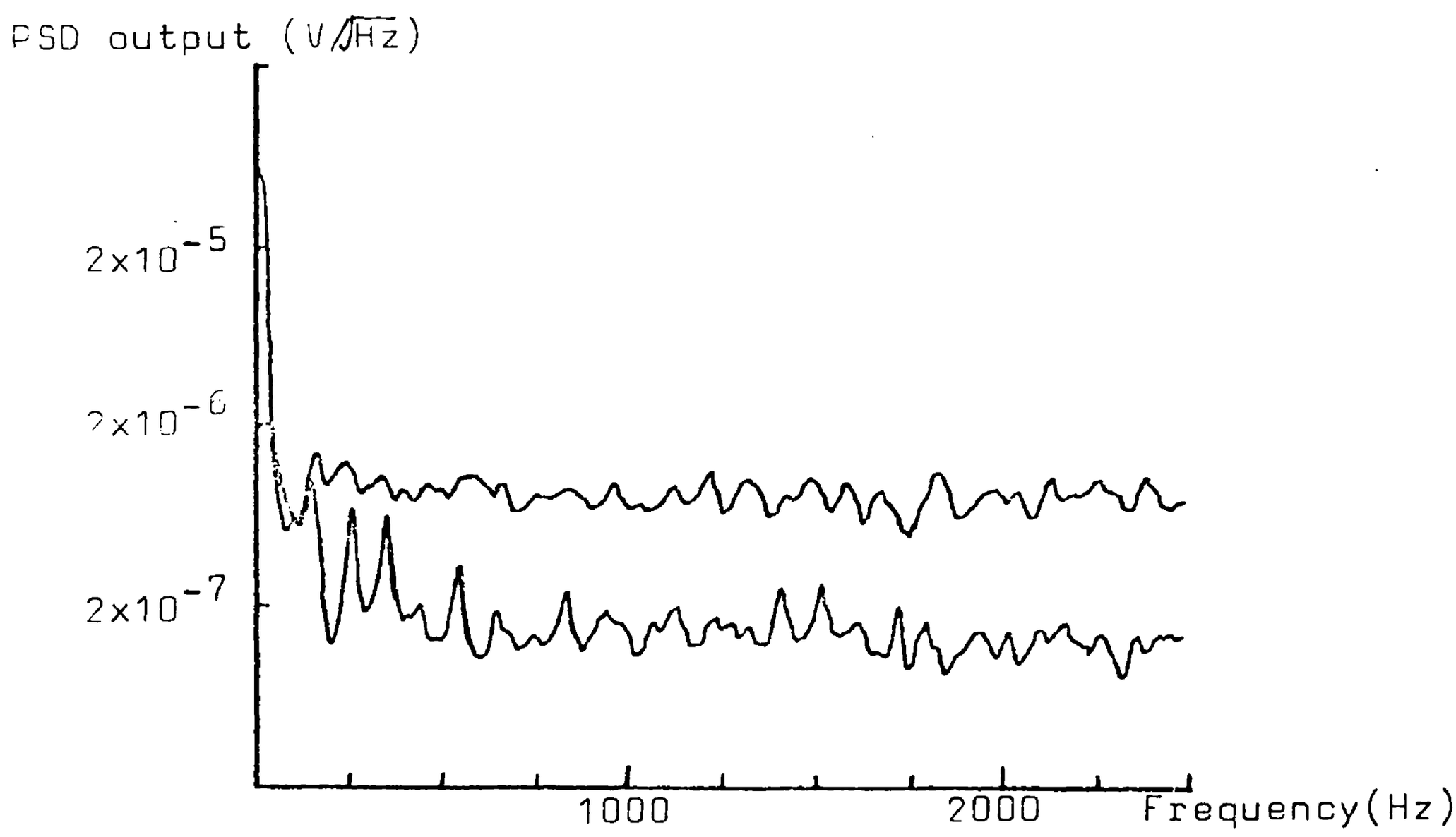

Fig 5·18: Output of one of the new preamplifier-PSD combinations. Top trace: shot noise on 0·4mW; bottom trace: no light on diode, i.e. amplifier noise.

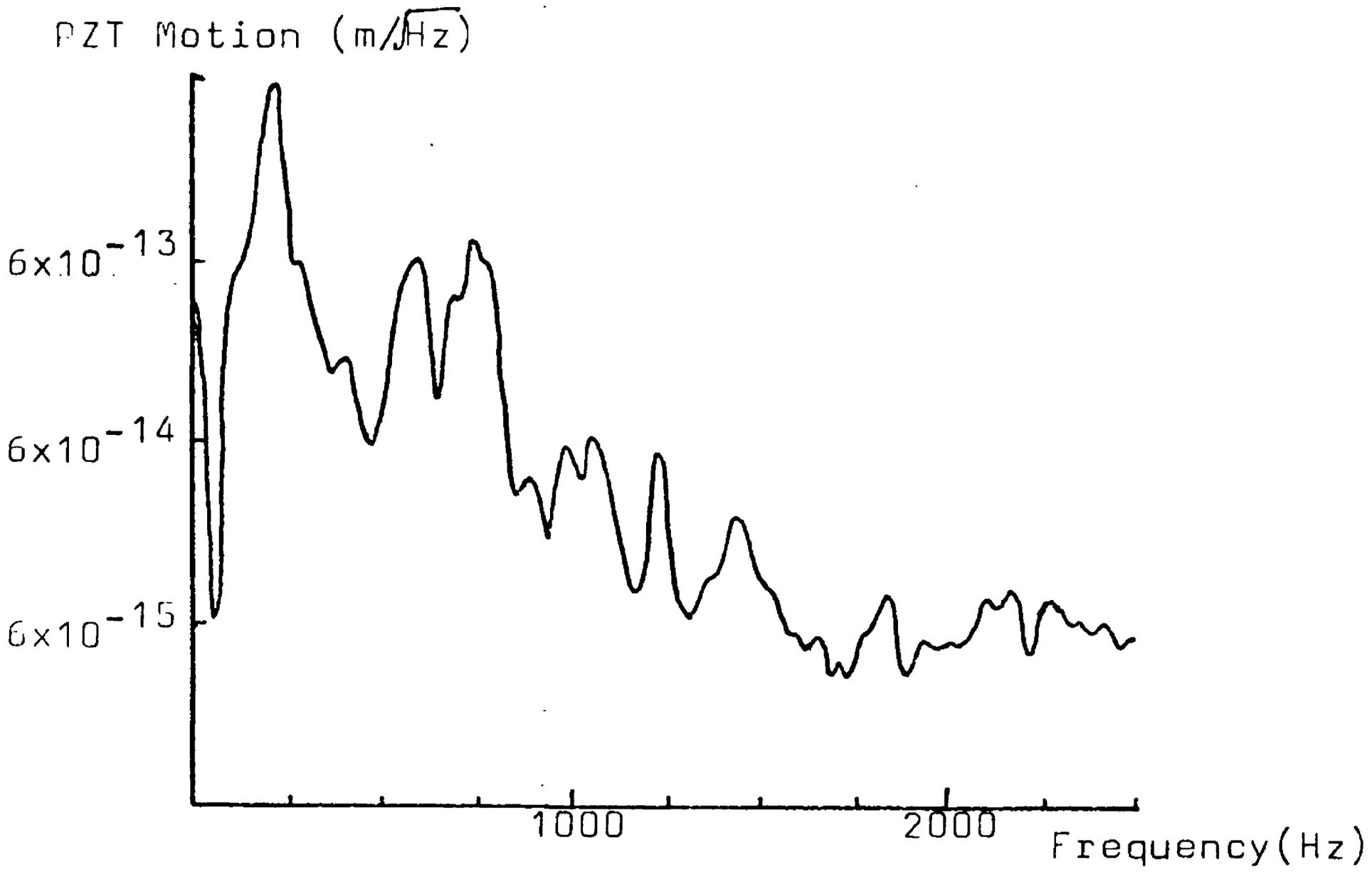

Fig 5·19(a): Detector sensitivity in a 2·5 kHz bandwidth.

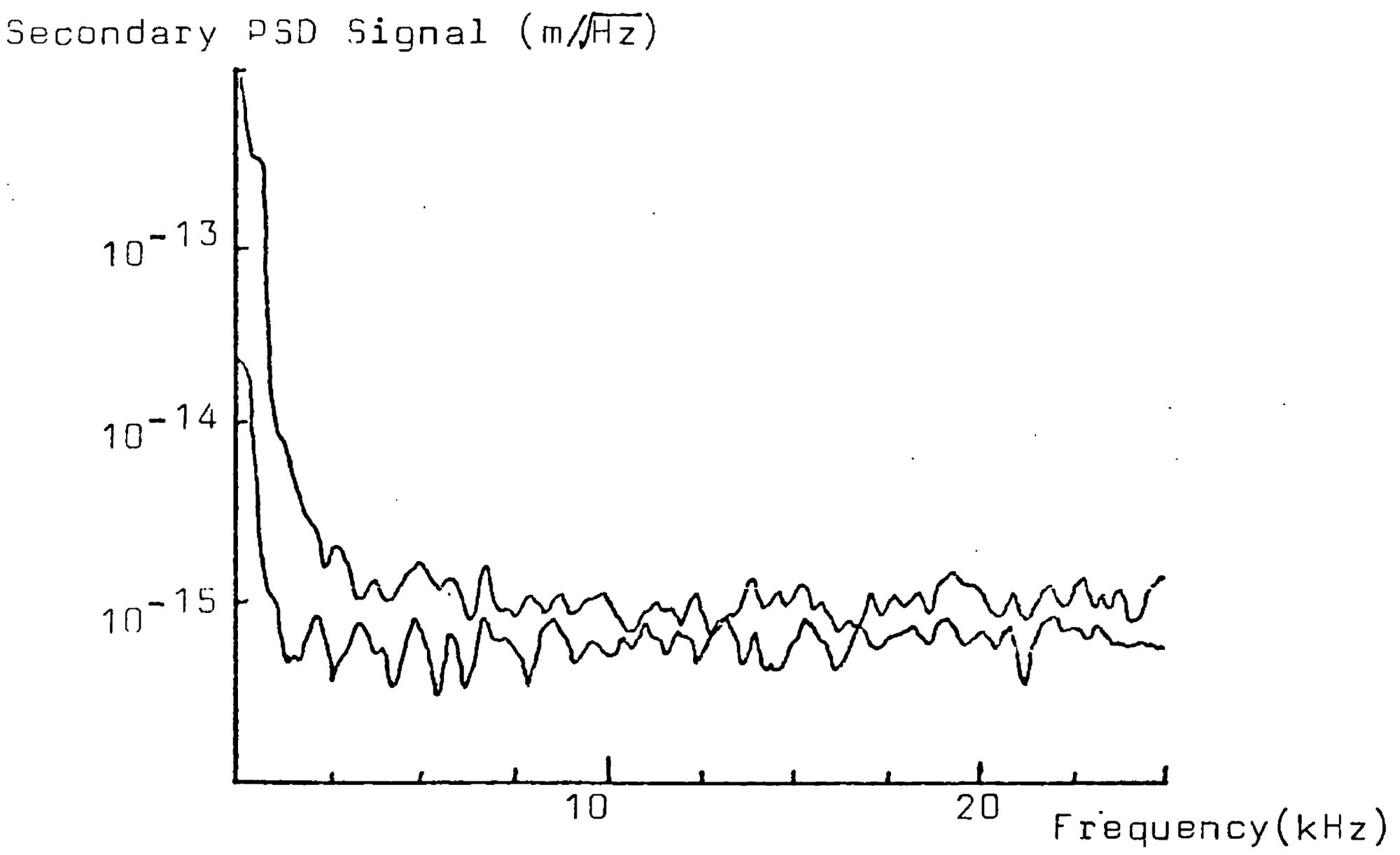

Fig 5·19(b): Detector sensitivity in a 25 kHz bandwidth. The lower trace shows the shot noise level in 3mW, the power on the secondary diode.

discrepancy may be explained (cf. 2·43) if the visibility was only a few per cent.

At this point, the deterioration in the mirrors made further measurements both impossible and futile.

Some of the measurements of the significance of the various noise sources are summarised in fig 5·20. It seems probable that the combination of three noise sources (beam frequency, intensity and positional fluctuations) is sufficient to explain the observed detector sensitivity above 750 Hz. The large peaks around 600 Hz, together with the smaller one at 1280 Hz, are associated with resonances of the suspension wires; these are excited by seismic noise or electrical noise in the wire-pulling or orientation control circuits.

This series of experiments made several things very clear: that mirrors must be found which give good finesse and visibility; that very good optical isolation is required; that if the sensitivity is to be significantly improved, the fluctuation levels of the laser beam frequency, intensity and position must <u>all</u> be reduced. A few of these points are discussed further in the next Chapter.

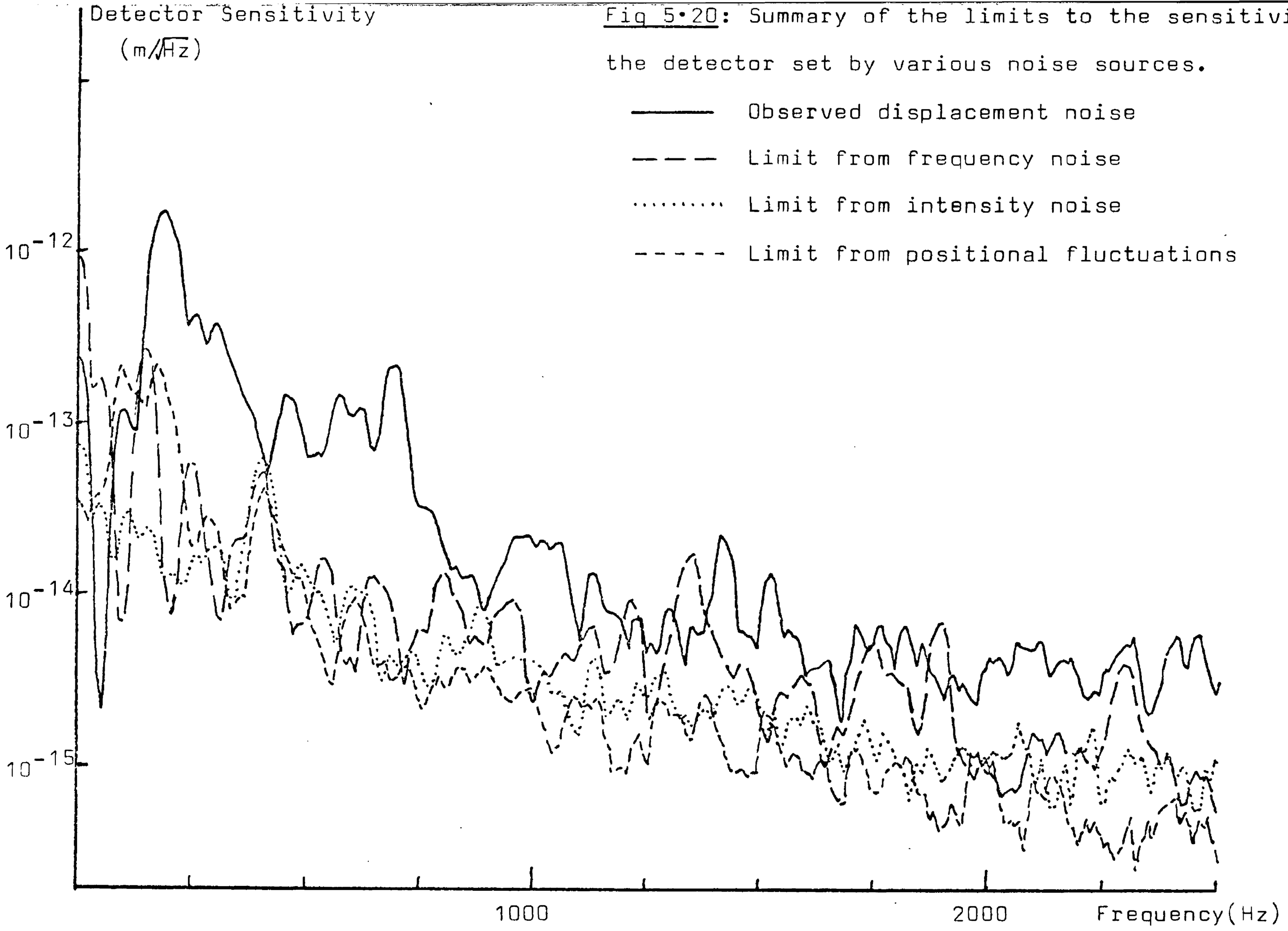

Fig 5·20: Summary of the limits to the sensitivity of the detector set by various noise sources.

——— Observed displacement noise

— — — Limit from frequency noise

····· Limit from intensity noise

- - - - - Limit from positional fluctuations

CHAPTER SIX

CONCLUSION AND FUTURE PROSPECTS

It has been seen both theoretically (Chapter 3) and experimentally (Chapter 5) that beam geometry fluctuations constitute a very serious limit to the sensitivity of the gravitational wave detector. Indeed, the noise produced by positional fluctuations must be reduced by a factor of $\sim 10^4$ if the desired sensitivity (i.e. shot noise on $\gtrsim 1$ W) is to be achieved at frequencies of several hundred Hz. While this is a large reduction, the work described in Chapter 4 on the development of suppression systems for beam geometry fluctuations should make it possible: the fast active system (section 4·3) will be able to suppress the positional fluctuations by a factor of 100, with the present mode-cleaning cavity (section 4·2) suppressing them by a further factor of 50. So a combination of these two well-developed techniques is already almost enough to make positional fluctuations unimportant.

The importance of more complex beam geometry fluctuations has also been demonstrated, though less precisely. These, too, will be suppressed by the mode-cleaning cavity. It is not yet clear whether the suppression factors attainable with the present cavity (~35 for beam size fluctuations) will be sufficient. If they are not, it may be possible to use a cavity with higher finesse: this will require, however, the use of mirrors with greater power-handling capacity or an increase in the length of the cavity. This problem of power density on the mirrors will become more severe as higher laser powers are achieved. If only a small reduction in the size of higher

order mode fluctuations is required, it may be easier to use an aperture system such as that described in section 4·1.

Thus, it seems that the techniques developed here for the suppression of beam geometry fluctuations should be sufficient to ensure that they do not place an important limit on the sensitivity of the gravitational wave detector.

It was seen in Chapter 3 that one of the factors which reduced the importance of beam size fluctuations was the high degree of symmetry facilitated by the optical recombination of the beams from the two cavities. With matching of the two finesses, such a recombination will also reduce the sensitivity of the interferometer to frequency noise. The importance of intensity noise should also be reduced in such a scheme: for a feedback voltage could be applied to the output Pockels cell to ensure that an interference minimum is accurately maintained; since this loop has a very high potential bandwidth (there is no PZT resonance to worry about) it should have a high DC loop gain, so the residual phase error should be small, reducing the coupling of low frequency intensity noise. When it is realised that the interfered output from the two cavities has the additional advantage of giving good fringe visibility (therefore better potential sensitivity), it seems clear that it is this signal which should be used as the measure of the relative length difference of the two arms of the interferometer.

In operation, the demodulated output of a photodiode observing this interfered light would be fedback onto the output Pockels cell to maintain the null. The fedback voltage would be a measure of the relative phase fluctuations of the interfering beams. This voltage could be fedback in turn to the secondary PZT mirror (with, perhaps, a low frequency component of the signal from the 10% splitter). The voltage applied to the PZT would then give the gravitational wave sensitivity in the region where the loop gain was high. At higher frequencies, where only the feedback loop to the output Pockels cell would have high loop gain, it would be the voltage applied to the Pockels cell which would give the detector output. When even this loop gain is negligible, it would be the output of the PSD which would represent the gravitational wave signal.

The combination of the use of optical recombination of the two beams, together with the mode cleaner (and the active system for positional fluctuations) should enable the detector noise level to be considerably improved. It is then likely that the thermal noise of internal vibrations of the test masses will become significant. This is due to their rather complex internal structure. Replacement of the end masses by solid, rigid structures should present few problems. The central mass, however, is considerably more difficult, for it must contain quite a large amount of complex optics. A likely solution is to retain the present central mass but place the cavity mirrors on rigid masses which would be separately suspended. This would provide vibration isolation between

the cavity mirrors and the main central mass. While a certain increase in complexity is evidently involved, this should pose no fundamental problems.

The discussion in Chapter 1 of likely source strengths and detector sensitivities made it clear that detected laser powers of 1W are required if gravitational waves are to be detected. This is perhaps a factor of 50 larger than the present detected power level in the Glasgow detector — ~20mW from a laser single-line output of ~200mW. These losses will have to be reduced by ensuring very good mirror quality (appropriate for the angle required) and using anti-reflection coating wherever possible. Greater laser power will also be required, however. Some increase may be attained by using very low-loss intra-cavity Pockels cells, such as balanced Brewster cut crystals in a single glass envelope. Indeed, single-line output powers of up to 2W have been achieved at Glasgow with an intra-cavity Pockels cell, though this has not been maintained for long periods.

An alternative method of increasing the available laser power is to eliminate the intra-cavity Pockels cell entirely. Instead, the laser would be stabilised by having its mirrors mounted on PZTs, together with an external Pockels cell. The PZTs would be used to stabilise the laser frequency with respect to a reference cavity, reducing the fluctuations to the point at which a phase correcting Pockels cell could be used to stabilise the light with respect to the interferometer cavities. The first loop could have a bandwidth of ~100 kHz, while the

second could easily operate to several MHz. Such a two-loop system has been tried by the Munich group (Billing et al 1981). The final frequency stability could well be better than that obtained with a one-stage system using an intra-cavity Pockels cell, while the absence of the lossy Pockels cell in the laser would result in a considerably higher laser output power. In addition, other lasers may be used to amplify this stabilised light (without the need for single-mode étalons), increasing the available power still further. A. Brillet at L'Université Paris Sud is reported to be investigating this technique.

Another way of increasing the effective light power is to recycle the light that would otherwise be rejected at the beamsplitter (Drever et al 1981). A possible way of doing this for a cavity detector is shown in fig 6·1. If the path lengths are adjusted to minimise the (already small) light power on the photodiodes, then the recycled light will have the correct phase to increase the light power. This is only useful when the losses for one cycle are small; in turn, it would only be sensible if the achievable storage time was comparable with period of the gravitational wave (otherwise more could be gained by increasing the storage time). If the fractional loss per cycle (i.e. the fraction of the power not returning eventually to the first mirror) is ρ, then the final power I_f for an incident power I_0 is just

$$I_f/I_0 = 1/\rho \qquad (6\cdot1)$$

So the sensitivity is improved (if shot-noise limited) by a factor of

$$\text{Sensitivity gain} = \rho^{-\frac{1}{2}} = 30(\rho/10^{-3})^{-\frac{1}{2}} \qquad (6\cdot2)$$

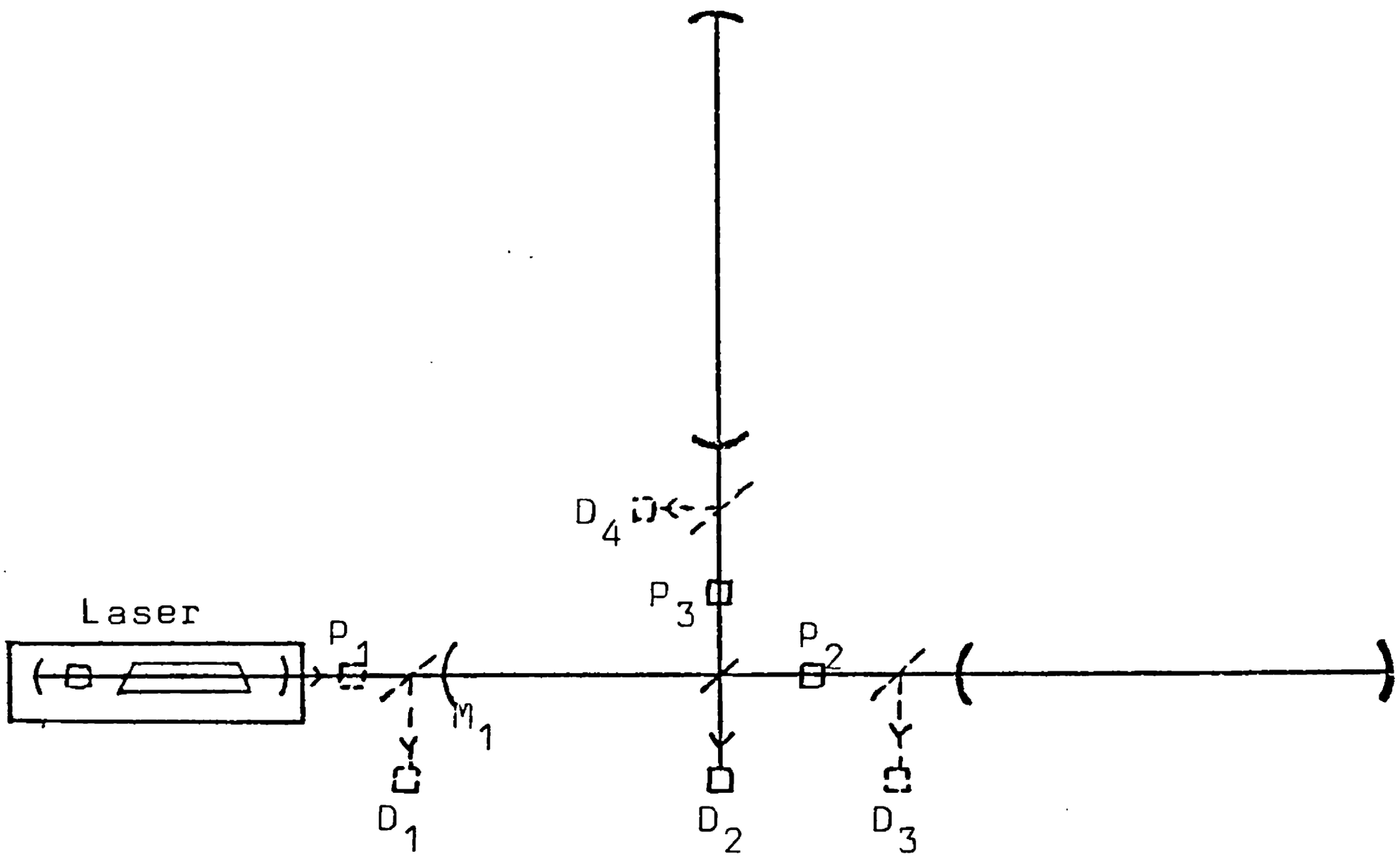

Fig 6·1: The optical arrangement of a cavity detector which uses "light recycling". The additional mirror M_1 is arranged so that it reflects back to the interferometer any light returning towards the laser; if the light on the diode D_1 is minimised, the effective incident power is increased; after Drever (1983).

It is clear that the losses must be small if any significant improvement is to be achieved.

If the losses are dominated by the absorption or scattering (coefficient A^2) at the cavity mirrors, then, for an input transmission $T_1^2 \gg A^2$ (i.e. low loss),

$$\rho = 2A^2/T_1^2 \qquad (6·3)$$

The mirror transmission should evidently be as large as possible compatible with keeping a long storage time, i.e.

$$\tau_s \gtrsim \tau_g/\pi \qquad (6\cdot4)$$

This gives

$$\rho \gtrsim c\tau_g A^2/2\pi l \qquad (6\cdot5)$$

So the possible improvement in the shot-noise limited sensitivity over the storage time limit would be

$$\text{Sensitivity gain} = (c\tau_g A^2/2\pi l)^{-\frac{1}{2}}$$
$$= 14(l/1\text{km})^{\frac{1}{2}}(A^2/10^{-4})^{-\frac{1}{2}} \qquad (6\cdot6)$$

With high quality mirrors and low loss optics, it would seem that the use of this recycling technique may allow an improvement of the sensitivity by an order of magnitude. With 1 W of incident light, this would give a shot-noise limited sensitivity of $h \sim 2\times10^{-21}$ for milli-second pulses.

The high light powers that recycling attempts to provide are required to reduce the photon-counting error. Caves (1981) has shown that the origin of both the photon counting error and the differential radiation pressure fluctuations in the two arms may be considered to lie in vacuum field fluctuations. The two types of beam fluctuation are the result of different <u>phases</u> (relative to the beam) of vacuum fluctuation. The noise levels in the two orthogonal phases are normally equal, leading to the standard expressions for photon counting error and radiation pressure fluctuations. Caves' suggestion was that it might be possible to reduce the noise level in one phase, at the expense of increasing it in the other (thus avoiding a violation of the Heisenberg Uncertainty Principle). Production of such a "squeezed state" in the vacuum at the normally unused port of the interferometer could

therefore reduce the fluctuations in photon number while increasing the radiation pressure fluctuations. The overall sensitivity of the detector could therefore be improved.

Squeezed states can, at least in principle, be produced by non-linear optical devices such as degenerate parametric amplifiers. It is by no means certain, however, that reasonable squeeze factors can be achieved (e.g. Walls 1983).

A major problem with squeezing is the transferance of noise from one phase to the other by losses in the system. The most obvious place at which this occurs is the photodiode, where the lack of efficiency means that the statistics of the light are only poorly reflected in the photocurrent. If only the light at the unused port was squeezed, this would totally prevent any possible sensitivity improvement. It may be possible, however, to also squeeze the output light, effectively amplifying the signal and noise of the output light until the diode noise is negligible. So inefficient ($\zeta \sim 0{\cdot}4$) photodiodes may not stop the use of the squeezing technique.

Losses will also occur at the cavity mirrors, inevitably degrading the squeezed state. This means that squeezing can only improve the detector sensitivity if it is not limited by mirror losses: for cavity detectors,

$$\text{Possible improvement factor} = (T_1^2/A^2)^{\frac{1}{2}} \qquad (6{\cdot}7)$$

Note that this is about the same factor as that obtainable from recycling.

Use of squeezed states will be difficult, but it may enable improvement of the shot-noise limited sensitivity

by up to an order of magnitude. This, possibly in combination with recycling, should enable shot-noise limited sensitivities of better than $h \sim 10^{-21}$ to be achieved.

Another way of further improving the sensitivity of an interferometer and so increasing the probability of detecting gravitational radiation is to use a technique which may be termed "periodic recycling" (Drever 1983). A possible optical arrangement with a cavity detector is indicated in fig 6·2. The incoming laser beam is divided at the beamsplitter M_1 into two equal halves, each of which enters one of the detector cavities through the high quality mirror M_2. The cavities are arranged to have a storage time comparable with half the gravitational wave period. On re-emerging from a cavity (with the maximum phase change given by 2·24), the beam is directed by the polarising beamsplitters into the other cavity, where most of the beam still sees the same sign of gravitational wave. The phase change thus increases. The shot noise limited sensitivity of the detector may therefore increase linearly with the number of cycles until the losses dominate. It should be noted that the resultant sensitivity will be an oscillatory function of gravitational wave frequency: an oscillatory output will therefore result if the gravitational waves are broad-band, as in a pulse.

The periodic recycling system may also be regarded as a pair of coupled oscillators (Drever, personal communication, 1983): the resonance is split into two normal modes, the separation being determined by the coupling

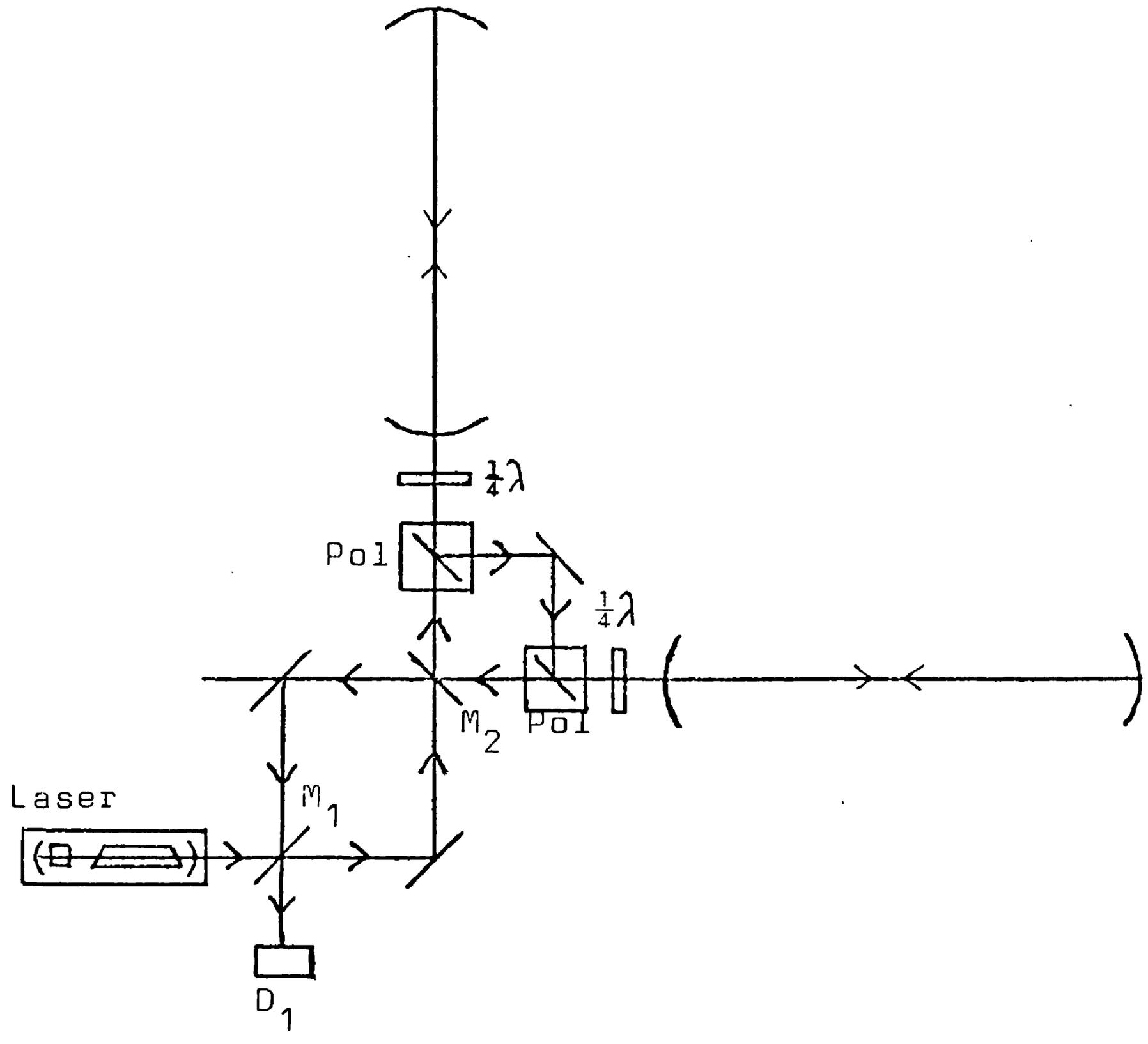

Fig 6·2: An optical arrangement for periodic recycling with a cavity detector, after Drever (1983)

constant (the reflectivity of M_2). If this latter quantity is correctly chosen ($1-R_2^2 \sim \omega_g/\nu_0$, with ω_g the GR frequency and ν_0 the free spectral range), both the "DC" light and one of the sidebands produced by the gravitational wave (cf. Appendix 2) will resonate. The possible improvement factor for a periodic source is therefore approximately equal to ν_0/ω_g. For a 1 km detector, this is a factor of approximately 25 at 1 kHz.

It is clear that periodic recycling promises to be a useful technique, particularly in the search for

continuous gravitationa radiation from souces such as fast pulsars. Together with squeezing and normal recycling, it shares the requirement for large detectors and low-loss optics. The possibility of using these advanced techniques, either separately or in combination, significantly increases the likelihood of gravitational radiation being detected. These techniques also enhance the potential advantages of laser interferometers over bar detectors. It is apparent that the technical difficulties associated with acheiving the required sensitivity are considerable. They do not, however, appear insuperable.

APPENDIX ONE

AN EXPERIMENTAL UPPER LIMIT TO THE GRAVITATIONAL RADIATION FROM THE MILLISECOND PULSAR PSR 1937+214

The pulsar PSR 1937+214 rotates at a frequency of 642 Hz, only a factor of two less than the theoretical upper limit for a neutron star. Soon after its discovery by Backer et al (1982), it was decided at Glasgow that it was worth attempting a direct search for gravitational radiation from this unusual object. A suitable detector was available in the form of a split bar originally used for searches for gravitational-wave pulses and for a stochastic background of gravitational radiation (Drever et al 1973, Hough et al 1975): the high bandwidth (~200Hz around 1 kHz) set by the latter application resulted in a reasonable sensitivity at 1284 Hz, twice the rotational frequency. With a mass of 300 kg, Q of 2,200, coupling coefficient β of 0·18, piezoelectric motion sensing, FET pre-amplifiers and room temperature operation, the detector noise level was $\sim 3\times10^{-18} m/\sqrt{Hz}$ at this frequency.

In order to obtain as good a sensitivity as possible, it was decided to integrate the signal from the detector for several hours. This requires, however, precise knowledge of the pulsar frequency. While a value for this at one time could be obtained from Jodrell Bank, it was necessary to calculate the apparent changes produced by Doppler shifting as the Earth revolved and rotated.

If $\underset{\sim}{r}$ and $\underset{\sim}{s}$ are the position vectors of the Earth and pulsar in barycentric-equatorial co-ordinates, the time delay of a pulse received at the centre of the Earth

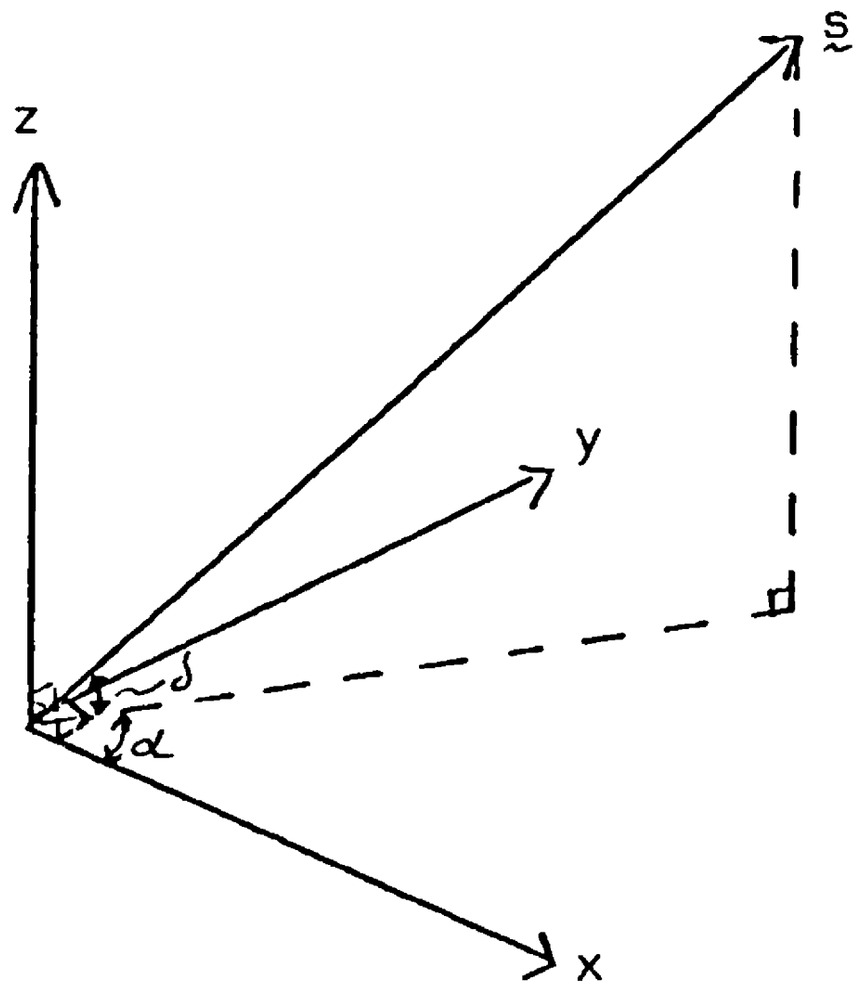

Fig A1·1: The rectangular barycentric-equatorial co-ordinate system (x,y,z); the declination and right ascension of a source are indicated.

relative to the solar system barycentre is

$$t_{EC} = (-1/c)\underset{\sim}{r}\cdot\underset{\sim}{s} \qquad (A1\cdot1)$$

It is convenient to use rectangular barycentric-equatorial co-ordinates, as indicated in fig A1·1. In terms of the declination δ and the right ascension α,

$$x = \cos\delta\cos\alpha \qquad (A1\cdot2)$$

$$y = \cos\delta\sin\alpha \qquad (A1\cdot3)$$

$$z = \sin\delta \qquad (A1\cdot4)$$

So if the Earth's position is (X,Y,Z), the time delay is

$$t_{EC} = (-1/c)(x_p X + y_p Y + z_p Z) \qquad (A1\cdot5)$$

Thus, the rate of change of the time delay as a result of the orbital motion is just

$$\dot{t}_{EC} = (-1/c)(x_p \dot{X} + y_p \dot{Y} + z_p \dot{Z}) \qquad (A1\cdot6)$$

The velocities $\dot{X},\dot{Y},\dot{Z}$ are tabulated in the Astronomical Almanac.

There is also due to the spin of the Earth: if the

pulsar altitude (elevation) is h, the time delay at an Earth radius ρ is

$$t_S = (\rho/c)\sinh \qquad (A1\cdot7)$$

The value of sinh may be calculated from

$$\sinh = \sin\phi\sin\delta + \cos\phi\cos\delta\cos HA \qquad (A1\cdot8)$$

where ϕ is the latitude and HA is the hour angle, obtained from the sidereal time τ ($HA = \tau - \alpha$); δ and α must be corrected to the present epoch. So

$$\dot{t}_S = -\dot{\tau}\cos\phi\cos\delta\sin(\tau-\alpha) \qquad (A1\cdot9)$$

A combination of (A1·6) and (A1·9) may be used to find the total rate of change of time delay, hence the Doppler shift.

The experiment took place between 20·15 on 6th December and 04·15 on 7th December 1982. The calculated values of twice the pulsar frequency for this period are shown in Table A1·1. The assumed periods, changed at the times indicated, were sufficiently accurate to ensure that the phase discrepancy between the assumed and "true" apparent pulsar waveforms was always less than 0·1 cycle.

Time for Changing Period	Doppler Shift $(\Delta\nu/\nu)\times10^{-7}$	Period During Run (ms)
20h	15·283	·778945039
23h	15·268	·778945096
0·30h	13·6066	·778945240
02·00h	11·299	·778945436
03h	9·5437	·778945570
04h	7·7959	·778945651

Table A1·1: Calculated values for twice the apparent frequency.

The experimental arrangement is indicated in fig A1·2. A 5 MHz crystal, referenced to the 60 kHz MSF standard frequency transmission, was used as a stable clock. A signal from this clock was divided by 3900 and used, in a two-phase lock-in amplifier, to beat the signal from the detector down to near 1·8 Hz. This greatly reduced data handling problems. Each phase of this low frequency signal was then averaged in 26 minute batches using the HP3582A spectrum analyser. The trigger for this averaging was obtained from the clock, using a system of pre-set scalars in the "leap-year" mode (Horowitz 1969) to ensure that exactly 7 cycles were averaged on each firing. It is these scalars that were adjusted to allow for the Dopp-ler shifts. The division of the data into 26 minute bat-ches allowed the signals at slightly different frequencies to be compared: the batches were coherently added in the HP85 computer, with phase shifts introduced to correspond to each frequency. The result of each of these integrat-ions was folded into one cycle and the amplitude of the signal found by least-square fitting. This gave the amp-litude of the detector output at each of ten frequencies around the expected frequency, results shown in fig A1·3. It can be seen that there is no evidence for a significant signal.

The calibration shown was found by using capacitor plates at the end of the bar to apply known forces and observing the resultant output. The radiation was assumed to be unpolarised. The varying sensitivity of the detec-tor, as its orientation relative to the pulsar changed during the experimental run, was also taken into account.

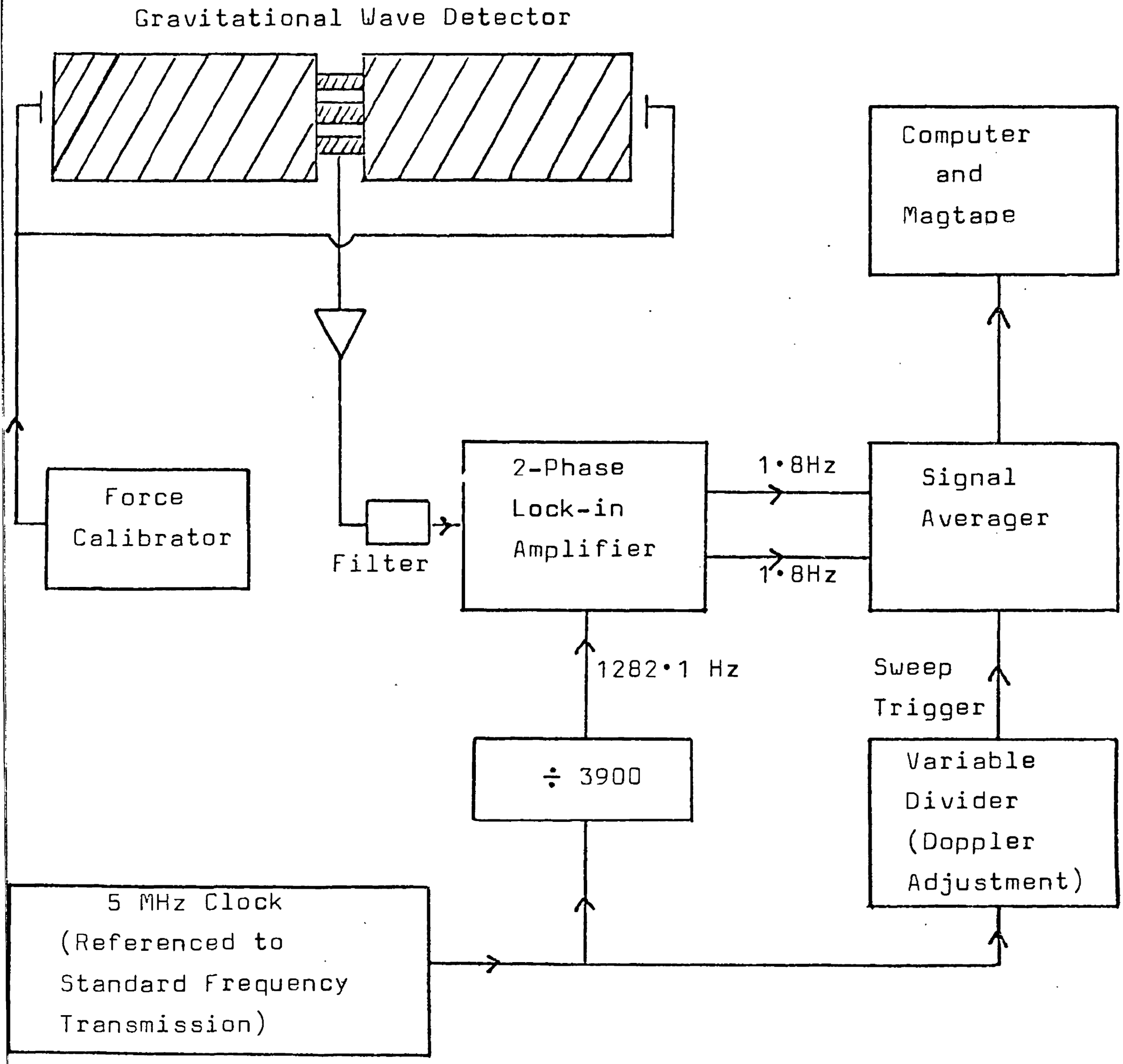

Fig A1·2: Schematic diagram of the detector and data recording system.

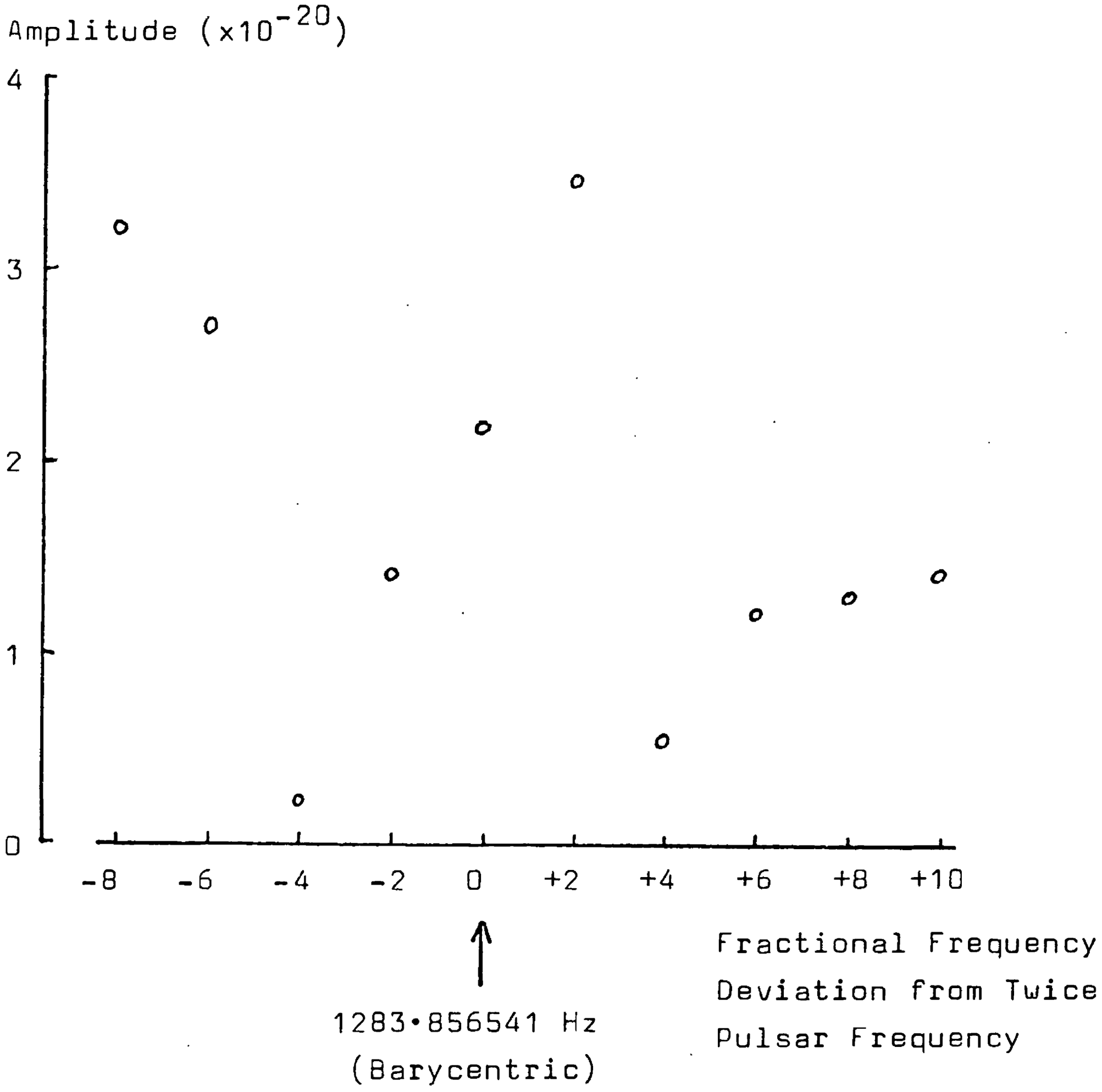

Fig A1·3: Detector output, expressed in terms of an equivalent gravitational wave amplitude, at ten barycentric frequencies.

If the signal at exactly twice the pulsar frequency is corrected for the noise power observed at other frequencies, it corresponds to a gravitational wave amplitude

$$h \sim \left[0{\cdot}8^{+1{\cdot}5}_{-0{\cdot}8}\right]\times 10^{-20}$$

While this result does not constitute a severe astrophysical constraint, it is an interesting and direct upper limit on the gravitational radiation from the millisecond pulsar.

APPENDIX TWO

AN ALTERNATIVE CALCULATION OF THE GRAVITATIONAL-WAVE SENSITIVITY OF A CAVITY

The phase change produced by an incident gravitational wave in the beam emerging from an optical cavity was calculated in section 2·1(i) by explicitly superposing the separate components of this beam. An alternative but equivalent method (Drever, personal communication, 1983) is to treat the gravitational wave as phase modulating the field inside the cavity (by $\Delta\phi = hkl\exp(i\omega_g t)$), producing sidebands whose amplitude is determined by the resonance of the cavity. The amplitude of the sidebands relative to the main beam is then (cf., for example, 2·14)

$$E_s = \frac{Fhkl\exp(i\omega_g t)}{(1-R_1R_2)}\left\{\frac{e^{i\delta} - R_1R_2}{1+F'\sin^2\delta/2}\right\} \qquad (A2\cdot1)$$

where $\delta = 2\pi\nu_g/\nu_0 = 4\pi l/\lambda_g$. For $\delta \ll 1$, (A2·1) may be written as

$$E_s = \frac{Fhkl\exp(i\omega_g t)}{\pi\left[1+(4Fl/\lambda_g)^2\right]}\left\{1 + i(4Fl/\lambda_g)\right\} \qquad (A2\cdot2)$$

Only the real part of the field is detected. For low storage times ($Fl/\lambda_g \ll 1$), the phase change produced by a gravitational wave is therefore

$$\Delta\phi = (F/\pi)hkl\cos\omega_g t \qquad (A2\cdot3)$$

If $Fl/\lambda_g \gg 1$, then

$$\Delta\phi = (hk\lambda_g/4\pi)\sin\omega_g t \qquad (A2\cdot4)$$

Alternatively, the magnitude of $\Delta\phi$ is

$$|\Delta\phi| = \tfrac{1}{2}kc\tau_s h\left[1+(2\pi\tau_s/\tau_g)^2\right]^{-\frac{1}{2}} \qquad (A2\cdot5)$$

where $\tau_s = 2Fl/\pi c$ and $\tau_g = 2\pi/\omega_g$.

These relations are identical to those derived in section 2·1(i). Note that for $\tau_s \gg \tau_g$, the phase change is about constant, at a value equal to one half of that obtained for a delay line of optimum length.

APPENDIX THREE

THE FEEDBACK SIGNAL REQUIRED FOR THE ACQUISITION OF LOCK

Even in the absence of high frequency phase noise, the swinging of the test masses at their natural pendulum frequency with the consequent sweeping through of the fringes means that high frequency position feedback signals are required if the cavities are to attain resonance. Crudely, if the duration of a fringe is τ, the feedback system must have gain out to a frequency of at least $1/\tau$ if it is to be able to lock on. The system must also have the range to cope with both low and high frequency signals. These factors should be understood if an appropriate feedback system is to be designed.

The signal giving the equivalent positional change of a test mass as a fringe sweeps through is (cf. 2·48)

$$\Delta x(t) = \frac{(\lambda/\pi)\sin\delta}{1+F'\sin^2\delta/2} \qquad (A3\cdot1)$$

For high finesse cavities, the only significant contributions to this are from the region where $\sin\delta \approx \delta$. Now if $\delta = \dot{\delta}t$ (i.e. uniform velocity of swing), the positional signal may be written

$$\Delta x(t) = (\lambda/\pi)\dot{\delta}t\left[1+(F\dot{\delta}t/\pi)^2\right]^{-1} \qquad (A3\cdot2)$$

Or,

$$\Delta x(t) = (\lambda/F)t\left[(\pi/F\dot{\delta})-it\right]^{-1}\left[(\pi/F\dot{\delta})+it\right]^{-1} \qquad (A3\cdot3)$$

Taking the Fourier transform to give the frequency spectrum gives (e.g. Bateman 1954):

$$\Delta x(f) = (\lambda/2F)\exp(-f/f_c) \qquad (A3\cdot4)$$

where $f_c = F\dot{\delta}/\pi$.

If the masses are swinging by one wavelength at 1 Hz, then $\dot{\delta}$ might be as high as 4πrad/s. With a finesse of 300,

this would give $f_c \sim 1$ kHz. The feedback loop would therefore require gain in a bandwidth larger than 1 kHz if the system is to be able to acquire lock at any part of a swing. The achievement of this necessary bandwidth in the locking loop of the secondary cavity is by no means easy.

The frequency spectrum A3·4 also indicates a problem with any feedback system which applies a <u>force</u> to the test masses, since the force required to produce a given displacement increases as the square of the frequency. Such a system is attractive because the double integration reduces the effect of electrical noise or pick-up at gravitational wave frequencies. The maximum acceleration required by (A3·4) occurs at a frequency $f = 2f_c$; with the parameters used above,

$$\ddot{x}(\max) \sim 2\times10^{-2} \text{m/s}^2$$

This is quite large. If a capacitative system were to be used, the required voltage with plate area A and separation d would be

$$V = (2md^2\ddot{x}/\varepsilon\varepsilon_0 A)^{\frac{1}{2}} \qquad (A3\cdot5)$$

With $A \sim 10^{-3}\text{m}^2$, $d \sim 1$ mm and $m \sim 3$ kg, the voltage required for the attainment of lock would be

$$V_{REQ} \sim 4 \text{ kV}$$

Thus, the use of such techniques does not look practical unless the effectiveness of the damping of the masses' swinging can be greatly increased.

APPENDIX FOUR

THE EFFECT OF MODE-MATCHING ON FRINGE VISIBILITY

The importance of obtaining a good a fringe visibility as possible was seen in Chapter 2; the significance of imperfect mode-matching is calculated here.

An incoming laser beam with a characteristic size w_1 different to that of the cavity beam w_2 will lead to a degraded fringe contrast, for two reasons: the overlap between the interfering beams will be poor and the excited amplitude of the intra-cavity beam will be reduced. If the interfering beams are

$$E_1 = E_0 \exp(-r^2/w_1^2) \qquad (A4\cdot1)$$

and $$E_2 = (\eta w_1/w_2) E_0 \exp(-r^2/w_2^2) \qquad (A4\cdot2)$$

where the factor (w_1/w_2) is included to ensure equal energies when the amplitude factor η (due to absorption or poor excitation) is equal to 1, then the ratio of minimum to maximum intensity is

$$I_{min}/I_0 = \frac{\int_0^\infty \left[E_0 \exp(-r^2/w_1^2) - (\eta w_1/w_2) E_0 \exp(-r^2/w_2^2)\right]^2 r\,dr}{\int_0^\infty E_0^2 \exp(-2r^2/w_1^2) r\,dr} \qquad (A4\cdot3)$$

So the visibility is

$$V = 4\eta (w_1/w_2 + w_2/w_1)^{-1} - \eta^2 \qquad (A4\cdot4)$$

The amplitude of the intra-cavity beam will be reduced when there is a mismatch, for energy will be transferred to higher order modes(principally the second for a small mismatch). If $|(w_1-w_2)/w_1| \ll 1$, use of (3·13) gives

$$I_0 \propto 1 - \tfrac{1}{2}(\Delta w/w)^2 \qquad (A4\cdot5)$$

or $$\eta = \eta_0 \left[1 - \tfrac{1}{4}(\Delta w/w)^2\right] \qquad (A4\cdot6)$$

The visibility is therefore

$$V = \frac{4\eta_0\left[1 - \frac{1}{4}(\Delta w/w)^2\right]}{\left[w_1/w_2 + w_2/w_1\right]} - \eta_0^2\left[1 - \frac{1}{4}(\Delta w/w)^2\right]^2 \qquad (A4\cdot7)$$

The significance of this may be seen by taking some examples. If $\eta_0 = 1$, the visibility with no mismatch is unity (100%); with $\Delta w/w = 0\cdot5$, the visibility drops to 85%. On the other hand, a value of $\eta_0 = 0\cdot25$ gives a visibility with no mismatch of 44%; with $\Delta w/w = 0\cdot5$, V = 38%.

Thus, the precise quality of the mode-matching has only a moderate effect on the fringe visibility.

APPENDIX FIVE

THE RESPONSE OF A QUADRANT PHOTODIODE TO POSITIONAL FLUCTUATIONS OF A LASER BEAM

A quadrant photodiode consists of four independent diodes arranged in the four quadrants of a circle (fig A5·1). If a light spot (e.g. a laser beam) is arranged to cover part of each of the four segments, then a measure of the position of the centroid of the spot may be obtained from the relative intensities (photocurrents) of the four quadrants. Probably the simplest such method is to subtract the currents from opposite quadrants in order to obtain the position signal; information about the two dimensions (x and y)is then obtained separately from the two pairs of diodes. The aim of this calculation is to obtain quantitatively, for such a system, the sensitivity to positional fluctuations of a laser beam of given size and positional offset, the non-linearity and dimensional cross-coupling. This will include an assessment of the importance of laser intensity noise and photocurrent shot noise. These results are relevant to the design of the system used to measure laser beam positional fluctuations (Chapter 3).

Consider the system shown in fig A5·1, where a laser beam of radius w is incident on a quadrant diode with a positional offset r and angular offset $\theta+\phi$ with respect to the diode, or θ with respect to an external Cartesian co-ordinate system. The measure of the x co-ordinate is the difference in photocurrent between qwadrants 1 and 3 :

$$i_x = i_1 - i_3 \qquad (A5\cdot1)$$

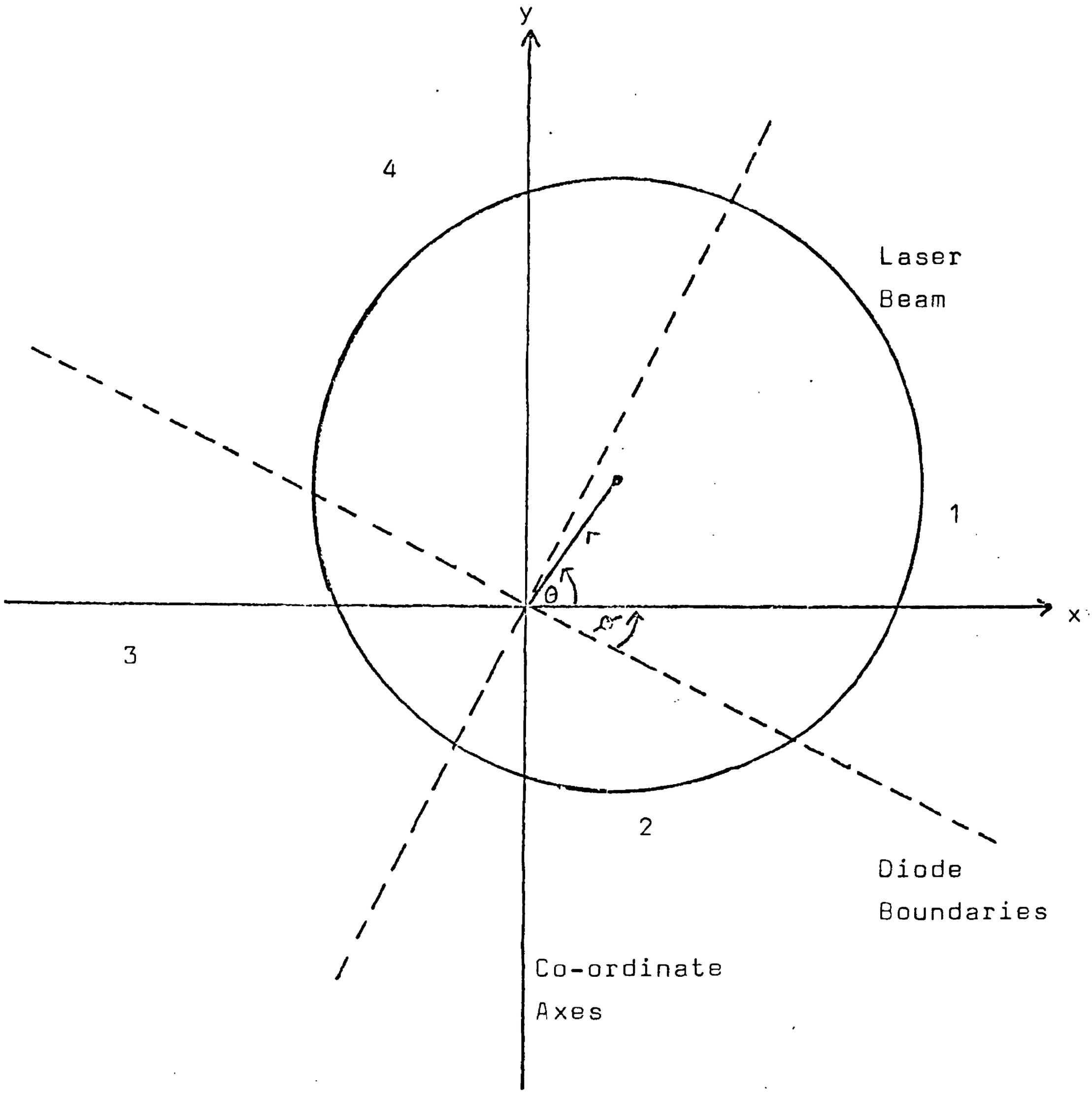

Fig A5•1: Schematic diagram of a laser beam incident on a quadrant diode. The centre of the laser beam is offset by a distance r and angle $\theta+\phi$, while the diode axes are rotated by an angle ϕ with respect to the external co-ordinates.

A measure of a small fluctuation δx is therefore

$$\delta i_x = \delta i_1 - \delta i_3 \qquad (A5\cdot2)$$

So we want to calculate the change in i_1, i_3 when x fluctuates, for arbitrary r, θ.

The laser beam is assumed to have an intensity distribution

$$I(\rho,t) = I(t)e^{-2\rho^2/w^2} = (w^2P(t)/\pi)e^{-2\rho^2/w^2} \qquad (A5\cdot3)$$

where ρ is the distance from the centre of the laser beam and P(t) is the total laser power at time t. The photocurrent in quadrant 1 is then

$$i_1(t) = \eta I(t)\int_{\alpha=-\phi}^{-\phi+\pi/2}\int_{\sigma=0}^{R_D} e^{-2\rho^2/w^2}\sigma\,d\sigma\,d\alpha \qquad (A5\cdot4)$$

where η is the power to current efficiency of the diode and R_D is the radius of the diode. In practice, $R_D - r \gg w$, so this limit may safely be taken as infinity. Application of the cosine rule then gives

$$i_1(t) = \frac{2\eta P(t)}{\pi w^2} e^{-2r^2/w^2}\int_{-\phi}^{-\phi+\pi/2}\int_{0}^{\infty}\exp\left[-2\sigma^2/w^2 + (4r\sigma/w^2)\cos(\theta-\alpha)\right]\sigma\,d\sigma\,d\alpha \qquad (A5\cdot5)$$

The integral over σ is standard (Gradshteyn and Rhyzhik 1965), giving

$$i_1(t) = (\eta P(t)/2\pi)e^{-2r^2/w^2}\int_{0}^{-\phi+\pi/2}\exp\left[(2r^2/w^2)\cos^2(\theta-\alpha)\right]\cdot \times \left[\sqrt{\pi/2} - \sqrt{2}\int_{0}^{\sqrt{2}r/w\cos(\theta-\alpha)} e^{-t^2}\,dt\right]d\alpha \qquad (A5\cdot6)$$

Each part of the integral can be evaluated in a straightforward, if rather messy, fashion by expressing it as a series and using standard integrals. This gives (pto.):

$$i_1(t) = \frac{\eta P(t)}{2\sqrt{2}\,\pi} e^{-2r^2/w^2} \left\{ \sum_{j=0}^{\infty} \frac{(\sqrt{2}r/w)^{2j}}{j!} \left[\frac{\pi/2}{2^{2j}} {}^{2j}C_j \right.\right.$$

$$\left.\left. + \frac{1}{2^{2j-1}} \sum_{k=0}^{j-1} {}^{2j}C_k \frac{\sin\left[\frac{\pi}{2}(j-k)\right]\cos\left[2(j-k)(\theta+\phi-\pi/4)\right]}{j-k} \right] \right.$$

$$\left. + \frac{2}{\sqrt{\pi}} \sum_{L=0}^{\infty} \frac{(\sqrt{2}r/w)^{2L+1}}{(2L+1)!!\,2^L} \sum_{k=0}^{L} {}^{2L+1}C_k \frac{2\sin\left[\frac{\pi}{4}(2L-2k+1)\right]\cos\left[(2L-2k+1)(\theta+\phi-\pi/4)\right]}{2L-2k+1} \right\}$$

(A5·7)

This results in a difference signal i_x of

$$i_x(t) = -\frac{\eta P(t)}{\sqrt{2}\,\pi} e^{-2r^2/w^2} \sum_{L=0}^{\infty} \frac{(\sqrt{2}r/w)^{2L+1}}{(2L+1)!!\,2^L} \sum_{k=0}^{L} {}^{2L+1}C_k \frac{4\sin\left[\frac{\pi}{4}(2L-2k+1)\right]\sin\left[\frac{\pi}{2}(2L-2k+1)\right]}{2L-2k+1}$$

(A5·8)

Defining the latter summation to be $f_1(\theta,\phi)$, we can proceed to calculate the change in i_x corresponding to beam positional changes δx, δy by differentiating with respect to r, θ and using

$$\delta i_x = (\partial i_x/\partial r)(\delta x\cos\theta + \delta y\sin\theta) + (\partial i_x/\partial\theta)(\delta y\cos\theta - \delta x\sin\theta)/r$$

(A5·9)

This leads to the result

$$\delta i_x = -\frac{\eta P(t)}{\sqrt{2}\,\pi} e^{-2r^2/w^2} \left\{ \delta x \left[\cos\theta \left(\sum_{L=0}^{\infty} \frac{(\sqrt{2}r/w)^{2L} \frac{\sqrt{2}}{w} f_L(\theta,\phi)}{(2L+1)(2L+1)!!\,2^L} - \frac{4r}{w^2} \sum_{L=0}^{\infty} \frac{(\sqrt{2}r/w)^{2L+1} f_L(\theta,\phi)}{(2L+1)!!\,2^L} \right) \right.\right.$$

$$\left.\left. - \frac{\sin\theta}{r} \sum_{L=0}^{\infty} \frac{(\sqrt{2}r/w)^{2L+1} f_L'(\theta,\phi)}{(2L+1)!!\,2^L} \right] \right.$$

$$+ \delta y \left[\sin\theta \left(\sum_{L=0}^{\infty} \frac{(\sqrt{2}r/w)^{2L} \frac{\sqrt{2}}{w} f_L(\theta,\phi)}{(2L+1)(2L+1)!!\,2^L} - \frac{4r}{w^2} \sum_{L=0}^{\infty} \frac{(\sqrt{2}r/w)^{2L+1} f_L(\theta,\phi)}{(2L+1)!!\,2^L} \right) \right.$$

$$\left.\left. + \frac{\cos\theta}{r} \sum_{L=0}^{\infty} \frac{(\sqrt{2}r/w)^{2L+1} f_L'(\theta,\phi)}{(2L+1)!!\,2^L} \right] \right\}$$

(A5·10)

Here $f_1'(\theta,\phi)$ is just the differential of $f_1(\theta,\phi)$ with respect to θ, i.e.

$$f_L'(\theta,\phi) = \sum_{k=0}^{L} {}^{2L+1}C_k \, 4\sin\left[\tfrac{\pi}{4}(2L-2k+1)\right]\sin\left[\tfrac{\pi}{2}(2L-2k+1)\right]\cos\left[(2L-2k+1)(\theta+\phi-3\pi/4)\right] \qquad (A5\cdot11)$$

Now the series in l converges quite strongly, with $\left[1/(2l+1)(2l+1)!!\,2^l\right]_{l=1} = 1/18$. So if we restrict attention to the region $r/w \lesssim 1$, it is reasonable to take only $l = 0$, giving

$$\delta i_x = \frac{2\sqrt{2}\,\eta P(t)}{\pi w}\left\{\left[\cos(\phi-\tfrac{1}{4}\pi) + (4r/w)\sin(\theta+\phi-\tfrac{3}{4}\pi)\right]\delta x + \left[\sin(\phi-\tfrac{1}{4}\pi) + (4r/w)\cos(\theta+\phi-\tfrac{1}{4}\pi)\right]\delta y\right\} \qquad (A5\cdot12)$$

The ratio of linear to non-linear terms is thus $w/4r$: as long as $r \ll w/4$, the difference current will be a linear and orthogonal measure of the positional fluctuations. In this limit, and with $\phi = \frac{1}{4}\pi$, the sensitivity becomes

$$\delta i_x = \frac{2\sqrt{2}\,\eta P(t)}{\pi w}\delta x \qquad (A5\cdot13)$$

For a positional fluctuation to be detectable, this change in current must be greater than the shot noise in the diode current:

$$\frac{2\sqrt{2}\,\eta P(t)}{\pi w}\delta x \gtrsim (2e\eta P\Delta f)^{\frac{1}{2}} \qquad (A5\cdot14)$$

where e is the electronic charge. So the minimum detectable displacement is

$$\delta x_{min} = \pi w(e\Delta f/4\eta P)^{\frac{1}{2}} = \pi w(\pi\hbar\nu\Delta f/2\xi P)^{\frac{1}{2}} \qquad (A5\cdot15)$$

where $\xi = (2\pi\hbar\nu/e)\eta$ is the quantum efficiency of the diode ($\sim 0\cdot35$). For a laser power P = 1 mW and beam size w = 0·2 mm, this gives

$$\delta x_{min} = 10^{-11}\,\mathrm{m/Hz}$$

If the beam is offset from the centre of the diode, then the difference current may be affected by a change in the

laser power. If these fluctuations are assumed to be of form

$$P(t) = P_0 + \delta P \cos\omega t$$

then, in order to see whether the intensity or position fluctuations dominate the diode output signal, it is necessary to compare $\frac{\partial i}{\partial \rho}.\frac{\partial \rho}{\partial t}\Delta t$ and $\frac{\partial i}{\partial x}.\frac{\partial x}{\partial t}\Delta t$. The criterion that the signal due to intensity noise is less than that due to displacement noise becomes

$$\frac{\delta x(\omega)}{r} > \sqrt{2}\sin(\theta+\phi-\tfrac{3}{4}\pi)\frac{\delta P(\omega)}{P_0} \qquad (A5\cdot16)$$

Or, ignoring the geometrical factor,

$$(\delta x/10^{-11}\,m/\sqrt{Hz}) > (r/10^{-6}\,m)(\frac{\delta P}{P_0}/10^{-5}\sqrt{Hz}) \qquad (A5\cdot17)$$

APPENDIX SIX

A METHOD FOR MEASURING FLUCTUATIONS IN BEAM SIZE

It was seen in Chapter 3 that fluctuations in the size of a laser beam may produce significant noise in the interferometer. It would evidently be useful to be able to observe these fluctuations. Now in principle, a change in the beam radius w may be measured by observing the change in intensity of the central portion of the beam relative to that of the outer portion (or to that of the whole beam). The aim of this calculation was to determine (and optimize) the sensitivity of such a system to beam size fluctuations and to evaluate possible contamination by positional fluctuations of the beam. The practicalities of the subtraction (or division) out of the intensity noise will not be discussed.

Consider the situation illustrated in fig A6·1, in which a laser beam of characteristic radius w is incident, with positional offset r, on a photodiode of radius r_c. The photocurrent is

$$i = \eta \int_{\theta=0}^{2\pi} \int_{\sigma=0}^{r_c} I(\sigma,\theta)\sigma\, d\sigma\, d\theta \qquad (A6\cdot1)$$

where η is the power to current efficiency of the diode and $I(\sigma,\theta)$ is the intensity distribution of the laser beam:

$$I(\sigma,\theta) = I_0 e^{-2\rho^2/w^2} = I_0 \exp[(-2r^2-2\sigma^2+4\sigma r\cos\theta)/w^2] \qquad (A6\cdot2)$$

So the current is

$$i = \eta I_0 e^{-2r^2/w^2} \int_{\sigma=0}^{r_c} \sigma e^{-2\sigma^2/w^2} \int_{\theta=0}^{2\pi} e^{4\sigma r\cos\theta/w^2}\, d\theta\, d\sigma \qquad (A6\cdot3)$$

The integral over θ gives an imaginary Bessel function which may be expanded to give (Gradshteyn and Rhyzhik 1965) a current of

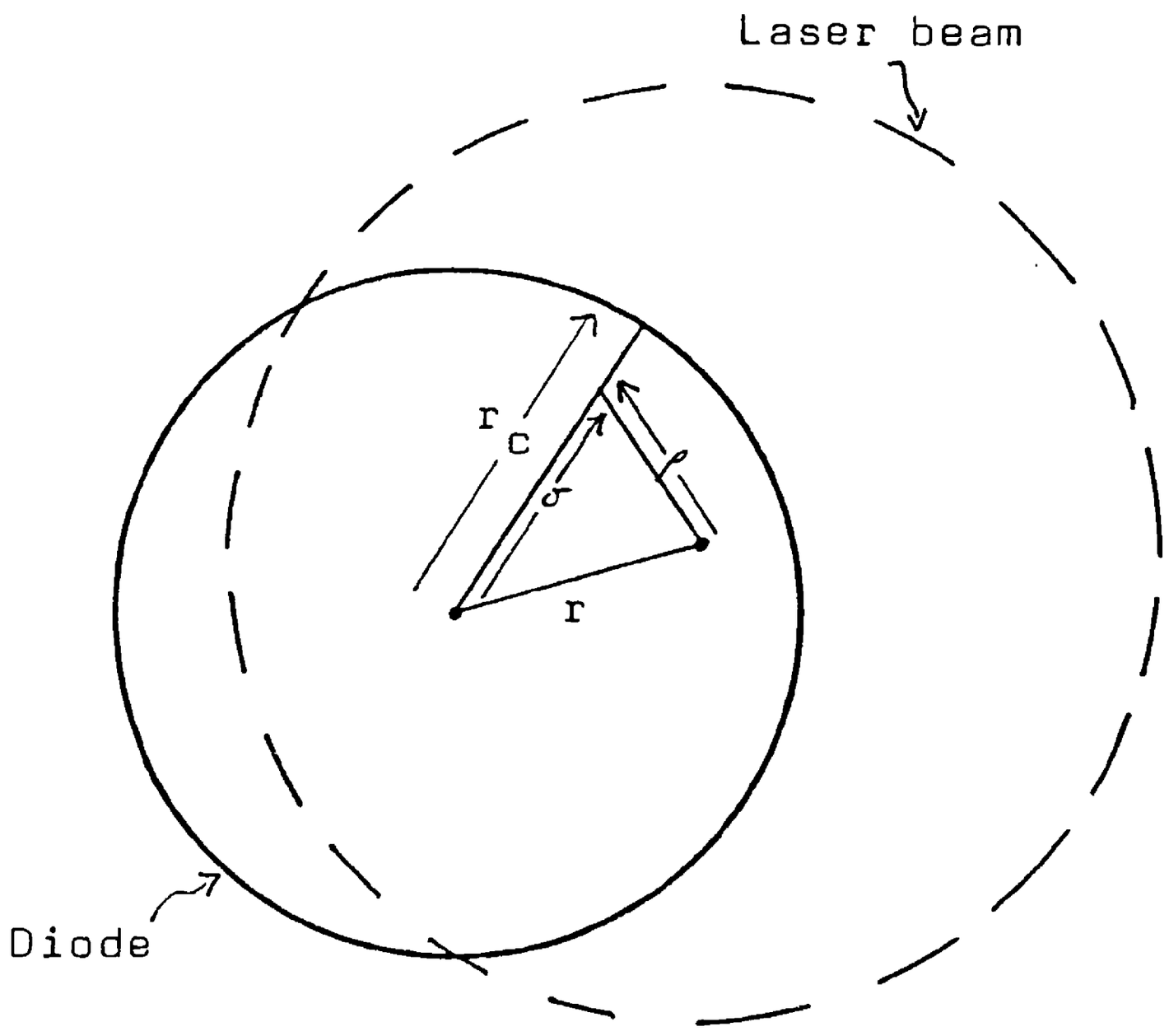

Fig A6·1: A schematic indication of a laser beam incident on a (smaller) photodiode, with positional offset (r,θ). ρ is the distance from the centre of the laser beam, which has a characteristic size w.

$$i = 2\pi\eta I_o e^{-2r^2/\omega^2} \int_0^{r_c} \sum_{k=0}^{\infty} \frac{(2r/\omega^2)^{2k} \sigma^{-2k+1} e^{-2\sigma^2/\omega^2}}{k!\ k!} \qquad (A6\cdot4)$$

This may now be integrated by parts to give

$$i = \eta P e^{-2r^2/\omega^2} \sum_{k=0}^{\infty} \frac{(\sqrt{2}r/\omega)^{2k}\left\{k! - e^{-2r_c^2/\omega^2} \sum_{L=0}^{k} \frac{(\sqrt{2}r_c/\omega)^{2(k-L)}\ 2k!!}{(2k-2L)!!\ 2^L}\right\}}{k!\ k!} \qquad (A6\cdot5)$$

Expanding this expression explicitly gives

$$i = \eta P e^{-2r^2/\omega^2}\left\{1 - e^{-2r_c^2/\omega^2} + 2r^2/\omega^2\left[1 - e^{-2r_c^2/\omega^2}\left(1 + r_c^2/\omega^2\right)\right] + O(r/\omega)^4\right\} \qquad (A6\cdot6)$$

If attention is restricted to the case of $r \ll \omega$, this leads to the result

$$\frac{\partial i}{\partial w} = (2\sqrt{2}\eta P r_c^2/w^3) e^{-2r_c^2/w^2} \qquad (A6\cdot7)$$

This current change produced by a beam size fluctuation is a maximum at $r_c/w = 1/\sqrt{2}$; this does not exactly correspond to the maximum signal to noise ratio if shot noise is assumed to dominate, yet is sufficiently close for this choice of effective aperture size to be a sensible one.

For $r_c/w = 1/\sqrt{2}$, the sensitivity becomes

$$\delta i = (2\sqrt{2}\eta P/e)(\delta w/w) = (\sqrt{2}\xi q P/\pi\hbar\nu e)(\delta w/w) \qquad (A6\cdot8)$$

where e is 2·718..., q is the electronic charge and ξ the quantum efficiency. The photocurrent shot noise then means that the minimum detectable beam size change is

$$\delta w_{min} = w(e(e-1)\pi\hbar\nu/2\xi P)^{\frac{1}{2}} \quad \text{per } \sqrt{\text{Hz}} \qquad (A6\cdot9)$$

Note that this is about the same as the corresponding limit to the measurement of positional fluctuations with a quadrant diode (see Appendix 5).

The diode current may also change because of beam positional fluctuations:

$$\delta i = -(4\eta P r_c^2/w^4) e^{-2r_c^2/w^2} r\delta r \qquad (A6\cdot10)$$

Thus, positional fluctuations will not be detected if the beam is centred to an accuracy of

$$\frac{r}{w} < \frac{\delta w}{\delta r} \qquad (A6\cdot11)$$

So, if it is desired to measure δw to within $\sim 10^{-11}\,m/\sqrt{Hz}$ and $w \sim 1$ mm, $\delta r \sim 10^{-9}\,m/\sqrt{Hz}$, the beam must be centred to within $\sim 10^{-5}$ m.

APPENDIX SEVEN

THE EFFECT OF FIRST ORDER MODE FLUCTUATIONS ON BEAM PROPAGATION

According to the formalism developed in section 3·2, a lateral displacement of the laser beam is represented by a change in the amplitude of the first order mode m = 1 which is <u>in phase</u> with the fundamental. The lateral displacement should evidently remain constant as the beam propagates, yet the first order mode gradually moves <u>out</u> of phase with the fundamental. Is this consistent? Similarly, it is not clear that a fluctuation in the first order mode which is 90^{o} out of phase with the fundamental should produce the observed properties of an angular change – a lateral displacement which increases linearly with distance along the beam. It is shown below, however, that it is the combination of the change in the relative phase of the modes and of the overall change in the beam size w which ensures the consistency of the two ways of viewing the situation.

Consider a fluctuation in A_1 which is directly in phase with the fundamental at a beam waist (size w_0), and should therefore represent a lateral displacement. A distance z away from the waist there will be a phase difference between the modes (cf. 3·4) of

$$\phi = \arctan(\lambda z/\pi w_0^2) \qquad (A7\cdot1)$$

The lateral displacement at this position will be determined by the in phase component of the fluctuation δA_1:

$$\delta A_1(//) = \delta A_1 \cos\phi \qquad (A7\cdot2)$$

$$\text{But} \quad \cos\phi = \left[1 + \tan^2\phi\right]^{-\frac{1}{2}} = \left[1 + (\lambda z/\pi w_0^2)^2\right]^{-\frac{1}{2}} \qquad (A7\cdot3)$$

and the beam size w varies with z as (Kogelnik and Li 1966):

$$w^2(z) = w_0^2\left[1 + (\lambda z/\pi w_0^2)^2\right] \qquad (A7\cdot4)$$

So the parallel component of the fluctuation is just

$$\delta A_1(//) = \delta A_1 w_0/w \qquad (A7\cdot5)$$

Now the displacement this produces is (cf. 3·15)

$$\delta X = \sqrt{2}\delta x/w \propto \delta A_1(//) = \delta A_1 w_0/w \qquad (A7\cdot6)$$

Thus the displacement δx is independent of w and of z: it is constant as required.

A similar argument can be used for an angular change: now the parallel component producing the displacement is

$$\delta A_1(//) = \delta A_1 \sin\phi \qquad (A7\cdot7)$$

and $\sin\phi = \lambda z/\pi w_0 w$

This gives a displacement δx of

$$\delta x/w \propto \lambda z/\pi w_0 w \qquad (A7\cdot8)$$

Thus, the displacement is proportional to the axial distance, as required.

Thus, the representation of beam positional changes as fluctuations in the amplitude of the first order mode gives the correct propagation properties of the beam.

APPENDIX EIGHT

A NOTE ON THE BEAM-CLEANING ACTION OF SINGLE-MODE FIBRES

Chapter 4 described three possible ways of reducing beam geometry fluctuations. An alternative, currently being investigated at MIT, might be to use a single-mode optical fibre. This idea is briefly explained below. The treatment of fibre modes follows that of Yariv (1976).

An optical fibre of diameter d may be treated as a waveguide, with discrete modes which may be considered to be the superposition of plane waves propagating at an angle $\theta = \arcsin(h/k_0 n_2)$ to the axis of the fibre; hd is a number characterising the mode, k_0 is the vacuum wavenumber and n_2 the refractive index in the fibre. The resultant field distribution inside the fibre, for even modes, is

$$E = E_0 \cos(hx) \exp(-i\beta z) \qquad (A8\cdot1)$$

where $\beta = k_0 n_2 \cos\theta$; x is the transverse direction, z the propagation. For odd modes,

$$E = E_0 \sin(hx) \exp(-i\beta z) \qquad (A8\cdot2)$$

Outside the fibre, the field decays exponentially:

$$E = E_0 \cos(hd) \exp\left[-p(1\times|-d) - i\beta z\right] \qquad (A8\cdot3)$$

where pd is an integer which has to satisfy the relations

$$pd = hd\tan(hd) \qquad (A8\cdot4)$$

$$\text{and} \quad (pd)^2 + (hd)^2 = k_0^2 d^2 (n_2^2 - n_1^2) \qquad (A8\cdot5)$$

with n_1 the refractive index of the cladding.

It is evident that an incoming even Gaussian mode will excite more than one even fibre mode, while an odd Gaussian mode will excite odd fibre modes. The two types of mode are, however, sufficiently similar for reasonably efficient coupling to be possible, for example, from the

T_{00} mode into the TE_1 mode and the T_{10} mode into the TE_2 mode. Beam geometry fluctuations require the presence of higher order waveguide modes.

Now if

$$0 < (n_2^2 - n_1^2)^{\frac{1}{2}} k_0 d < \pi \qquad (A8\cdot6)$$

the waveguide will only support one mode without attenuation. Such a single mode fibre may therefore serve as a method of reducing the geometry fluctuations of a laser beam.

To calculate the decay length of a mode in the fibre, it is convenient to view the field as a superposition of plane waves. These are reflected off the side of the fibre with a reflection coefficient R. If the angle of propagation is θ, the number of bounces in a length l is

$$N = (l/d)\tan\theta \approx hl/k_0 n_2 d \qquad (A8\cdot8)$$

The amplitude after N bounces is reduced by R^N, or

$$A/A_0 = \exp(lhd.\ln R/k_0 n_2 d^2) \qquad (A8\cdot9)$$

If θ is less than the critical angle, R = 1 and the mode does not decay. For higher modes, lnR is negative-definite and the mode decays in a characteristic length

$$l_c = \frac{-k_0 n_2 d^2}{(hd)\ln R} \qquad (A8\cdot10)$$

As an example, consider the decay of the TE_2 mode, which would produce positional fluctuations. This has

$$\pi/2 < hd < \pi \qquad (A8\cdot11)$$

Taking $n_2 \sim 1\cdot5$, $\ln R \sim -0\cdot1$ ($R \sim 0\cdot9$), $\lambda \sim 5\times10^{-7}$m and $d \sim 10\mu$m (fairly pessimistic) gives a decay length of about 1cm. So even a 5cm length of fibre would give a potential suppression factor of over 100.

It is evident that, at least in principle, single-mode

optical fibres have considerable potential as suppressors of laser beam geometry fluctuations. It is not yet clear, however, whether associated practical problems will severely constrain their use.

REFERENCES

Arnett, W.D. (1979) In "Sources of Gravitational Radiation" Ed. Smarr, L. (CUP)

Ashworth, M., Lyne, A.G. and Smith, F.G. (1983) Nature 301, 313

Backer, D.C., Kulkarni, S.R., Heiles, C., Davies, M.M. and Goss, W.M. (1982) Nature 300, 615

Backer, D.C., Kulkarni, S.R. and Taylor, J.M. (1983)Nature 301, 314

Bagayev, S.N., Chebotayev, V.P., Dychkov, A.S. and Goldort, V.G. (1981) Appl. Phys 25, 161

Bateman, H. (1954) "Table of Integral Transforms" Vol I (McGraw-Hill, New York)

Billing, H., Winkler, W., Schilling, R., Rüdiger, A., Maischberger, K. and Schnupp L. (1981) In "Quantum Optics, Experimental Gravitation and Measurement Theory" Eds. Meystre, P. and Scully, M.O. (Plenum Press)

Blair, D.G. (1983) In "Gravitational Radiation" Eds. Deruelle,N and Piran, T. (North-Holland, Amsterdam)

Boriakoff, V., Buccheri, R. and Fauci, F. (1983) Nature 304, 417

Boyd, G.D. and Gordan, J.P. (1961) Bell Syst. Tech. J. 40, 489

Braginsky, V.B. (1977) In "Proceedings of the International Meeting on Experimental Gravitation" Ed. Bertotti, B. (Accad. Naz. dei Lincei, Rome)

Braginsky, V.B. (1983) In "Gravitational Radiation" Eds. Deruelle, N. and Piran, T. (North-Holland, Amsterdam)

Braginsky, V.B., Grishchuk, L.P., Doroshkevich, A.G., Zel'dovich, Ya.B., Novikov, I.D. and Sazhin, M.V. (1974) JETP 38, 865

Braginsky,V.B. and Menskii, M.B. (1971) JETP Lett. 13, 417

Braginsky,V.B. and Nazarenko, V.S. (1971) In "Proceedings of the Conference on Experimental Tests of Gravitation Theories, Nov. 11-13 1970" JPL Tech. Mem. 33

Braginsky,V.B., Zel'dovich,Ya.B. and Rudenko, V.N. (1969) JETP Lett. 10,280

Brillet, A. and Tourrenc, P. (1983) In "Gravitational Radiation" Eds. Deruelle, N. and Piran, T. (North-Holland, Amsterdam).

Carr, B.J. (1980) Astr. Astrophys. 89, 6

Caves, C.M. (1979) Phys. Lett. 80B, 323

Caves, C.M. (1981) Phys. Rev. D23, 1693

Caves, C.M., Drever, R.W.P., Sandberg, V.D., Thorne, K.S. and Zimmerman, M. (1980) Rev. Mod. Phys. 52, 341

Clark, J.P.A. (1979) In "Sources of Gravitational Radiation" Ed. Smarr, L. (CUP)

Clark, J.P.A. and Eardley, D.M. (1977) Ap.J 215, 311

Decher, R., Randall, J.L., Bender, P.L. and Faller, J.E. (1980) SPIE 228, 149

Detweiler, S.L. (1979) In "Sources of Gravitational Radiation" Ed. Smarr, L. (CUP)

Douglass, D.H. and Braginsky, V.B. (1979) In "General Relativity, an Einstein Centenary Survey" Eds. Hawking, S.W. and Israel, W. (CUP)

Drever, R.W.P. (1983) In "Gravitational Radiation" Eds. Deruelle, N. and Piran, T. (North-Holland, Amsterdam)

Drever, R.W.P., Ford, G.M., Hough, J., Kerr, I., Munley, A.J., Pugh J.R., Robertson, N.A. and Ward, H. (1980) Proc GR9, Jena (In press)

Drever, R.W.P., Hall, J.L., Kowalski, F.V., Hough, J., Ford, G.M., Munley, A.J. and Ward, H. (1983) Appl. Phys. B31, 97

Drever, R.W.P., Hough, J., Bland, R. and Lessnoff, G.W. (1973) Nature 246, 340

Drever, R.W.P., Hough, J., Munley, A.J., Lee, S-A, Spero, R., Whitcombe, S.E., Ward, H. Ford, G.M., Hereld, M, Robertson, N.A., Kerr, I. Pugh, J.R., Newton, G.P., Meers, B.J., Brooks III, E.D. and Gursel, Y. (1981) In "Quantum Optics, Experimental Gravitation and Measurement Theory" Eds. Meystre, P. and Scully, M.O. (Plenum Press)

Eardley, D.M. (1983) In "Gravitational Radiation" Eds. Deruelle, N. and Piran, T. (North-Holland, Amsterdam)

Edelstein, W.A., Hough, J., Pugh, J.R. and Martin, W. (1978) J. Phys. E 11, 710

Eddington, A.S. (1922) "The Mathematical Theory of Relativity" (CUP)

Epstein, R. and Clark, J.P.A. (1979) In "Sources of Gravitational Radiation" Ed. Smarr, L. (CUP)

Forward, R.L. (1978) Phys. Rev. D17, 379

Gibbons, G.W. and Hawking, S.W. (1971) Phys. Rev. D4, 2191

Giffard, R.P. (1976) Phys. Rev. D14, 2478

Gradsheytn, I.S. and Ryzhik, I.M. (1965) "Table of Integrals, Series and Products" (Academic Press)

Grishchuk, L. (1977) Ann. N.Y. Acad. Sci. 302, 439

Heffner, H. (1962) Proc. IRE 50, 1604

Hellings, R.W. (1983) In "Gravitational Radiation" Eds. Deruelle, N. and Piran, T. (North-Holland, Amsterdam)

Helmcke, J., Lee, S-A. and Hall, J.L. (1982) Appl. Opt. 21, 1686

Hirakawa, H., Tsubono, K. and Fujimoto, M. (1977)
Phys. Rev. D17, 1919

Horowitz, P. (1969) Rev. Sci. Instr. 40, 369

Hough, J., Drever, R.W.P., Ward, H., Munley, A.J., Newton, G.P., Meers, B.J., Hoggan, S. and Kerr, G.A. (1983)
Nature 303, 216

Hough, J., Pugh, J.R., Bland, R. and Drever, R.W.P. (1975)
Nature 254, 498

Kogelnik, H. and Li, T. (1966) Proc. IEEE 54, 1312

Man, C.N., Brillet, A. and Cerez, P. (1978) J.Phys. E 11, 19

Mashhoon, B., Carr, B.J. and Hu, B. (1981) Ap. J. 246, 569

Meyer, R.E., Sanders, G.A. and Ezekiel, S. (1983) MIT Preprint

Michelson, P.F. (1983) In "Gravitational Radiation" Eds.
Deruelle, N. and Piran, T. (North-Holland, Amsterdam)

Mironovskii, V.N. (1966) Sov. Astron. 9, 762

Misner, C.W., Thorne, K.S. and Wheeler, J.A. (1973)
"Gravitation" (Freeman, San Francisco)

Moss, G.E., Miller, L.R. and Forward, R.L. (1971) Appl.
Opt. 10, 2495

Munley, A.J. (1982) PhD Thesis, Glasgow University.

Papaloizou, J. and Pringle, J.E. (1978) MNRAS 184, 501

Pegoraro, F. and Radicati, L.A. (1980) J. Phys. A 13, 2411

Ress, M.J. (1983) In "Gravitational Radiation" Eds,
Deruelle, N. and Piran, T. (North-Holland, Amsterdam)

Robertson, N.A. (1981) PhD Thesis, Glasgow University.

Rüdiger, A., Schilling, R., Schnupp, L., Winkler, W.,
Billing, H. and Maischberger, K. (1981) Opt. Act.
28, 641

Rüdiger, A., Schilling, R., Schnupp, L., Winkler, W., Billing, H. and Maischberger, K. (1982) Max Planck Preprint MPQ 68

Saenz, R.A. and Shapiro, S.L. (1978) Ap. J. 221, 286

Saenz, R.A. and Shapiro, S.L. (1979) Ap. J. 229, 1107

Saenz, R.A. and Shapiro, S.L. (1981) Ap. J. 244, 1033

Saulson, P.P. (1982) MIT Preprint

Schilling, R., Schnupp, L., Winkler, W., Billing, H., Maischberger, K. and Rüdiger, A. (1981) J. Phys. E 14, 65

Smith, F.G. (1977) "Pulsars" (CUP)

Starobinsky, A.A. (1979) JETP 30, 682

Taylor, J.H. and Weisberg, J.M. (1982) Ap.J. 253, 908

Thorne, K.S. (1980) Rev. Mod. Phys. 52, 285

Thorne, K.S. (1983) In "Gravitational Radiation" Eds. Deruelle, N. and Piran, T. (North-Holland, Amsterdam)

Thorne, K.S., Caves, C.M., Sandberg, V.D. and Drever, R.W.P. (1979) In "Sources of Gravitational Radiation" Ed. Smarr, L. (CUP)

Walls, D.F. (1983) Nature 306,141

Weber, J. (1960) Phys. Rev. 117, 306

Weber, J. (1967) Phys. Rev. Lett. 18, 498

Weber, J. (1970a) Phys. Rev. Lett. 22, 1320

Weber, J. (1970b) Phys. Rev. Lett. 24, 276

Weber, J. (1970c) Phys. Rev. Lett. 25, 180

Weiss, R. (1972) Quart. Prog. Rep. Res. Lab. Elect. MIT 105, 54

Weiss, R. (1979) In "Sources of Gravitational Radiation" Ed. Smarr, L. (CUP)

Weksler, M., Vager, Z. and Neumann, G. (1980) Appl. Opt. 19, 2717

White, S.D.M. and Rees, M.J. (1978) MNRAS 183, 341

Will, C.M. (1979) In "General Relativity, an Einstein Centenary Survey" Eds, Hawking, S.W. and Israel, W. (CUP)

Wilson, J.R. (1979) In "Sources of Gravitational Radiation" Ed. Smarr, L. (CUP)

Yariv, A. (1976) "Introduction to Optical Electronics" (Holt, Rinehart and Winston, New York)

Zel'dovich, Ya.B. and Polnarev, A.G. (1974) Sov. Astron. 18, 17

Zimmerman, M. (1978) Nature 271, 524

Zimmerman, M. (1980) Phys. Rev. D21, 891

Zimmerman, M. and Szedenits, E. (1979) Phys. Rev. D20, 351

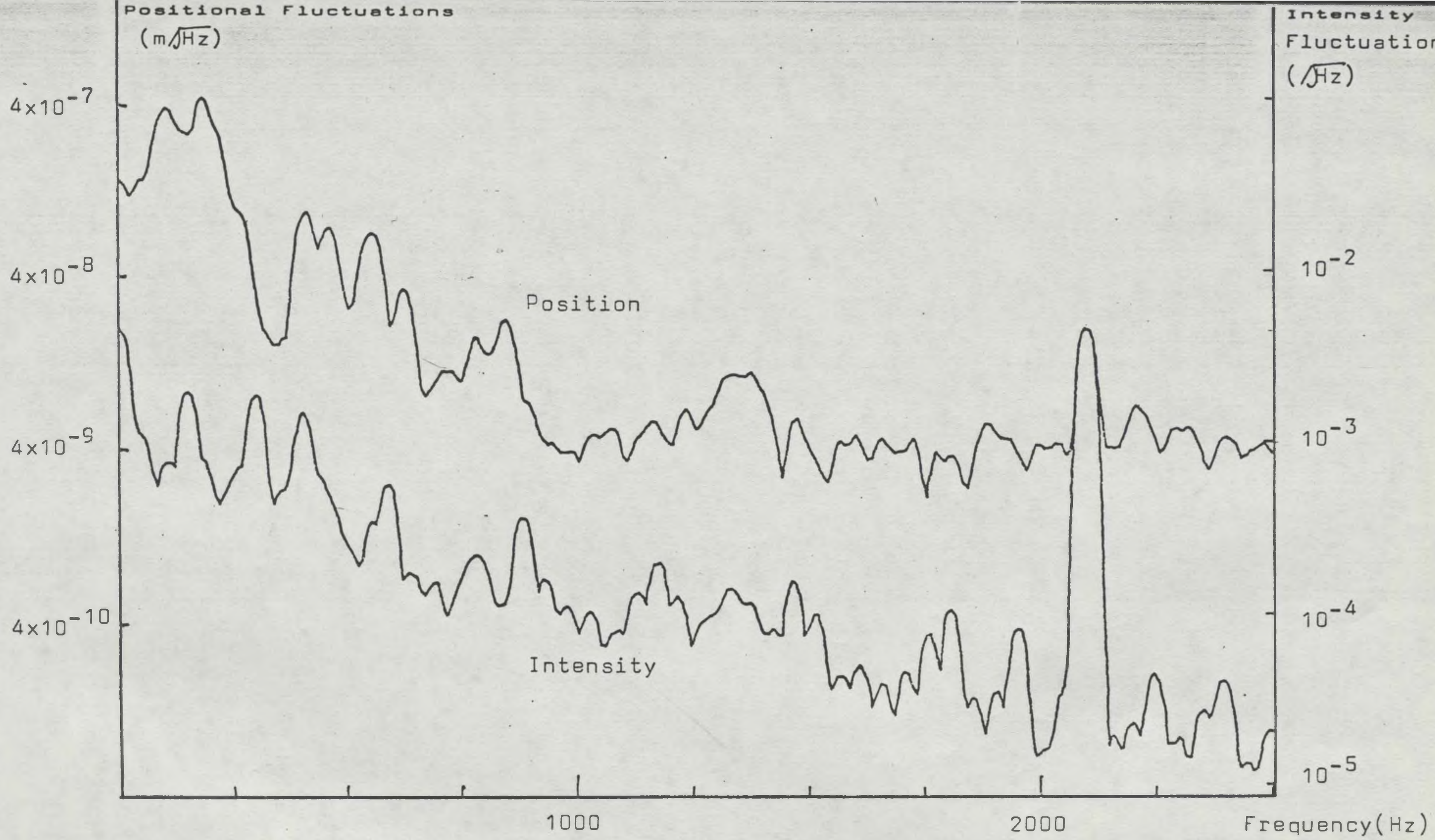

Fig 3·4: A spectrum of the positional fluctuations of the Spectra 170 Ar^+ laser, measured on the central mass where w ~1mm. The effect of a modulation of the intensity at ~2 kHz can be seen, together with a spectrum of the corresponding intensity noise.

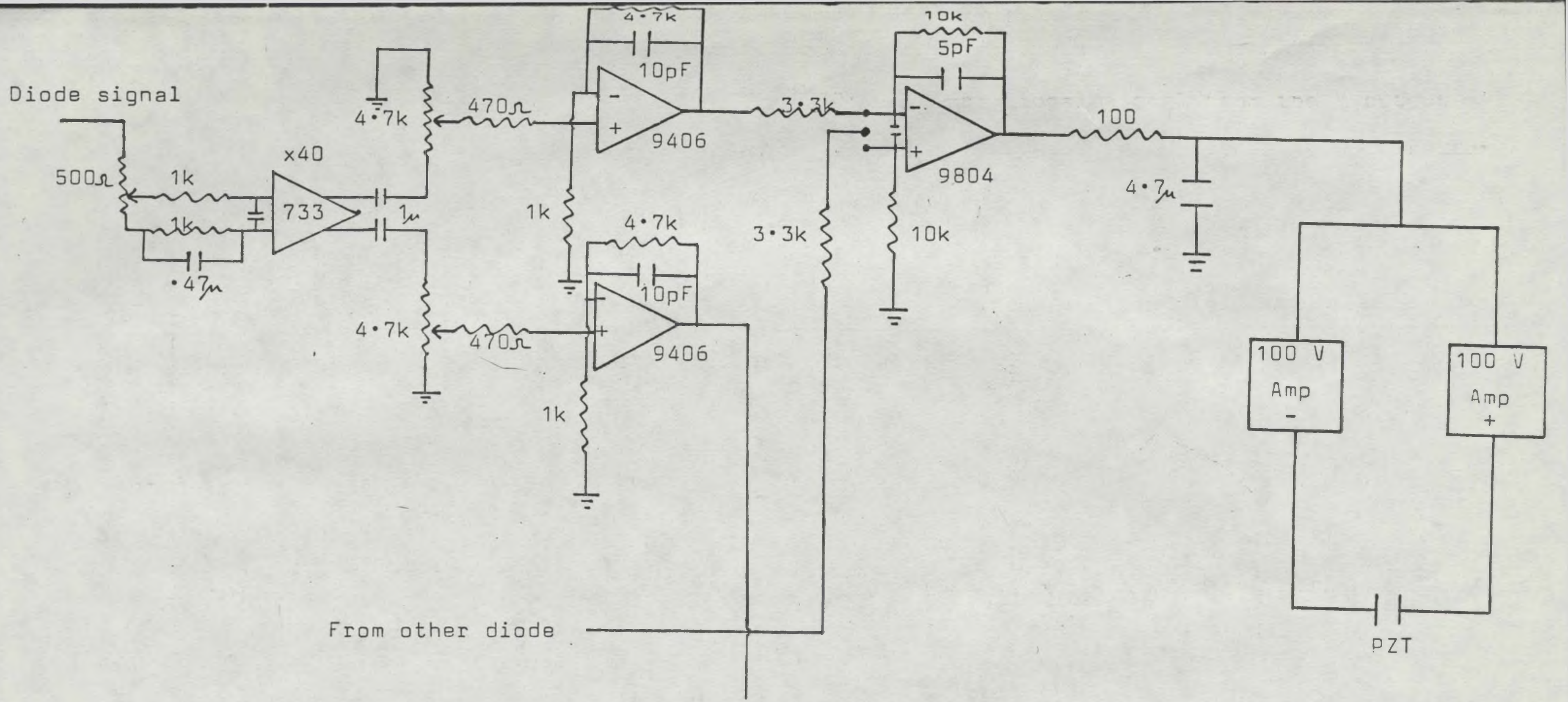

Fig 4·19: Part of the circuit diagram for one dimension, one transducer of the fast beam position stabilisation system.